

International Atomic Energy Agency

INDC(CCP)-150/LJH

**IN DC**

**INTERNATIONAL NUCLEAR DATA COMMITTEE**

Evaluation of Nuclear Data for  $^{242}\text{Pu}$  in the  
 $10^{-5}$  eV - 15 MeV Neutron Energy Region

Translation of a Collection of Scientific Papers Published  
by the Heat and Mass-Exchange Institute of the  
Byelorussian Academy of Sciences in Minsk in 1979

Edited by A.K. Krasin

Translated by the IAEA  
July 1980

---

**IAEA NUCLEAR DATA SECTION, WAGRAMERSTRASSE 5, A-1400 VIENNA**

Reproduced by the IAEA in Austria  
July 1980  
80-3674

Evaluation of Nuclear Data for  $^{242}\text{Pu}$  in the  
 $10^{-5}$  eV - 15 MeV Neutron Energy Region

Translation of a Collection of Scientific Papers Published  
by the Heat and Mass-Exchange Institute of the  
Byelorussian Academy of Sciences in Minsk in 1979

Edited by A.K. Krasin

Translated by the IAEA  
July 1980

UDC 539.173.4

This collection of papers sets out the results of the evaluation of nuclear constants for  $^{242}\text{Pu}$  in the  $10^{-5}$  eV-15 MeV energy region.

The evaluation is based on all the experimental data available as of September 1979. Extensive use is made of the results of nuclear modelling calculations which are further developed in this collection of papers. The evaluated data are written in the ENDF/B format and are presented as a print-out.

EVALUATION OF NUCLEAR DATA FOR  $^{242}\text{Pu}$  IN THE REGION OF RESOLVED  
AND UNRESOLVED RESONANCES ( $10^{-5}$  eV-200 keV)

G.V. Antsipov, L.A. Bakhanovich, V.A. Kon'shin, V.M. Maslov,  
G.B. Morogovskij, E.Sh. Sukhovitskij, Yu.V. Porodzinskij

1. INTRODUCTION

The extensive development of nuclear power calls for a highly accurate knowledge of the nuclear constants of fissile and construction materials. In order to design and develop fast reactors, a sufficiently firm knowledge of the neutron cross-sections of the plutonium isotopes is required since the core of a fast or thermal reactor may contain 55-60%  $^{239}\text{Pu}$ , 20-25%  $^{240}\text{Pu}$ , 10-15%  $^{241}\text{Pu}$  and 5-10%  $^{242}\text{Pu}$ . Furthermore,  $^{242}\text{Pu}$  is a source isotope for the accumulation of  $^{244}\text{Cm}$  which, together with  $^{242}\text{Cm}$ , is a source of neutron activity in the nuclear fuel.

This and the next two papers<sup>\*</sup> give an evaluation of the nuclear constants for  $^{242}\text{Pu}$  in the  $10^{-5}$  eV-15 MeV region, together with the results of work done in the Institute on the formulation of methods for evaluating and setting up complete files (self-consistent sets) of evaluated nuclear constants, as are required for reactor calculations and other applications. The evaluation made use of all the experimental data available as of September 1979. These data are quite scarce and essentially refer only to the resonance parameters and fission cross-sections. In deriving evaluated data we therefore drew extensively on nuclear modelling calculations.

The evaluated data were recorded on ES computer magnetic tape and sent to the Nuclear Data Centre in Obninsk. The group constants divided into the standard 26 groups, as derived from this evaluation, are given in the third article (see this collection, p. 92 ).

Table 1.1 gives the Q values and thresholds of various neutron reactions with the  $^{242}\text{Pu}$  nucleus. The threshold value (for negative Q) is given by the expression:

$$T = \frac{m_n + M_{242}}{M_{242}} \cdot (-Q) = 1.00417 \cdot (-Q),$$

<sup>\*</sup>/ See present collection, p.p. 42 and 92.

where  $M_n$  is the neutron mass (1.00866522) and  
 $M_{242}$  is the mass of the  $^{242}\text{Pu}$  nucleus (242.058768).

Table 1.1

Q values and thresholds for neutron reactions with the  $^{242}\text{Pu}$  nucleus

Reaction	Q value, MeV	Threshold, MeV
$^{242}\text{Pu} (n,2n) ^{241}\text{Pu}$	- 6,301	6,327
$^{242}\text{Pu} (n,3n) ^{240}\text{Pu}$	- 11,542	11,590
$^{242}\text{Pu} (n,4n) ^{239}\text{Pu}$	- 18,075	18,150
$^{242}\text{Pu} (n,\gamma) ^{243}\text{Pu}$	5,037	
$^{242}\text{Pu} (n, d) ^{241}\text{Np}$	- 4,658	4,678
$^{242}\text{Pu} (n, t) ^{240}\text{Np}$	- 4,371	4,389
$^{242}\text{Pu} (n, ^3\text{He}) ^{240}\text{U}$	- 4,260	4,280
$^{242}\text{Pu} (n, ^4\text{He}) ^{239}\text{U}$	9,786	
$^{242}\text{Pu} (n, np) ^{241}\text{Np}$	- 6,883	6,912
$^{242}\text{Pu} (n, nd) ^{240}\text{Np}$	- 10,629	10,673
$^{242}\text{Pu} (n, nt) ^{239}\text{Np}$	- 9,535	9,575
$^{242}\text{Pu} (n, n^3\text{He}) ^{239}\text{U}$	- 10,793	10,838
$^{242}\text{Pu} (n, n^4\text{He}) ^{238}\text{U}$	4,982	

The ground state of the  $^{242}\text{Pu}$  nucleus has spin  $0^+$ .

In reactors  $^{242}\text{Pu}$  is produced by sequential neutron capture in the nuclei of  $^{239}\text{Pu}$ ,  $^{240}\text{Pu}$  and  $^{241}\text{Pu}$ .  $^{242}\text{Pu}$  is converted via  $\alpha$  decay into  $^{238}\text{U}$  with a half-life of  $(3.702 \pm 0.014) \times 10^5$  years [1]. The spontaneous fission lifetime for  $^{242}\text{Pu}$  is  $7 \times 10^{10}$  years.

## 2. NUCLEAR DATA FOR $^{242}\text{Pu}$ IN THE THERMAL AND EPITHERMAL REGIONS ( $10^{-5}$ - $10$ eV)

The  $^{242}\text{Pu}$  nucleus undergoes virtually no fissions up to  $\sim 0.5$  MeV and so the most important processes in this energy region are  $(n,\gamma)$  and  $(n,n)$  reactions.

Measurements in this energy region may be broken down into two categories: measurements at the thermal value and measurements of the energy dependence which may be used to determine the parameters of the first resonance.

Measurements at the thermal value can be further broken down into two types: direct measurements at 0.0253 eV and measurements in the Maxwellian spectrum.

Several authors [2-6] have carried out integral measurements of  $\sigma_{\gamma}$  at the thermal value (at 0.0253 eV) by the activation method and obtained cross-section values which were not in satisfactory agreement. Moreover, differential  $\sigma_t$  measurements have been made [7-11] and in Refs [8, 9]  $\sigma_{\gamma}$  was calculated from  $\sigma_t$  on the basis of specific assumptions concerning the  $\sigma_p$  value. All these data are shown in Table 2.1. There are no measurements of the  $\sigma_n$  elastic scattering cross-section for  $^{242}\text{Pu}$ . However, the coherent scattering length  $a$  was measured in Ref. [12] and was found to be  $(0.81 \pm 0.01) \times 10^{-12}$  cm. The scattering cross-section, which may be defined as  $4\pi a^2$ , is  $8.24 \pm 0.21$  b. This measurement is very important for the determination of the potential scattering cross-section  $\sigma_p$ . Apart from these data, let us mention two more values of  $\sigma_{\gamma}^{2200}$ : 18 and 23 b [13].

Table 2.1

Experimental data on  $\sigma_t^{2200}$  and  $\sigma_{\gamma}^{2200}$  for  $^{242}\text{Pu}$

Paper	$\sigma_{\gamma}$ , b	$\sigma_p$ , b	$\sigma_n$ , b	$\sigma_t$ , b	Target	Remarks
Studier [2]	$30 \pm 10$					Activation method, reactor spectrum
Butler [3]	$19.8 \pm 1.0$					Activation method, result corrected by Durham and Molson [4]
Halperin [5]	$24.4 \pm 1.0$					Activation method
Folger [6]	20					" "
Durham [4]	$18.7 \pm 0.7$					" "
Auchampaugh [7]				$39.8 \pm 1.6$	$\text{PuO}_2$	Differential trans- mission measurements
Young [8]	$22 \pm 2$	I4		$39 \pm 1$	$\text{PuO}_2$	" "
Young [9]	$18.5 \pm 2.0$	I0.7	8.4	$26.9 \pm 2.0$	$\text{PuO}_2$	" "
Young [11]	$18.5 \pm 1.0$	I0.7	8.4	$26.9 \pm 1.0$	Pu metal and $\text{PuO}_2$	" "
Lander [12]				$3.24 \pm 0.21$		Diffraction
Calculation in terms of weighted average parameters of the first resonance	18.35	I0.7	8.45	26.80		

A fact which stands out in Table 2.1 is that the  $\sigma_{\gamma}$  values, which may be derived from the  $\sigma_t$  measurements [7, 8] at reasonable  $\sigma_p$  values, are anomalously high. This is due [11] to the use of a  $PuO_2$  powder target and to the presence of water in the sample. If due allowance is made for the scattering effects by small particles and for the water, the  $\sigma_t^{2200}$  value is reduced by 12.2 b (6.3 b + 5.9 b) so that the transmission data correspond with the activation analysis data on  $\sigma_{\gamma}^{2200}$ . In fact the results from special  $\sigma_t$  measurements using a metal target [11] were in excellent agreement with the  $\sigma_t$  measurements on a powder oxide target [9] when allowance was made for the above-mentioned corrections.

The most reliable data on  $\sigma_t^{2200}$  for  $^{242}\text{Pu}$  are thus those given in Refs [9, 11], and they will be used from now on in this paper. It is also interesting to note that the latest  $\sigma_t$  [9, 11] and  $\sigma_n$  [12] data are in excellent agreement with the  $\sigma_{\gamma}$  value measured by Durham and Molson's activation method [4].

Table 2.2 gives the existing estimates of the thermal cross-sections for  $^{242}\text{Pu}$  [11, 14-16] together with the results of the present evaluation as described below.

Table 2.2  
Various evaluations of the  $^{242}\text{Pu}$  thermal cross-sections

Paper	$\sigma_t$ , b	$\sigma_a$ , b	$\sigma_p$ , b	$\sigma_t$ , b	$\sigma_f$ , b
Young, Simpson [11]	$26.9 \pm 1.0$			$19.0 \pm 0.6$	
Caner, Yiftah [14]	$26.8 \pm 1.0$	$8.3 \pm 1.4$		$18.5 \pm 1.0$	
Mughabghab, Garber [15]	$26.5 \pm 0.5$	$5.0 \pm 0.2$		$18.5 \pm 0.4$	0.2
Benjamin et al. [16]				18.7	0
ENDF/B-III	26.9	8.4		18.5	0
This paper	$26.9 \pm 1.0$	$8.25 \pm 0.21$	$10.5 \pm 0.29$	$18.6 \pm 1.0$	0.0007

Table 2.3  
Resonance parameters of the first  $^{242}\text{Pu}$  resonance

Paper	$E_r$ , eV	$\Gamma_n$ , MeV	$\Gamma_n^o$ , MeV	$\Gamma_\gamma$ , MeV	$\Gamma$ , MeV
Egelstaff et al. [17]	$2.67 \pm 0.02$	$1.7 \pm 0.8$	$1.0 \pm 0.5$		
Cote et al. [18]	$2.65 \pm 0.01$	$1.9 \pm 0.2$	$1.2 \pm 0.1$	$25.1 \pm 2.6$	$27.0 \pm 2.7$
Leonard et al. [19]	2.65				
Auchampaugh et al. [7]	$2.64 \pm 0.01$	$1.92 \pm 0.10$	$1.18 \pm 0.06$	$25.5 \pm 1.0$	$27.4 \pm 1.0$
Young, Reader [9]	$2.63 \pm 0.04$		$1.22 \pm 0.05$	$25.0 \pm 1.5$	
	$2.68 \pm 0.04$		$1.12 \pm 0.09$	$31 \pm 5$	
Caner, Yiftah [14]	$2.65 \pm 0.01$		$1.19 \pm 0.03$	$26.0 \pm 1.0$	
Mughabghab, Garber [15]	$2.67 \pm 0.01$	$2.00 \pm 0.08$	$1.22 \pm 0.05$	$25 \pm 2$	$27 \pm 2$
Weighted average from papers [7, 9, 17, 18]	2.66		$1.19 \pm 0.03$	$25.5 \pm 0.8$	
Estimate in this paper	2.66		$1.21 \pm 0.04$	$25.5 \pm 0.8$	

The  $^{242}\text{Pu}$  cross-sections in the thermal and epithermal regions are mainly determined by the parameters of the first resonance, since the next two resonances have narrow neutron widths and the third is rather far away, so that its contribution to the cross-sections in the given energy region is small. Table 2.3 shows the resonance parameters based on the data taken from various papers, their weighted average values allowing for the errors quoted by the authors (we used values as a preliminary estimate) and the parameter estimates obtained by us. All the parameters are in agreement to within the error limits quoted by the authors, and there was no need for  $\Gamma_n^o$  renormalization because of differences in  $E_r$ .

To obtain evaluated cross-sections in the thermal and epithermal regions, we used provisional estimates of the parameters of the first resonance, the  $\sigma_\gamma$  data at the thermal value, the  $\sigma_t^{2200}$  value from Ref. [11], the coherent scattering length from Ref. [12] and the experimental  $\sigma_t$  data [9, 11] in the region up to 2 eV which were available to us. The first resonance parameters were selected in such a way as to provide the best description of the experimental data on the condition that the adjusted values of the parameters matched the weighted averages from Table 2.3 to within the error limits.

The cross-section calculation made allowance for all resonance contributions by means of the formulae:

$$\bar{\sigma}_n(E) = 4\pi R^2 + 4\pi \chi^2 \sum_i \left( \frac{r_{ni}}{r_i} \right)^2 \left( \frac{E}{E_{ri}} \right) \Psi + \sqrt{4\pi \chi^2} \sqrt{4\pi R^2} \sum_i \frac{r_{ni}}{r_i} \left( \frac{E}{E_{ri}} \right)^{1/2} \chi; \quad (2.1)$$

$$\bar{\sigma}_{\delta(\chi)}(E) = 4\pi \chi^2 \sum_i \frac{r_{ni} r_{f(i)}}{r_i} \left( \frac{E}{E_{ri}} \right)^{1/2} \Psi, \quad (2.2)$$

where  $4\pi R^2 = \left( \frac{A+1}{A} \right)^2 \times \frac{K}{E}$ ; A is the atomic number; K =  $2.60382 \times 10^6$  b·eV;  $4\pi R^2$  is the potential scattering cross-section; and  $\Psi$  and  $\chi$  are functions which allow for the resonance broadening due to thermal motion of the nuclei and the experimental resolution. In the region below the energy of the first resonance, no allowance was made in the cross-section calculations for interference between potential and resonance scattering originating from all resonances except the first, i.e. it was assumed that this contribution is compensated by resonances on the energy axis symmetrical to 0.

The adjusted parameters are shown in Table 2.3. The calculation using the weighted average parameters of the first resonance is generally in agreement with the experimental data to within the error limits. However, in order to improve the calculation, the reduced neutron width was taken to be somewhat larger. A comparison between the calculation and the  $\sigma_t$  experimental results from Refs [9, 11] shows that the energy dependence is in good agreement throughout the region, except below 0.005 eV where the discrepancy reaches ~ 7% (see Fig. 2.1). In order to compensate for this discrepancy, it was necessary to introduce a resonance on the negative energy axis. As a result of a self-consistent fit, we recommend the following parameters for the negative and first resonances:

$E_r = -0.001$ eV	$E_r = 2.66 \pm 0.02$ eV
$\Gamma_n^0 = -0.002688$ MeV	$\Gamma_n^0 = 1.21 \pm 0.04$ MeV
$\Gamma_f^0 = 0.0$	$\Gamma_f^0 = 0.0$
$\Gamma_\gamma^0 = 0.001085$ MeV	$\Gamma_\gamma^0 = 25.5 \pm 0.8$ MeV

The following cross-sections were calculated at the thermal point from these parameters and taken as evaluated data:

$$\sigma_{\gamma} = 18.636 \text{ b}$$

$$\sigma_n = 8.247 \text{ b}$$

$$\sigma_p = 10.50 \text{ b}$$

$$\sigma_f = 0.0007 \text{ b}$$

$$\sigma_t = 26.884 \text{ b}$$

R was found to equal  $0.91409 \times 10^{-12} \text{ cm.}$

### 3. NEUTRON CROSS-SECTIONS FOR $^{242}\text{Pu}$ IN THE RESOLVED RESONANCE REGION

We assumed that the resolved resonance region for  $^{242}\text{Pu}$  extends up to 1 keV, since measurements in the higher energy region [21, 22] cannot be used for resonance analysis.

The rather large average spacing between resonances facilitates parameterization and the analysis of the results. However, we had access to very few numerical data from experiments on cross-sections, and the analysis had to be based on parameters, thus inevitably affecting the accuracy of the resulting evaluated data. A number of  $\sigma_t$  and  $\sigma_f$  measurements were available in the given energy region [7, 9, 11, 21, 23]. However, either there is no detailed information on the experimental conditions [7, 11, 23] or there are no numerical data from the experiments [9] or allowance for  $^{239}\text{Pu}$  and  $^{241}\text{Pu}$  impurities in the sample was not entirely correct, thus giving rise both to negative cross-sections and to an anomalously high background at energies corresponding to the positions of the resonances for these impurities [21, 23].

There were obviously not enough experimental data available to provide a self-consistent set of resonance parameters directly (in particular, there were no data on  $\sigma_{\gamma}$  and  $\sigma_n$  whatsoever). The evaluation in the resolved resonance region was therefore based on parameters introduced by the authors of the experimental papers.

$^{242}\text{Pu}$  resonance parameters are given in Refs [4, 9, 10, 14, 17, 18, 20-28]. However, Refs [10, 14, 20] contain evaluations and were accordingly not used in our analysis. Let us give a brief review of the papers used in the analysis.

1. Cote et al. [18] measured transmission and obtained values for the parameters of two resonances at 2.65 eV and 53.6 eV. For the 2.65 eV resonance, two samples of differing thickness were used so that  $\Gamma_{\gamma}$  could be determined. The  $\Gamma_{\gamma}$  value was taken to be the same for the 53.6 eV resonance as for the first resonance.

2. Pattenden [24] measured transmission by the time-of-flight method below 850 eV (the area method was used up to 320 eV). The best resolution was 15 ns/m. A  $\text{PuO}_2$  sample containing 91%  $^{242}\text{Pu}$  was used in the experiment.
3. Auchampaugh et al. [7] measured the  $^{242}\text{Pu}$  total cross-section  $\sigma_t$  in the 0.75-389 eV region by the time-of-flight method using  $\text{PuO}_2$  samples containing 99.41 and 97.080%  $^{242}\text{Pu}$ .  $\Gamma_n^o$  values were derived by analysing the area and shape of the peaks. The authors also quoted the value  $S_o = (0.95 \pm 0.40) \times 10^{-4}$ .
4. Young et al. [9] analysed  $\sigma_t$  measurements on a  $\text{PuO}_2$  sample containing 99.88%  $^{242}\text{Pu}$  and quote  $\Gamma_n^o$  and  $\Gamma_\gamma$  values up to 150 eV. They also quote  $S_o = (0.99 \pm 0.44) \times 10^{-4}$  and  $\langle D \rangle = 16.5$  eV. The resonance absorption integral proved to be  $1110 \pm 60$  b.
5. Bergen et al. [23] measured  $\sigma_f$  by the explosion technique in the 51-5000 eV region using the time-of-flight method and a sample containing 99.8%  $^{242}\text{Pu}$  placed 214.6 m from the source. The authors quote  $\sigma_o \Gamma_f$  values over the range 53-790 eV.
6. Auchampaugh et al. [21] also measured  $\sigma_f$  by the explosion technique, investigating the 20 eV-10 MeV range with a sample containing 99.91%  $^{242}\text{Pu}$ . The authors quote  $A_f = \frac{\pi}{2} \sigma_o \Gamma_f$  values over the range 370 eV-4 keV.
7. James [25] measured  $\sigma_t$  in the 16 eV-35 keV region using the time-of-flight method. The cross-sections were measured in relation to  $^{235}\text{U}$  on a  $\text{PuO}_2$  sample containing 99.89%  $^{242}\text{Pu}$ . The author gives  $\sigma_o \Gamma_f$  parameters and values for resonances at 767 and 799 eV.
8. Auchampaugh and Bowman [26] measured  $\sigma_t$  by the time-of-flight method in the 600 eV-81 keV region. Parameters in the region up to 4 keV were obtained for resonances with a significant  $\Gamma_f$  value. The authors combined the fission data from Ref. [21] with the transmission data to obtain  $\Gamma_n$  and  $\Gamma_f$  values.
9. Simpson et al. [27] measured transmission over the 15 eV-30 keV range. The measurements were performed on three metal samples of differing thickness at 77 K. The authors quote parameter values in the 20-500 eV region.

10. Poortmans et al. [22] measured the  $\sigma_t$ ,  $\sigma_\gamma$  and  $\sigma_n$  cross-sections in the region up to 1.3 keV. The area technique was used to obtain  $\Gamma_n^o$  values for 71 resonances and  $\Gamma_\gamma$  values for 25 resonances. The experimental resolution varied from 5 to 1.5 ns/m and the baseline from 60 m in the  $\sigma_\gamma$  measurements to 30 m in the  $\sigma_t$  and  $\sigma_n$  measurements. The  $\text{PuO}_2$  sample contained 99.8%  $^{242}\text{Pu}$ . The authors quote the following average resonance parameters:

$$\langle \Gamma_\gamma \rangle = 21.9 \pm 0.4 \text{ (stat.)} \pm 1.0 \text{ (syst.) MeV};$$

$$\langle \Gamma_n^o \rangle = 1.52 \text{ MeV};$$

$$\langle D \rangle = 17.02 \text{ eV};$$

$$S_o = (0.89 \pm 0.10) \times 10^{-4}.$$

11. Hockenbury et al. [28] measured transmission in the resonance region on a metallic sample containing 92.55%  $^{242}\text{Pu}$  and quote  $\Gamma_n$  values for five resonances over the 205-383 eV range.

None of the authors made a simultaneous determination of  $\Gamma_n^o$ ,  $\Gamma_\gamma$  and  $\Gamma_f$ , and only in Refs [22, 27] were both  $\Gamma_n^o$  and  $\Gamma_\gamma$  values derived together. The  $\Gamma_n^o$  or  $\Gamma_n$  values are the most reliable, although for a number of resonances the differences between them exceed the error limits.

$\Gamma_f$  values were obtained by the authors of Refs [23, 26] on the basis of the  $\sigma_0 \Gamma_f$  and  $\frac{\pi}{2} \sigma_0 \Gamma_f$  values and of the  $\Gamma_n$  and  $\Gamma_\gamma$  values used by them. It should also be pointed out that the energy resolution in Ref. [23] was considerably worse than in Ref. [21] which is the source of the  $\frac{\pi}{2} \sigma_0 \Gamma_f$  values used in Ref. [26] to obtain the  $\Gamma_f$  values. Where there were two  $\Gamma_f$  values, we therefore gave preference to the measurements from Ref. [21].

Only the parameters from Poortmans et al. [22] cover almost the entire resonance region in which we are interested. Furthermore, as stated above, these parameters were obtained by a simultaneous analysis of the  $\sigma_t$ ,  $\sigma_\gamma$  and  $\sigma_n$  cross-sections, which makes them particularly reliable. We therefore used these parameters as the basis for our evaluation.

The evaluated resonance energies were taken from Ref. [22]. For those resonances which had been omitted from that paper, we used the energies in Ref. [27] (where they were available) and, failing these, the resonance energies quoted by other authors.

The reduced neutron widths  $\Gamma_n^o$  and their errors were taken from Ref. [22] and where these values were not available, we used the weighted averages and corresponding errors from other papers. The average value  $\langle \Gamma_n^o \rangle$  was  $1.30 \pm 0.20$  MeV. This value is in good agreement with the value  $\langle \Gamma_n^o \rangle = 1.362$  MeV which is obtained by averaging the weighted values for each resonance. Figure 3.1 compares the Porter-Thomas distribution with the  $\Gamma_n^o / \langle \Gamma_n^o \rangle$  distribution histogram for  $\langle \Gamma_n^o \rangle = 1.3$  MeV.

We had available  $\Gamma_\gamma$  values from Refs [9, 22, 27]. These values were obtained by various methods (both by the area method [9, 27] and by shape analysis [22]), so that the calculation of the weighted averages for each resonance may yield incorrect  $\Gamma_\gamma$  values. For the same reasons, it was not possible to normalize the  $\Gamma_\gamma$  values to the selected  $\Gamma_n^o$  values for each resonance.

Bearing in mind that the most accurate  $\Gamma_\gamma$  values came, in our opinion, from Ref. [22] we treat the  $\Gamma_\gamma$  values from that paper as recommended values and, for resonances for which these values were missing, we took the average value  $\langle \Gamma_\gamma \rangle = 22.609$  MeV. The resonance capture integral  $I_\gamma$  in the region 0.5-500 eV proved to be 1115.67 b which is in good agreement with the  $I_\gamma$  values obtained in Refs [8, 15], i.e.  $1090 \pm 60$  b and  $1130 \pm 60$  b, respectively.

It is very difficult to determine the fission widths  $\Gamma_f$  in the resolved resonance region because fission in this region is of the sub-barrier type, i.e. the  $\Gamma_f$  values are very small and therefore depend very much on the  $\Gamma_n^o$  and  $\Gamma_\gamma$  values assumed for each resonance since the  $\Gamma_f$  values are obtained by measuring the areas beneath the fission curve. Moreover, there is a strong dependence on the experiment's energy resolution since poor resolution makes it difficult to select the limits for numerical integration. The  $\Gamma_f$  values were derived from the values  $A_B = \sigma_0 \Gamma_f$  and  $A_A = \frac{\pi}{2} \sigma_0 \Gamma_f$  [21, 23] by means of the formula  $A_B = 4\pi \Gamma^2 \frac{n_f}{\Gamma}$  and  $A_A = 2\pi \Gamma^2 \frac{n_f}{\Gamma}$  in Refs [23, 26]. In Ref. [23]

the  $\Gamma_n^o$  and  $\Gamma_\gamma$  values were taken from Ref. [10] and in Ref. [26] intrinsic  $n$  and  $\Gamma_\gamma$  values were used. The calculations of  $\Gamma_f$  using the  $\Gamma_n^o$  and  $\Gamma_\gamma$  values assumed by us showed that, for resonances where  $A_B$  and  $A_A$  are measured, the  $\Gamma_f$  values derived from  $A_A$  [21] are considerably smaller than the  $\Gamma_f$  values derived from  $A_B$  [23]. This is because the experimental resolution is better in Ref. [21] than in Ref. [23]. Thus, where there were two  $\Gamma_f$  values

obtained on the basis of Refs [21, 23] using our recommended  $\Gamma_n^o$  and  $\Gamma_Y$  values, preference was given to the  $\Gamma_f$  values obtained from Ref. [21]. If the  $\Gamma_f(E)$  dependence is plotted, the  $\Gamma_f$  values clearly form two groups of levels which correspond to the two levels in the second dip of the double-humped fission barrier at 474.6 and 761.7 eV.

If  $\langle D \rangle$  is determined by simple averaging, allowing for all resonances, the result is  $\langle D \rangle = 14.725$  eV. On the other hand, if no levels are omitted due to the resolution, the energy dependence of the increasing number of levels may be expressed as  $\sum N_i = AE_i + B$ . In our case, we then obtain  $\langle D \rangle = 14.233 \pm 0.536$  eV, which is in good agreement with the above  $\langle D \rangle$  value (Fig. 3.2).

Figure 3.3 compares the Wigner distribution with the  $D/\langle D \rangle$  histogram. An estimate of the energy dependence of the increasing number of levels in the range up to 1 keV shows that no S levels are omitted due to the energy resolution, although levels might be uniformly omitted over the entire energy scale owing to incorrect allowance for background. All the recommended values are shown in Table 3.1.

Figure 3.1 shows that there is a certain excess of resonances with low  $\Gamma_n^o$ . Moreover, the histogram depicting the distribution of level spacings is biased towards the low D region compared with the Wigner distribution (see Fig. 3.3). If it is assumed that some narrow S resonances in Table 3.1 are in fact broad p resonances, the histograms agree much better with the theoretical distributions. We are referring to the resonances at 14.6, 106.0, 141.43, 219.0, 271.95, 274.95, 281.0, 327.6, 379.63, 425.15 and 494.75 eV which have anomalously low  $\Gamma_n^o$  values. However, this visual criterion is obviously inadequate and a much stricter check is required. A check of both hypotheses, viz. (1) "levels are S levels" or (2) "possible p levels are considered" using Kolmogorov's criterion [29] and the  $\chi^2$  distribution showed that there are at least no statistical grounds for assuming that p levels are present rather than absent. Both assumptions fall within the 95% confidence range, although hypothesis (2) above gives test values which are closer to the centre than hypothesis (1). Both hypotheses are equally valid. One more test for p resonances was carried out using the method proposed in Ref. [30]. The test is the size of the  $g\Gamma_n(E)$  value:

$$g\Gamma_n(E) = \frac{\langle g\Gamma_n' \rangle \langle g\Gamma_n^o \rangle (2,197222 - \ln \frac{\langle g\Gamma_n' \rangle}{\langle g\Gamma_n^o \rangle}) \cdot (\kappa R)^2 \sqrt{E}}{\langle g\Gamma_n^o \rangle - E \cdot (\kappa R)^2 \langle g\Gamma_n' \rangle}$$

Table 3.1  
Evaluated  $^{242}\text{Pu}$  resonance parameters

Parameter	$E_r$ , eV	$\Gamma_n^o$ , MeV	$\Gamma_n$ , MeV	$\Gamma_\gamma$ , MeV	$\Gamma_f$ , MeV
1	2	3	4	5	6
I	2,66	1,21 ± 0,04	1,97 ± 0,07	25,5 ± 0,8	
2	14,60	0,016 ± 0,003	0,061 ± 0,013	22,609	
3	22,56	0,065 ± 0,006	0,31 ± 0,03	22,609	
4	40,93	0,073 ± 0,007	0,47 ± 0,04	22,609	
5	53,46	7,11 ± 0,40	52 ± 2	21,2 ± 1,7	0,043
6	67,57	0,54 ± 0,02	4,4 ± 0,2	23 ± 3	0,047
7	88,44	0,056 ± 0,01	0,53 ± 0,1	22,609	0,043
8	106,00	0,06 ± 0,03	0,06 ± 0,4	22,609	
9	107,27	1,64 ± 0,1	17,00 ± 1,0	21 ± 2	0,049
10	131,30	0,53 ± 0,02	6,1 ± 0,2	24,5 ± 7,0	0,053
II	141,43	0,010 ± 0,002	0,12 ± 0,02	22,609	
I2	149,6	1,18 ± 0,04	14,50 ± 0,5	21 ± 2	0,049
I3	163,3	0,057 ± 0,005	0,47 ± 0,06	22,609	
I4	204,7	3,30 ± 0,020	52 ± 3	20 ± 2	0,055
I5	209,7	0,031 ± 0,007	0,45 ± 0,10	22,609	
I6	215,2	0,35 ± 0,02	5,2 ± 0,3	22,609	0,125
I7	219,0	0,014 ± 0,007	0,2 ± 0,1	22,609	
I8	232,6	0,33 ± 0,02	5,0 ± 0,3	22,609	0,108
I9	264,3	0,018 ± 0,006	0,3 ± 0,1	22,609	
I0	271,95	0,010 ± 0,002	0,16 ± 0,03	22,609	
21	273,5	1,00 ± 0,03	16,00 ± 0,5	22 ± 2	0,093
22	274,95	0,010 ± 0,002	0,17 ± 0,03	22,609	
23	281,05	0,008 ± 0,003	0,13 ± 0,05	22,609	
24	298,60	0,50 ± 0,02	3,7 ± 0,3	26 ± 7	
25	303,50	1,02 ± 0,05	17,8 ± 0,8	22,5 ± 2,0	0,066
26	319,90	11,2 ± 2,2	200 ± 4	22 ± 3	0,079
27	327,60	0,028 ± 0,017	0,5 ± 0,3		
28	332,40	3,84 ± 0,82	70,0 ± 15,0	25 ± 3	0,109
29	374,20	0,31 ± 0,02	6,0 ± 0,3		0,031
30	379,63	0,014 ± 0,002	0,27 ± 0,04		
31	382,20	2,76 ± 0,26	54 ± 5	22,5 ± 2	0,021
32	396,10	0,13 ± 0,05	2,5 ± 1,0	22,609	
33	399,7	0,10 ± 0,05	2 ± 1	22,609	
34	410,5	0,39 ± 0,02	8,0 ± 0,5	22,609	0,019
35	424,0	0,24 ± 0,02	5,0 ± 0,4	22,609	0,052
36	425,15	0,0134 ± 0,002	0,28 ± 0,04	22,609	
37	474,6	0,018 ± 0,009	0,4 ± 0,2	22,609	0,953
38	482,3	1,07 ± 0,27	23,6 ± 0,6	23,5 ± 2,0	0,304
39	491,75	0,012 ± 0,003	0,267 ± 0,067	22,609	
40	503,9	6,68 ± 2,23	150 ± 50	22,609	0,041
41	536,2	4,32 ± 0,22	100 ± 5	21 ± 2	0,073
42	548,3	3,16 ± 0,13	74 ± 3	25 ± 2	0,095
43	576,1	1,25 ± 0,21	30 ± 5		0,042

Table 3.1 (continued)

Parameter	$E_r$ , eV	$\Gamma_n^o$ , MeV	$\Gamma_n$ , MeV	$\Gamma_\gamma$ , MeV	$\Gamma_f$ , MeV
1	2	3	4	5	6
44	594.7	1.56 $\pm$ 0.16	38.0 $\pm$ 4.0	21 $\pm$ 2	0.036
45	599.5	0.45 $\pm$ 0.04	II $\pm$ I	22,609	0.098
46	610.7	0.57 $\pm$ 0.08	I4 $\pm$ 2	22,609	0.070
47	638.2	0.20 $\pm$ 0.04	5 $\pm$ I	22,609	
48	665.0	0.10 $\pm$ 0.02	2.7 $\pm$ 0.5	22,609	
49	669.2	0.54 $\pm$ 0.08	I4 $\pm$ 2	22,609	0.099
50	692.9	1.71 $\pm$ 0.11	45 $\pm$ 3	22 $\pm$ 2	0.227
51	711.3	4.87 $\pm$ 0.37	I30 $\pm$ 10	I9.5 $\pm$ 2.0	0.060
52	727.4	0.11 $\pm$ 0.07	3 $\pm$ 2	22,609	
53	736.6	3.68 $\pm$ 0.18	I00 $\pm$ 5	22,609	0.596
54	751.8	4.99 $\pm$ 0.18	I37 $\pm$ 5	22,609	1.496
55	761.7	0.12 $\pm$ 0.05	3.3 $\pm$ 1.5	22,609	33.52
56	788.5	1.89 $\pm$ 0.5	53 $\pm$ 14	22,609	1.259
57	793.5	3.02 $\pm$ 1.42	85 $\pm$ 40	22,609	0.074
58	823.8	0.07 $\pm$ 0.03	2 $\pm$ I	22,609	0.444
59	837.5	1.31 $\pm$ 0.07	38 $\pm$ 2	20 $\pm$ 3	0.059
60	856.1	1.26 $\pm$ 0.07	37 $\pm$ 2	22 $\pm$ 3	0.150
61	865.1	0.34 $\pm$ 0.03	I0 $\pm$ I		0.062
62	877.6	2.09 $\pm$ 0.10	62 $\pm$ 3	26 $\pm$ 3	0.049
63	886.2	0.71 $\pm$ 0.0	22 $\pm$ 1.5	29 $\pm$ 10	0.040
64	922.5	2.11 $\pm$ 0.10	64 $\pm$ 3	18 $\pm$ 3	0.046
65	935.4	0.36 $\pm$ 0.07	II $\pm$ 2	22,609	
66	939.6	0.33 $\pm$ 0.10	I0 $\pm$ 3	22,609	
67	949.1	0.45 $\pm$ 0.05	I4 $\pm$ 1.5	26 $\pm$ 6	
68	977.9	0.46 $\pm$ 0.05	I4.5 $\pm$ 1.5	22,609	
69	1004.0	1.36 $\pm$ 0.09	43 $\pm$ 3	22,609	

The  $\langle \Gamma_n^o \rangle$  value was based on the assumption that  $S_1 = 2.5 \times 10^{-4}$ . It was found that all the resonances in Table 3.1 are S resonances.

Thus, there are at least no statistical grounds at present to associate any of the known  $^{242}\text{Pu}$  resonances with p resonances.

The following average values were obtained from the evaluation of the resonance parameters and these will henceforth be used for the calculations in the unresolved resonance region:

$$\langle \Gamma_n^o \rangle = 1.30 \pm 0.20 \text{ MeV}$$

$$\langle \Gamma_\gamma \rangle = 22.61 \pm 0.65 \text{ MeV}$$

$$\langle D \rangle = 14.233 \pm 0.536 \text{ eV}$$

$$S_0 = (0.91 \pm 0.15) \times 10^{-4}$$

#### 4. AVERAGE RESONANCE PARAMETERS AND NEUTRON CROSS-SECTIONS IN THE UNRESOLVED RESONANCE REGION

In this section we shall consider the 1-200 keV region in which we may confine our attention to the contribution from S, p and d waves. The average cross-sections were evaluated on the basis of average parameters which were determined both from the data in the resolved resonance region and from the condition describing the experimental data in terms of average cross-sections. The maximum p method is used to estimate the average  $^{242}\text{Pu}$  resonance parameters; this method is based on the minimization of the square-law functional [31].

$$F(p) = [\sigma_T - \sigma_T(p)]^T V^{-1} [\sigma_T - \sigma_T(p)] + (P_0 - p)^T W_0^{-1} (P_0 - p). \quad (4.1)$$

where  $\sigma_T$  is the vector of experimental cross-sections with a covariance matrix  $V$ ,  $\sigma_T(p)$  is the theoretical cross-section vector and  $P_0$  is the vector of the initial average parameters which are derived from data in the resolved resonance region with a covariance matrix  $W_0$ . This method is, however, restricted by the lack of experimental information on all types of cross-sections.

In the given energy region, several measurements of the total cross-section  $\sigma_t$  have been made [19, 26, 27]. However, the graphical data which we obtained from Young and Reeder's paper [? 9] covering the region up to 8 keV are not sufficient to allow an evaluation to be made and can be used only to check for contradictions. The experimental data from Refs [26, 27] covering the region 0.6-81 keV and up to 30 keV respectively would have been very useful in determining the average resonance parameters for the p wave, but these data were not available.

Among the experimental  $\sigma_f$  data available in the given energy region [21, 23, 25, 32], the results of Auchampaugh et al. [21] are the most interesting as far as the evaluation of the average resonance parameters is concerned. Bergen and Fullwood's measurements [23] are much less accurate ( $\sim 60\%$ ) and their data are considerably higher than the data from Ref. [21] which agree with other  $\sigma_f$  measurements at higher energies (see Fig. 4.1). Moreover, the data from Refs [23, 25, 32] only partially cover the energy region of interest.

The  $\sigma_\gamma$  cross-section was measured by Hockenbury et al. [28] in the 6–70 keV region with 6% accuracy and by Wissak and Kappeler [33] in the 10–90 keV region. The data agree (see Fig. 4.2) but the quality of the measurements is much lower in Ref. [33] than in Ref. [28] since the authors obtained the ratios  $\sigma_\gamma^{(242\text{Pu})}/\sigma_\gamma^{(238\text{U})}$  and  $\sigma_\gamma^{(242\text{Pu})}/\sigma_\gamma^{(197\text{Au})}$ . Owing to the actual indeterminacy of the  $\sigma_\gamma^{(238\text{U})}$  data, the accuracy of the  $\sigma_\gamma^{(242\text{Pu})}$  values derived from them does not exceed 20%. The latest  $\sigma_\gamma^{(197\text{Au})}$  estimates [34, 35] virtually coincide but it is difficult to use the  $\sigma_\gamma^{(197\text{Au})}$  cross-section as a standard in the region below 100 keV in order to achieve accurate cross-section measurements [36]. The difficulties are caused by the resonance structure, and special attention must be paid to the energy spectrum of the neutron beam when comparing the  $\sigma_\gamma$  data. The real accuracy of the  $\sigma_\gamma^{(242\text{Pu})}$  data derived from the ratios  $\sigma_\gamma^{(242\text{Pu})}/\sigma_\gamma^{(197\text{Au})}$  also amounts to ~20%.

#### 4.1. Average level spacing $\langle D \rangle_r$

In order to determine the average spacing  $\langle D \rangle_r$  between levels with given spin  $J$  and parity  $\Pi$ , we used the relation between the Fermi-gas model, which assumes that there are no separate collective-type motions, and the parity dependence:

$$\langle D(U) \rangle_r = \frac{48\sqrt{2} \alpha^{1/4} (U-\delta)^{5/4} \tilde{\zeta}^3}{2J+1} \exp \left[ -2\sqrt{a(U-\delta)} + \frac{(J+0.5)^2}{2\tilde{\zeta}^2} \right],$$
$$\tilde{\zeta}^2 = \frac{g}{\pi^2} \langle m^2 \rangle \sqrt{a(U-\delta)},$$
$$U = S_n + E. \quad (4.2)$$

The  $\delta$  parameter is the correction for even-odd differences in the density of the levels, which is 0.61 MeV for  $^{243}\text{Pu}$  [37]. The mean square of the magnetic quantum numbers  $\langle m^2 \rangle$  is selected either in accordance with a quasi-classical evaluation ( $\langle m^2 \rangle = 0.24 \text{ A}^{2/3}$ ), which we in fact used, or in a form resulting from  $m^2$  averaging over the filled shell model states lying below the Fermi bound ( $\langle m^2 \rangle = 0.146 \text{ A}^{2/3}$ ) [38, 39]. The basic level density parameter  $\alpha$  is determined from the data on neutron resonance density:  $\langle D_{\text{obs}} \rangle = \langle D(S_n - \delta) \rangle_{\frac{1}{2+}}$ . The energy of neutron separation from the  $^{243}\text{Pu}$  nucleus is  $S_n = 5.037 \pm 0.025 \text{ MeV}$  [40];  $\langle D \rangle_{\text{obs}}$  was obtained in Section 3 and is  $14.23 \pm 0.54 \text{ eV}$ . Parameter  $\alpha$  proved to be  $31.81 \pm 0.17 \text{ MeV}^{-1}$ . The error quoted is governed only by the uncertainties in  $\langle D \rangle_{\text{obs}}$  and  $S_n$ .

Since the energy region is close to the normalization point ( $\text{Sn} - \delta$ ),  $\langle D \rangle_r$  does not change noticeably when allowance is made for the contribution from rotational and vibrational modes to the level density [41, 42]. For this reason, and since the shell correction for  $^{243}\text{Pu}$  is slight, there is no need to make allowance for the decrease in shell effects as the excitation energy increases [43].

#### 4.2. Average neutron $\langle \Gamma_n \rangle_r$ and inelastic $\langle \Gamma_{n'} \rangle_r$ widths

The average neutron widths were determined via the strength functions, as follows:

$$\langle \Gamma_n \rangle_r = S_\ell \langle D \rangle_r E^{1/2} P_\ell v_r. \quad (4.3)$$

where  $v_r$  is the number of neutron exit channels for the  $r$  state of the compound nucleus, which is 1 for an even-even target nucleus. The penetration factors  $P_\ell$  are determined by the expressions:

$$\begin{aligned} P_0 &= 1; \\ P_1 &= (\kappa\alpha)^2 / [1 + (\kappa\alpha)^2]; \\ P_2 &= (\kappa\alpha)^4 / [9 + 3(\kappa\alpha)^2 + (\kappa\alpha)^4], \end{aligned} \quad (4.4)$$

where the neutron wave number is  $K = 2.196771 \times 10^{-3} AW \sqrt{E/(1+AW)}$ , the  $^{242}\text{Pu}$  isotopic mass is  $AW = 239.9793$ , and the radius of the scattering channel, taken as the sum of the radii of the nucleus and the neutron is  
 $\alpha = [0.123(AW \times 1.008665)^{1/3} + 0.08] \times 10^{-12} \text{ cm} = 0.84656 \times 10^{-12} \text{ cm.}$

The average inelastic widths  $\langle \Gamma_{n'} \rangle_r$  were determined by a formula analogous to that in expression (4.3):

$$\langle \Gamma_{n'} \rangle_r = \langle D \rangle_r \sum_{q\ell} S_{\ell'} (E - E_q)^{1/2} P_{\ell'} (E - E_q) v_{J\ell'q}, \quad (4.5)$$

where  $\ell'$  is the orbital moment of the scattered neutron,

$E_q$  is the energy of the excited level and

$v_{J\ell'q}$  is the number of inelastic neutron exit channels.

Two levels are excited in the region up to 200 keV:  $E_1 = 44 \text{ keV}$  with spin  $2^+$  and  $E_2 = 146 \text{ keV}$  with spin  $4^+$ .

The basic set of strength functions comprised the following values:  $S_0 = 0.91 \times 10^{-4}$ ;  $S_1 = 2.5 \times 10^{-4}$ ; and  $S_2 = 0.91 \times 10^{-4}$ . The value  $S_0 = (0.91 \pm 0.10) \times 10^{-4}$  was obtained in Section 3. The value  $S_1 = 2.5 \times 10^{-4}$  was obtained by Hockenbury et al. [28] from the description of the  $\langle \sigma_\gamma \rangle$  cross-section. A similar value, i.e.  $S_1 = 2.57 \times 10^{-4}$ , was obtained in Ref. [44] using a generalized optical model. Since the main contribution to the cross-sections in the energy region under consideration comes from S and p waves, the assumption that  $S_2 = S_0$  made by Dresner [45] has only a slight effect on the accuracy of the theoretical cross-sections.

#### 4.3. Average radiation widths $\langle \Gamma_\gamma \rangle_r$

The average radiation widths  $\langle \Gamma_\gamma \rangle_r$  were calculated in the dipole electric transition approximation:

$$\langle \Gamma_f \rangle_r = \langle D \rangle_r \int_0^U f(u, \epsilon) \sum_{j=13-11}^{1M} p(u-\epsilon, j') d\epsilon. \quad (4.6)$$

The spectral factor  $f(u, \epsilon)$ , including the energy and multipolarity dependence of the matrix components of the radiative transitions, was derived from the photo-absorption cross-section for a deformed nucleus as described by the superposition of two Lorentz curves:

$$f(u, \epsilon) \approx \sum_{i=1}^2 \left( \frac{1}{3} \right) \frac{\Gamma_{i\sigma} \epsilon^4}{(\epsilon^2 - E_{i\sigma}^2)^2 + (\Gamma_{i\sigma} \epsilon)^2}. \quad (4.7)$$

Values averaged over heavy nuclei [39] were used as the giant dipole resonance parameters,  $E_{i\sigma}$  and  $\Gamma_{i\sigma}$ , since there are no measurements for  $^{243}\text{Pu}$ :  $E_{1\sigma} = 11$  MeV,  $\Gamma_{1\sigma} = 2.9$  MeV,  $E_{2\sigma} = 14$  MeV and  $\Gamma_{2\sigma} = 4.5$  MeV.

Expression (4.7) was used in preference to the familiar Weisskopf expression  $f(u, \epsilon) \sim \epsilon^3$  because it provides a better description of the fission widths  $\Gamma_{\gamma f}$  after preliminary  $\gamma$ -emission in the case of heavy fissionable nuclei [46].

The theoretical  $\langle \Gamma_\gamma \rangle_r$  widths were normalized to the value obtained in Section 3, i.e.  $\langle \Gamma_\gamma \rangle_{\text{obs}} = \langle \Gamma_\gamma \rangle_{\frac{1}{24}} = 22.6$  MeV, which together with the condition  $E \ll U$  can be used to describe the level density of a compound nucleus within the framework of the Fermi-gas model.

#### 4.4. Average fission widths $\langle \Gamma_f \rangle_r$

The structure observed in the  $^{242}\text{Pu}$  sub-threshold fission cross-section [21, 23, 25, 47] is explained by the double-humped fission barrier predicted by Strutinsky [48]. The existence of quasi-steady states in the second dip which are related to the first-dip states is in fact responsible for the observed grouping of levels with anomalously large fission widths.

The average fission width  $\langle \Gamma_f \rangle_r$  can be expressed as the sum of the widths for separate channels:

$$\langle \Gamma_f \rangle_r = \sum_{k=1}^4 \langle \Gamma_f \rangle_{rk} = \frac{\langle D \rangle_r}{2\pi} \sum_{k=1}^4 P_{frk}, \quad (4.8)$$

where  $P_{frk}$  is the penetrability of the k-th fission barrier which, for a single-humped parabolic barrier, can be determined by the Hill-Wheeler expression [49]:

$$P_{frk} = \left\{ 1 + \exp \left[ \frac{2T}{\hbar \omega_{rk}} (\epsilon_{frk} - E) \right] \right\}^{-1}. \quad (4.9)$$

Various methods of calculating the penetration of a double-humped fission barrier have been investigated [50-53]. The authors of Ref. [51] used a quasi-classical approximation to obtain the penetration of a barrier with humps of arbitrary shape in a deep sub-barrier region. The penetration factor is energy-dependent like a resonance and varies from  $P_{\max} = 4P_A P_B / (P_A + P_B)^2$  to  $P_{\min} = P_A P_B / 4$ , where  $P_A$  and  $P_B$  are the penetrations of humps A and B. As a result of averaging over the range between the levels, the penetration  $\bar{P}$  satisfies the relation

$$\bar{P} = \sqrt{P_{\max} P_{\min}}. \quad (4.10)$$

Reference [54] compares a precise numerical calculation of a barrier penetration approximated by three parabolas with the results from a quasi-classical approximation. The comparison shows that the quasi-classical results are considerably higher in the vicinity of the lower hump's peak. However, the fission barrier parameters used in this paper are such that in the given energy region  $P_A$  and  $P_B$  are much less than unity.

For a barrier approximated by two inverted humps, the authors of Ref. [52] obtained an analytical expression which also holds in the near-barrier region, unlike the corresponding expression in Ref. [51]. The maximum and minimum penetration values in Ref. [52] are determined as follows:

$$P_{\max} = \frac{P_A P_B}{1 + \sqrt{(1-P_A)(1-P_B)}}. \quad (4.11)$$

The penetration of humps A and B is much less than unity, and  $P_{\max}$ ,  $P_{\min}$  and  $\bar{P}$  satisfy expression (4.10). This approach was also used in the present paper to calculate the  $\langle \Gamma_f \rangle_r$  widths. It was assumed that the number of channels was 1 for the  $\frac{1}{2}^+$  state and obeyed the  $(2J + 1)$  law for p and d states, and the penetrations  $P_A$  and  $P_B$  were calculated using formula (4.9). The successful application of this algorithm to  $^{240}\text{Pu}$  [55] gives grounds for hoping that it can also satisfactorily describe the experimental  $\langle \sigma_f \rangle$  data for  $^{242}\text{Pu}$ .

Owing to a shortage of experimental data, no distinction can be drawn between the  $E_A^K$ ,  $E_B^K$ ,  $\hbar\omega_A^K$  and  $\hbar\omega_B^K$  fission barrier curves for the r state. We therefore did not allow for splitting of both the inner and outer humps and assumed their parameters to be the same for all states. The parameters  $E_A = 6.04$ ,  $E_B = 5.44$ ,  $\hbar\omega_A = 0.8$  and  $\hbar\omega_B = 0.52$  MeV, obtained by the author of Ref. [39] from a description of  $\langle \sigma_f \rangle$  in the higher energy region, do not match the experimental data of Ref. [21] in the unresolved resonance region (see Fig. 4.1). By slightly modifying the height of the humps so that  $E_A = 5.94$  MeV and  $E_B = 5.64$  MeV, we obtained a thoroughly satisfactory description of  $\langle \sigma_f \rangle$  (see Fig. 4.1). Furthermore, the parameters make a better fit with the conditions assigned to  $E_A$ ,  $E_B$ ,  $\hbar\omega_A$  and  $\hbar\omega_B$  in Ref. [21] where the  $^{242}\text{Pu}$  resonance parameters were analysed in the sub-threshold energy region.

This approach assumes that the states in the second dip are purely vibrational. However, several experimental results show that allowance must be made for the possible dissipation of vibrational states in the second dip into intermediate states of the compound nucleus [56, 57]. The dissipation of the oscillations associated with fission, which is simulated by introducing an imaginary part into the potential and thus producing an absorbed flux R, broadens and shortens the resonances. Using an approximation of the equidistant spectrum of intermediate states, the authors of Ref. [58] obtained the following expression for  $\bar{P}$ :

$$\bar{P} - P_d \cdot \sqrt{(P_{\max} - P_d)(P_{\min} - P_d)} = R \frac{P_d}{P_A + P_B}, \quad (4.12)$$

where

$$\begin{aligned} P_{\max} &= P_d + \frac{R P_d}{4 \gamma \hbar \omega}; \\ P_{\min} &= P_d + \frac{R P_d}{4 \gamma \hbar \omega}; \\ \gamma &= \frac{P_A + P_B}{4}; \end{aligned} \quad (4.13)$$

P<sub>d</sub> is the penetration corresponding to direct fission. Expression (4.12) is analogous to (4.10) except that its physics implications are different since it refers only to the absorbed part of the flux.

Reference [21] noted a sharp increase in the average fission width in the 10-100 keV region. One possible explanation is the weak decay of the vibrational level, thus providing further justification for using this method to calculate  $\langle \Gamma_f \rangle_r$ .

#### 4.5. Partial-width distribution laws

In order to calculate the average cross-sections of reactions running through a compound nucleus, the laws governing the distribution of partial widths must be known. The expression for the average cross-section  $\langle \sigma_{nx} \rangle$  takes the form [59, 60]

$$\langle \sigma_{nx} \rangle = \frac{B}{E} \sum_r \frac{\Gamma_r}{\langle \Gamma_r \rangle_r} \cdot \left\langle \frac{\Gamma_{nr} \Gamma_{xr}}{\Gamma_r} \right\rangle, \quad (4.14)$$

where  $B = 4.124506 \times 10^6$  b.eV for  $^{242}\text{Pu}$ . Shaker and Luk'janov have proposed a general distribution covering several channels which make different  $\alpha_k$  contributions to the average width [61]. Where the channel contributions are equal ( $\alpha_k = 1/v$ ,  $k = 1, 2, \dots, v$ ), this distribution is reduced to the well-known Porter-Thomas distribution with  $v$  degrees of freedom. This distribution can be used to describe fluctuations in the neutron, radiation and inelastic widths for the following reasons. The contribution to the neutron widths  $\langle \Gamma_n \rangle_r$  for an even-even nucleus always yields one channel. The number of radiation channels for excitation energies of the order of the neutron binding energy is large, and there are sufficient grounds for assuming that  $v_r = \infty$ . When the  $\langle \Gamma_{n'} \rangle_r$  widths are determined - see expression (4.5) - no distinction is drawn between states with different neutron spin projections, and so for S- and p-wave states the number of degrees of freedom can be associated with the number of exit channels. The widths  $\langle \Gamma_{n'} \rangle_{3/2^+}$  and  $\langle \Gamma_{n'} \rangle_{5/2^+}$  include contributions from scattering widths with two excited levels. However, the contribution from the  $4^+$  level is much smaller and therefore  $v$ , expressed as

$$v_{\text{eff}} = \frac{\left( \sum_q \langle \Gamma_{n'q} \rangle_r \right)^2}{\sum_q \left( \langle \Gamma_{n'q} \rangle_r \right)^2}, \quad (4.15)$$

is close to unity.

The distribution of fission widths  $\Gamma_{fr}$  is a different matter. As a result of the double-humped fission barrier, the fission-width distribution differs from the Porter-Thomas distribution. The latter generally applies only to  $\gamma_{fr}^2$  widths, which are related to the fission widths as follows:

$$\Gamma_{fr}(E) = 2\gamma_{fr}^2 P_{fr}(E), \quad (4.16)$$

where  $P_{fr}(E)$  represents the barrier penetration for fission from state  $r$ , which varies non-monotonically in this case. The authors of Ref. [51] have proposed the following method, also used in this paper, for taking the fluctuations in the fission widths into account. The law governing the distribution of the penetration  $p$ , which is derived from the energy dependence of the penetrability in a quasi-classical approximation, is as follows:

$$W(p) = \left[ \frac{2}{\pi} p \sqrt{(P_{max}-p)(p-P_{min})} \right]^{-1} \quad (4.17)$$

and it may also be used to express fluctuations of the local average widths  $\tilde{\Gamma}_{fr}$ . However, local fluctuations are described by the Porter-Thomas distribution  $P_V(\Gamma_{fr}/\tilde{\Gamma}_{fr})$ . Then the distribution of the quantity  $\kappa = \Gamma_{fr}/\langle \Gamma_{fr} \rangle_r = \frac{\Gamma_{fr}}{\tilde{\Gamma}_{fr}} \cdot \frac{\tilde{\Gamma}_{fr}}{\langle \Gamma_{fr} \rangle_r} = \frac{\Gamma_{fr}}{\langle \Gamma_{fr} \rangle_r} \cdot \frac{1}{\kappa}$  may be defined as:

$$\omega(z) = \int_0^\infty p_\kappa(y) W(z/y) \frac{dy}{y}. \quad (4.18)$$

The authors of Ref. [58] have proposed a somewhat different method for describing fluctuations in the fission widths. The distribution in expression (4.17) links the average width fluctuations with the fluctuations in the direct fission penetration (see Section 4.4), the period of which amounts to a few hundred keV. At the same time the characteristic structure period in the fission cross-section amounts to a few hundred eV ( $\sim 600$  eV for  $^{242}\text{Pu}$  [21]). By expressing the fission penetration as [58, 62]

$$P_f = P_d + P_d', \quad (4.19)$$

where  $P_a$  is the penetrability for nuclear fission via intermediate states in the second dip, we can obtain substantial variations in  $P_f$  over an interval of  $\approx 1 \text{ keV}$ , which is equal to the level spacing in the second dip. The  $\omega(p)$  distribution obtained in Ref. [58] takes the form

$$\omega(p) = (\bar{p} - p_d) [\pi(p - p_d) \sqrt{(p_{\max} - p)(p - p_{\min})}]^{-1}, \quad (4.20)$$

where  $p_{\max}$  and  $p_{\min}$  are determined by expression (4.11).

In this paper we adopted a simpler approach requiring a knowledge of fewer parameters, and we used formulae (4.17) and (4.18). Table 4.1 shows the numbers of degrees of freedom for the Porter-Thomas distributions of the widths of all processes and states. The number of degrees of freedom  $v_{fr}$ , determined by the number of open fission channels, is related to the Porter-Thomas distribution  $Pv(\Gamma_{fr}/\tilde{\Gamma}_{fr})$  describing local fluctuations in  $\Gamma_{fr}$  with respect to the mean values.

Table 4.1

Number of degrees of freedom  $v_{fr}$  in the Porter-Thomas distributions for  $^{242}\text{Pu}$  partial widths

$\Gamma$	$\lambda_{nr}$	$\lambda_{n'r}$	$\lambda_{fr}$	$v_{fr}$
$1/2^+$	I	2	I	
$1/2^-$	I	I	2	
$3/2^-$	I	2	4	$\infty$
$3/2^+$	I	I	4	
$5/2^+$	I	I	6	

#### 4.6. Analysis of average $^{242}\text{Pu}$ resonance parameters

The quality of the average parameters is judged by the extent to which they fit the data obtained in the resolved resonance region and by the description of the average cross-sections. In this section we shall use virtually all the information from the resolved resonance region:  $\langle D \rangle_{\text{obsv}}$ ,  $\langle \Gamma_Y \rangle_{\text{obsv}}$ ,  $S_0$  and  $\sigma_p$ , which is the potential scattering cross-section. Let us examine the comparison with the experimental data on average cross-sections.

The total cross-section  $\langle \sigma_t \rangle$  was calculated using the formula

$$\langle \sigma_t \rangle = \frac{4\pi}{k^2} \sum_l (2l+1) S_l \sin^2 \varphi_l + \frac{2\pi^2}{k^2} \sum_l (2l+1) \sqrt{S_l} \sigma_p - \frac{4\pi^2}{k^2} \sum_l (2l+1) \sqrt{S_l} \sigma_p \sin^2 \varphi_l, \quad (4.21)$$

where the first term represents the potential scattering cross-section, the second the compound nucleus production cross-section and the third takes into account interference from potential and resonance scattering. The phase shifts  $\varphi_l$  were determined as:

$$\begin{aligned} \varphi_0 &= kR; \\ \varphi_1 &= kR - \arctg(kR); \\ \varphi_2 &= kR - \arctg \left[ \frac{3kR}{3 - (kR)^2} \right], \end{aligned} \quad (4.22)$$

where the scattering radius  $R$  is derived from the condition that in the low energy region  $\sigma_p = 4\pi R^2$ . The evaluated  $\sigma_p$  is 10.5 b.

Figure 4.3 shows a comparison of the theoretical and experimental data on  $\langle \sigma_t \rangle$ . Unfortunately, the data available from Young and Reeder [?9] can be used only to confirm that there is no contradiction with the  $\sigma_p$  and  $S_0$  values used by us.

The  $\langle \sigma_Y \rangle$  cross-section was calculated from formula (4.14) without allowing for fission competition since the fission widths in this region are narrow ( $\sigma_f \sim 10$  mb), and considerable amounts of machine time are required in order to achieve the desired accuracy using the real fission width distribution. As stated above, it was assumed that the  $S_1$  value, initially set at  $2.5 \times 10^{-4}$ , would be calculated more accurately later on the basis of the experimental data on  $\langle \sigma_Y \rangle$ . However, the comparison in Fig. 4.2 shows this not to be necessary. The systematics of the strength functions  $S_1$  for heavy nuclei lead us to the conclusion that, for  $^{242}\text{Pu}$ ,  $S_1$  is known with 25% accuracy. We should point out that the p-wave contribution to the  $\langle \sigma_Y \rangle$  cross-section at 7 keV and the d-wave contribution at 175 keV are comparable to the S-wave contribution.

$\langle \sigma n' \rangle$  was calculated in the same way as  $\langle \sigma \gamma \rangle$ . Figure 4.4 shows that the S-wave contribution is minimal since only the d-wave contributes to the exit channel.

The fission cross-section  $\langle \sigma_f \rangle$  was calculated from formula (4.14) by the Monte Carlo method, owing to the complexity of the law governing the fission-width distribution. The number of histories was selected so that the error in  $\langle \sigma_f \rangle$  due to the finiteness of the selection did not exceed 20%. A considerable amount of machine time would be required in order to improve the accuracy of the calculations, and the experimental data below 100 keV are no more accurate. The comparison in Figure 4.1 with the results from experiments shows that the agreement is entirely satisfactory.

The average resonance parameters thus maintain the fit with the experimental cross-sections, and the results of the calculations based on these parameters can therefore be used as evaluated data.

Table 4.2 shows the estimated  $^{242}\text{Pu}$  cross-sections in the 1-200 keV region ( $\langle \sigma_n \rangle$  and  $\langle \sigma_{n'} \rangle$ , allowing for direct processes). Table 4.3 shows the partial cross-sections  $\langle \sigma_f \rangle_r$  which are difficult to calculate.

Table 4.2  
Evaluated data on average  $^{242}\text{Pu}$  cross-sections  
in the 1-200 keV region

E, keV	$\langle \sigma_n \rangle, \delta$	$\langle \sigma_\gamma \rangle, \delta$	$\langle \sigma_{n'} \rangle, \delta$	$\langle \sigma_f \rangle, \delta$	$\langle \sigma_t \rangle, \delta$
I	12,470	3,201	0	0,018	22,689
1,5	18,116	2,447	0	0,015	20,578
2	17,268	2,054	0	0,013	19,335
2,5	16,668	1,817	0	0,012	18,497
3	16,223	1,650	0	0,011	17,884
4	15,588	1,440	0	0,010	17,038
5	15,155	1,309	0	0,009	16,473
6	14,838	1,217	0	0,009	16,064
7	14,596	1,146	0	0,009	15,751
8	14,406	1,089	0	0,008	15,503
9	14,252	1,042	0	0,008	15,302
10	14,125	1,000	0	0,008	15,133
15	13,717	0,857	0	0,008	14,582
20	13,501	0,758	0	0,007	14,269
25	13,366	0,686	0	0,007	14,059
30	13,268	0,629	0	0,007	13,904
40	13,123	0,549	0	0,007	13,679
50	12,957	0,463	0,081	0,008	13,509
60	12,742	0,387	0,230	0,008	13,367
70	12,543	0,335	0,351	0,009	13,238
80	12,359	0,300	0,449	0,009	13,117
90	12,188	0,274	0,530	0,010	13,002
100	12,025	0,255	0,598	0,010	12,888
110	11,718	0,266	0,709	0,012	12,665
140	11,413	0,210	0,805	0,014	12,442
160	11,129	0,198	0,873	0,017	12,217
180	10,845	0,190	0,932	0,020	11,987
200	10,561	0,186	0,981	0,023	11,751

Table 4.3

Partial fission cross-sections for  $^{242}\text{Pu}$   
in the 1-200 keV region

E, keV	<G+>r, mb				
	1/2 +	1/2 -	3/2 -	3/2 +	5/2 +
1	16,2	0,6	1,2	0,0	0,0
1,5	12,8	0,7	1,5	0,0	0,0
2	10,5	0,8	1,7	0,0	0,0
2,5	9,2	0,9	1,9	0,0	0,0
3	8,0	0,9	2,1	0,0	0,0
4	6,7	1,0	2,3	0,0	0,0
5	5,7	1,1	2,5	0,0	0,0
6	5,0	1,2	2,6	0,0	0,0
7	4,5	1,2	2,8	0,0	0,0
8	4,1	1,3	2,8	0,0	0,0
9	3,8	1,3	2,9	0,0	0,0
10	3,6	1,4	2,9	0,0	0,0
15	3,0	1,4	3,2	0,0	0,0
20	2,7	1,4	3,3	0,0	0,0
25	2,5	1,4	3,4	0,0	0,0
30	2,3	1,5	3,4	0,0	0,0
40	2,1	1,5	3,7	0,0	0,0
50	1,9	1,6	4,1	0,0	0,1
60	1,8	1,8	4,4	0,1	0,1
70	1,7	2,0	4,8	0,1	0,1
80	1,6	2,1	5,0	0,1	0,2
90	1,6	2,2	5,4	0,2	0,2
100	1,6	2,4	5,9	0,2	0,3
120	1,8	2,8	6,7	0,3	0,4
140	2,0	3,2	7,8	0,4	0,6
160	2,3	3,8	9,0	0,6	0,9
180	2,7	4,3	11,2	0,7	1,1
200	3,3	5,2	12,2	0,9	1,4

It is interesting to compare our evaluation with the data of Caner and Yiftah [14] and Lagrange and Jary [63]. It should be remembered that the latter results were obtained by generalized optical and statistical modelling. The main parameters are compared in Table 4.4.

Table 4.4

Comparison of average  $^{242}\text{Pu}$  parameters in the unresolved resonance region with the data from Refs [14, 63]

Paper	$\langle D \rangle_{\text{obsv}}$ eV	$\langle \Gamma \rangle_{\text{obsv}}$ MeV	$S_0 \cdot 10^{-4}$	$S_1 \cdot 10^{-4}$	$\Theta_p, \delta$
Caner, Yiftah [14]	$13.7 \pm 1.2$	$28 \pm 1$	$1.17 \pm 0.23$	$\begin{cases} J=1/2 \\ J=3/2 \end{cases}$	$\begin{cases} 0.520 \\ 0.675 \end{cases}$
Lagrange, Jary [63]	16.5	27	1.00	2.63	
Present paper	$14.23 \pm 0.54$	$22.6 \pm 0.7$	$0.91 \pm 0.15$	2.5	10.5

There are obviously very considerable differences between the parameters.

Figure 4.3 shows that the shape of the  $\langle \sigma_t \rangle$  cross-section in Ref. [14] differs from the data in Ref. [63] and in the present paper, although these two sources are in good agreement with one another. Moreover, the data in Ref. [14] on  $\langle \sigma_\gamma \rangle$  (Fig. 4.2) do not agree with the experimental results in Refs [28] and [35], whereas the data from Lagrange and Jary and the present paper are in good agreement with those results and virtually coincide. The differences (Fig. 4.1) are due to the different approaches and parameters used in the calculations.

#### 4.7. Analysis of errors in the evaluated average cross-sections in the 1-200 keV region

In order to determine the accuracy of the evaluated average cross-sections, all sources of error must be analysed: uncertainties associated with the model approximation, experimental errors and the extent to which the estimates fit the experimental results, and uncertainties due to errors in the parameter calculations.

The model used to calculate  $\langle \sigma_n \rangle$ ,  $\langle \sigma_{n^*} \rangle$ ,  $\langle \sigma_\gamma \rangle$  and  $\langle \sigma_t \rangle$  cannot give rise to substantial errors by virtue of the condition  $E \ll S_n$ , standardization in terms of  $\langle D \rangle_{\text{obsv}}$  and  $\langle \Gamma_\gamma \rangle_{\text{obsv}}$ , the low value of the  $\langle \sigma_f \rangle$  cross-section and also owing to the fact that the narrow-resonance approximation and the accepted partial-width distribution laws are valid in this energy region.

The uncertainty in  $\langle \sigma_f \rangle$  must be assessed on the basis of the experimental errors, which are rather high according to the data in Ref. [21]. Furthermore, there may be a significant intermediate structure in  $\langle \sigma_f \rangle$  caused by the double-humped fission barrier. An analysis of all the experimental data shows that the real error in the evaluated  $\langle \sigma_f \rangle$  data will amount to 50% at 1-10 keV and then decrease to 7% in the 100-200 keV region.

In order to analyse the uncertainties due to errors in the parameters, let us assume that the average distances  $\langle I \rangle_r$  and widths  $\langle \Gamma_\gamma \rangle_r$  are known with the same accuracy as  $\langle D \rangle_{\text{obsv}}$  and  $\langle \Gamma_\gamma \rangle_{\text{obsv}}$ . This is possible since all level density models give virtually the same results and the  $\langle \Gamma_\gamma \rangle_r$  values are virtually equal to the  $\langle \Gamma_\gamma \rangle_{\text{obsv}}$  values.

We should point out the high accuracy of  $\sigma_p$  (2.8%),  $\langle \Gamma_\gamma \rangle_{\text{obsv}}$  (3.1%) and  $\langle D \rangle_{\text{obsv}}$  (3.8%).  $S_0$  is determined with 16% accuracy and  $S_1$  with 25% accuracy.

An analysis of partial contributions to  $\langle \sigma_t \rangle$  shows that the error may be estimated adequately by taking into account the error in the S-wave contribution to the potential scattering cross-section and the S- and p-wave contributions to the compound nucleus production cross-section, which are caused by the uncertainties in  $\sigma_p$ ,  $S_0$  and  $S_1$ . The relative partial and total errors in  $\langle \sigma_t \rangle$  are shown in Table 4.5.

Table 4.5

Relative partial and total errors in the theoretical cross-section  $\langle \sigma_t \rangle$

E, keV	Source of error				$\Delta \langle \sigma_t \rangle / \langle \sigma_t \rangle$
	$\Delta \sigma_p$	I	$\Delta S_0$	I	
1	0,013		0,087		0,088
5	0,018		0,053		0,057
10	0,019		0,041		0,048
20	0,020		0,030		0,044
40	0,020		0,023		0,046
100	0,020		0,015		0,055
200	0,019		0,012		0,064

The total error in the theoretical cross-section  $\langle \sigma_t \rangle$  amounts to 5-9%. The real error may be somewhat larger owing to unforeseen contributions and to the possible  $\delta$  dependence of the radius  $R$ . The total error in  $\langle \sigma_t \rangle$  was therefore increased by 1%.

In considering the uncertainty in the theoretical cross-section  $\langle \sigma_\gamma \rangle$ , let us confine our attention to the 1-40 keV region where only S- and p-wave contributions need be taken into account and there is no competition from inelastic scattering. Let us also ignore competition from fission channels and the effect of fluctuations in the neutron widths, which do not exceed 30%. Let us also assume  $\langle D(u) \rangle_p = \langle D(Sn) \rangle_p$  and  $\langle \Gamma_\gamma \rangle_p = \text{const}$ . Then expression (4.14) can be written for  $\langle \sigma_\gamma \rangle$  as

$$\langle \sigma_\gamma \rangle = \frac{\beta}{E} \langle r_\gamma \rangle \sum_r \frac{\theta_r}{\langle D \rangle_r} \frac{\langle \Gamma_n \rangle_r}{\langle \Gamma_n \rangle_r + \langle r_\gamma \rangle}, \quad (4.23)$$

which is convenient for analysis. Uncertainties in  $\langle \Gamma_\gamma \rangle$ ,  $\langle D \rangle_r$  and  $\langle \Gamma_n \rangle_r$  are the sources of error in the  $\langle \sigma_\gamma \rangle$  value. The relative partial and total errors in  $\langle \sigma_\gamma \rangle$  are shown in Table 4.6.

Table 4.6

Relative partial and total errors in  $\langle \sigma_\gamma \rangle$

E, keV	Source of error			$\frac{\Delta \langle \sigma_\gamma \rangle}{\langle \sigma_\gamma \rangle}$
	$\Delta \langle \Gamma_\gamma \rangle$	$\Delta \langle D \rangle_r$	$\Delta \langle \Gamma_n \rangle_r$	
1	0,018	0,034	0,053	0,065
5	0,014	0,025	0,042	0,051
10	0,012	0,023	0,072	0,077
20	0,011	0,024	0,063	0,068
40	0,014	0,024	0,042	0,050

The minimum contribution to  $\langle \sigma_\gamma \rangle$  errors comes from the uncertainty in the  $\langle \Gamma_\gamma \rangle$  value, and the maximum contribution from the uncertainty in  $\langle \Gamma_n \rangle_r$  which is governed in turn by the uncertainty in  $S_\ell$  and  $\langle D \rangle_r$ . The error in the theoretical cross-section  $\langle \sigma_\gamma \rangle$  due to the inaccuracy of

the basic parameters amounts to 5-8%. The 8% value must of course also be assigned to the error throughout the 1-200 keV region because, although the error decreases as the energy increases, there is a growing influence from a number of factors which we have not taken into consideration. In order to make a final estimate of the error in the  $\langle \sigma_{\gamma} \rangle$  values we have obtained, the fit with the experimental data must also be considered (Fig. 4.2). The theoretical curve and experimental data from Hockenbury et al. [28] are in agreement within the error limits quoted by them. However, it can be seen that the error in the region below 40 keV must be increased to 10%.

Let us now evaluate the error in the theoretical cross-section  $\langle \sigma_n \rangle$  which may be written as follows in the 1-40 keV region:

$$\langle \sigma_n \rangle = \langle \sigma_p \rangle_0 + \langle \sigma_{comp} \rangle_0 + \langle \sigma_{comp} \rangle_1 - \langle \sigma_p \rangle_1 - \langle \sigma_r \rangle_1. \quad (4.24)$$

Table 4.7 shows the uncertainties in  $\langle \sigma_n \rangle$  calculated from the data from Table 4.6. The same table shows the uncertainty in  $\langle \sigma_n \rangle$  calculated on the assumption that the error in  $\langle \sigma_{\gamma} \rangle$  is 8% and the  $\sigma_p$  error is doubled ( $\Delta \langle \sigma_n \rangle / \langle \sigma_n \rangle$ ).

Table 4.7

Theoretical uncertainties in the  $\langle \sigma_n \rangle$  cross-section

E, keV	Source of error				$\Delta \langle \sigma_n \rangle$	$\Delta \langle \sigma_n \rangle$
	$\Delta \langle \sigma_p \rangle_0$	$\Delta \langle \sigma_{comp} \rangle_0$	$\Delta \langle \sigma_{comp} \rangle_1$	$\Delta \langle \sigma_r \rangle$	$\langle \sigma_n \rangle$	$\langle \sigma_n \rangle$
1	0,015	0,101	0,004	0,009	0,103	0,106
5	0,019	0,059	0,012	0,004	0,063	0,072
10	0,021	0,044	0,018	0,005	0,052	0,064
20	0,021	0,033	0,026	0,004	0,047	0,060
40	0,021	0,024	0,036	0,002	0,049	0,060

The following uncertainties in the  $\langle \sigma_n \rangle$  cross-section estimates can thus be derived from Table 4.7: 8% at 1 keV and 6% at 5-20 keV, rising linearly to 8.5% at 200 keV.

The errors in the theoretical cross-section  $\langle \sigma n^* \rangle$  were obtained by analysing its sensitivity to the parameters of the p-wave, which is the main contributor. The  $S_1$  uncertainty is the main source of error in this case. The  $\langle \sigma n^* \rangle$  error decreases with energy and was estimated to be 20% at 50 keV, 13% at 100 keV and 9% at 200 keV.

Table 4.8 shows the final accuracy of the evaluated data on average  $^{242}\text{Pu}$  cross-sections in the 1-200 keV region.

Table 4.8

Errors in the evaluated data on average  $^{242}\text{Pu}$  cross-sections in the 1-200 keV region

E, keV	$\frac{\Delta \langle \sigma_s \rangle}{\langle \sigma_s \rangle}, \%$	$\frac{\Delta \langle \sigma_x \rangle}{\langle \sigma_x \rangle}, \%$	$\frac{\Delta \langle \sigma_n \rangle}{\langle \sigma_n \rangle}, \%$	$\frac{\Delta \langle \sigma_{n'} \rangle}{\langle \sigma_{n'} \rangle}, \%$	$\frac{\Delta \langle \sigma_d \rangle}{\langle \sigma_d \rangle}, \%$
I	2	3	4	5	6
I	50	10	II	-	10
5	50	10	7	-	7
10	50	10	6	-	6
20	30	10	6	-	5
40	20	10	6	-	6
100	7	8	7	13	7
200	7	8	8,5	9	7

REFERENCES

1. Bulyanitsa, L.S., Gejdel'man, A.M., Egorov, Yu.S., Krizhanskij, L.M., Lipovskij, A.A., Preobrazhenskaya, L.D., Lovtseyus, A.V., Khol'nov, Yu.V., Period poluraspada  $^{242}\text{Pu}$  (Half-life of  $^{242}\text{Pu}$ ), Izvestiya AN SSSR, Ser. Fizich., 40 (1976) 2075.
2. Studier M.H., Maeder D., Wapstra A.M. A New Isomer in Lead. Phys.Rev., 93, 1954, 1433.
3. Butler J.P., Lounsbury M., Merritt J.S. The Neutron Capture Cross Sections of  $^{238}\text{Pu}$ ,  $^{242}\text{Pu}$  and  $^{243}\text{Am}$  in the Thermal and Epicadmium Regions. Can. J. Phys., 35, 1957, 147.
4. Durham R.W., Molsen F. Capture Cross Section of  $^{242}\text{Pu}$ . Can. J. Phys., 48, 1970, 715.
5. Halperin J., Oliver J.H. ORNL-3679, 1964, 13.
6. Folger R.L., Smith J.A., Brown L.C., Overman R.F., Holcomb H.P. Fol 1 Measurements of Integral Cross Sections of Higher Mass Actinides, Proc. Conf. on Neutron Cross Sections and Technology, Washington, 2, 1960, 1279.
7. Auchampaugh G.F., Bowman C.D., Coops M.S., Fultz S.C. Neutron Total Cross Section of  $^{242}\text{Pu}$ . Phys. Rev., 146, 1966, 840.
8. Young T.E., Roeder S.D., IN-1132, 1968.
9. Young T.E., Roeder S.D. Total Neutron Cross Section of  $^{242}\text{Pu}$ . Nucl. Sci. Eng., 40, 1970, 389.
10. Dunford O.L., Alter H. Neutron Cross Sections for  $^{238}\text{Pu}$ ,  $^{242}\text{Pu}$  and  $^{244}\text{Cm}$ . NAA-SR-12271, 1967.
11. Young T.E., Simpson F.B., Tate R.E. The Low-Energy Total Neutron Cross Section of Plutonium-242. Nucl. Sci. Eng., 43, 1971, 341.
12. Lander G.H., Mudler M.H. Coherent Scattering Amplitude of  $^{240}\text{Pu}$  and  $^{242}\text{Pu}$ . Acta Crystallogr., B 27, 1971, 2284.
13. Ice C.H. Production of Transplutonium Elements at Savannah River, DP-MS-66-69, 1966.
14. Caner M., Jiftah S. Nuclear Data for Plutonium-242, IA 1275, 1975.
15. Mughabghab S.F., Garber D.I. Neutron Cross Sections, Resonance Parameters, BNL-325, 3d ed., 1973.
16. Benjamin R.W., Vandavelde V.D., Correll T.C., McCrosson F.J. A Consistent Set of Transplutonium Multigroup Cross Sections. Proc. Conf. on Neutron Cross Sections and Technology, Washington, 1, 1975, 224.

17. Egelstaff F.A., Gayther D.B., Nicholson K.P. J. Nucl. Eng., 6, 1958, 303.
18. Cote R.E., Bollinger L.M., Burnes R.F., Diamond H. Slow-Neutron Cross Sections of  $^{240}\text{Pu}$ ,  $^{242}\text{Pu}$  and  $^{243}\text{Pu}$ . Phys. Rev., 114, 1959, 505.
19. Leonard B.R., Odecaarden R.H. Bull. Am. Phys. Soc., 6, 1961, 6.
20. Young T.E., Grimsoy R.A. ANCR -1016, 1971.
21. Auchampaugh G.F., Farrell J.A., Bergen D.W. Neutron-Induced Fission Cross Sections of  $^{242}\text{Pu}$  and  $^{244}\text{Pu}$ . Nucl. Phys., A 171, 1971, 31.
22. Poortmans F., Vanpraet G.J. Neutron Resonance Parameters of  $^{242}\text{Pu}$ . Nucl. Phys., A 207, 1973, 342.
23. Bergen D.W., Fullwood R.R. Neutron-Induced Fission Cross Section of  $^{242}\text{Pu}$ . Nucl. Phys., A 163, 1971, 577.
24. Pettenden N. EANDC-50 B, 1965.
25. James J.D. Fission Components in  $^{242}\text{Pu}$  Resonances. Nucl. Phys., A 123, 1969, 24.
26. Auchampaugh G.F., Bowman G.D. INDS (USA)-36 "U", 1971, 121.
27. Simpson O.B., Simpson O.D., Miller H.G., Harvey J.A., Hill N.W. Neutron Resonance Parameters of  $^{242}\text{Pu}$  below 500 eV. USNDC-3, 1972, 2.
28. Hockenbury R.W., Senislo A.J., Kaushal N.N. KeV Capture Cross Section of  $^{242}\text{Pu}$ . Proc. Conf. on Neutron Cross Section and Technology, Washington, 2, 1975, 584.
29. Kendall, M.G., Stuart, A., Statisticheskie vyyody i svyazi (Statistical deductions and relations), Moscow, "Nauka" (1973) 616. Owen, D.V., Sbornik statisticheskikh tablits (Compendium of statistical tables), Moscow, V.Ts. AN SSSR (1966) 424.
30. Bollinger L.M., Thomas G.E. P-Wave Resonances of  $^{238}\text{U}$ . Phys. Rev., 171, 1968, 1293.
31. Nikolaev, M.N., Manturov, G.N., Sovmestnaya otsenka nejtronnykh sechenij i uglovых raspredelenij uprugo rasseyanniykh nejtronov na urane-238 v oblasti nerazreshennykh rezonansov (Joint evaluation of neutron cross-sections and angular distributions of elastically scattered neutrons on uranium-238 in the unresolved resonance region). Materialy 4-j Vsesoyuznoj Konferentsii po nejtronnoj fizike, part 4, Kiev (1977) 108.

32. Behrens J.W., Newbury R.S., Magana J.W. Measurements of the Neutron-Induced Fission Cross Sections of  $^{240}\text{Pu}$ ,  $^{242}\text{Pu}$  and  $^{244}\text{Pu}$  Relative to  $^{235}\text{U}$  from 0.1 to 30 MeV. Nucl.Sci.Eng., 66, 1978, 433.
33. Wissak K., Kappeler F. Neutron Cross Section Ratios of  $^{240}\text{Pu}$ ,  $^{242}\text{Pu}$ ,  $^{238}\text{U}$  and  $^{197}\text{Au}$  in the Energy Range from 10 to 90 keV. Nucl.Sci.Eng., 66, 1978, 363.
34. Magurno B.A. ENDF/B-IV Cross Section Measurement Standards, BNL-NCS-50464, August 1975.
35. Vinogradov, V.N., Manokhin, V.N., Platonov, V.P., Rabotnov, N.S., Tolstikov, V.A., Otsenka secheniya radiatsionnogo zakhvata bystrykh nejtronov zolotom-197 (Evaluation of the  $^{197}\text{Au}$  radiative capture cross-section for fast neutrons), Materialy 3-j Vsesoyuznoj Konferentsii po nejtronnoj fizike, part 1, Kiev (1975) 165.
36. Jackson H.E. Review of Standard Reference Data and Important Cross Section Discrepancies, ANL/ND-77-1, Nov.1976, p.21.
37. Gilbert A., Cameron A.G.W. A Composite Nuclear Level Density Formula with Shell Corrections. Can.J.Phys., 43, 1965, 1446.
38. Malyshev, A.V., Plotnost' urovnej i struktura atomnykh yader (Level density and structure of atomic nuclei), Moscow, Atomizdat (1969).
39. Lynn, J.E., Systematics for neutron reactions of the actinide nuclei, AERE-R7468 (1974).
40. Kravtsov, V.A., Massy atomov i energii svyazi yader (Atomic masses and binding energies of nuclei), Moscow, Atomizdat (1974).
41. Ignatyuk, A.V., Isteikov, K.Yu., Smirenkin, G.N., Sistemmatika parametrov plotnosti urovnej (Systematics of level-density parameters), Materialy 4-j Vsesoyuznoj Konferentsii po nejtronnoj fizike, part 1, Kiev (1977) 60.

42. Blokhin, A.I., Ignatyuk, A.V., Platonov, V.P., Tolstikov, V.A., Vliyanie kollektivnykh effektov v plotnosti urovnej na energeticheskuyu zavisimost' sechenij radiatsionnogo zakhvata bystrykh nejtronov (Influence of collective level-density effects on the energy dependence of the radiative capture cross-sections for fast neutrons), Voprosy atomnoj nauki i tekhniki, ser. "Yadernye Konstanty", 21 (1976) 3.
43. Ignatyuk, A.V., Smirenkin, G.N., Tishin, A.S., Fenomenologicheskoe opisanie energeticheskoy zavisimosti parametra plotnosti urovnej (Phenomenological description of the energy dependence of the level-density parameter), Yadernaya fizika, 23 (1975) 485.
44. Lagrange, C., Calculs dans le cadre du modele optique en voies couplees de sections efficaces neutroniques pour  $^{236}$ ,  $^{238}$ ,  $^{240}$ ,  $^{242}$ ,  $^{244}$ Pu dans le domaine d'energie 1 keV-20 MeV (Calculations within the framework of the optical model in coupled paths of neutron cross-sections for  $^{236}$ ,  $^{238}$ ,  $^{240}$ ,  $^{242}$ ,  $^{244}$ Pu in the 1 keV-20 MeV energy range) INDC (FR) 16/L (1977).
45. Dresner, L., Inelastic scattering of neutrons by  $^{238}$ U below 1 keV, Nucl. Sci. Eng., 10 (1963) 142.
46. Sukhovitskij, E.Sh., Klepatskij, A.B., Kon'shin, V.A., Antsipov, G.V., Uchet protsessa  $(n, \gamma f)$  pri raschete shirin radiatsionnogo zakhvata i srednikh sechenij delyashchikhsya yader (Allowance for the  $(n, \gamma f)$  process in calculating radiative capture widths and average cross-sections of fissionable nuclei), Materialy 4-j Vsesoyuznoj konferentsij po nejtronnoj fizike, part 4, Kiev (1977) 68.
47. Auchampaugh G.F., Bowman O.D. Parameters of the Subthreshold Fission Structure in  $^{242}$ Pu. Phys. Rev.C., 7, 1973, 2085.
48. Strutinsky V.M. Shell Effects in Nuclear Masses and Deformation Energies. Nucl.Phys., A 95, 1967, 420.
49. Hill D.L., Wheeler J.A. Nuclear Constitution and the Interpretation of Fission Phenomena. Phys.Rev., 89, 1953, 1102.
50. Wong C.Y., Bang J. Penetration of a Double Barrier. Phys. Letters, 29 B, 1969, 143.

51. Gaj, E.V., Ignatyuk, A.V., Rabotnov, N.S., Smirenkin, G.N., Dvugorbyj bar'er i delenie yader nejtronami (Double-humped barrier and fissioning of nuclei by neutrons), *Yadernaya fizika* 10 (1969) 542.
52. Tyapin, A.S., Marshalkin, V.E., Pronitsaemost' dvugorbogo potentsial'nogo bar'era (Penetrability of a double-humped potential barrier), *Yadernaya fizika* 18 (1973) 277.
53. Masterov, V.S., Seregin, A.A., Pronitsaemost' dvugorbogo bar'era v kvaziklassicheskom priblizhenii (Penetrability of a double-humped barrier in a quasi-classical approximation), *Yadernaya fizika* 27 (1978) 1464.
54. Cramer, J.D., Nix, J.R., Exact calculations of the probability through two-peaked fission barriers, *Phys. Rev. C*, 2 (1970) 1048.
55. Antsipov, G.V., Kon'shin, V.A., Sukhovitskij, E.Sh., Otseka nejtronnykh sechenij  $^{240}\text{Pu}$  v oblasti nerazreshennykh rezonansov (Evaluation of the neutron cross-sections of  $^{240}\text{Pu}$  in the unresolved resonance region) Materialy 3-j vsesoyuznoj konferentsii po nejtronnoj fizike, part 2, Kiev (1975) 21.
56. Bondorf, J.P., Damping effects in the transmissions through the double-humped fission barrier, *Phys. Letters*, 31 B (1970) 1.
57. Ignatyuk, A.V., Rabotnov, N.S., Smirenkin, G.N., Soldatov, A.S., Tsipenyuk, Yu.M., Podbar'ernoje fotodelenie chetno-chetnykh yader (Sub-barrier photo-fission of even-even nuclei) *Zh. Ehks. Teor. Fiz.* 61 (1971) 1284.
58. Tyapin, A.S., Marshalkin, V.E., Raspredelenie delitel'nykh shirin v modeli dvugorbogo bar'era geleniya (Distribution of fission widths in the double-humped fission barrier model), *Voprosy atomnoj nauki i tekhniki, ser. "Yadernye Konstanty"*, 23 (1976) 105.

59. Hauser W., Feshbach H. The Inelastic Scattering of Neutrons. Phys.Rev., 87, 1952, 366.
60. Lane A.M., Lynn J.E. Fast Neutron Capture Below 1 MeV: Cross Sections for  $^{238}\text{U}$  and  $^{232}\text{Th}$ , Proc.Phys.Soc., A 70, 1957, 557.
61. Shaker M.O., Lukyanov A.A. The Generalized Porter- Thomas Distribution. Phys.Letters, 19, 1965, 197.
62. Lynn J.E., Back B.B. Sub-Barrier Fission Probability for Double - Humped Barrier. J.Phys., A 7, 1974, 395.
63. Lagrange Ch., Jary J. Coherent Optical and Statistical Model Calculations of Neutron Cross Sections for  $^{240}\text{Pu}$  and  $^{242}\text{Pu}$  between 10 keV and 20 MeV, NEANDC (E) 198 "L", INDC (FR) 30/L, 1978.

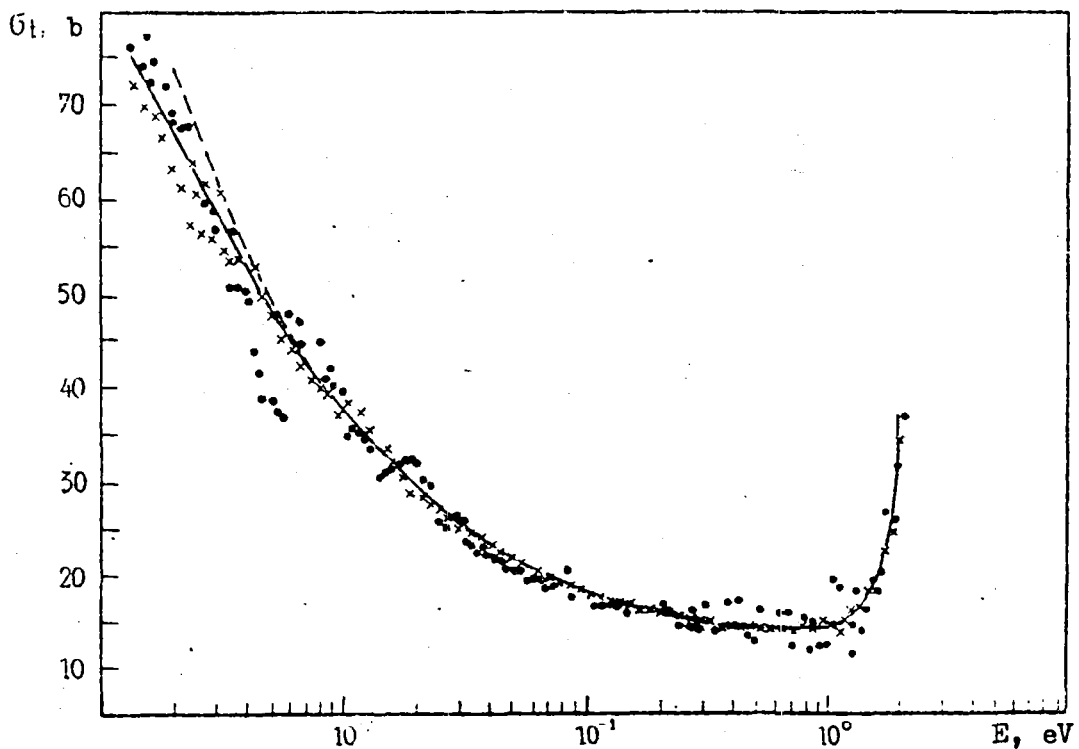


Fig. 2.1. Comparison of theoretical (—) and experimental data on  $\sigma_t$  of  $^{242}\text{Pu}$  in the region up to 2 eV: - - - represents the calculation without allowance for negative level, • - represents the data from Young and Reeder's paper [9] and x - the data from Young et al. [11].

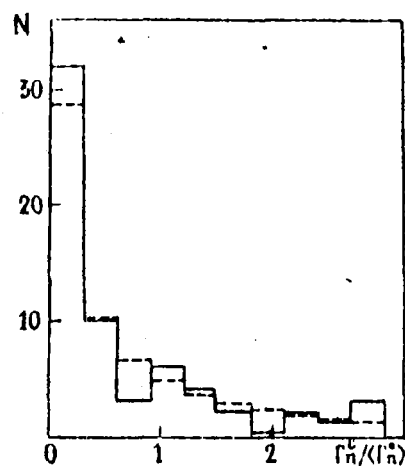


Fig. 3.1. Comparison of Porter-Thomas distribution (---) and  $\Gamma_n^e / \langle \Gamma_n^e \rangle$  distribution histograms for  $\langle \Gamma_n^e \rangle = 1.3 \text{ MeV}$ .

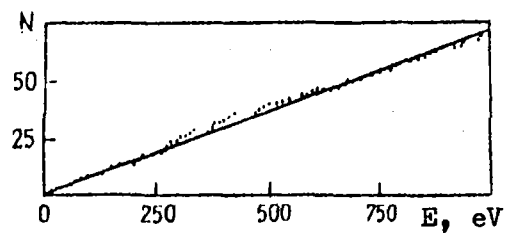


Fig. 3.2. Increase in number of levels as a function of energy.

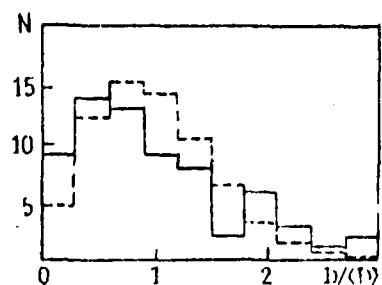


Fig. 3.3. Comparison of Wigner distribution histogram (---) with the  $D/\langle D \rangle$  distribution histogram (—) based on the data in Table 3.1.

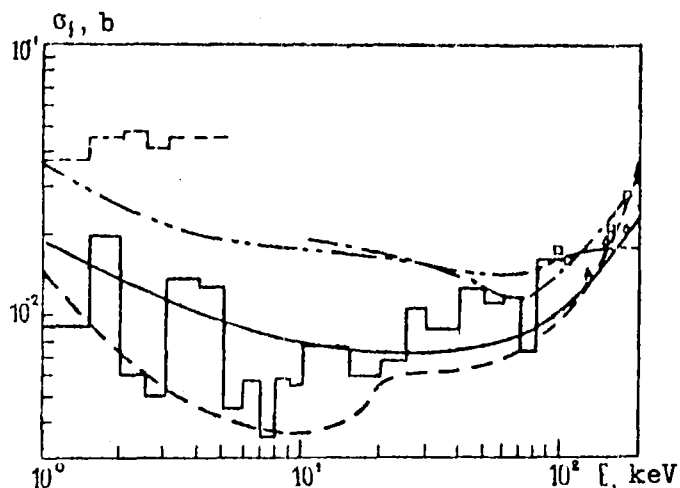


Fig. 4.1. Comparison of theoretical and experimental data on  $\langle \sigma_f \rangle$  for  $^{242}\text{Pu}$  in the 1-200 keV region. - - - represents the data from Bergen and Fullwood's paper [23], - - - from Auchampaugh et al. [21], - - - - from Caner and Yiftah [14] and - - - - from Lagrange and Jary [63]. - - - - - represents the calculation based on Lynn's parameters [39] and - - - - the evaluated data in this paper.

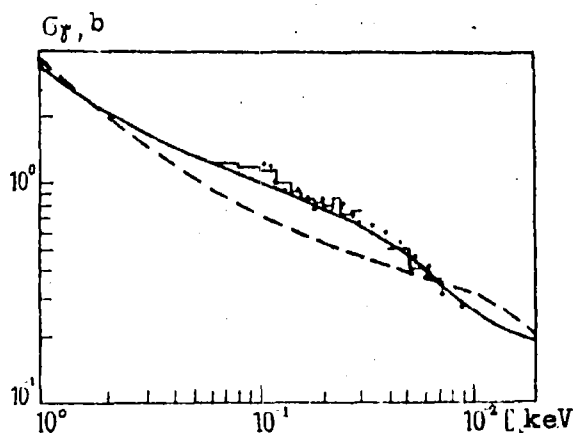


Fig. 4.2. Comparison of experimental and evaluated data on  $\langle \sigma_\gamma \rangle$  for  $^{242}\text{Pu}$ . - - - is taken from Hockenbury et al. [28], - - - from Wissak and Kappeler [33], - - - - from Caner and Yiftah [14] and - - - is the result from this paper.

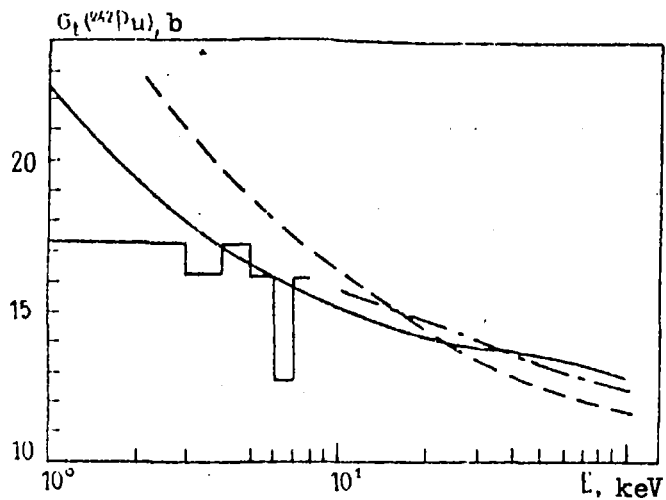


Fig. 4.3. Comparison of experimental and evaluated data on  $\langle\sigma_t\rangle$  for  $^{242}\text{Pu}$ .  
\_\_\_\_\_ is taken from Young and Reeder's paper [9], \_\_\_\_\_ from  
Caner and Yiftah [14], \_\_\_\_\_ from Lagrange and Jary [63] and  
\_\_\_\_\_ is the result from this paper.

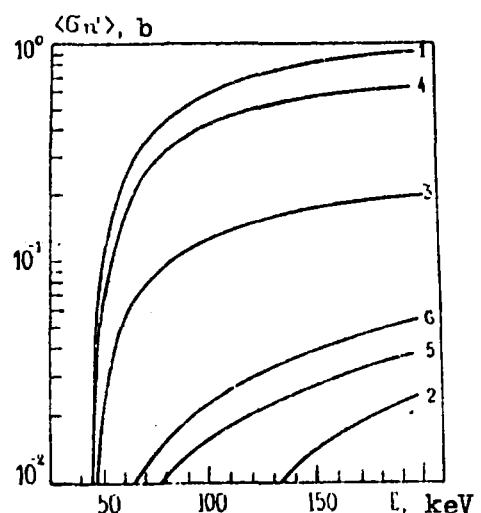


Fig. 4.4. Total (curve 1) and partial (curves 2-6) inelastic scattering cross-sections for channels  $1/2^+$ ,  $1/2^-$ ,  $3/2^-$ ,  $3/2^+$  and  $5/2^+$  respectively.

ABSTRACT

UDC 539.173.4

EVALUATION OF NUCLEAR DATA FOR  $^{242}\text{Pu}$  IN THE REGION OF RESOLVED AND UNRESOLVED RESONANCES ( $10^{-5}$  eV-200 keV). G.V. Antsipov, L.A. Bakhanovich, V.A. Kon'shin, V.M. Maslov, G.B. Morogovskij, E.Sh. Sukhovitskij, Yu.V. Porodzinskij, Coll. "Evaluation of nuclear data for  $^{242}\text{Pu}$  in the  $10^{-5}$  eV-15 MeV neutron energy region". Minsk, Heat- and Mass-Exchange Institute, BSSR Academy of Sciences, 1979, pp. 3-52.

Neutron data for  $^{242}\text{Pu}$  are evaluated in the resolved and unresolved resonance regions. In the  $10^{-5}$ -1 keV region, the evaluation is based on the Breit-Wigner resonance parameters. In the unresolved resonance region, all types of average cross-section and width are calculated. The authors quote average parameters and cross-sections in the 1-200 keV region and analyse the errors in the evaluated data.

Thirteen tables, eight figures, 63 bibliographical references.

EVALUATION OF NEUTRON CROSS-SECTIONS FOR  $^{242}\text{Pu}$  IN THE 0.2-15.0 MeV REGION ON THE BASIS OF EXPERIMENTAL DATA AND THEORETICAL MODELS

G.V. Antsipov, L.A. Bakhanovich, A.R. Benderskij, V.A. Zenevich,  
A.B. Klepatskij, V.A. Kon'shin and E.Sh. Sukhovitskij

In the 0.2-15 MeV energy region for  $^{242}\text{Pu}$  experimental data on the energy dependence of neutron cross-sections are totally lacking, except for the fission cross-section. In performing the evaluation it was therefore necessary to make wide use of the various theoretical models, namely optical, statistical and pre-equilibrium decay models and also the results of the systematics on the neighbouring nuclei.

The fission cross-section was evaluated on the basis of experimental data; it is therefore hoped that proper allowance for the competition of fission will substantially raise the accuracy of the other calculated cross-sections.

1. EVALUATION OF THE FISSION CROSS-SECTION  $\sigma_f$  FOR  $^{242}\text{Pu}$  IN THE 0.1-15 MeV REGION

Of the available  $\sigma_f$  measurements for  $^{242}\text{Pu}$  [1-9] only the data of Alkhazov et al. [1] are absolute; the others were obtained in relation to the  $\sigma_f$  for  $^{235}\text{U}$ . In the evaluation of  $\sigma_f$  ( $^{242}\text{Pu}$ ) all existing experimental data were considered. The data on the  $\sigma_f$  ( $^{242}\text{Pu}$ )/ $\sigma_f$  ( $^{235}\text{Pu}$ ) ratio were converted into absolute values of  $\sigma_f$  ( $^{242}\text{Pu}$ ) with the use of the evaluated data of Ref. [10] on  $\sigma_f$  ( $^{235}\text{U}$ ) obtained with consideration of the correlation of experimental data. The renormalization could not be performed only for the data of Bergen and Fullwood [6] since they did not indicate the exact source of the  $\sigma_f$  ( $^{235}\text{U}$ ) values used by them.

Comparison of the derived cross-sections  $\sigma_f$  ( $^{242}\text{Pu}$ ) shows the following. The data of Kupriyanov et al. [2] and Meadows [3] are in good agreement with one another. In the region up to 0.8 MeV their data also agree with those of Butler [9] although in the region above 1 MeV they lie considerably higher (by ~8%). The data of Fomushkin and Gutnikova [7] lie systematically below all others. This may be the result of inaccurate allowance for the contribution of other isotopes to fission, owing to poor target purity (73.3%  $^{242}\text{Pu}$ ). Moreover, these

data have a large scatter around the average curve. The data of Behrens et al. [4] and Bergen and Fullwood [6] agree, on the whole, with one another. However, the data of the latter in the entire region and those of the former in the region up to 1.5 MeV lie somewhat above the data of Kupriyanov et al. [2]. The data of Auchampaugh et al. [5] lie between the four other sets of data [2-6]. In the region above 4 MeV there are only two sets of data [2,4]. In the region above 6 MeV the data of Behrens et al. lie ~3% below the data of Kupriyanov et al. [2]. They also lie considerably below the absolutely measured value of Alkhazov et al. [1] at 14.8 MeV.

Considering all the experiments, including the data available with us, we concluded that the evaluation of  $\sigma_f(^{242}\text{Pu})$  in the region up to 7 MeV should be based on the data of Kupriyanov et al. [2]. These data are in good agreement with those of Meadows [3], although the latter are available only in the form of a graph and are preliminary. Besides, Meadows does not give the errors of his data. The data of Bergen and Fullwood [6] were not taken into account in the evaluation because they were impossible to renormalize. Moreover, in their experiment [6] a strong anisotropy of fission fragments was observed, especially above 1 MeV, and the measurements were carried out only for two angles. Lastly, these data have a large statistical scatter around the average curve in comparison with the data of Ref. [2]. Butler's data [9] were available only in the form of a graph. The data of Formushkin et al. [8] exhibit a considerable systematic difference from all the other available data.

In the region above 6 MeV the data of Behrens et al. [4] lie on an average ~3% below those of Ref. [2] and ~6.5% below those of Alkhazov et al. [1] at 14.8 MeV, while in the region of low energies they lie somewhat above the data of Kupriyanov et al. [2]. Renormalization of the data of Behrens et al. to the absolutely measured value of Alkhazov et al. [1] does not impair their agreement with the data of Kupriyanov et al. [2]. Therefore, in the region above 7 MeV the evaluation of  $\sigma_f(^{242}\text{Pu})$  was based on the data of Behrens et al. [4] renormalized to the value of Alkhazov et al. [1] at the 14.8 MeV point.

A further justification for the choice of the data of Kupriyanov et al. [2] to be used as reference for evaluation in the region up to 7 MeV is also provided by the comparison with the value of the average

cross-section  $\bar{\sigma}_f(^{242}\text{Pu})$  over the  $^{252}\text{Cf}$  fission spectrum measured by Alkhazov et al. [1]. During the averaging it was assumed that the  $^{252}\text{Cf}$  fission neutron spectrum was governed by a Maxwellian distribution although this may not be true of the whole energy region. Thus, Knitter et al. [11] did not observe deviations from a Maxwellian distribution in the 0.15-15.0 MeV region, while Batenkov et al. [12] found similar deviations in the region below 0.7-0.8 MeV.

Calculation for the  $^{252}\text{Cf}$  spectrum temperature  $T = 1.42 \pm 0.05$  MeV gives a value averaged over the  $^{252}\text{Cf}$  spectrum of  $\bar{\sigma}_f = 1.13 \pm 0.01$  b (the error is due only to the temperature error) for the evaluated data of  $\sigma_f(^{242}\text{Pu})$ . It is somewhat higher than the experimental value of Alkhazov et al. ( $\bar{\sigma}_f = 1.095 \pm 0.020$  b). It should be borne in mind, however, that the value of  $\bar{\sigma}_f$  calculated from other data can only be higher. The evaluated data on  $\sigma_f(^{242}\text{Pu})$ , on the  $\sigma_f(^{242}\text{Pu})/\sigma_f(^{235}\text{U})$  ratio and on the  $\sigma_f(^{235}\text{U})$  used are given in Table 1.1. The evaluated and experimental data on  $\sigma_f(^{242}\text{Pu})$  are given in Figs 1.1-1.4. Comparison of the data of the present evaluation with those of Caner and Yiftah [13] and Lagrange and Jary [14] shows considerable disagreement (up to ~40%) in the 0.1-0.3 MeV region. Considerable disagreement with the data of Ref. [13] is also observed in the 6-10 MeV region.

Let us now consider the question of the accuracy of the  $\sigma_f(^{242}\text{Pu})$  data. The evaluation in the region up to 7 MeV was based on the data of Ref. [2] on the  $\sigma_f(^{242}\text{Pu})/\sigma_f(^{235}\text{U})$  ratio, having an error of 2.2-2.5% above 1 MeV rising to 5.7% with decrease in energy to 0.127 MeV. Another most complete set of data [4] on the cross-section ratio has an accuracy of 1.8-3% in the 1-15 MeV region, which falls to 18% at 0.1 MeV. Both series of data agree within the errors cited by the authors. Hence it is valid to evaluate the accuracy of the  $\sigma_f(^{242}\text{Pu})/\sigma_f(^{235}\text{U})$  ratio at 3% in the 1-7 MeV region, reducing it to 6% at 0.1 MeV.

In the region above 7 MeV the accuracy of the  $\sigma_f(^{242}\text{Pu})/\sigma_f(^{235}\text{U})$  ratio will also be lower. The  $\sigma_f(^{242}\text{Pu})$  value derived from the ratio of Ref. [4] and from  $\sigma_f(^{235}\text{U})$  [10] at 14.8 MeV and the absolute value of Ref. [1] differ by 6%, agreeing only at the boundary of the error range; hence, the error of the  $\sigma_f(^{242}\text{Pu})/\sigma_f(^{235}\text{U})$  ratio at this energy can be evaluated at 5%. Although the absolute measurement of Ref. [1] at 14.8 MeV has an accuracy of 2.8%, the error of  $\sigma_f(^{242}\text{Pu})$  in the 7-15 MeV region will be somewhat higher. Considering the above and bearing in

mind that the accuracy of  $\sigma_f(^{235}\text{U})$  is evaluated at 3% [10] in the whole energy range under consideration, we present in Table 1.2 the evaluated uncertainties in the values of  $\sigma_f(^{242}\text{Pu})/\sigma_f(^{235}\text{U})$  and  $\sigma_f(^{242}\text{Pu})$ .

## 2. USE OF THE COUPLED CHANNEL METHOD FOR EVALUATION OF $^{242}\text{Pu}$ NUCLEAR DATA

Recently the coupled channel method has come into extensive use for evaluation and prediction of the neutron cross-sections of actinides. For heavy nuclei the dependence between the different channels is quite strong, and the coupled channel method is effective [15,16]. Born's method of distorted waves [17] is being used with success in regions where deformation of the nucleus  $\beta$  is small ( $\beta \approx 0.1$ ). At higher values of  $\beta$  the differential elastically and inelastically scattered neutron cross-sections are not described satisfactorily by the distorted wave method since the low-lying collective states influence not only the inelastic scattering processes but also the elastic channel. It is preferable in this case to use the coupled channel method, i.e. to seek an accurate solution of the quantum-mechanical problem of scattering on a deformed non-spherical potential having an internal structure.

The most rigorous solution of this problem was suggested by Bohr and Mottelson [15]. Later the coupled channel method was developed in a number of papers [18-21] and incorporated in computer programs [16,22-25]. We give the principal formulae of the method, following Tamura [16].

The generalized Hamiltonian of the system of target nucleus and incident neutron can be presented in the form

$$H = T + H_T + V(r, \theta, \varphi), \quad (2.1)$$

where  $T$  is the operator of the incident-neutron kinetic energy,  $H_T$  the Hamiltonian of the target-nucleus internal motion and  $V(r, \theta, \varphi)$  the interaction potential. The total wave function of the system  $\psi$  is the solution of the Schrödinger equation

$$H\psi = E\psi. \quad (2.2)$$

This function can be expanded with respect to the full set of eigenfunctions of operators  $T$  and  $H_T$ :

$$\begin{aligned} \psi &= \frac{1}{2} \sum_{J,M} R_{nljnjn}(z) \left( Y_{ljnjn} \otimes \Phi_{jn} \right)^{JM} = \\ &= \frac{1}{2} \sum_{JM} R_{nljnjn}(z) \sum_{m_j m_n} \langle j_n l_n m_j M_n | JM \rangle Y_{ljnjn m_j m_n} \Phi_{jn M_n}, \end{aligned} \quad (2.3)$$

where  $\mathcal{Y}_{Lj\mu}$  is the spherical spin-angular function with orbital moment  $\mu$  and total moment  $j\mu$ ;  $\Phi_{I_n M_n}$  is the wave eigenfunction of the Hamiltonian of the target nucleus with moment  $I_n$  and its projection  $M_n$  and satisfies the Schrödinger equation:

$$H_T \Phi_{I_n M_n} = E_n \Phi_{I_n M_n}, \quad (2.4)$$

$J$  and  $M$  are the total moment of the system and its projection on the  $z$  axis, respectively. The interaction potential  $V(r, \theta, \varphi)$  is chosen in the generally accepted form with a radial Woods-Saxon dependence and its derivative:

$$\begin{aligned} V(r, \theta, \varphi) = & -\frac{V_s}{1 + \exp \frac{r - R_s}{a_s}} - i W_c \left[ \frac{d}{1 + \exp \frac{r - R_w}{a_w}} + \frac{1-d}{\exp \left( \frac{r - R_w}{a_w} \right)^2} \right] - \\ & - \frac{4i W_d \exp \frac{r - R_p}{a_p}}{\left( 1 + \exp \frac{r - R_p}{a_p} \right)^2} - \left( \frac{\hbar}{m_e c} \right)^2 \frac{1}{a_s^2} \frac{V_s \exp \frac{r - R_s}{a_s}}{\left( 1 + \exp \frac{r - R_s}{a_s} \right)^2} (\vec{l} \cdot \vec{\sigma}), \end{aligned} \quad (2.5)$$

where  $\theta, \varphi$  are angles in the centre-of-mass system.

Considering axial symmetry, the radius of the nucleus is presented in the form

$$R_L = R_{L0} \left( 1 + \sum_s p_s Y_{s0}(\theta') \right), \quad (2.6)$$

where  $\theta'$  represents angles in the co-ordinate system connected with the nucleus. Then potential (2.5) can be written as

$$V(r, \theta, \varphi) = V_{\text{diag}} + V_{\text{coupl}}(r) \quad (2.7)$$

$$V_{\text{coupl}} = \sum_{\lambda \mu} V^\lambda(r) D_{\mu 0}^\lambda(\theta_i) Y_{\lambda \mu}(\theta, \varphi). \quad (2.8)$$

Here  $D_{\mu 0}^\lambda(\theta_i)$  is the matrix of rotation and  $\theta_i$  represents Euler angles between the laboratory system of co-ordinates and the system connected with the nucleus.

$$V^\lambda(r) = 4 \pi \int V(r - R_{L0} \left( 1 + \sum_s p_s Y_{s0}(\theta') \right)) Y_{\lambda 0}(\theta) d(\phi, \theta'), \quad (2.9)$$

and  $V_{\text{diag}} = V^{\lambda=0}$

Substituting (2.3), (2.4) and (2.7-2.9) into (2.2), multiplying the left side by  $(Y_{l_{n+j_n}} \otimes \Phi_{I_n})^{JM}$  and integrating over all the co-ordinates except the radial variable  $r$ , we obtain a system of connected equations

$$\begin{aligned} & \left( \frac{d^2}{dr^2} - \frac{l_n(l_n+1)}{r^2} - \frac{2\mu}{\hbar^2} V_{\text{diag}} + 1 \right) R_{nl_{n+j_n}}^J(z) = \\ & = \frac{2\mu}{\hbar^2} \sum_{\lambda \in \Lambda_{l_n}} \langle (Y_{l_{n+j_n}} \otimes \Phi_{I_n})^{JM} | V_{\text{coupl}} | (Y_{l_{n+j_n}} \otimes \Phi_{I_n})^{JM} \rangle R_{nl_{n+j_n}}^J(z). \end{aligned} \quad (2.10)$$

In order to calculate the matrix elements in the right-hand part of (2.10), we need to know the form of the wave function of the target nucleus. For axially symmetric nuclei usually the rigid rotator model is chosen

$$\Phi_{I_n M_n} = [(2I_n + 1)/8\pi^2]^{1/2} D_{K M_n}^{I_n}(\theta'), \quad (2.11)$$

where  $K$  is the projection of moment  $I_n$  on the symmetry axis of the nucleus. Then the matrix coupling element can easily be calculated

$$\begin{aligned} \langle (Y_{l_j} \otimes \Phi_I)^{JM} | V_{\text{coupl}} | (Y_{l_j} \otimes \Phi_I)^{JM} \rangle &= \frac{1}{\sqrt{4\pi}} \sum_{\lambda \neq 0} U^\lambda(z) \sqrt{(2j+1)(2j'+1)} \times \\ &\times \sqrt{(2I+1)} \langle j j' \gamma_2 - \gamma_1 | \lambda 0 \rangle \langle I' \lambda K O | I K \rangle W(j i j' I'; J \lambda) \times \\ &\times (-1)^{J - \gamma_2 - I + j + j' - \gamma_1 (e' - e)} \end{aligned} \quad (2.12)$$

In this manner, we can now solve Eq. (2.10) for radial wave functions  $R_{nl_{n+j_n}}^J(z)$ . If we connect this solution with the asymptotic one in the region outside the boundary of the nucleus, where the influence of the residual potential can be neglected, we obtain the coefficients of the  $C$  matrix.

Let us determine the form of the asymptotic function. The initial state of the system is characterized by a plane wave of unit amplitude in the entrance channel

$$\Psi_{\text{inc}} = \frac{1}{\sqrt{v_1}} \exp(i k_1 z) \Phi_{I, M, J, S, M}, \quad (2.13)$$

(where  $v_1$  is incident neutron velocity) or in the representation of the total moment of the system  $J$

$$\begin{aligned} \Psi_{\text{inc}} &= \sqrt{\frac{4\pi}{v_1}} \frac{1}{2k_1 z} \sum_{JM, l_m, m_j} (2l+1)^{1/2} \langle l_S 0 M_s | j M_s \rangle \langle j I, m, M, J M \rangle \times \\ &\times (-2i F_e) (Y_{l_j} \otimes \Phi_{I, J})^{JM} \end{aligned} \quad (2.14)$$

The total asymptotic wave function takes the following form

$$\Psi_{as} = \sqrt{\frac{4\pi}{V_1 k_1^2}} \sum_{JM} (2e+1)^{1/2} \langle l'sm_s | jm_s \rangle \langle j' I_1 m_1 M_1 | JM \rangle \sum_{n \neq j} \delta_{n1} \delta_{s1} \delta_{j1} F_e^{(n)} + \\ + \left( \frac{k_1}{k_n} \right)^{1/2} (2e+1)^{1/2} C_{ej;nej}^T (G_e^{(n)} + F_e^{(n)}) (Y_{ej} \otimes \Phi_{In})^{JM}, \quad (2.15)$$

where  $F_e^{(n)}$  and  $G_e^{(n)}$  are the regular and irregular Coulomb functions, respectively. It is implied that in the entrance channel  $\Psi_{as}$  is the superposition of the plane incident wave and the diverging spherical one, while in the others they are diverging spherical waves. The asymptotic wave function determines the scattering amplitude:

$$X_{m_1 M_1, m_2 M_2} (\theta, \varphi) = \frac{\sqrt{4\pi}}{k_n} \sum_{\substack{l'm_1 m_2 \\ m_1' m_2'}} (2e+1)^{1/2} C_{l'm_1 m_2'}^T \langle l'sm_s | jm_s \rangle \times \\ \times \langle j_1 m_1 M_1 | JM \rangle \langle l'sm_s | j'm_2 \rangle \langle j' I_1 m_1 M_1 | JM \rangle Y_{l'm_2'} (\theta, \varphi). \quad (2.16)$$

It is now easy to write the expressions for the differential  $\frac{d\sigma_n}{d\Omega}$  and integral  $\sigma_n$  cross-sections for elastic and direct inelastic scattering at levels:

$$\frac{d\sigma_n}{d\Omega} = \frac{1}{2(2I_1+1)} \sum_{m_1 M_1, m_2 M_2} | X_{m_1 M_1, m_2 M_2} (\theta, \varphi) |^2 = \\ = \frac{(-1)^{I_1 - I_2}}{2(2I_1+1) k_1^2} \sum_{\substack{j_1 j_2 \\ j_1' j_2' \\ l_1 l_2 \\ l_1' l_2' \\ e_1 e_2 \\ e_1' e_2'}} C_{l_1 j_1 m_1 l_1' j_1' m_1'}^T C_{l_2 j_2 m_2 l_2' j_2' m_2'}^T (2J_1+1)(2J_2+1) \sqrt{(2j_1+1)(2j_2+1)} \times \\ \times \sqrt{(2j_1'+1)(2j_2'+1)} \sum_{\substack{l_1 l_2 \\ l_1' l_2' \\ e_1 e_2 \\ e_1' e_2'}} R_l(\cos\theta) \frac{1}{4} [1 + (-1)^{l_1+l_2-L}] [1 + (-1)^{l_1'+l_2'-L}] \times \\ \times \langle j_1 j_2 | \gamma_{z-1/2} | L \rangle \langle j_1' j_2' | \gamma_{z-1/2} | L' \rangle W(J_1 j_1' J_2 j_2' ; I_1 L) W(J_1 j_1' J_2 j_2' ; I_2 L), \quad (2.17)$$

where averaging has been performed over the initial states and summation over the final states.

Integrating (2.17) over angles, we obtain the integral cross-section at the level

$$\sigma_n = \frac{2\pi}{k_1^2 (2I_1+1)} \sum_{J \in ej} (2J+1) | C_{ej;nej}^T |^2. \quad (2.18)$$

The total cross-section is determined by the optical theorem

$$\sigma_t = \frac{2\pi}{k_1^2 (2I_1+1)} \sum_{J \in ej} (2J+1) \operatorname{Im} C_{ej;ej}^T. \quad (2.19)$$

We determine the compound nucleus formation cross-section as

$$\begin{aligned}\sigma_c &= \sigma_t - \sum_n \sigma_n = \\ &= \frac{2\pi}{k_i^2(2j+1)} \sum_{r \neq j} (2j+1) \left( \text{Im} C_{ij,nej}^T - \sum_{n \neq j} |C_{ij,nej}^T|^2 \right).\end{aligned}\quad (2.20)$$

By comparing expression (2.20) with the expression for  $\sigma_c$  of the spherical optical model, we can obtain the generalized penetration factors

$$T_{ij}^T = 4 \left( \text{Im} C_{ij,1ej}^T - \sum_{n \neq j} |C_{ij,nej}^T|^2 \right). \quad (2.21)$$

Application of the coupled channel method requires considerable mathematical work because of the impossibility of analytical calculations so that complicated computer programs have to be developed. However, in view of computational difficulties, even in the most sophisticated nuclear data evaluation program [22], as is mentioned in Ref. [26], the optical potential parameters were not determined automatically by using the  $\chi^2$ -criterion.

In order to apply the coupled channel method to evaluate nuclear constants, we developed the COUPLE program for the EHSM-6 computer. Special studies were made to determine the optimal conditions for numerical calculation. In the numerical calculations we used the results which Kikuchi [23] and Dzyuba et al. [25] had obtained in their studies of the influence of the various physical approximations on the cross-section values calculated. The COUPLE program was combined with the optimization problem of the search for the potential parameters by the method of conjugate gradients, which best describe the initial experimental data.

The C-matrix coefficients and the neutron cross-sections  $\sigma_t$ ,  $\sigma_{24}$ ,  $\sigma_{44}$  calculated by this program were compared in respect of  $^{238}\text{U}$  with the calculations by the JUPITOR program, which had been suggested as a test by Kikuchi [23]. The comparison showed that the C-matrix coefficients differed by not more than  $10^{-4}$  and the neutron cross-sections by not more than 0.1%. Such an agreement with the results of Kikuchi [23] is achieved with allowance for the fact that Kikuchi used the old value of the constant of conversion of energy into wave number  $k = 0.2178 \frac{M}{M+1} \sqrt{E_{\text{lab}}}$ , where  $E$  is in MeV and  $k$  in Fermi $^{-1}$ . In our calculations the refined constant equal to 0.219677 was used.

The coupled channel method can be used to calculate  $\sigma_t$ ,  $\sigma_c$ ,  $S_0$ ,  $S_1$ ,  $\sigma_n^{0+}$ , the angular distributions of elastically and non-elastically scattered neutrons and the direct-excitation cross-sections for the first levels. In order to determine the potential parameters we can directly use only the experimental data on  $S_0$ ,  $S_1$ ,  $\sigma_p$  and  $\sigma_t$ . The overwhelming majority of data on the angular distributions of elastically scattered neutrons cannot be used to obtain the optimal potential parameters because they contain either an isotropic part due to the compound contribution at low energies or an often unknown contribution of the unresolved lower levels at high energies. In most cases, therefore, we can only compare the theoretical data on the angular distributions of elastically scattered neutrons with experimental data, but not use the latter for obtaining the potential parameters.

By way of example, we give the potential parameters for  $^{238}\text{U}$  obtained by us. As experimental data, from which the potential parameters were derived, we took  $S_0$ ,  $S_1$ ,  $\sigma_p$  in the region of energies of the order of a few keV and  $\sigma_t$  in the 20 keV-15 MeV region. In the second step of fitting, apart from these data, we also used the most accurate experimental data on the angular distributions of elastically scattered neutrons [27,28] at 2.5 and 3.4 MeV, in which the contribution of the lower levels is clearly distinguished. However, it should be noted that, in spite of the high quality of the experimental data in Ref. [27], there is an inconsistency between the high value of  $\sigma_t$  at 3.4 MeV and the comparatively low value of the differential elastic scattering cross-section at small angles obtained in that work.

The potential was expanded in Legendre polynomials up to and including  $\lambda = 6$ , and the calculations were performed with consideration of the coupling of three levels ( $0^+ - 2^+ - 4^+$ ). After optimization we obtained the following values of the potential parameters for  $^{238}\text{U}$ :

$$V_R = 47.5 - 0.3 E_n, \quad \alpha_n = 0.62 \varphi, \quad R_n = 7.644092 \varphi \quad (r_{\infty} = 1.233485 \varphi)$$

$$W_D = \begin{cases} 2.7 + 0.4 E_n & \text{for } E_n < 10 \text{ MeV}, \quad \alpha_n = 0.58 \varphi, \quad R_n = 7.808108 \varphi \\ 6.7 & \text{for } E_n > 10 \text{ MeV} \quad (r_{\infty} = 1.26 \varphi) \end{cases}$$

$$V_s = 7.5 \text{ MeV}, \quad \beta_{s0} = 0.216, \quad \beta_{s1} = 0.067, \quad W_c = 0.$$

The values of the strength functions and potential scattering radius for  $^{238}\text{U}$  calculated with these potential parameters are given in Table 2.1.

The calculated values of  $\sigma_t(^{238}\text{U})$  agree with the experimental values to within 1-3% in the region from 50 keV to 15 MeV.

Figures 2.1 and 2.2 compare the calculated (using the above potential) and experimental data on neutron angular distributions for the elastic ( $0^+$ ), the first excited ( $2^+$ ) and the second excited ( $4^+$ ) levels for  $^{238}\text{U}$  at 2.5 and 3.4 MeV. The figures show satisfactory agreement between experimental and calculated data although the structure in the angular distribution of inelastically scattered neutrons at level  $2^+$  is not sufficiently well reproduced in calculation, and this may be due to the need to take into account the coupling of several additional channels, as is noted in Ref. [27]. It will be seen from a comparison of the results of calculation by the coupled channel method and those by the spherical optical model with the potential parameters of Lambropoulos [29] that the experimental data on angular distributions, especially for large angles, are described much better by the former method. This indicates that the contributions of the various partial waves to the cross-section are calculated more correctly in the coupled channel method.

The potential parameters for  $^{238}\text{U}$  obtained by us agree satisfactorily with the first version of the parameters of Lagrange [22] and differ somewhat from the second version of the potential given in Ref. [27], which was obtained by heavily "weighting" the experimental data on the angular distributions of elastically and inelastically scattered neutrons.

The calculated neutron cross-section values, especially at low energies, are sensitive to the choice of deformation parameters. The information on the shape of nuclei comes mainly from studies by the method of Coulomb excitation of nuclei [30] and inelastic scattering of electrons [31], which give the proton distribution in the nucleus. The values of the obtained deformation parameters  $\beta_{20}$  and  $\beta_{40}$  depend on the assumed form of charge distribution in the nucleus (thus, according to the data of Ref. [30] for  $^{238}\text{U}$  in the case of uniform charge distribution  $\beta_{20} = 0.253$ , in the case of Fermi distribution  $\beta_{20} = 0.283$  and in the case of charge distribution with a hard core  $\beta_{20}$  varies from 0.252 to 0.200 as a function of the constant density radius). Besides, it is necessary to distinguish the charge deformation parameters of the nucleus, which can be determined by electromagnetic measurements, and the deformation parameters of the nuclear potential, which can be obtained from experiments on inelastic scattering at energies above the Coulomb barrier.

Hendrie et al. [32] experimentally determined the potential deformation parameters for  $^{238}\text{U}$  from  $(\alpha, \alpha')$  experiments, which are sensitive to proton and neutron distribution in nuclei. The values were:

$\beta_{20} = 0.20 \pm 0.01$ ,  $\beta_{40} = 0.06 \pm 0.01$ ,  $\beta_{60} = -0.012 \pm 0.01$ . The experiments of Moss et al. [33] on  $(p, p')$  scattering gave considerably higher values:  $\beta_{20} = 0.27 \pm 0.01$ ,  $\beta_{40} = 0.017 \pm 0.015$ ,  $\beta_{60} = -0.015$ .

Theoretical calculations of the deformation parameters for the ground state of actinides by the Strutinsky shell correction method [34] were carried out by Nilsson et al. [35] using the deformation potential of a harmonic oscillator, by Garssev et al. [36], by Goetz et al. [37] and by Pauli [38] using the Woods-Saxon potential. The experimental and theoretical values of the deformation parameters for  $^{238}\text{U}$  and  $^{242}\text{Pu}$  are given in Table 2.2.

Moreover, in the study of the neutron spectra of single-particle states Braid et al. [39] obtained  $\beta_{20} = 0.24 \pm 0.01$  for  $^{238}\text{U}$ .

Thus, the calculation results of Refs [35, 37-39] agree with one another and with the experimental data of Hendrie et al. [32] to within ~10% and also with the results of analysis of experimental data [27] by the coupled channel method. Therefore, the  $^{242}\text{Pu}$  neutron cross-sections were calculated with the deformation parameter values of Refs [35] and [37] slightly renormalized on the basis of the evaluated values for  $^{238}\text{U}$ :  $\beta_{20} = 0.228$ ,  $\beta_{40} = 0.057$ .

The geometric parameters  $r_{OR}$ ,  $a_R$ ,  $z_{OD}$ ,  $a_D$  are taken to be identical for  $^{238}\text{U}$  and  $^{242}\text{Pu}$ . The depths of the real and imaginary parts of the potential were also changed slightly in accordance with the isotopic dependence  $\sim 17\frac{N-Z}{A}$  and  $\sim 9\frac{N-Z}{A}$ , respectively [14]. Calculation with such a potential gives unsatisfactory values of cross-sections and strength functions for  $^{242}\text{Pu}$ :  $S_0 = 1.15 \times 10^{-4}$ ,  $S_1 = 3.0 \times 10^{-4}$ ,  $R' = 9.07 \mu$ , our evaluated value being  $S_0 = 0.91 \pm 0.15 \times 10^{-4}$ . Therefore, in evaluating  $^{242}\text{Pu}$  we used the same potential parameters as in the case of  $^{238}\text{U}$ . This is especially justified since the calculated predictions of  $\beta_{20}$  for  $^{242}\text{Pu}$  and  $^{238}\text{U}$  differ, as will be seen from Table 2.2, by 0.012, which is significantly lower than the accuracy of the value of  $\beta_{20}$  for  $^{238}\text{U}$ , namely 0.02. Fig. 2.3 gives the values, calculated with the above potential parameters, for total cross-section  $\sigma_t$ , compound nucleus formation cross-section  $\sigma_c$  and elastic scattering  $\sigma_n^{el}$  and direct inelastic scattering  $\sigma_{n'}^{2+, 4+}$  cross-sections in the  $10^{-2}$ -10 MeV region. Fig. 2.4 represents the differential elastic scattering cross-section of 1.3 MeV neutrons by the  $^{242}\text{Pu}$  nucleus and the contribution of direct elastic scattering to this cross-section.

### 3. USE OF THE STATISTICAL THEORY OF NUCLEAR REACTIONS TO CALCULATE NEUTRON CROSS-SECTIONS

The partial cross-sections for the interaction of neutrons with the  $^{242}\text{Pu}$  nucleus in the 0.2-5.0 MeV region was calculated with the help of

the Hauser-Feshbach formalism [40]. Since in the above energy region, in the case of  $^{242}\text{Pu}$ , only the fission cross-section is known experimentally (see Section 1), the evaluation of the radiative capture  $\sigma_\gamma$  and inelastic scattering  $\sigma_n$ , cross-sections can be based only on calculations by theoretical models. Of special importance in this connection is the correctness of the theoretical concepts used in the calculation of the widths of these processes, especially the question of the energy dependence of radiative capture widths, which is closely connected with the choice of a particular level density model of the nucleus.

In the energy region under consideration the target nucleus has both a discrete and a continuous level spectrum. In the discrete spectrum region the calculations used the Hauser-Feshbach formalism, as modified by Lane and Lynn [41]. The fluctuations of neutron and fission widths were taken into account on the assumption that their distribution follows the Porter-Thomas law [42]. In the region of energies higher than the boundary of the discrete and continuous level spectra of the target nucleus the unmodified Hauser-Feshbach formalism is ordinarily used [40]. However, in the case of many nuclei, including  $^{240}\text{Pu}$ , the discrete level spectrum is experimentally not allowed to be so high that the effects of fluctuation and correlation of widths can be neglected at its boundary, as will be seen from Figs 3.1 and 3.2. In Refs [43, 44] it has been shown that in the case of a large number of reaction channels with comparable magnitudes of contributions a good approximation is the modification of the Hauser-Feshbach formalism [40], suggested by Tepel et al. [43], which takes into account the effect of correlation of the entrance and the exit elastic channels. Our calculations show that at small energies  $^{242}\text{Pu}$  cross-sections  $\sigma_\gamma$ ,  $\sigma_f$  and  $\sigma_n$ , calculated by the conventional formalism [41] and those by the formalism of Ref. [43] differ considerably (Figs 3.1 and 3.2), but even at 1.1 MeV the calculated values of the cross-sections satisfactorily agree with one another. Therefore, in the region above 1.1 MeV the formalism of Ref. [43] was used.

### 3.1. Calculation of neutron penetrations

For calculations by the statistical model neutron penetrations were computed by the optical model with a spherical potential of the form

$$V(z) = -V_0 f(z) - l W_D g(z) + V_{\infty} h(z)(l \vec{\sigma}), \quad (3.1)$$

where

$$\begin{aligned} f(z) &= [1 + \exp(\frac{z-R_1}{\alpha_1})]^{-1}, \\ g(z) &= 4 \exp(\frac{z-R_2}{\alpha_2}) / [1 + \exp(\frac{z-R_1}{\alpha_1})]^2, \\ h(z) &= (\frac{\pi}{m_{xc}})^2 \frac{1}{z} \frac{df(z)}{dz}, \\ R_1 &= r_1 A^{1/3}, \quad R_2 = r_2 A^{1/3}. \end{aligned} \quad (3.2)$$

We took the following values of potential parameters which most satisfactorily describe the total interaction cross-section  $\sigma_t$  and the inelastic interaction cross-section  $\sigma_{nx}$  for the  $^{239}\text{Pu}$  nucleus:

$$\begin{aligned} W_p &= 6.490 + 0.041 E_n \text{ (MeV)}, \\ V_{so} &= 7.0 \text{ MeV}, \\ r_1 &= 1.287 \text{ fm}, \quad r_2 = 1.315 \text{ fm}, \\ Q_1 &= 0.486 \text{ fm}, \quad \alpha_1 = 0.712 \text{ fm}. \end{aligned} \quad (3.3)$$

In the case of  $^{242}\text{Pu}$ , there are practically no experimental data on optical cross-sections. Comparison of the strength functions evaluated by us  $S_0 = (0.91 \pm 0.15) \times 10^{-4}$  and  $S_1 = (2.5 \pm 0.5) \times 10^{-4}$  with the calculated values  $S_0 = 1.007 \times 10^{-4}$  and  $S_1 = 2.885 \times 10^{-4}$  shows that they agree within the errors of the evaluated quantities. The calculated potential scattering cross-section at 1 keV  $\sigma_p = 11.058 \text{ b}$  also agrees satisfactorily with the evaluated figure of 10.5 b. The calculated cross-sections  $\sigma_t$ ,  $\sigma_c$ ,  $\sigma_p$  for  $^{242}\text{Pu}$  in the 1 keV-5 MeV region are given in Fig. 3.3.

### 3.2. The level spectra of the $^{242}\text{Pu}$ , $^{243}\text{Pu}$ , $^{238}\text{U}$ and $^{239}\text{U}$ nuclei for neutron cross-section calculations

In the present work a number of calculations were performed for the  $^{238}\text{U}$  nucleus; therefore, apart from  $^{242}\text{Pu}$  and  $^{243}\text{Pu}$ , we consider the level spectra of  $^{238}\text{U}$  and  $^{239}\text{U}$ . In the case of the  $^{239}\text{U}$  and  $^{243}\text{Pu}$  nuclei, we shall confine ourselves to presenting the continuous spectrum, since consideration of the  $\gamma$ -transitions to discrete levels has little effect on  $\sigma_\gamma$ .

The discrete level spectrum of  $^{242}\text{Pu}$  was chosen from the results of Refs [45,46] since earlier studies do not provide any additional information. The data of Refs [45,46] and the level scheme adopted are given in Table 3.1. The table also presents the level scheme recommended in Ref. [47], which became available after the calculations had been made. It does not differ significantly from the scheme adopted and has no substantial effect on the results of cross-section calculations.

The level scheme for the  $^{238}\text{U}$  nucleus is taken from Ref. [29].

In the region of energies higher than the energy of the last allowed level  $E_{q \max}$ , the continuous level spectrum has to be used for the calculation of process widths. At present, the relationship of the Fermi-gas model is used most extensively

$$\rho_{\text{Fr}}(u, J, \eta) = \frac{2J+1}{4\sqrt{2\pi} \sigma^2} \rho(u) \exp\left[-\frac{(J + \gamma_1)^2}{2\sigma^2}\right], \quad (3.4)$$

where  $\rho(u)$  is the total level density:

$$\rho(u) = \frac{\sqrt{x}}{12\alpha^{1/4} u^{5/4}} \exp\left[2\sqrt{\alpha(u-\delta)}\right], \quad (3.5)$$

$$u = E + \delta_n, \quad (3.6)$$

$$\sigma^2 = \frac{6}{x^2} \langle m^2 \rangle \sqrt{\alpha(u-\delta)}. \quad (3.7)$$

These expressions contain only two parameters: the basic level density parameter  $\alpha$  and correction  $\delta$  for even-odd differences in level density, since the mean square of the magnetic quantum numbers  $\langle m^2 \rangle$  is chosen either on the basis of the quasi-classical evaluation ( $\langle m^2 \rangle = 0.24 \text{ A}^{2/3}$ ) used by us or in a form which follows from averaging  $m^2$  over the occupied states of the shell model lying below the Fermi level ( $\langle m^2 \rangle = 0.146 \text{ A}^{2/3}$ ) [48,49]. Parameter  $\alpha$  is determined from the observed density of neutron resonances  $\rho_{\text{obs}}(S_n) = 1/\langle D(S_n) \rangle_{\text{obs}}$ .

In recent years the Fermi-gas model for level density calculation has undergone substantial development, extending its range of application to a considerable extent. On the basis of the clear correlation between parameter  $\alpha$  and shell correction  $\delta W$  in the mass formula of Ref. [51], Ignatyuk et al. [50] took into account the diminution of the shell effects in level density with rise in the excitation energy, using for the purpose the expression

$$\alpha(u) = \tilde{\alpha} [1 + f(u) \delta W/u], \quad (3.8)$$

where  $f(U) = 1 - \exp(-\gamma U)$ ,  $\tilde{\alpha}$  is the asymptotic value of  $\alpha(U)$  at high excitation energies. In Ref. [52] parameter  $\tilde{\alpha}$  was represented in the form of the following dependence on mass number:

$$\tilde{\alpha} = \alpha A + \beta A^{1/2}. \quad (3.9)$$

In the present work, however, it was determined from the  $\langle D(S_n) \rangle_{obs}$  data in order to make allowance for the individual characteristics of the nuclei. The values of parameter  $\gamma$  were taken from Ref. [52].

It should be noted that the effect of the energy dependence of parameter  $\alpha$  is most substantial for nuclei near the closed shells. In the case of the nuclei studied in the present work, the magnitude of the shell corrections is relatively small and the influence of this effect will be much less.

Further development of the level density theory is associated with consideration of the contribution of collective motions of nucleons – rotational and vibrational; the need for taking them into account has been pointed out in a number of theoretical studies [53–55]. Here the expression for level density can be written in the form [56]

$$\rho(U, J, \Pi) = K_{rot} K_{vib} \rho_{sr}(U, J, \Pi), \quad (3.10)$$

where  $\rho_{sr}(U, J, \Pi)$  is determined by relation (3.4),  $K_{rot}$  and  $K_{VIB}$  are the coefficients of increase in level density due to contributions from rotational and vibrational motions. In Refs [52, 56–57] simple evaluations convenient for calculations were obtained for  $K_{rot}$  and  $K_{VIB}$ :

$$K_{rot} = F_1 I = F_1 \sqrt{U/\alpha}, \quad (3.11)$$

$$K_{vib} = \exp(0.25 U^{\gamma}), \quad (3.12)$$

where  $F_1$  is the moment of inertia of the deformed nucleus in relation to the axis perpendicular to the axis of symmetry.

The presence of a multiplier of sufficiently large magnitude in (3.10) considerably reduces parameter  $\alpha$  in comparison with the conventional expression (3.4).

At present, for the calculation of nuclear level densities an ever-increasing interest is being shown in the superfluid nucleus model, which

correctly takes into account the residual correlation-type interactions.

A simple version of this model which is convenient for calculations is suggested in Ref. [58]. In the superfluid model level density is written in the form of (3.4) [59], the difference being in the determination of  $\sigma^2$  and total density  $\rho(u)$ , which can be represented by the expression

$$\rho(u) = \frac{\exp[S(\beta, d_z, d_n)]}{(2\pi)^{3/2} |\text{Det}(\beta, d_z, d_n)|^{1/2}}, \quad (3.13)$$

where  $\beta$  is a reciprocal of thermodynamic temperature  $t$ ,  $d_{z,N} = \lambda_{z,N}\beta$  ( $\lambda_{z,N}$  represents the chemical potentials for the proton and neutron components) and  $\text{Det}(\beta, d_z, d_n)$  is the determinant from the second derivatives of entropy:

$$\text{Det}(\beta, d_z, d_n) = \begin{vmatrix} D_{\beta\beta} & D_{\beta d_z} & D_{\beta d_n} \\ D_{d_z\beta} & D_{d_z d_z} & 0 \\ D_{d_n\beta} & 0 & D_{d_n d_n} \end{vmatrix} \quad (3.14)$$

According to Ref. [58] the quantities needed for determining level density in the superfluid nucleus model can be found in the following manner:

$$S = 2\alpha \frac{t_c^2}{t} [1 - f^2(t)], \quad (3.15)$$

$$\sigma^2 = \frac{6\alpha}{\pi^2} \langle m^2 \rangle t_c [1 - f^2(t)], \quad (3.16)$$

$$U = \frac{3}{2} \alpha t_c [1 - f^2(t)] = U_c [1 - f^2(t)], \quad (3.17)$$

$$\text{Det} = \frac{18\alpha^2 t_c^8}{\pi^4} [1 + f^2(t)]^2 [1 - f^2(t)], \quad (3.18)$$

where function  $f(t)$  satisfies the equation

$$f(t) = t h \left[ \frac{t_c}{t} f(t) \right]. \quad (3.19)$$

Quantity  $t_c$  in (3.15)-(3.18) is the critical temperature which is related in the given model to the correlation function of the ground state  $\Delta_0$  as  $t_c = \Delta_0/2$ .

Above the phase transition point  $t_c$  function  $f(t) = 0$  and it is necessary to use the relations of the Fermi-gas model, where the excitation energy is related to temperature by the expression

$$U = at^2 + \frac{1}{8} 2\Delta_0^2. \quad (3.20)$$

It should be noted that in the given version of the model the magnitude of energy shift  $E_{kong}$  and the phase transition point  $t_c$  are lower than in the approximation of a constant matrix element of paired interaction ( $E_{kong} = \frac{5\alpha}{2\pi} \Delta_0$ ,  $t_c = 0.567 \Delta_0$ ). This can result in a noticeable variation in level density.

This approach is valid for even-even nuclei. However, as shown in Ref. [60], the relations of the superfluid model are also valid for odd and odd-odd nuclei if the excitation energy is defined in the following manner:

$$U = U_{\text{even}} + \begin{cases} \Delta_0 & \text{for odd nuclei,} \\ 2\Delta_0 & \text{for odd-odd nuclei} \end{cases} \quad (3.21)$$

In the present study  $\Delta_0$  was determined as  $\Delta_0 = 12.5 A^{-1/2}$  MeV [52]. Above it was assumed that the correlation functions of the ground states of the proton and neutron components were equal  $\Delta_{oz} = \Delta_{on} = \Delta_0$ .

The level density models considered lead to a different energy dependence of level density (Fig. 3.4), and this affects the cross-section values calculated by the statistical model.

In the present study we used a variant of the superfluid model with allowance for collective motions. The contribution of the rotational and vibrational motions to level density was taken into account by introducing multipliers (3.11) and (3.12) into formula (3.4).

In calculating level density by the different models for the  $^{242}\text{Pu}$ ,  $^{243}\text{Pu}$ ,  $^{238}\text{U}$  and  $^{239}\text{U}$  nuclei, we used the values of parameters given in Tables 3.2 and 3.3.

### 3.3. Description of the fission process

In the energy region under consideration it is physically justified to use, in the case of  $^{242}\text{Pu}$ , the conventional concept of the single-humped fission barrier. The fission penetrations were calculated by the Bohr-Hill-Wheeler model [65] on the assumption of a continuous spectrum of fission transition states. The total fission penetration for state  $J\pi$  of the compound nucleus at excitation energy  $E_n + S_n$  is described by the formula

$$T_{fjn}(E_n) = \int_0^{\infty} \frac{1}{1 + \exp[-\frac{2\pi(E_n - V_F - \epsilon)}{\hbar\omega_F}]} g_F(\epsilon, J, \pi) d\epsilon, \quad (3.22)$$

where

$$g_F(\epsilon, J, \pi) = C_F (2J+1) \exp\left[-\frac{(J+\frac{1}{2})^2}{2\sigma^2}\right] \exp\left(-\frac{\epsilon}{\theta_F}\right) \quad (3.23)$$

is the density of the fission transition states in the constant temperature model [49] at an energy exceeding the fission threshold by  $\epsilon$ . The fission threshold  $V_F$  calculated from the neutron binding energy was assumed to be 0.5 MeV and the curvature of all fission barriers  $\hbar\omega_F = 0.5$  MeV. The density parameters of the fission transition states were  $C_F = 0.5$ ,  $\theta_F = 0.3$ ,  $\sigma = 5.7$ . With these parameters we can satisfactorily describe the fission cross-section in the 0.2-1.1 MeV region (Fig. 3.2). Since it was not possible to achieve a good description of  $\sigma_f$  in the 0.2-5.0 MeV region by a single set of parameters, the competition between fission and the inelastic scattering and radiative capture processes in the 1.1-5.0 MeV region was taken into account by representing the fission penetrations in the form

$$T_{fjn} = (2J+1) \exp\left[-\frac{(J+\frac{1}{2})^2}{2\sigma^2}\right] T_f \quad (3.24)$$

where  $T_f$  was determined from normalization of the calculated fission cross-section to that evaluated from experimental data.

### 3.4. Radiative neutron capture by the $^{242}\text{Pu}$ nucleus

For  $^{242}\text{Pu}$  experimental data on  $\sigma_\gamma$  are available only in the region up to 80 keV [66, 67], and hence the evaluation of this cross-section has to be based on theoretical calculations. Since calculation of this cross-section is very sensitive to the level density model used, the question of choice of model must be studied on nuclei whose  $\sigma_\gamma$  has been well investigated experimentally over a wide energy region, for example  $^{238}\text{U}$  [68, 70].

The radiative capture penetration was calculated by the cascade theory of gamma-quantum emission [71] with consideration of the competition of the  $(n, \gamma n')$  and  $(n, \gamma f)$  reactions in a manner similar to Ref. [72]. In the case of the nucleus under consideration, the expression for radiative capture penetration is

$$T_{\gamma\gamma n}(E_n) = 2\pi \int \sum_{\substack{E_n + E_\gamma = E_{\gamma\gamma} \\ A+1}}^{\epsilon_n + \epsilon_\gamma = \epsilon_{\gamma\gamma}} g(E_n + E_\gamma - \epsilon_\gamma, J_{\gamma\gamma} \eta_n) f(E_n, \epsilon_\gamma) d\epsilon_\gamma. \quad (3.25)$$

Since the problem of intensity of magnetic dipole transitions is at the discussion stage, only electric dipole transitions were considered. The calculation was performed both for a spectral factor in the form proposed by Weisskopf and for a spectral factor with a Lorentz energy dependence generalized for deformed nuclei [49]

$$f(E_n, \epsilon_\gamma) \approx \frac{8}{3} \frac{N_A e^2}{A \hbar c} \frac{1.4}{m_e c^2} \sum_{i=1}^2 \frac{\Gamma_{G_i} \epsilon_\gamma^4}{(\epsilon_\gamma^2 - \epsilon_{G_i}^2)^2 + (\Gamma_{G_i} \epsilon_\gamma)^2}, \quad (3.26)$$

with the average giant resonance parameters for actinides [49]:

$$\epsilon_{G_1} = 11 \text{ MeV}, \epsilon_{G_2} = 14 \text{ MeV}, \Gamma_{G_1} = 2.9 \text{ MeV}, \Gamma_{G_2} = 4.5 \text{ MeV}.$$

The calculated values of  $\sigma_\gamma$  with the Lorentz factor were substantially higher than the experimental data [73]. However, this fact does not unambiguously lead to the conclusion that it is preferable to use the Weisskopf spectral factor. Since penetration depends on the level density of the compound nucleus, it can be assumed that the disagreement with experiment is due to the incorrectness of the level density model used. It has been shown in Ref. [74] that consideration of the collective effects in the level density of a nucleus substantially improves the agreement of the experimental data on  $\sigma_\gamma$  with the data calculated using the Lorentz spectral factor. In Ref. [74] the calculation for  $^{238}\text{U}$  was made only up to 1.0 MeV and no account was taken of the competition of the fission process. In order to choose a model for the calculation of  $\sigma_\gamma$  for the  $^{242}\text{Pu}$  nucleus, we calculated  $\sigma_\gamma$  for  $^{238}\text{U}$  in the 0.1-3.0 MeV region with allowance for the competition of fission for the different level density models with both types of spectral factor. In the calculations we used the spherical optical potential and the level scheme from Ref. [29]. The radiative capture width was normalized to the evaluated value of  $\langle \Gamma_\gamma \rangle_{\text{obs}} = 23.5 \text{ MeV}$  [75]. The calculation results are compared with the experimental data in Fig. 3.5. In the present work we did not undertake to describe in detail

the cross-section  $\sigma_\gamma$  for  $^{238}\text{U}$ , which is an independent subject of study requiring consideration of the deformation of the  $^{238}\text{U}$  nucleus and the uncertainty of experimental values  $\langle D \rangle_{\text{obs}}$  and  $\langle \Gamma_\gamma \rangle_{\text{obs}}$ . The errors in  $\langle D \rangle_{\text{obs}}$  and  $\langle \Gamma_\gamma \rangle_{\text{obs}}$  do not lead to any smaller magnitudes of error in the calculated  $\sigma_\gamma$ . Meanwhile the discrepancy in  $\langle \Gamma_\gamma \rangle_{\text{obs}}$  reaches 7% [76, 77] and that in  $\langle D \rangle_{\text{obs}}$  30% [63, 76, 78]. The calculations used  $\langle D \rangle_{\text{obs}} = 17.7$  eV [63], the value of  $\langle D \rangle_{\text{obs}}$  given in Ref. [76] being 20.8 eV. Calculation shows that the difference in  $\sigma_\gamma$  for these values of  $\langle D \rangle_{\text{obs}}$  is ~15% (Fig. 3.6).

Our analysis showed that the use of the conventional Fermi-gas model for level density results in a considerable difference between the calculated  $\sigma_\gamma$  for both the spectral factors and the experimental data (Fig. 3.5), which cannot be attributed to the uncertainty of the potential and of the values of  $\langle \Gamma_\gamma \rangle_{\text{obs}}$  and  $\langle D \rangle_{\text{obs}}$ . If we use level density with allowance for collective motions and level density from the superfluid model of the nucleus, the calculated cross-sections  $\sigma_\gamma$  exhibit a much better agreement with experiment. Consideration of the energy dependence of parameter  $\alpha$  has very little influence on calculated  $\sigma_\gamma$  in the energy region considered, for example at 3.0 MeV the difference is not higher than 4%. There is greater justification for using the spectral factor with a Lorentz dependence, as is indicated by the results of description of radiative strength functions [79] and the experimentally measured widths of the  $(n, \gamma f)$  process [72]. The calculated curve of  $\sigma_\gamma$  for the level density from the superfluid model of the nucleus and the Lorentz spectral factor generally shows better agreement with experimental data than the curve calculated by the Fermi-gas model with allowance for collective motions and the Lorentz spectral factor. However, because of some uncertainty in the parameters of the superfluid model variant used, especially in the phase transition energy, it cannot be affirmed that a similar relationship between these two calculated curves will also occur in the case of other nuclei. Calculations of  $\sigma_\gamma$  ( $^{242}\text{Pu}$ ) show (Fig. 3.7) that for  $^{242}\text{Pu}$  the cross-section  $\sigma_\gamma$  calculated using the level density from the superfluid model with consideration of collective motions is higher than that calculated for density from the Fermi-gas model with allowance for collective motions. It should be noted that when the level density from the superfluid model is used, calculation for the Weisskopf spectral factor in the region up to 1.0 MeV gives higher values of  $\sigma_\gamma$  than those obtained in case of the Lorentz spectral factor. The above uncertainty requires further studies. Therefore, in the evaluation of  $\sigma_\gamma$  ( $^{242}\text{Pu}$ ) we used the results of calculations for level densities from the Fermi-gas

model with consideration of collective motions and the Lorentz spectral factor. The radiation widths were normalized to our evaluated value of  $\langle \Gamma \rangle_{\gamma \text{ obs}} = 22.6 \text{ MeV}$ . The calculations of  $\sigma_{\gamma}^{(242\text{Pu})}$  for the different level density models are given in Fig. 3.7. It is to be noted that in the region of energies from the boundary of the discrete and continuous level spectra of the target nucleus (1.15 MeV) to 2.0 MeV the calculation gives somewhat high values of  $\sigma_{\gamma}$  because of underestimating the level density of the residual nucleus in this region. The sectors of the calculated curves in Fig. 3.7 in the 1.15–2.0 MeV region are adjusted with allowance for the general character of the energy dependence of  $\sigma_{\gamma}$ .

### 3.5. Inelastic neutron scattering by the $^{242}\text{Pu}$ nucleus

For an experimentally known fission cross-section the basic condition for reliability of calculations of the total inelastic scattering cross-section is the correct value of neutron penetrations. In the case of deformed nuclei of the  $^{242}\text{Pu}$  type the most correct description of neutron penetrations is given by the coupled channel method. However, errors in the calculations of partial cross-sections by the statistical model, which are due to the use of the spherical optical potential, can be offset to a considerable extent by renormalizing to the compound nucleus formation cross-section  $\sigma_c$  calculated by the coupled channel method.

If the calculated fission cross-section is fitted to the experimental data, the choice of the level density model will have practically no effect on the value of the total inelastic scattering cross-section. But the difference in the level density of the target nucleus from the various models leads to a change in the ratio of the scattering cross-sections at discrete and continuous level spectra and to a change in the excitation cross-sections for discrete levels (Fig. 3.8). Hence it follows that the choice of the level density model can substantially affect the characteristics of the calculated scattered neutron spectra.

## 4. CALCULATION OF THE $(n,2n)$ , $(n,3n)$ , $(n,n'f)$ AND $(n,2nf)$ CROSS-SECTIONS

The cross-sections of the  $(n,2n)$ ,  $(n,3n)$ ,  $(n,n'f)$  and  $(n,2nf)$  reactions and the neutron spectra accompanying these reactions were calculated by the statistical model with allowance for the possibility of pre-equilibrium neutron emission. The model uses the experimental data for nuclei occurring at the subsequent stages of decay of the nucleus. The method is described in detail in Ref. [80].

The formula for calculating the  $(n,2n)$  cross-section takes the form

$$\begin{aligned} \sigma_{n,2n}(E_n) = & \sigma_{n,n'x} \int_{S_{nA}}^{E_n} \left( \frac{\sigma_{nn'x}}{\sigma_{ne} - \sigma_{np}} \right)_{A-1, E-S_{nA}} \chi_p^1(E) dE \int_{S_{nA}}^{E_n-S_{nA}} \left( \frac{\sigma_{1}}{\sigma_{ne}} \right)_{A-2, E-S_{nA}} \chi_p^2(E) dE + \\ & + \sigma_{np} \int_{S_{nA}}^{E_n} \left( \frac{\sigma_{nn'x}}{\sigma_{ne} - \sigma_{np}} \right)_{A-1, E-S_{nA}} \chi_{np}^1(E) dE \int_{S_{nA}}^{E_n-S_{nA}} \left( \frac{\sigma_{1}}{\sigma_{ne}} \right)_{A-2, E-S_{nA}} \chi_{np}^2(E) dE. \end{aligned} \quad (4.1)$$

Similar formulae can be obtained for  $\sigma_{n,3n}$ ,  $\sigma_{n,n'f}$  and  $\sigma_{n,2nf}$ . Here  $\sigma_{n,n'x} = \sigma_{ne} - \sigma_{ny} - \sigma_{nf} - \sigma_{hp}$ ;  $\sigma_{ne}$ ,  $\sigma_{ny}$  are the evaluated cross-sections for nuclei occurring at the subsequent stages of decay,  $\sigma_{hp}$  the cross-section with emission of the first neutron from a nucleus not in equilibrium  $\chi_p^n(E)$  the spectrum of the residual excitations of the nucleus after the emission of the n-th neutron: case (p) - the first neutron is emitted from an equilibrium nucleus, case (hp) - the first neutron is emitted from a nucleus which has not attained statistical equilibrium. In the case of the  $^{242}\text{Pu}$  nucleus, the contribution of the pre-equilibrium processes to the inelastic interaction cross-section was calculated as in Ref. [80], and was found to be 7% for the incident neutron energy of 7 MeV, 12% for 9 MeV, 16% for 12 MeV and 20% for 15 MeV.

The evaluated cross-sections for  $^{241}\text{Pu}$ ,  $^{240}\text{Pu}$  and  $^{239}\text{Pu}$  and all constants needed for the calculations were taken from our evaluated data files.

Figure 4.1 gives the calculations of the  $(n,2n)$  and  $(n,3n)$  cross-sections for  $^{242}\text{Pu}$  and compares them with the evaluations of Refs [14, 81].

The calculation results for the  $(n,n'f)$  and  $(n,2nf)$  reactions and the secondary neutron spectra are given in the paper dealing with the evaluation of the angular and energy distributions of secondary neutrons for  $^{242}\text{Pu}$ .

## 5. EVALUATED CROSS-SECTIONS FOR $^{242}\text{Pu}$ IN THE 0.2-15 MeV REGION

The evaluated cross-section  $\sigma_f$  was obtained in Section 1. As evaluated data on the total interaction cross-section  $\sigma_t$ , the compound nucleus formation cross-section and the potential elastic scattering cross-section, we used the coupled channel data (Section 2), which are connected in the low-energy region (0.2 MeV) with the results of cross-section calculation from strength functions evaluated by us in the region of unresolved resonances. For evaluation of  $\sigma_\gamma$  and  $\sigma_n$ , and the elastic scattering cross-section through the compound nucleus we used the results of the statistical model

calculations (Section 3) renormalized to the evaluated compound nucleus formation cross-section and connected in the low-energy region (0.2 MeV) with the cross-sections calculated from strength functions in the region of unresolved resonances. During renormalization we took into account the change in  $\sigma_f$  used in considering the competition of the fission process. The cross-sections of direct excitation of the first two levels were taken from the coupled channel calculations. The cross-sections for the  $(n,2n)$  and  $(n,3n)$  processes were obtained in Section 4. In the high energy region it is necessary to take into account the contribution of direct and semi-direct mechanisms to  $\sigma_\gamma$ . Since this contribution varies little in the case of neighbouring nuclei, in order to take it into account we used the  $^{238}\text{U}$  data in the high-energy region [82-84], which agree with the calculation by the formula proposed by Lane and Lynn [85]

$$\sigma_\gamma^{\text{np}} = k \frac{Z^2}{A} \left( \frac{E+4}{E_{\gamma^*}} \right)^3, \quad (5.1)$$

where  $k \sim 10^{-3}$ , E is expressed in MeV and  $\sigma_\gamma^{\text{np}}$  in mb.

The evaluations of cross-sections  $\sigma_t$ ,  $\sigma_n$ ,  $\sigma_\gamma$ ,  $\sigma_{n'}$ ,  $\sigma_{n,2n}$  and  $\sigma_{n,3n}$  in the 0.2-15 MeV region are given in Tables 5.1 and 5.2.

Cross-sections  $\sigma_f$ ,  $\sigma_{n,2n}$  and  $\sigma_{n,3n}$  are compared with the results of other evaluations in Section 1.4. The comparison of cross-sections  $\sigma_\gamma$  and  $\sigma_n$ , is given in Figs 5.1 and 5.2.

REFERENCES

- [1] ALKHAZOV, I.D., KASATKIN, V.P., KOSTOCHKIN, O.I., MALKIN, L.Z., PETRZHAK, K.A., FOMICHEV, A.V., SHKAPOV, V.I., in: Proceedings of the Third All-Union Conference on Neutron Physics, Kiev, parts 6 and 9, (1975) (in Russian).
- [2] KUPRIYANOV, V.M., FURSOV, B.I., MASLENNIKOV, B.K., SURIN, V.M., SMIRENKO, G.N., At. Energ. 46 (1979) 35.
- [3] MEADOWS, J.W., Proc. of the NEANDC/NEACRP Specialist Meeting on Fast Fission Cross-Sections, held at ANL, June 28-30 (1976).
- [4] BEHRENS, J.W., NEWBURY, R.S., MANAGA, J.W., Nucl. Sci. Eng., 66 (1978) 433.
- [5] AUCHAMPAUGH, G.F., FARRELL, J.A., BERGEN, D.W., Nucl. Phys., A171 (1971) 31.
- [6] BERGEN, D.W., FULLWOOD, R.R., Nucl. Phys., A163 (1971) 577.
- [7] POMUSHKIN, Eh.F., GUTNIKOVA, E.K., Yad. Fiz. 10 (1969) 917.
- [8] POMUSHKIN, Eh.F., GUTNIKOVA, E.K., ZAMYATNIN, Yu.S., MASLENNIKOV, B.K., BELOV, V.N., SURIN, V.M., NASYROV, F., PASHKIN, N.F., Yad. Fiz. 5 (1967) 966.
- [9] BUTLER, D.K., Phys. Rev., 117 (1960) 1305.
- [10] KON'SHIN, V.A., SUKHOVITSKIJ, E.Sh., ZHARKOV, V.F., Determination of errors in evaluated data allowing for correlations and the evaluation of  $\sigma_f(^{235}\text{U})$ ,  $\alpha(^{235}\text{U})$ ,  $\alpha(^{239}\text{Pu})$  and  $\sigma_f(^{239}\text{Pu})$  for BOYaD-3. Report, Institute of Heat and Mass Exchange, Byelorussian SSR Academy of Sciences (1978) (in Russian).
- [11] KNITTER, M.H., PAULSER, A., LISKIEN, H., ISLAM, M.M., Atomkern-energie, 22 (1973) 84.
- [12] BATENKOV, O.I., BLINOV, M.V., VITENKO, V.A., KRISYUK, I.T., TUZ, V.T., in: Proceedings of the Third All-Union Conference on Neutron Physics, Kiev, part 5 (1975) 114 (in Russian).
- [13] CANER, M., YIFTAH, S., IA-1275 (1973).
- [14] LAGRANGE, Ch., JARY, J., NEANDC(E)198"l", INDC(FR)30/L (1978).
- [15] BOHR, A., MOTTELSON, B., Kgl. Danske Vidensk. Selsk., Mat.-Fys. Medd., 27 (1953) 16.
- [16] TAMURA, T., Rev. of Mod. Phys., 37 (1965) 679.
- [17] BASSEL, R.H., SATCHLER et al., Phys. Rev., 110 (1958) 1080.
- [18] MARGOLIS, B., TROUBETZKOY, E.S., Phys. Rev., 106 (1957) 105.
- [19] CHASE, D.M., WILETS, L., EDMONDS, A.R., Phys. Rev., 110 (1958) 1080.
- [20] YOSHIDA, S., Proc. Phys. Soc. (London), A69 (1956) 668.

- [21] BUCK, B., Phys. Rev., 130 (1963) 712.
- [22] LAGRANGE, Ch., Proc. of the EANDC Topical Discussion on "Critique of Nuclear Models and Their Validity in the Evaluation of Nuclear Data", (1975) 58.
- [23] KIKUCHI, Ya., Proc. of a Panel on Neutron Nuclear Data Evaluation, Vienna, (1971) 305.
- [24] IGNATYUK, A.V., LUNEV, V.P., SHORIN, V.S., in: Problems of Atomic Science and Technology, Ser. "Nuclear Constants", No. 13 (1974) 59 (in Russian).
- [25] DZYUBA, B.M., MARSHALKIN, V.E., POVYSHEV, V.M., TYAPIN, A.S., in: Problems of Atomic Science and Technology, Ser. "Nuclear Constants", No. 23 (1976) 147 (in Russian).
- [26] DELAROCHE, J.P., LAGRANGE, Ch., SALVY, J., Nuclear Theory in Neutron Nuclear Data Evaluation, IAEA-190 1 (1976) 251.
- [27] HAOUAT, G., LACHKAR, J., LAGRANGE, Ch., PATIN, Y., SIGAUD, J., SHAMU, R.E., NEANDC (E)-196 "L", INDC (FR)-29/L, (1978).
- [28] HAOUAT, G., SIGAUD, J., LACHKAR, J., LAGRANGE, Ch., DUCHEMIN, B., PATIN, Y., NEANDC (E) 180 "L", INDC (FR)-13/L, (1978).
- [29] LAMBROPOULOS, P., Nucl. Sci. Eng., 46 (1971) 356.
- [30] BEMIS, C.E., Jr., McGOWAN, F.K., FORD, J.L.C., Jr., MILNER, W.T., STELSON, P.H. and ROBINSON, R.L., Phys. Rev., C8, (1973) 1466.
- [31] COOPER T. et al. Phys. Rev., 13, (1976) 1083.
- [32] HENDRIE, D.L., et al., Phys. Rev. Lett., 30 (1973) 571.
- [33] MOSS, J.M., et al., Phys. Rev. Lett., 26 (1971) 1488.
- [34] STRUTINSKY, V.M., "Shells" in Deformed Nuclei, Nucl. Phys. A122 (1968).
- [35] NILSSON, S.G., TSANG, C.F. et al., Nucl. Phys., A131 (1969) 1.
- [36] GAREEV, F.A., IVANOVA, S.P., PASHKEVICH, V.V., Yad. Fiz. 11 (1970) 1200.
- [37] GOETZ, U., PAULI, H.C., et al., Nucl. Phys., A192 (1972) 1.
- [38] PAULI, H.C., Phys. Rev., 7C (1973) 35.
- [39] BRAID, T.H., et al., Phys. Rev., (1970) 1C, 275; 4 (1971) 247.
- [40] HAUSER, W., FESHBACH, H., Phys. Rev., 87 (1952) 366.
- [41] LANE, A.M., LYNN, J.E., Proc. Phys. Soc., A70 (1957) 557.
- [42] PORTER, C.E., THOMAS R.G., Phys. Rev., 104 (1956) 483.
- [43] TEPEL, J.W., HOFMANN, H.M., WEIDENMÜLLER, H.A., Phys. Lett., 49B (1974) 1.
- [44] MOLDAUER, P.A., Phys. Rev., C14 (1976) 764.
- [45] MAHER, J.V., ERSKINE, J.R., FRIEDMAN, A.M., SIEMSSEN, R.H., SCHIFFER, J.P., Phys. Rev., C5 (1972) 1380.

- [46] ELZE, Th.W., HUIZENGA, J.R., Nucl. Phys., A187 (1972) 545.
- [47] Evaluation from Nuclear Data Sheets (1977).
- [48] MALYSHEV, A.V., Level Density and Structure of Atomic Nuclei, Atomizdat, Moscow (1969) (in Russian).
- [49] LYNN, J.E., AERE-R7468 (1974).
- [50] IGNATYUK, A.V., SMIRENKO, G.N., TISHIN, A.S., Yad. Fiz. 23 (1975) 485.
- [51] MYERS, W.D., SWIATECKI, W.S., Ark. Fysik, 36 (1967) 593.
- [52] IGNATYUK, A.V., ISTEKOV, K.K., SMIRENKO, G.N., in: Proceedings of the Fourth All-Union Conference on Neutron Physics, Kiev, part 1 (1977) 60 (in Russian).
- [53] SOLOVIEV, V.G., MALOV, L.A., Nucl. Phys., A196 (1972) 433.
- [54] BJORNHOLM, S., BOHR, A., MOTTELSON, B., Physics and Chemistry of Fission, IAEA, Vienna (1974) 1 367.
- [55] MALOV, L.A., SOLOVIEV, V.G., VORONOV, V.V., Nucl. Phys., A224 (1974) 396.
- [56] BLOKHIN, A.I., IGNATYUK, A.V., SOKOLOV, Yu.V., in: Proceedings of the Third All-Union Conference on Neutron Physics, Kiev, part 3 (1975) 8 (in Russian).
- [57] IGNATYUK, A.V., Nuclear Theory in Neutron Nuclear Data Evaluation, IAEA, Vienna (1976) 1 211.
- [58] IGNATYUK, A.V., SHUBIN, Yu.N., Izv. Akad. Nauk SSSR, Ser. Fiz. 37 (1973) 1947.
- [59] IGNATYUK, A.V., SOKOLOV, Yu.V., SHUBIN, Yu.N., Yad. Fiz. 18 (1973) 989.
- [60] IGNATYUK, A.V., SOKOLOV, Yu.V., in: Proceedings of the Second All-Union Conference on Neutron Physics, Kiev, part 2 (1976) 32 (in Russian).
- [61] GILBERT, A., CAMERON, A.G.W., Can. J. Phys., 43 (1965) 1446.
- [62] KRAVTSOV, V.A., Atomic Masses and Binding Energies of Nuclei, Atomizdat, Moscow (1974) (in Russian).
- [63] MUGHABGHAB, S.F., GARBER, D.I., BNL-325, 3 ed (1973).
- [64] ANTSIPOV, G.V., KON'SHIN, V.A., MOROGOVSKIY, G.B., SUKHOVITSKIY, E.Sh., in: Nuclear Constants No. 25 (1977) 32 (in Russian).
- [65] HILL, D.L., WHEELER, J.A., Phys. Rev., 89 (1953) 1102.
- [66] HOCKENBURY, R.W., SANISLO, A.J., KANSHAL, N.N., Proc. Conf. on Neutron Cross-Section and Technology, Washington, 2 (1975) 584.
- [67] WISSAK, K., KAPPELER, F., Nucl. Sci. Eng., 66 (1978) 363.
- [68] YOENITZ, W.P., Nucl. Sci. Eng., 57 (1975) 300.

- [69] LINDNER, M., NAGLE, R.J., LANDRUM, H.J., Nucl. Sci. Eng., 59 (1976) 381.
- [70] HANNA, R.C., and ROSE, B., J. Nucl. En., 8 (1959) 197.
- [71] BLATT, J., WEISSKOPF, V., Theoretical Nuclear Physics, Foreign Languages Publishing House, Moscow (1954) (Russian translation).
- [72] SUKHOVITSKIJ, E.Sh., KLEPATSKIJ, A.B., KON'SHIN, V.A., ANTSIPOV, G.V., in: Proceedings of the Fourth All-Union Conference on Neutron Physics, Moscow, part 4 (1977) 68 (in Russian).
- [73] FRICKE, M.P., et al., Nuclear Data for Reactors, IAEA, Vienna 2 (1970) 265.
- [74] BLOKHIN, A.I., IGNATYUK, A.V., PLATONOV, V.P., TOLSTIKOV, V.A., Preprint FEhI-655 (in Russian).
- [75] USA Nuclear Data Library ENDF/B-IV.
- [76] RAHN, et al., Phys. Rev., 6 (1972) 1854.
- [77] ROSEN, J., DESJARDINS, J.S., RAINWATER, J., HAVENS, W.W., Phys. Rev., 118 (1960) 687.
- [78] DE SAUSSURE, G., OLSEN, D.K., PAREZ, R.B., DIFILIPPO, F.C., ORNL/TM-6152 (ENDF-257) (1978).
- [79] BARTHOLOMEW, et al., Advance Nuclear Physics 7 (1974) 232.
- [80] KON'SHIN, V.A., ANTSIPOV, G.V., SUKHOVITSKIJ, E.Sh., BAKHANOVICH, L.A., KLEPATSKIJ, A.B., MOROGOVSKIJ, G.B., PORODZINSKIJ, Yu.V., Evaluation of  $^{241}\text{Pu}$  nuclear data in the  $10^{-3}$  eV-15 MeV neutron energy region. Preprint, Institute of Heat and Mass Exchange, Byelorussian SSR Academy of Sciences, part 5 (1979) (in Russian).
- [81] BAXMAN, C.I., YOUNG, P.G., LA - 7482 - PR (1978).
- [82] PERKIN, J.L., O'CONNOR, L.P., COLEMAN, R.F., Proc. Phys. Soc., 72 (1958) 505.
- [83] BARRY, J.F., BUNCE, J., WHITE, P.H., J. Nucl. Energy, A/B18 (1964) 48.
- [84] PANITKIN, Yu.G., SHERMAN, L.E., At. Ehnerg. 39 (1975) 17.
- [85] LANE, A.M., LYNN, J.E., Nucl. Phys., 11 (1959) 646.

Table 1.1

Evaluated values of  $\sigma_s(^{242}\text{Pu})$ ,  $\sigma_t(^{235}\text{U})$  and  
 $\sigma_s(^{242}\text{Pu})/\sigma_t(^{235}\text{U})$  in the 0.1-15 MeV region

$E_n, \text{MeV}$	$\sigma_s(^{242}\text{Pu}), \text{b}$	$\sigma_t(^{235}\text{U}), \text{b}$	$\sigma_s(^{242}\text{Pu})/\sigma_t(^{235}\text{U})$
	1	2	3
0,10	0,070	1,555	0,006
0,12	0,012	1,522	0,006
0,14	0,014	1,478	0,009
0,16	0,017	1,438	0,012
0,18	0,020	1,399	0,014
0,20	0,023	1,366	0,017
0,22	0,027	1,336	0,020
0,24	0,033	1,311	0,025
0,26	0,038	1,289	0,029
0,28	0,044	1,270	0,035
0,30	0,053	1,250	0,042
0,32	0,061	1,233	0,049
0,34	0,072	1,221	0,059
0,36	0,080	1,215	0,066
0,38	0,091	1,214	0,075
0,40	0,102	1,212	0,084
0,42	0,116	1,205	0,096
0,44	0,130	1,196	0,109
0,46	0,153	1,186	0,129
0,48	0,179	1,176	0,152
0,50	0,206	1,166	0,177
0,55	0,277	1,146	0,242
0,60	0,359	1,128	0,313
0,65	0,451	1,113	0,405
0,70	0,555	1,105	0,502
0,75	0,667	1,101	0,604
0,80	0,800	1,117	0,716
0,85	0,972	1,144	0,850
0,90	1,122	1,180	0,951
0,95	1,239	1,204	1,029
1,00	1,335	1,215	1,099
1,10	1,452	1,220	1,190

Table 1.1 continued

I	1	2	3	4
I,20	I,447	I,226	I,180	
I,40	I,389	I,299	I,116	
I,60	I,388	I,258	I,103	
I,80	I,424	I,276	I,116	
2,00	I,448	I,284	I,128	
2,20	I,415	I,275	I,110	
2,40	I,381	I,259	I,097	
2,60	I,380	I,239	I,114	
2,80	I,385	I,222	I,133	
3,00	I,378	I,205	I,144	
3,20	I,368	I,193	I,147	
3,40	I,356	I,182	I,147	
3,60	I,343	I,171	I,147	
3,80	I,329	I,159	I,147	
4,00	I,314	I,147	I,146	
4,50	I,275	I,117	I,141	
5,00	I,239	I,087	I,139	
5,50	I,251	I,052	I,189	
6,00	I,446	I,139	I,270	
6,50	I,750	I,386	I,263	
7,00	I,934	I,600	I,209	
7,50	2,037	I,755	I,161	
8,00	2,094	I,820	I,151	
8,50	2,112	I,824	I,158	
9,00	2,106	I,812	I,162	
9,50	2,087	I,800	I,159	
10,00	2,064	I,786	I,156	
10,50	2,014	I,776	I,151	
11,00	2,022	I,770	I,142	
11,50	2,002	I,750	I,139	
12,00	I,985	I,768	I,123	
13,00	2,025	I,922	I,054	
14,00	2,134	2,071	I,030	
15,00	2,163	2,108	I,026	

Table 1.2

Evaluated uncertainties in the values of  
 $\bar{\sigma}_f(^{242}\text{Pu})/\bar{\sigma}_f(^{235}\text{U})$  and  $\bar{\sigma}_f(^{242}\text{Pu})$

E, MeV	$\Delta \frac{\bar{\sigma}_f(^{242}\text{Pu})}{\bar{\sigma}_f(^{235}\text{U})}, \%$	$\Delta \bar{\sigma}_f(^{242}\text{Pu}), \%$
0,1	6,0	6,7
0,5	4,7	5,6
1 - 7	3,0	4,3
9	3,5	4,6
11	4,0	5,0
13	4,5	5,4
15	5,0	5,8

Table 2.1

Comparison of theoretical data and data evaluated from  
experiments on  $S_0$ ,  $S_1$ ,  $R'$  for  $^{238}\text{U}$

Obtained by	$S_0, 10^{-4}(\text{eV})^{-1/2}$	$S_1, 10^{-4}(\text{eV})^{-1/2}$	$R', \Phi$
Evaluation	$1,0 \pm 0,1$	$1,92 \pm 0,30$	$9,4 \pm 0,3$
Calculation	1,06	2,16	9,23

Table 2.2

Values of deformation parameters for  $^{238}\text{U}$  and  $^{242}\text{Pu}$

Nucleus	Nilsson's calculation [35]		Goetz's calculation [37]		Experiment of Ref. [32]	
	$\beta_{20}$	$\beta_{40}$	$\beta_{20}$	$\beta_{40}$	$\beta_{20}$	$\beta_{40}$
$^{238}\text{U}$	0.222	0.065	0.228	0.063	$0.20 \pm 0.01$	$0.06 \pm 0.01$
$^{242}\text{Pu}$	0.234	0.055	0.240	0.048	-	-
Nucleus	Experiment of Ref. [33]		Calculation by the coupled channel method		Used in the present evaluation	
$^{238}\text{U}$	$0.27 \pm 0.01$	0.017	$0.216 \pm 0.02$		0.216	
$^{242}\text{Pu}$	-	-	-		0.216	

Table 3.1  
Discrete level spectrum of the  $^{242}\text{Pu}$  nucleus

Maher et al. [45]		Elze et al. [46]		[47]		Present work	
$E_\gamma, \text{keV}$	$\Gamma \text{n}$						
0	0+	0	0+	0	0+	0	0+
45	2+	46	2+	44,54	2+	46	2+
146	4+	148	4+	147,2	4+	148	4+
		308	6+	305,9	6+	308	6+
		.519	8+	517,6	8+	519	8+
				778,7	I0+		
		781	I-	780,3	(I-)	781	I-
		833	3-	832,3	3-	833	3-
		865		865		865	/ I-/
		927	5-	927	(5-)	927	5-
956	0+			956	(0+)	956	0+
				985,6			
995	(2+)	992		995	(2+)	995	(2+)
		I020	3-	I019,4	3-	I020	3-
				I039,6			
				I064,0	(4-)		
				I086,7	I2+		
II07		II02	(2+)	II02	(2+)	II02	(2+)
		II22	(5-)	II22	(5-)	II22	(5-)
				II52,2	(2-)		
		I204		I204			
		I259		I259			
		I501		I501			
		I613		I613			
		I638		I638			
		I650	(3-)	I650			
		I683		I683			
		I701		I701			
		I776		I776			
		I825		I825			
				I826,5	'4+,5+)		
				2092,3			
				2437,5			

Table 3.2  
Values of  $\langle D \rangle_{\text{obs.}}$ ,  $S_n$  and level density parameters  
for  $^{242}\text{Pu}$ ,  $^{243}\text{Pu}$ ,  $^{238}\text{U}$  and  $^{239}\text{U}$

Compound nucleus	$\langle D \rangle_{\text{obs.}}$ , eV	$\delta W$ , MeV [51]	$\delta$ , MeV [61]	$S_n$ , MeV [62]
$^{238}\text{U}$	2,5 / 49 /	- I,39	I,I2	6,143
$^{239}\text{U}$	I7,7 / 63 /	- I,35	0,69	4,804
$^{242}\text{Pu}$	I,34 / 64 /	- I,8	I,II	6,301
$^{243}\text{Pu}$	I4,23	- I,9	0,6I	5,037

Table 3.3

Values of parameter  $\alpha$  for the various level density models

Model	$^{238}\text{U}$	$^{239}\text{U}$	$^{242}\text{Pu}$	$^{243}\text{Pu}$
1	2	3	4	5
Fermi-gas	31.09	33.26	29.13	31.81
Fermi-gas with consideration of dependence $\alpha(u)$ <sup>*/</sup>	33.28	35.59	31.83	35.00
Fermi-gas with consideration of collective modes	19.10	20.07	17.74	19.25
Fermi-gas with consideration of dependence $\alpha(u)$ and collective modes <sup>*/</sup>	20.35	21.37	19.26	21.04
Superfluid model with consideration of collective modes	21.63	21.10	19.20	20.05

<sup>\*/</sup> In the case of level density models with consideration of dependence  $\alpha(u)$ , the asymptotic value of  $\alpha$  is given.

Table 5.1  
 Evaluated data on  $^{242}\text{Pu}$  cross-sections in  
 the 0.2-15.0 MeV region

E, MeV	$\sigma_t, \text{b}$	$\sigma_{n+}, \text{b}$	$\sigma_p, \text{b}$	$\sigma_n, \text{b}$	$\sigma_{n,2n}, \text{b}$	$\sigma_{n,3n}, \text{b}$
0.20	11.751	10.561	0.186	0.981		
0.22	11.508	10.286	0.179	1.016		
0.24	11.271	10.018	0.172	1.048		
0.26	11.019	9.736	0.166	1.079		
0.28	10.772	9.469	0.160	1.099		
0.30	10.523	9.196	0.156	1.110		
0.32	10.259	8.907	0.153	1.138		
0.34	9.992	8.612	0.151	1.157		
0.36	9.747	8.343	0.150	1.174		
0.38	9.520	8.088	0.149	1.192		
0.40	9.281	7.818	0.149	1.212		
0.42	9.092	7.598	0.149	1.229		
0.44	8.921	7.397	0.149	1.245		
0.46	8.745	7.186	0.149	1.257		
0.48	8.589	6.994	0.149	1.267		
0.50	8.453	6.819	0.149	1.279		
0.55	8.195	6.467	0.149	1.302		
0.60	7.956	6.132	0.149	1.316		
0.65	7.773	5.852	0.148	1.322		
0.70	7.621	5.598	0.147	1.321		
0.75	7.475	5.304	0.140	1.364		
0.80	7.339	5.029	0.132	1.378		
0.85	7.227	4.763	0.123	1.369		
0.90	7.146	4.545	0.112	1.367		
0.95	7.067	4.354	0.105	1.369		
1.00	7.002	4.187	0.100	1.380		
1.10	6.894	3.910	0.092	1.440		
1.20	6.813	3.758	0.086	1.522		
1.40	6.789	3.610	0.080	1.716		
1.60	6.837	3.473	0.076	1.900		

Table 5.1 continued

	1	2	3	4	5	6	7
1,00	6,960	3,435	0,070	2,031			
2,00	7,152	3,512	0,061	2,131			
2,20	7,331	3,604	0,051	2,201			
2,40	7,475	3,802	0,040	2,252			
2,60	7,589	3,931	0,030	2,248			
2,80	7,665	4,046	0,021	2,213			
3,00	7,713	4,141	0,016	2,179			
3,20	7,740	4,214	0,013	2,145			
3,40	7,764	4,293	0,011	2,104			
3,60	7,768	4,324	0,009	2,092			
3,80	7,757	4,339	0,008	2,081			
4,00	7,745	4,354	0,007	2,070			
4,50	7,646	4,315	0,006	2,049			
5,00	7,400	4,129	0,005	2,028			
5,50	7,179	3,929	0,005	1,991			
6,00	6,952	3,724	0,005	1,777	0,0		
6,50	6,748	3,536	0,005	1,455	0,002		
7,00	6,559	3,350	0,005	1,226	0,035		
7,50	6,391	3,216	0,005	0,988	0,145		
8,00	6,232	3,071	0,004	0,668	0,395		
8,50	6,078	2,932	0,004	0,443	0,587		
9,00	5,917	2,813	0,004	0,363	0,651		
9,50	5,835	2,711	0,004	0,348	0,685		
10,00	5,723	2,607	0,004	0,328	0,720		
10,50	5,676	2,568	0,004	0,317	0,743		
11,00	5,650	2,553	0,004	0,313	0,758		
11,50	5,645	2,572	0,004	0,309	0,765	0,0	
12,00	5,649	2,592	0,004	0,302	0,765	0,001	
13,00	5,677	2,675	0,004	0,289	0,514	0,170	
14,00	5,725	2,763	0,004	0,288	0,256	0,280	
15,00	5,775	2,825	0,004	0,238	0,172	0,323	

Table 5.2

## Discrete level excitation cross-sections for $^{242}\text{Pu}$

Table 5.2 continued

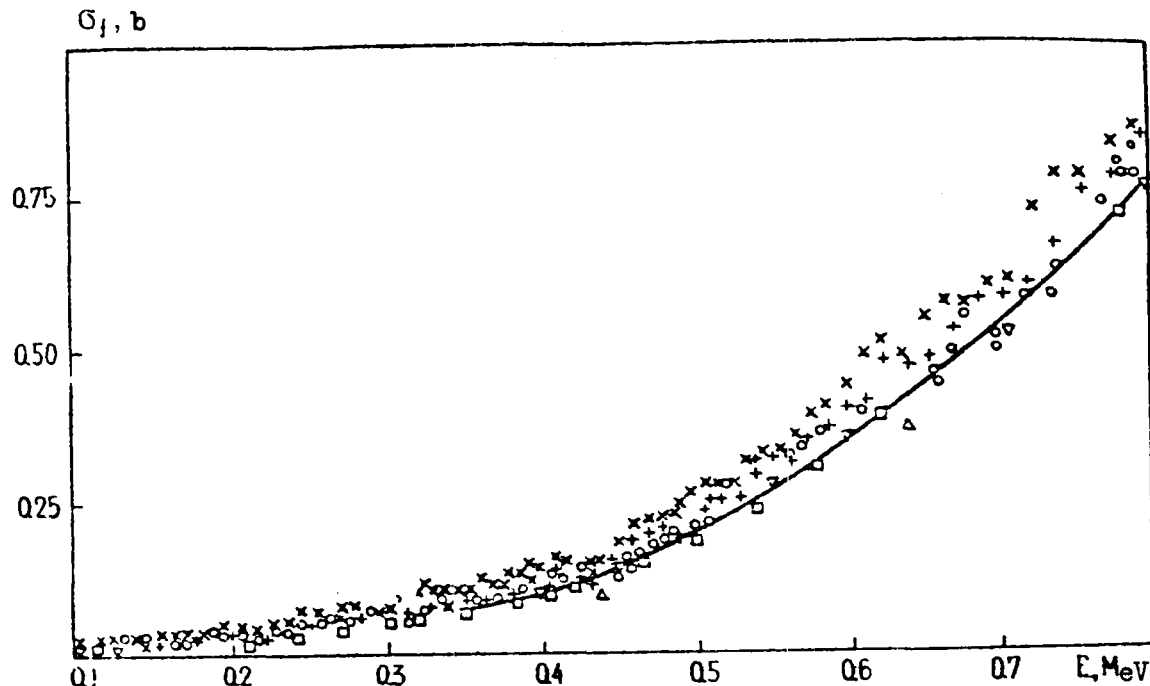


Fig. 1.1. Experimental and evaluated data on  $\sigma_f(^{242}\text{Pu})$  in the 0.1-0.8 MeV region: -evaluated data,  $\square$  -Kupriyanov et al. [2];  $\nabla$  -Meadows [3],  $+$  -Behrens et al. [4],  $\bullet$  -Auchampaugh et al. [5],  $x$  -Bergen et al. [6]  $\Delta$  -Fomushkin and Gutnikova [7],  $\circ$  -Butler [9]  $\bullet$  -Fomushkin et al.[8],  $\blacksquare$  -Alkhazov et al. [1],  $\oplus$  -renormalized data of Behrens et al. [4].

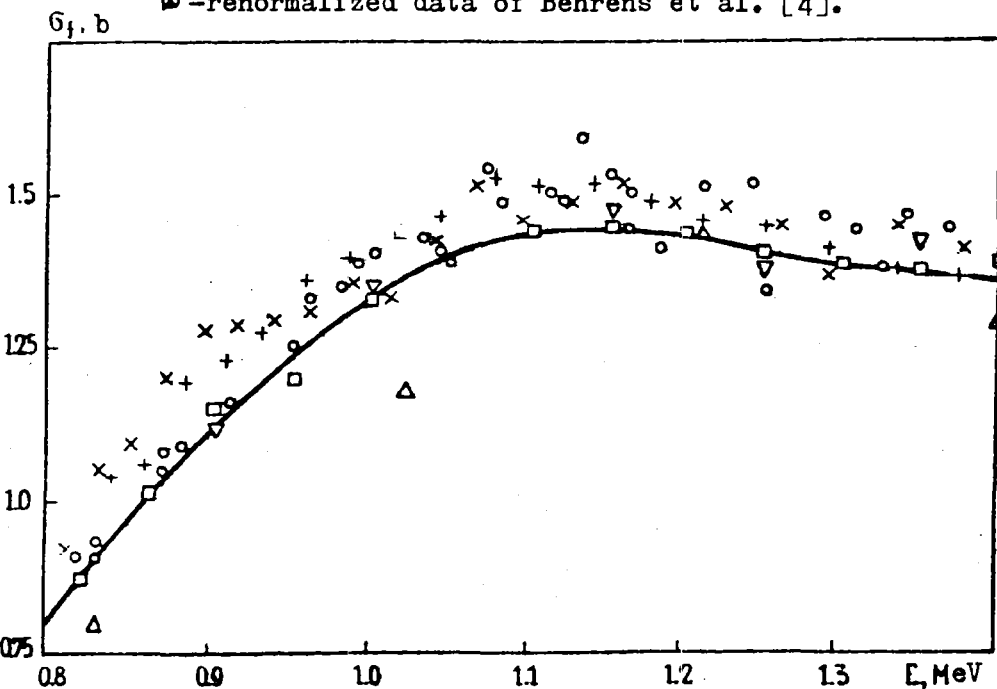


Fig. 1.2. Experimental and evaluated data on  $\sigma_f(^{242}\text{Pu})$  in the 0.8-1.4 MeV region (notations as in Fig. 1.1).

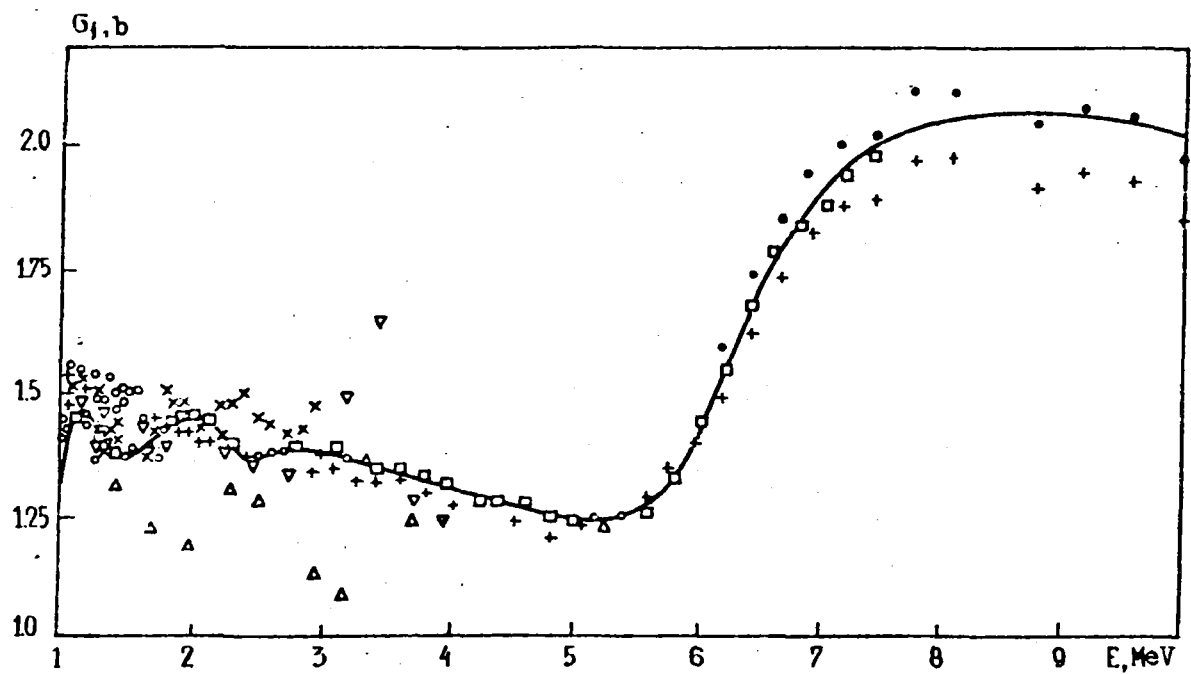


Fig. 1.3. Experimental and evaluated data on  $\sigma_f(^{242}\text{Pu})$  in the 1-10 MeV region (notations as in Fig. 1.1).

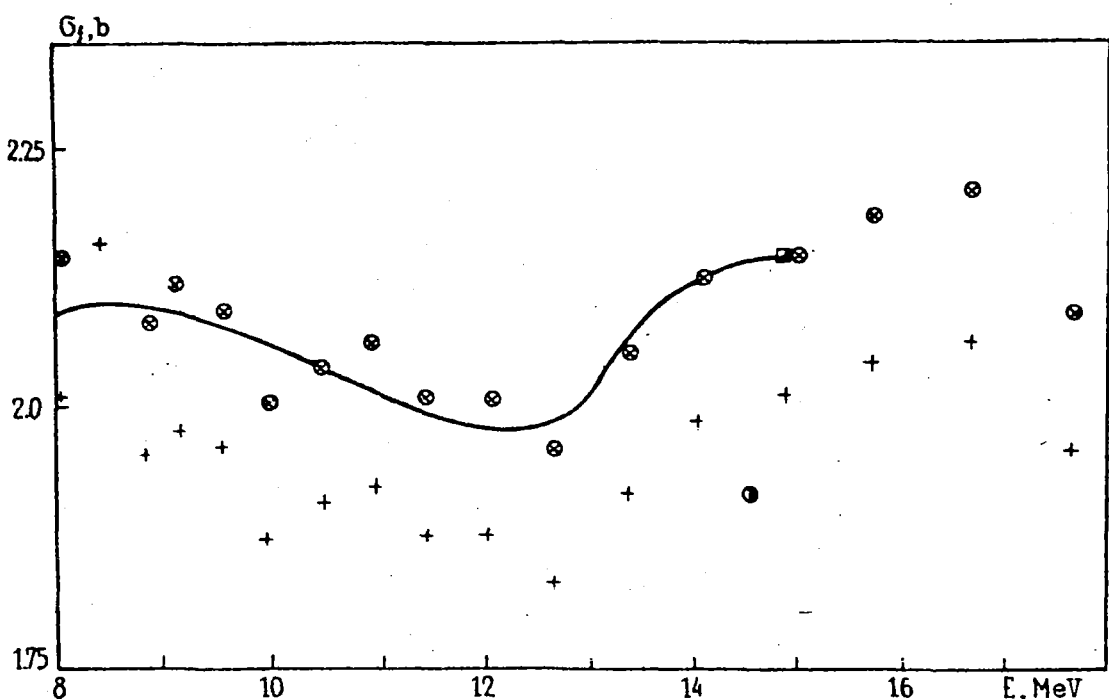
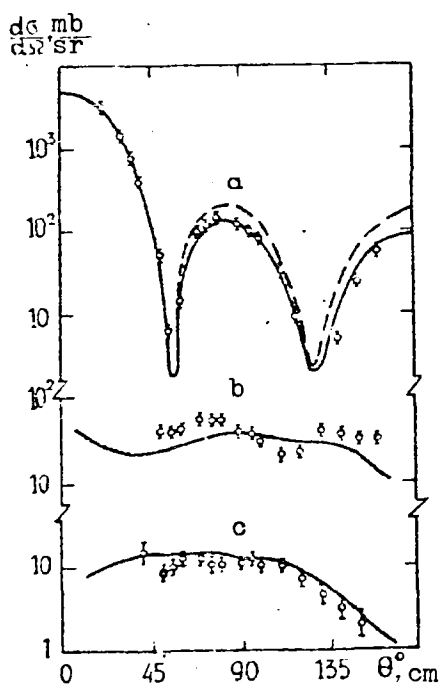
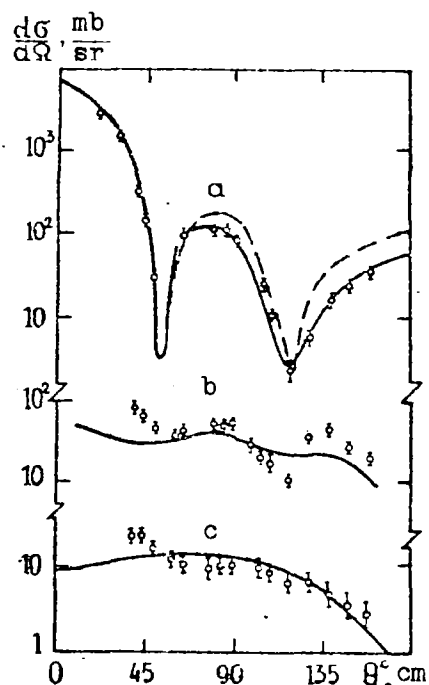


Fig. 1.4. Experimental and evaluated data on  $\sigma_f(^{242}\text{Pu})$  in the 8-15 MeV region (notations as in Fig. 1.1).



**Fig. 2.1.** Comparison of calculated and experimental (○) data on angular distributions of 2.5 MeV neutrons scattered at levels (a -  $0^+$ , b -  $2^+$ , c -  $4^+$ ) of the main rotational band of the  $^{238}\text{U}$  nucleus: — present work; - - - calculation by the spherical potential of Lambropoulos [29]



**Fig. 2.2.** Comparison of calculated and experimental data on angular distributions of 3.4 MeV neutrons scattered by the  $^{238}\text{U}$  nucleus (for notations see Fig. 2.1).

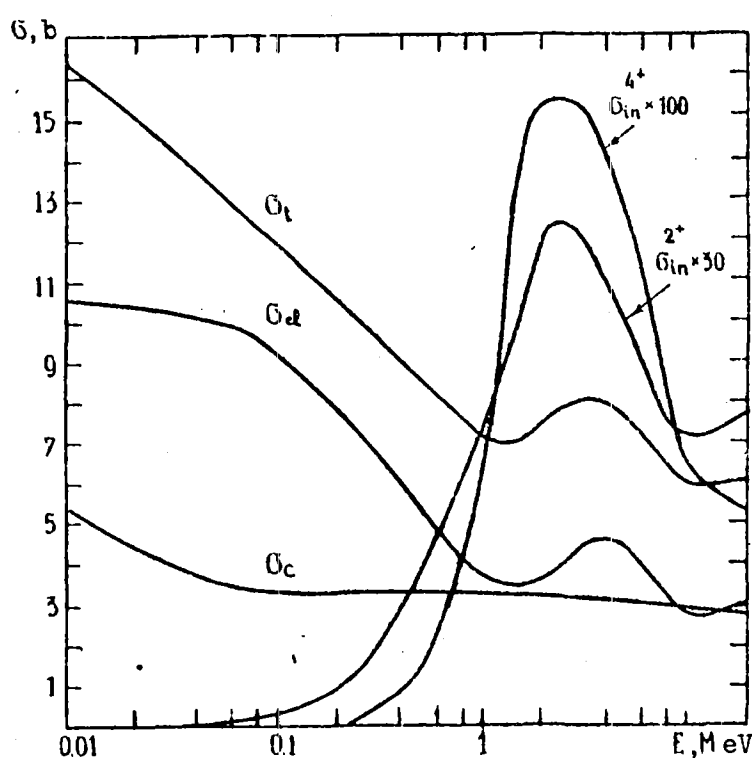


**Fig. 2.3.** Cross-sections of interaction of neutrons with the  $^{242}\text{Pu}$  nucleus in the 0.01-15 MeV region calculated by the coupled channel method.

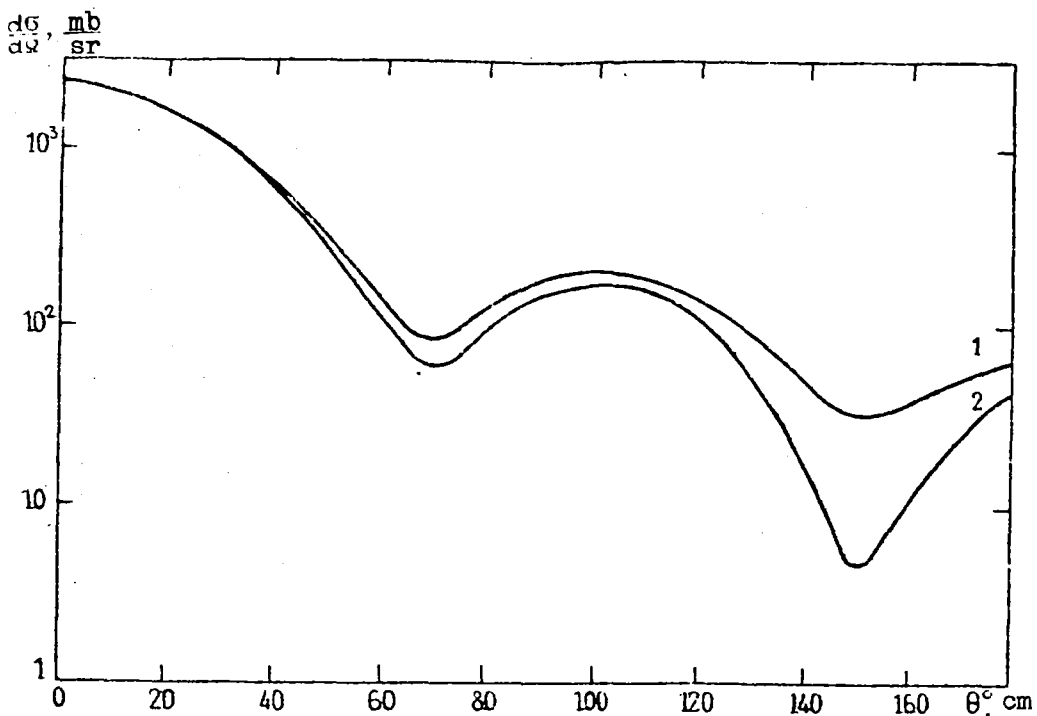


Fig. 2.4. Angular distribution of 1.3 MeV neutrons elastically scattered by the  $^{242}\text{Pu}$  nucleus: (1) total elastic scattering; (2) direct part of elastic scattering.

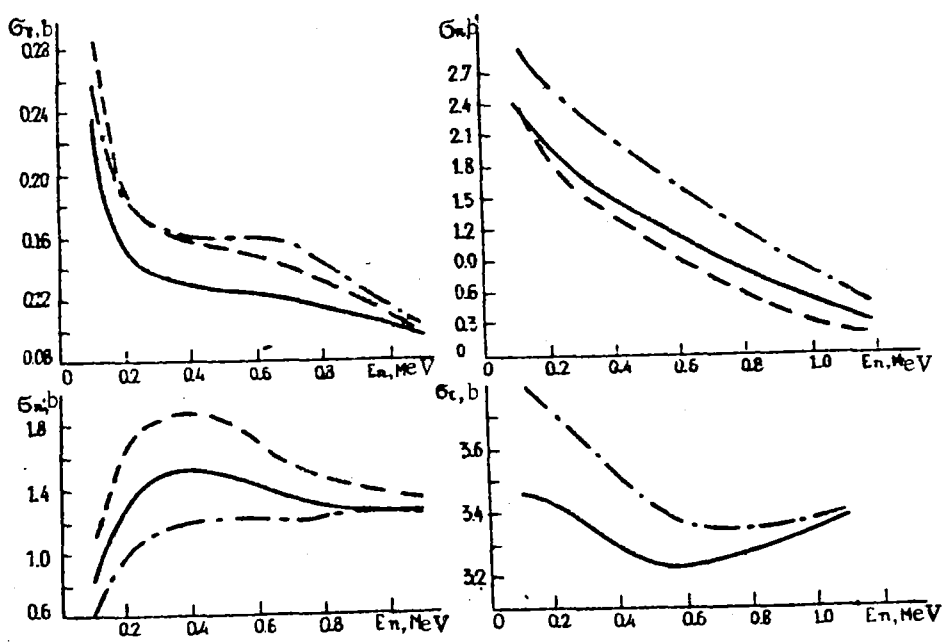
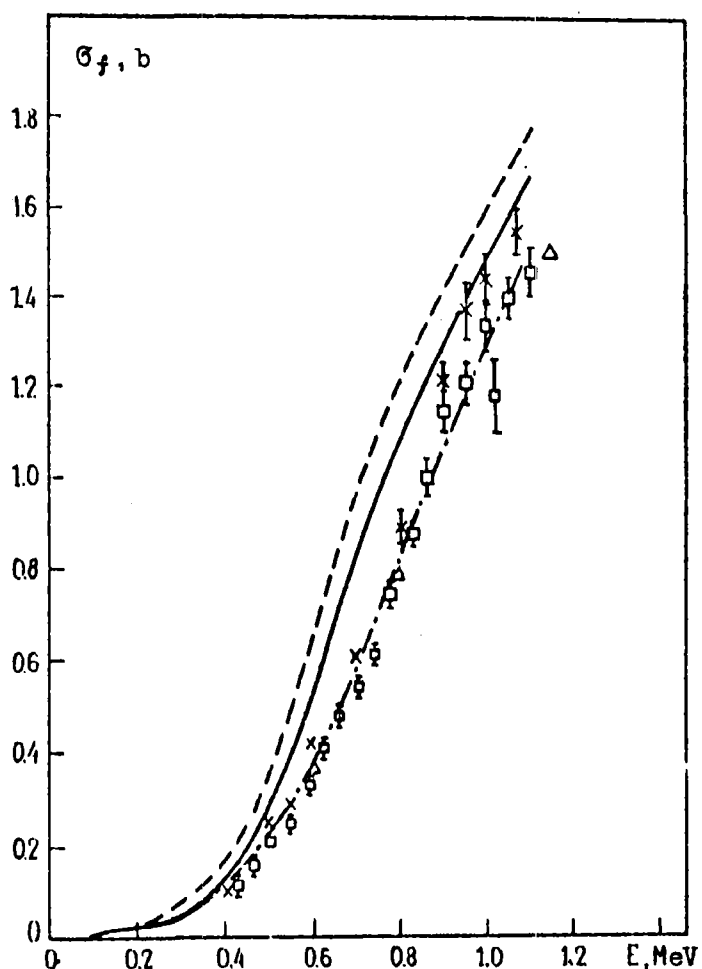


Fig. 3.1. Cross-sections  $\sigma_\gamma$ ,  $\sigma_n$ ,  $\sigma_{n\bar{n}}$ , and  $\sigma_c$  for  $^{242}\text{Pu}$  calculated by various formalisms: - · - - calculation with the S factor; - - - - calculation without the S factor; — - Tepel et al.



**Fig. 3.2.** Comparison of cross-section  $\sigma_f$  calculated by various formalisms with experimental data:  
- - - calculation with the S factor;  
- - - calculation without the S factor;  
— — — Tepel et al.

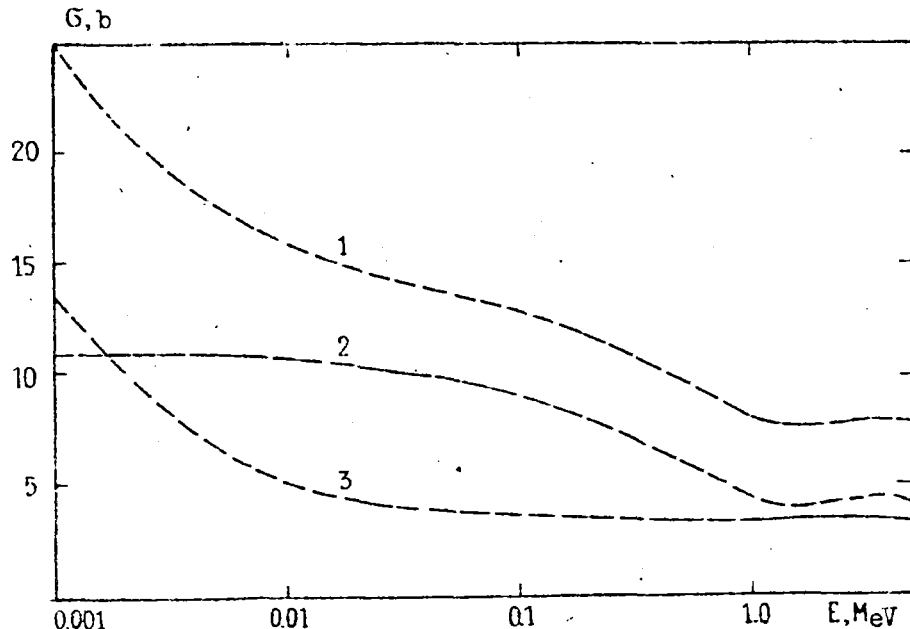


Fig. 3.3. Optical cross-sections of  $^{242}\text{Pu}$ : (1) total inter-action cross-section  $\sigma_t$ ; (2) potential scattering cross-section  $\sigma_{sc}$ ; (3) compound nucleus formation cross-section  $\sigma_c$ .

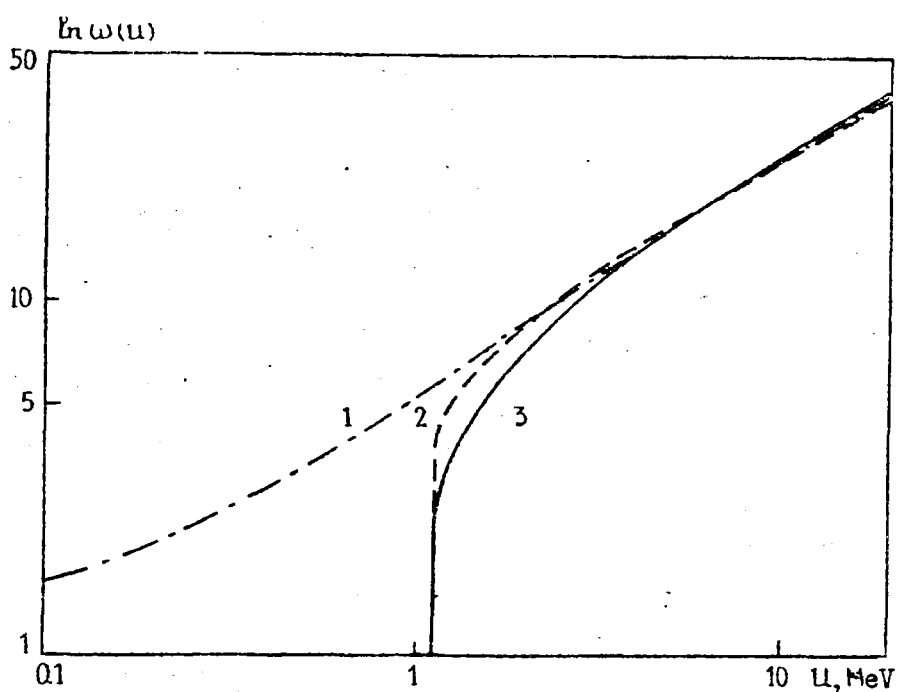


Fig. 3.4. Density of the states of  $^{242}\text{Pu}$ : — Fermi-gas model; - - - Fermi-gas model with consideration of the contribution of collective motions; - · - superfluid model with consideration of the contribution of collective motions.

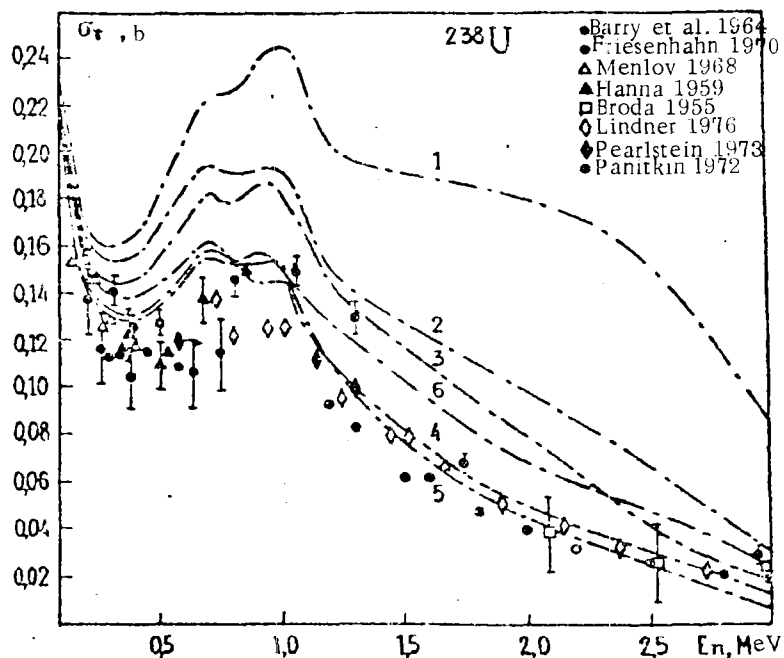
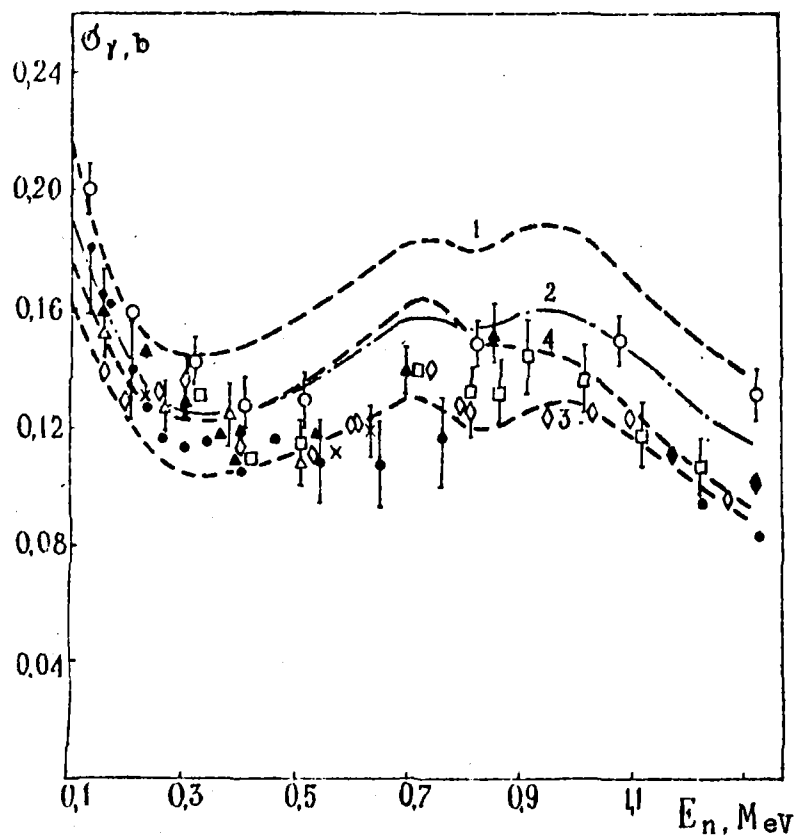


Fig. 3.5. Comparison of  $\sigma_\gamma$  for  $^{238}\text{U}$  calculated by the various level density models with experimental data: (1) Fermi-gas model, Lorentz factor; (2) Fermi-gas model, Weisskopf factor; (3) Fermi-gas model with consideration of collective motions, Lorentz factor; (4) superfluid model, Weisskopf factor; (5) Fermi-gas model with consideration of collective motions, Weisskopf factor; (6) superfluid model, Lorentz factor.



**Fig. 3.6.** Comparison of  $\sigma_{\gamma}$  for  $^{238}\text{U}$  calculated for level densities from the Fermi-gas model with consideration of collective motions and the Lorentz spectral factor for different values of  $\langle D \rangle_{\text{obs}}$  with experimental data: (1)  $\langle D \rangle_{\text{obs}} = 17.7 \text{ eV}$  [63]; (2)  $20.8 \text{ eV}$  [76]; (3)  $24.8 \text{ eV}$ ; (4)  $24.8 \text{ eV}$ , deformed potential.

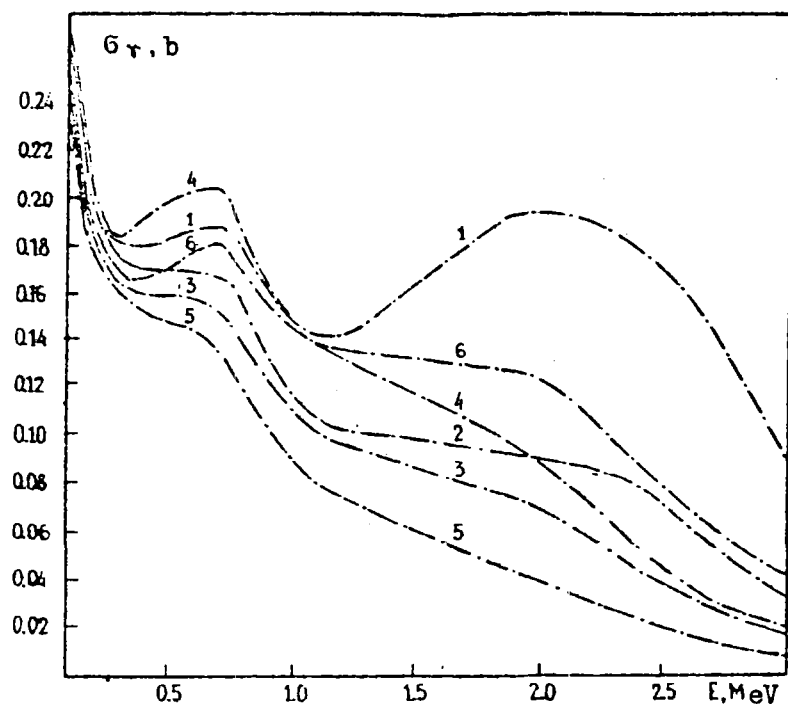


Fig. 3.7. Comparison of calculated values of  $\sigma_\gamma(^{242}\text{Pu})$  for the various level density models (for notations see Fig. 3.5).

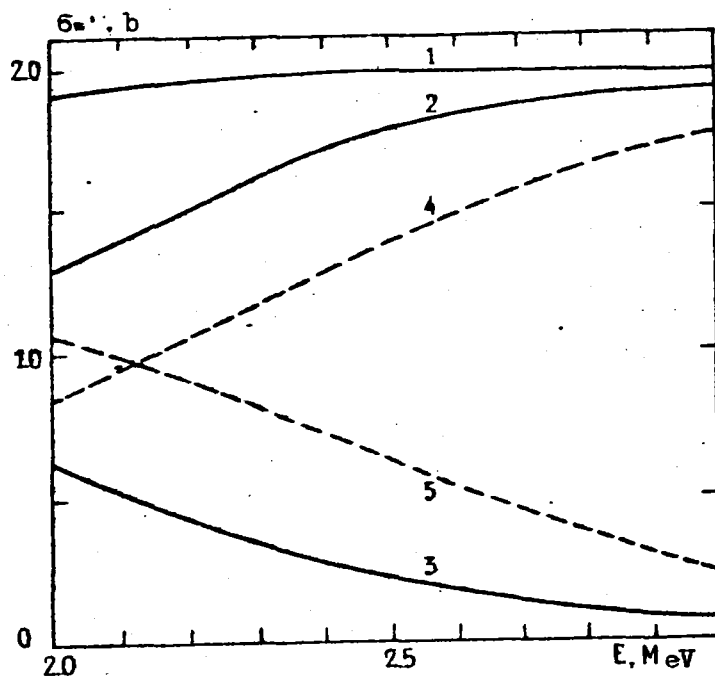
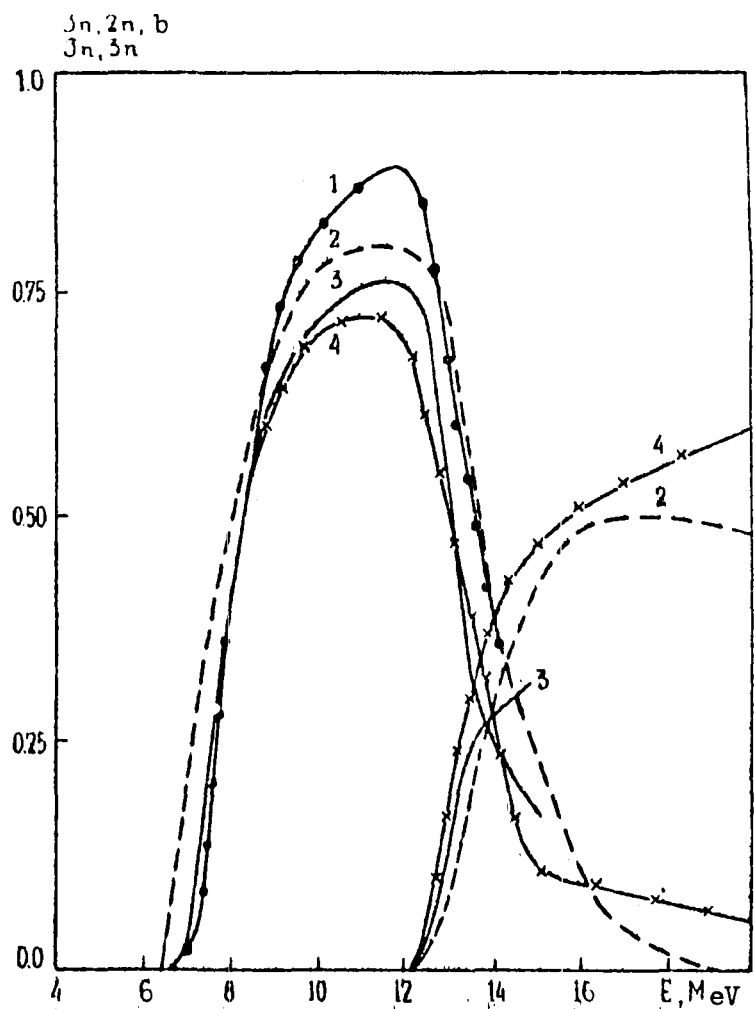
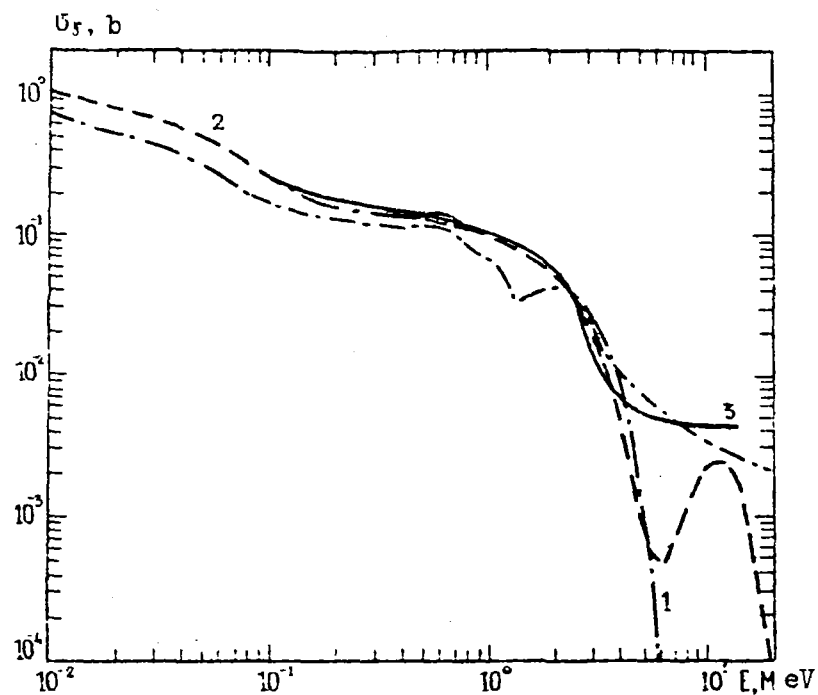


Fig. 3.8. The ratio between the neutron inelastic scattering cross-sections at the discrete and continuous level spectra of  $^{242}\text{Pu}$  for the various level density models: (1) total inelastic scattering cross-section; (2) scattering cross-section at the continuous spectrum for the level density from the Fermi-gas model with consideration of collective motions; (3) scattering cross-section at the discrete spectrum for the same level density; (4) scattering cross-section at the continuous spectrum for the level density from the Fermi-gas model; (5) scattering cross-section at the discrete spectrum for the same level density.



**Fig. 4.1.** Comparison of the various evaluations of the  $(n,2n)$  and  $(n,3n)$  reaction cross-sections: (1) Ref. [14]; (2) Ref. [81]; (3) present evaluation; (4) ENDF/B-4.



**Fig. 5.1.** Comparison of the various evaluations of  $\sigma_\gamma(^{242}\text{Pu})$ : (1) Ref. [14]; (2) Ref. [81]; (3) present evaluation; (4) ENDF/B-4.

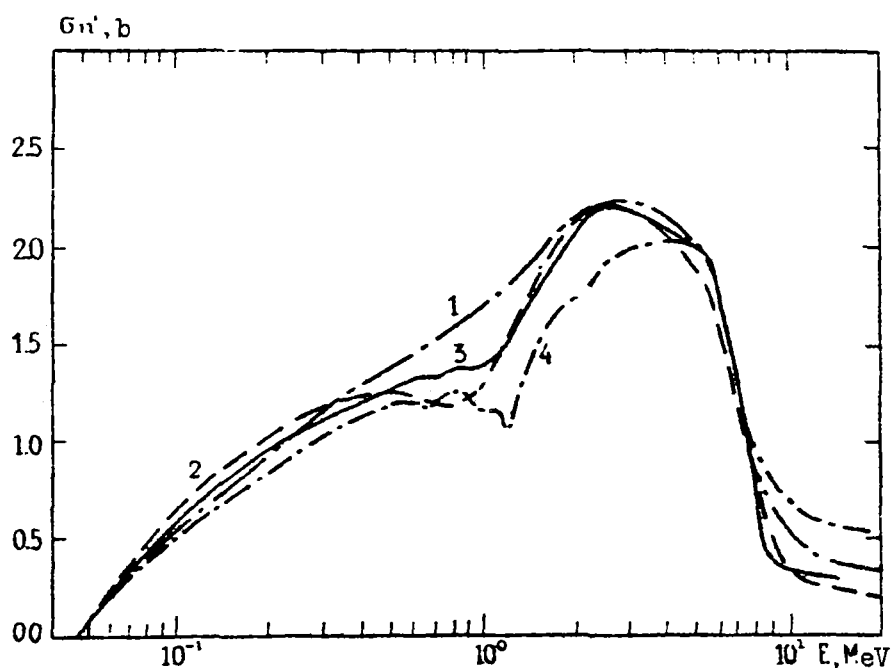


**Fig. 5.2.** Comparison of the various evaluations of  $\sigma_n(^{242}\text{Pu})$ : (1) Ref. [14]; (2) Ref. [81]; (3) present evaluation; (4) ENDF/B-4.

UDC 539.173.4

EVALUATION OF NEUTRON CROSS-SECTIONS FOR  $^{242}\text{Pu}$  IN THE  
0.2-15.0 MeV REGION ON THE BASIS OF EXPERIMENTAL DATA  
AND THEORETICAL MODELS

G.V. Antsipov, L.A. Bakhanovich, A.R. Benderskij,  
V.A. Zenevich, A.B. Klepatskij, V.A. Kon'shin,  
E.Sh. Sukhovitskij, in: Evaluation of  $^{242}\text{Pu}$  Nuclear  
Data in the  $10^{-5}$  eV - 15 MeV Neutron Energy Region,  
A.V. Lykov Institute of Heat and Mass Exchange  
(ITMO), Byelorussian SSR Academy of Sciences, Minsk  
(1979) 53-111

The authors have analysed the experimental data on the  $^{242}\text{Pu}$  fission cross-section in the 0.2-15 MeV region. For lack of experimental data the other types of cross-sections have been calculated by various theoretical models. Cross-sections  $\sigma_t$ ,  $\sigma_n$ ,  $\sigma_\gamma$ ,  $\sigma_{n'}$ ,  $\sigma_{n,2n}$  and  $\sigma_{n,3n}$  of  $^{242}\text{Pu}$  in the 0.2-15 MeV region have been evaluated on the basis of experimental data and calculation.

EVALUATION OF THE CHARACTERISTICS OF SECONDARY NEUTRONS AND GAMMA RAYS IN THE INTERACTION BETWEEN NEUTRONS AND THE  $^{242}\text{Pu}$  NUCLEUS

V.A. Zenevich, A.B. Klepatskij, A.K. Krasin, V.M. Maslov  
and Yu.V. Porodzinskij

In the present study we have evaluated the following characteristics of secondary neutrons and gamma rays for the  $^{242}\text{Pu}$  nucleus: the average number of secondary neutrons per fission event, the fission neutron spectrum, the angular and energy distributions of secondary neutrons from the  $(n,n)$ ,  $(n,n')$ ,  $(n,2n)$ ,  $(n,3n)$ ,  $(n,n'f)$  and  $(n,2nf)$  reactions and the energy spectrum of secondary gamma rays. Because of the total lack of experimental data the evaluation had to be performed by using calculations based on theoretical models (generalized optical, statistical and pre-equilibrium-decay models) and on the results of the systematics for other better-known nuclei. As a specific case of the use of the evaluation results for all  $^{242}\text{Pu}$  nuclear data we have in this study derived and presented the group constants of  $^{242}\text{Pu}$  in the standard 26-group representation. In addition, the evaluated nuclear data for  $^{242}\text{Pu}$  were recorded on magnetic tape in the ENDF/B format and are presented in the form of a print-out.

1. ENERGY DEPENDENCE OF  $\bar{\nu}_p(^{242}\text{Pu})$

There are no experimental data on  $\bar{\nu}_p(^{242}\text{Pu})$ . In our evaluation we therefore proceed from the systematics proposed by Howerton [1] in which the dependence of  $\bar{\nu}_p$  on atomic number, mass number and neutron energy is represented in the form of a Taylor expansion of the function of three variables close to some particular values, where the value of the function is well-known from experiment. Cutting off the expansion after three first-order terms and the cross term containing the product of mass by energy, he obtained the expression

$$\begin{aligned} \bar{\nu}(A, Z, E) = & 2.33 + 0.06[2 - (-1)^{A+1-Z} - (-1)^Z] + \\ & + 0.15(Z - 92) + 0.02(A - 235) + \\ & + [0.13 + 0.006(A - 235)](E - E_1), \end{aligned} \quad (1.1)$$

in which the constants were determined from experimental data. Here  $E_f$  is the fission threshold energy.

In the case where fission is preceded by the emission of one or more neutrons, expression (1.1) takes a more general form:

$$\bar{V}(A, Z, E) = \sum_{n=0}^M R_n \left\{ n + \bar{V}_{Th}(A-n, Z) + \bar{V}_1(A-n, Z) [E - E_B(A, Z) + E_B(A-n, Z) - n E_T(n) - E_f(A-n, Z)] \right\}, \quad (1.2)$$

where M is the number of possible fission modes,  $E_B(A, Z)$  the total binding energy of a nucleus of charge Z and mass A,  $E_f(A-n, Z)$  the fission barrier of a nucleus of charge Z and mass (A-n) and  $E_T(n)$  the average energy of pre-fission neutrons,

$$\bar{V}_1(A, Z) = 0.130 + 0.006(A-235); \quad (1.3)$$

$$\bar{V}_{Th}(A, Z) = 2.33 + 0.06[2 - (-1)^{\frac{A+1-Z}{2}}] + 0.15(2-92) + 0.02(A-235); \quad (1.4)$$

$$R_0(E) = \sigma_f(E) / \sigma_{nf}(E);$$

$$R_1(E) = \sigma_{n,n}(E) / \sigma_{nf}(E); \quad (1.5)$$

$$R_2(E) = \sigma_{n,2n}(E) / \sigma_{nf}(E);$$

$$\sigma_{nf}(E) = \sigma_f(E) + \sigma_{n,nf}(E) + \sigma_{n,2nf}(E). \quad (1.6)$$

The value of the fission threshold energy entering into (1.1) was determined in Ref. [1] by normalizing to unity the weighted mean values of the ratios of the calculated and measured  $\bar{v}(E)$ . In the case of the  $^{232}\text{Th}$ ,  $^{233}\text{U}$  and  $^{234}\text{U}$  nuclei in the region up to 4 MeV and the  $^{235}\text{U}$ ,  $^{236}\text{U}$ ,  $^{238}\text{U}$ ,  $^{239}\text{Pu}$ ,  $^{240}\text{Pu}$  and  $^{241}\text{Pu}$  nuclei in the region up to 6 MeV the  $\bar{v}$  data obtained showed sufficiently good agreement with experiment. At the same time, the  $E_f$  values so determined differ from those obtained by analysing fission cross-section data. However, the  $E_f$  value is not critical in the calculation of  $\bar{v}(E)$ . Thus, the value of  $\bar{v}(E)$  calculated for  $^{240}\text{Pu}$  at  $E_f = 0.31$  MeV (adjusted value) differs from  $\bar{v}(E)$  at  $E_f = 0.6$  MeV (experimental value) by not more than 1.5%.

In the present study the value of  $E_f(^{242}\text{Pu})$  was taken as 0.87 MeV on the basis of the systematics of Ref. [1]

$$E_f(A, Z) = 13.6 - 0.36Z^2/(A+1) + 0.2[2 - (-1)^{\frac{A+1-Z}{2}}] - S_n. \quad (1.7)$$

It should be noted that the actual error in  $\bar{v}$  due to the uncertainty of  $E_f$  is about 1%.

In order to calculate  $\bar{v}_p(E)$  at energies where fission may occur with the preliminary emission of one or two neutrons, we need to know the  $\sigma_{n,n'f}/\sigma_{nF}$  and  $\sigma_{n,2nf}/\sigma_{nF}$  ratios and the average energies of pre-fission neutrons.

The  $\sigma_{n,n'f}/\sigma_{nF}$  and  $\sigma_{n,2nf}/\sigma_{nF}$  ratios were calculated on the basis of our evaluation of  $\sigma_{nF}$ . The average energies of pre-fission neutrons  $E_T(n)$  were calculated with allowance for the pre-equilibrium stage of the process. It should be noted that the calculations of  $\bar{v}_p(E)$  are only slightly sensitive to the values of  $E_T(n)$  [2]. The data on  $R_n$  and  $E_T(n)$  used in the calculations are given in Table 1.1.

In order to evaluate the energy dependence of the total number of secondary neutrons per fission event, we used the results of Krick and Evans [3]. They measured the yield of delayed fission neutrons in the 0.6-1.3 MeV region with an accuracy of ~30%. The average value of  $\bar{v}_d$  is 0.016. The measurements of  $\bar{v}_d(E)$  for the  $^{233}U$ ,  $^{235}U$  and  $^{238}U$  nuclei [3, 4] show that in the region up to ~4 MeV the value of  $\bar{v}_d$  remains practically constant and then falls by ~40% up to 15 MeV. A similar energy dependence of  $\bar{v}_d$  was assumed for the  $^{242}Pu$  nucleus as well. The  $\bar{v}_d(E)$  values used in the present evaluation are given in Fig. 1.1.

The evaluated data on  $\bar{v}(E)$  are given in Table 1.2. The actual error of the data is ~3%.

## 2. FISSION NEUTRON SPECTRUM OF $^{242}Pu$

No measurements are available for the induced fission neutron spectra of  $^{242}Pu$ , so that data can be obtained only by using the systematics for the nuclei studied. In general, the spectra being measured can be approximated by a Watt distribution

$$N_w(E') = C_w S_h [2(wE')^{1/2} / T_w] \exp(-E'/T_w) \quad (2.1)$$

or by a Maxwellian distribution

$$N_m(E') = C_m E'^{1/2} \exp(-E'/T_m) \quad (2.2)$$

The existing systematics depend on the magnitudes of  $T_m$  or on the average spectrum energies  $\bar{E}$  which are linked by the relationship

$$\bar{E}^2 = \frac{3}{2} T_m \quad (2.3)$$

and are based on the theoretical conclusion of Terrell [5] that  $\bar{E}$  is connected with the average number of neutrons per fission  $\bar{\nu}(E)$  by the expression  $\bar{E} \sim [1 + \bar{\nu}(E)]^{1/2}$ . Howerton and Doyas [6] extended Terrell's conclusion to the presence of the reactions  $(n, n'f)$  and  $(n, 2nf)$ ; and by treating experimental data they obtained

$$T_M = 0.358 + 0.510 [1 + \bar{\nu}(E)]^{1/2}, \quad (2.4)$$

where

$$\bar{\nu}(E) = [\bar{\nu}_t(E)G_{nf}(E) - G_{nif}(E) - 2G_{n,2nf}(E)] / G_{nf}(E). \quad (2.5)$$

They also obtained the linear dependence

$$T_M = 0.997 + 0.125 \bar{\nu}(E), \quad (2.6)$$

which can be used with the same confidence as (2.4).

Manero and Kon'shin [7] have shown that  $\bar{\nu}_p$  depends little on the atomic number for identical values of Z. Hence it can be concluded that this occurs also in the case of the average fission spectrum energies. This will also be seen from consideration of Table 2.1, which gives the data on Pu isotopes for thermal neutrons.

With regard to  $^{242}\text{Pu}$ , measurements are available for the spontaneous fission neutron spectrum [10], which can serve as the criterion for verifying the applicability of the systematics to the given nucleus. Calculation by expressions (2.4) and (2.6) ( $\bar{\nu} = 2.15$ ) gives  $T_M = 1.26$  MeV, which agrees with the value of  $T_M = 1.21 \pm 0.07$  [11]. In this study we therefore propose for the fission neutron spectrum of  $^{242}\text{Pu}$  the use of expression (2.2) with the energy dependence (2.4) of temperature and the energy dependence  $\bar{\nu}_t(E)$  given in Section 1. The calculated values of  $T_M$  are contained in Table 2.2.

In representing the fission neutron spectrum analytically, we should bear in mind that the Maxwellian distribution does not approximate it in the whole energy region of secondary neutrons. Recent measurements (e.g. Ref. [7]) show an excess of low-energy neutrons, evidently reflecting the contribution of neutrons which are not associated with the motion of fragments. Besides, according to the preliminary results of Auchampaugh et al. [13], in the variation of primary neutron energy from 1.7 to 17.4 MeV,  $T_M$  was constant to within  $\pm 1\%$  for both  $^{235}\text{U}$  and  $^{238}\text{U}$ . At 22.5 MeV there was only a slight hardening of the fission spectrum.

### 3. ANGULAR DISTRIBUTIONS OF SECONDARY NEUTRONS

For elastic and inelastic scattering at levels  $2^+$  and  $4^+$  the angular distributions of scattered neutrons were obtained in calculations by the coupled channel method with addition of the isotropic (in the centre-of-mass system) part of elastic and inelastic scattering through the compound nucleus. For all other target-nucleus levels the angular distribution of inelastically scattered neutrons is taken to be isotropic. The calculations by the coupled channel method were performed with the use of the potential parameters given in our paper on the evaluation of the cross-sections of interaction of 0.2-15 MeV neutrons with the  $^{242}\text{Pu}$  nucleus. The differential elastic and inelastic scattering cross-sections at levels  $2^+$  and  $4^+$  are given in the form of a Legendre polynomial expansion

$$\frac{d\sigma_n(\theta)}{d\Omega} = \frac{\sigma_n}{4\pi} \left[ 1 + \sum_{l=1}^{l_{\max}} A_{ln} P_l(\cos\theta) \right], \quad (3.1)$$

where  $P_l(\cos\theta)$  represents Legendre polynomials of power  $l$  and  $n = 1, 2, 3$  is the level number.

The expansion coefficients  $A_{ln}$  for elastic and inelastic scattering at levels  $2^+$  and  $4^+$  are given in Tables 3.1-3.3, respectively.

### 4. ENERGY DISTRIBUTIONS OF SECONDARY NEUTRONS IN THE $(n,n')$ , $(n,2n)$ AND $(n,3n)$ REACTIONS

The energy distributions of secondary neutrons in the  $(n,n')$ ,  $(n,2n)$  and  $(n,3n)$  reactions were calculated by the statistical cascade model. Allowance was made for the possibility of emission of the first neutron before establishment of equilibrium in the compound nucleus and for the competition of fission, inelastic scattering and capture at the subsequent stages of decay. The calculation model is described in Ref. [14]. The contribution of the pre-equilibrium processes as a function of energy is taken as 0.06, 0.11 and 0.19 at 6, 9 and 15 MeV, respectively. The values of the level density parameters, neutron binding energies and fission barriers for the  $^{242}\text{Pu}$ ,  $^{241}\text{Pu}$  and  $^{240}\text{Pu}$  nuclei needed for the calculations were taken from the present work and from our evaluations [15, 16] for these nuclei. Because of their bulk the tables are not given in the text. The spectra will be found in the Appendix, where the complete file of  $^{242}\text{Pu}$  data is given in the form of a print-out.

## 5. THE SPECTRA OF GAMMA RAYS ACCOMPANYING THE PROCESSES OF INELASTIC INTERACTION OF NEUTRONS WITH THE $^{242}\text{Pu}$ NUCLEUS

The spectra of gamma rays accompanying the  $(n,n')$ ,  $(n,2n)$ ,  $(n,3n)$  and  $(n,\gamma)$  reactions were calculated in a dipole approximation by a statistical model, as was suggested in Ref. [17]. The required excitation functions of nuclei before gamma ray emission were obtained in the cross-section calculations for these reactions. The spectrum of gamma rays accompanying fission was not calculated because of the difficulty of calculating the excitation function of fragments. Hence the fission gamma spectrum was taken to be equal to the spectrum measured experimentally in Ref. [18]. It was assumed to be independent of the incident neutron energy. This is evidently a valid assumption, for fission energy is much higher than neutron energy. The total spectrum of gamma rays from the inelastic processes of interaction of neutrons with the  $^{242}\text{Pu}$  nucleus is given in the Appendix.

## 6. GROUP REPRESENTATION OF EVALUATED DATA FOR $^{242}\text{Pu}$

From the evaluated nuclear data for  $^{242}\text{Pu}$  we calculated the group constants in the standard 26-group representation. For this purpose, we used the set of GREKO programs, which allow calculations to be carried out with any group structure. The averaging was performed either over an arbitrary spectrum in point representation or over a group of standard spectra (Maxwell spectrum, Fermi spectrum, fission spectrum and so on). The algorithm for the calculation of the group constants is similar to that of Ref. [19].

In calculating the group cross-sections in the region of resolved resonances, the cross-sections calculated with a non-uniform step can be used with effect; this permits linear interpolation with a given accuracy for a minimum number of integration points. Thus, the procedure of averaging the group constants with a given accuracy over spectra  $f(E) = E^n$  ( $n = -1, 0, 1$ ) in interval  $\Delta E$

$$\langle \sigma_x \rangle = \frac{\int \sigma_x(E) f(E) dE}{\int f(E) dE} \quad (6.1)$$

with the use of cross-sections calculated at points with a step which permits linear interpolation of

$$\sigma_x(E) = \frac{\sigma_x(E_{L+}) - \sigma_x(E_L)}{E_{L+} - E_L} (E - E_L) + \sigma_x(E_L) \quad (6.2)$$

with the necessary accuracy amounts to calculating the algebraic sums, and this considerably reduces computer time:

for  $n = -1$

$$\langle \sigma_x \rangle = \sum_{i=1}^{N-1} [A_i(E_{i+1}-E_i) + (\sigma_x(E_i) - A_i E_i) \ln \frac{E_{i+1}}{E_i}] / \ln \frac{E_{i+1}}{E_1}; \quad (6.3)$$

for  $n = 0$

$$\langle \sigma_x \rangle = \sum_{i=1}^{N-1} [A_i \frac{E_{i+1}^2 - E_i^2}{2} + (\sigma_x(E_i) - A_i E_i)(E_{i+1} - E_i)] / (E_{i+1} - E_i); \quad (6.4)$$

for  $n = +1$

$$\langle \sigma_x \rangle = \sum_{i=1}^{N-1} [A_i \frac{E_{i+1}^3 - E_i^3}{3} + (\sigma_x(E_i) - A_i E_i) \left( \frac{E_{i+1}^2 - E_i^2}{2} \right)] / \left( \frac{E_{i+1}^2 - E_i^2}{2} \right), \quad (6.5)$$

where  $A_i = [\sigma_x(E_{i+1}) - \sigma_x(E_i)] / (E_{i+1} - E_i)$  and  $N$  is the number of points in group  $\Delta E$ .

In the calculation of the inelastic transition matrices account was taken of the possibility of pre-equilibrium emission of neutrons. This leads to the hardening of the inelastic scattering spectrum and consequently to an increase in the matrix elements of inelastic transitions from the given group to those nearest to it and to the group itself. The matrices of inelastic transitions due to the  $(n,2n)$  and  $(n,3n)$  reactions were calculated separately.

The group constants averaged over three standard spectra  $f(E) = E^n$  ( $n = -1, 0, 1$ ) in the region up to 1 keV are given in Table 6.1 and those for the remaining groups in Table 6.2; for  $E \leq 2.5$  MeV the averaging was performed over the Fermi spectrum and above 2.5 MeV over the fission neutron spectrum. Table 6.3 gives the inelastic transition matrix. Besides, Tables 6.4 and 6.5 contain the matrices of inelastic scattering due to the  $(n,2n)$  and  $(n,3n)$  reactions.

REFERENCES

1. Howerton R.J. Nucl.Sci.Eng., 62, 1971, 438.
2. Howerton R.J. Nucl.Sci.Eng., 46, 1971, 42.
3. Krick M.S., Evans A.E. Nucl.Sci.Eng., 47, 1972, 311.
4. Masters O.F., et.al. Nucl.Sci.Eng., 36, 1969, 202.
5. Terrell J. Phys.Rev., 113, 1959, 527.
6. Howerton R.J., Doyas R.J. Nucl.Sci.Eng., 46, 1971, 414.
7. Manero F., Kon'shin V.A. Atomic Energy Review, 10, 1972, 637.
8. Zamyatin, Yu.S., et al. in: Nuclear Data for Reactors (Proc. Conf. Helsinki (1970) 2, IAEA, Vienna, (1970) 183.
9. Smith A.B. Private Communication, 1971, in Reference 7.
10. Belov, L.M., et al., Yad. Fiz. 9 (1969) 727
11. Nefedov, V.N., et al., in: Proceedings of the Fourth All-Union Conference on Neutron Physics, Kiev, part 3 (1977) 205 (in Russian).
12. Smith A.B. et.al. Phys.Rev., 123, 1961, 2140.
13. Auchampaugh G.P. et.al. USNDO-3, 1972, p.118 and USNDO-7, 1973, p.127.
14. Kon'shin, V.A., et al., Report No. 6, ITMO AN BSSR, Minsk (1979) (in Russian).
15. Kon'shin, V.A., et al., Reports Nos 2-6, ITMO AN BSSR, Minsk (1979) (in Russian).
16. Antsipov, G.V., et al., in: Proceedings of the Third All-Union Conference on Neutron Physics, Kiev, part 2 (1975) 34 (in Russian).
17. Strutinskiij, V.M., et al., Zh. Ehksp. Teor. Fiz. 38 (1960) 598.
18. Verbinsky V.V. et.al. Phys.Rev., 7, 1973, 1173.
19. Abagyan, L.P., et al., Group Constants for Nuclear Reactor Calculations, Atomizdat (1964) (in Russian).
20. Data Formats and Procedures for the Evaluated Nuclear Data File, ENDF. Revised by D. Garber et. al. BNL-NCS-50496, 1975.

Table 1.1

Values of  $R_n$  and  $E_T(n)$  for the  $^{242}\text{Pu}$  nucleus

$E$ , MeV	$R_1$	$R_2$	$E_T(1)$ MeV	$E_T(2)$ MeV
5,5	0,041		0,02	
6,0	0,177		0,16	
6,5	0,323		0,28	
7,0	0,387		0,40	
7,5	0,421		0,52	
8,0	0,441		0,61	
8,5	0,448		0,70	
9,0	0,454		0,77	
9,5	0,456		0,82	
10,0	0,457		0,85	
10,5	0,457		0,88	
11,0	0,456		0,90	
11,5	0,453		0,93	
12,0	0,451	0,010	1,01	0,01
13,0	0,439	0,043	1,46	0,42
14,0	0,418	0,100	2,13	0,64
15,0	0,403	0,130	2,82	0,76

Table 1.2

Evaluated data on  $\bar{\nu}_p(E)$  and  $\bar{\nu}_t(E)$  for  $^{242}\text{Pu}$

E, MeV	$\bar{\nu}_p$	$\bar{\nu}_t$	E, MeV	$\bar{\nu}_p$	$\bar{\nu}_t$
	2	3	4	5	6
0,1·10 <sup>-10</sup>	2,740	2,756	0,34	2,799	2,815
2,53·10 <sup>-9</sup>	2,740	2,756	0,36	2,802	2,818
9·10 <sup>-8</sup>	2,741	2,757	0,38	2,806	2,822
0,010	2,742	2,758	0,40	2,809	2,825
0,016	2,743	2,759	0,42	2,813	2,829
0,022	2,744	2,760	0,44	2,816	2,832
0,027	2,745	2,761	0,46	2,819	2,835
0,033	2,746	2,762	0,48	2,823	2,839
0,039	2,747	2,763	0,50	2,826	2,842
0,045	2,748	2,764	0,55	2,835	2,851
0,051	2,749	2,765	0,60	2,844	2,860
0,056	2,750	2,766	0,65	2,852	2,868
0,062	2,751	2,767	0,70	2,861	2,877
0,068	2,752	2,768	0,75	2,869	2,895
0,074	2,753	2,769	0,80	2,878	2,891
0,080	2,754	2,770	0,85	2,887	2,903
0,086	2,755	2,771	0,90	2,895	2,911
0,091	2,756	2,772	0,95	2,904	2,920
0,10	2,759	2,774	1,00	2,912	2,928
0,12	2,761	2,777	1,1	2,930	2,946
0,14	2,764	2,780	1,2	2,947	2,963
0,16	2,768	2,784	1,4	2,981	2,997
0,18	2,771	2,787	1,6	3,016	3,032
0,20	2,775	2,791	1,8	3,050	3,066
0,22	2,778	2,794	2,0	3,084	3,100
0,24	2,782	2,798	2,2	3,119	3,135
0,26	2,785	2,801	2,4	3,153	3,169
0,28	2,789	2,805	2,6	3,188	3,204
0,30	2,792	2,808	2,8	3,222	3,238
0,32	2,795	2,811	3,0	3,256	3,272
3,2	3,291	3,307	8,0	4,093	4,100
3,4	3,325	3,341	8,5	4,171	4,177
3,6	3,360	3,376	9,0	4,250	4,256
3,8	3,394	3,410	9,5	4,330	4,336
4,0	3,428	3,443	10,0	4,413	4,419
4,5	3,514	3,529	10,5	4,495	4,501
5,0	3,600	3,614	11,0	4,578	4,584
5,5	3,689	3,702	11,5	4,661	4,667
6,0	3,778	3,789	12,0	4,739	4,745
6,5	3,862	3,872	13,0	4,870	4,876
7,0	3,940	3,950	14,0	4,978	4,984
7,5	4,016	4,023	15,0	5,092	5,098

Table 2.1

Values of  $T_M$  for Pu isotopes in thermal neutron fission

Isotope	$T_M$ , MeV	Reference
$^{238}\text{Pu}$	$1,35 \pm 0,04$	/8/
$^{239}\text{Pu}$	$1,39 \pm 0,02$	/9/
	$1,35 \pm 0,04$	/10/
	$1,38 \pm 0,04$	/11/
$^{241}\text{Pu}$	$1,335 \pm 0,034$	/12/

Table 2.2

Values of  $T_M$  for the fission neutron spectra of  $^{242}\text{Pu}$

E, MeV : $T_M$ , MeV	E, MeV : $T_M$ , MeV	E, MeV : $T_M$ , MeV
1 : 2	3 : 4	5 : 6
$10^{-11}$ : 1,341	$2,53 \cdot 10^{-3}$ : 1,341	0,01 : 1,342
0,1 : 1,344	0,2 : 1,346	0,4 : 1,350
0,6 : 1,355	0,8 : 1,359	1,1 : 1,364
1,6 : 1,377	2,0 : 1,386	3,0 : 1,407
4,0 : 1,428	5,0 : 1,448	6,0 : 1,448
7,0 : 1,488	8,0 : 1,505	9,0 : 1,471
10,0 : 1,542	11,0 : 1,553	12,0 : 1,524
13,0 : 1,589	14,0 : 1,601	15,0 : 1,542

Table 3.1

## Coefficients of Legendre polynomial expansion of angular distributions of elastically scattered neutrons

Energy, MeV Coefficients	0.001	0.003	0.01	0.03	0.10	0.25	0.50	0.75	1.00	1.50	2.00	3.00	4.00	5.00	6.00	7.00	8.00	9.00	10.00	11.00	12.00	13.00	14.00
A <sub>1</sub>	0.000533	0.001048	0.007227	0.025829	0.085359	0.220531	0.306736	0.381542	0.460292	0.560700	0.680722	0.752215	0.839349	0.859453	0.866759	0.877366	0.895059	0.882910	0.864176	0.864792	0.851055	0.830071	
A <sub>2</sub>	0.000304	0.000517	0.000521	0.007347	0.04989	0.103945	0.168593	0.243685	0.379467	0.509700	0.625002	0.688182	0.727244	0.747315	0.752061	0.748269	0.739640	0.730659	0.727604	0.715196	0.714771		
A <sub>3</sub>				0.000005	0.000026	0.000554	0.030554	0.084556	0.165476	0.308201	0.401426	0.482963	0.550202	0.601196	0.636091	0.652706	0.652042	0.642333	0.634062	0.628704	0.628262	0.576758	
A <sub>4</sub>					0.000010	0.000368	0.035290	0.022061	0.060587	0.178258	0.292846	0.390398	0.429578	0.478666	0.519967	0.542115	0.556097	0.558190	0.556325	0.548461	0.555865	0.545347	
A <sub>5</sub>						0.000101	0.000106	0.030129	0.004132	0.045961	0.123181	0.234374	0.296040	0.345255	0.383010	0.425170	0.451876	0.467301	0.476443	0.477184	0.469370	0.516560	
A <sub>6</sub>							0.000001	0.000016	0.000250	0.001526	0.012697	0.041691	0.109419	0.163560	0.212370	0.261023	0.306873	0.345684	0.375098	0.397295	0.411032	0.406175	0.405337
A <sub>7</sub>								0.000016	0.000115	0.001540	0.008609	0.037088	0.076700	0.119185	0.160353	0.203767	0.247780	0.287466	0.322060	0.346405	0.384615	0.416790	
A <sub>8</sub>									0.000006	0.000128	0.001506	0.010336	0.032103	0.064343	0.102285	0.141675	0.182057	0.221307	0.259302	0.290297	0.339102	0.366534	
A <sub>9</sub>										0.000006	0.000172	0.002041	0.010128	0.027529	0.055990	0.134993	0.175992	0.214243	0.246279	0.286771	0.334170		
A <sub>10</sub>											0.000014	0.000268	0.002127	0.001375	0.022698	0.07523	0.089317	0.124629	0.165016	0.200091	0.253652	0.280526	
A <sub>11</sub>												0.000015	0.000043	0.002274	0.007771	0.019883	0.041378	0.070209	0.104008	0.137305	0.150521	0.129472	
A <sub>12</sub>													0.000055	0.000445	0.001700	0.005718	0.014329	0.023724	0.049633	0.076435	0.112021	0.156642	
A <sub>13</sub>														0.000003	0.000058	0.000321	0.001226	0.004003	0.009360	0.019588	0.033930	0.072124	0.106526
A <sub>14</sub>															0.000008	0.000053	0.000242	0.001015	0.002889	0.006556	0.012400	0.034742	0.057244
A <sub>15</sub>																0.000004	0.000021	0.000195	0.000623	0.001644	0.003508	0.013498	0.032620
A <sub>16</sub>																	0.000028	0.000107	0.000324	0.000784	0.004536	0.010355	
A <sub>17</sub>																		0.000002	0.000009	0.000034	0.000094	0.001253	0.003035
A <sub>18</sub>																			0.000059	0.000067	0.000027	0.000027	0.000102

Table 3.2

Coefficients of Legendre polynomial expansion of angular distributions of inelastically scattered neutrons at level  $2^+$

Energy, MeV Coef- ficients	0,12	0,25	0,50	0,75	1,00	1,50	2,00	3,00	4,00	5,00	6,00	7,00	9,00	9,00	10,00	11,00	13,00	15,00
A <sub>1</sub>	-0,000679	-0,005970	-0,014360	-0,022763	-0,035612	-0,043235	-0,051316	0,076631	0,137398	0,158619	0,179045	0,207589	0,247317	0,281164	0,325898	0,359810	0,414722	0,452213
A <sub>2</sub>	-0,000762	-0,003945	-0,011447	-0,015593	-0,021372	-0,036680	-0,069726	-0,072885	-0,082774	-0,053084	-0,059773	-0,055832	-0,041075	-0,017890	0,012337	0,039823	0,095826	0,141260
A <sub>3</sub>	0,000051	0,001396	0,004215	0,004110	0,005505	0,015206	0,029348	0,051777	-0,006369	-0,030470	-0,053870	-0,069050	-0,076259	-0,077243	-0,071029	-0,061273	-0,022798	0,009553
A <sub>4</sub>	0,000024	-0,000619	-0,001592	-0,004068	-0,006128	0,005015	0,021415	0,026488	0,029951	0,016967	0,001773	-0,013307	-0,025270	-0,031232	-0,023766	-0,010463	0,009657	
A <sub>5</sub>	-0,000005	-0,000073	-0,000058	-0,000177	0,002151	0,012792	0,035144	0,036469	0,022056	0,023155	0,031740	0,028398	0,017627	0,059769	0,049504	0,009172	0,023704	
A <sub>6</sub>	0,000010	0,000105	0,000492	0,001953	0,002274	0,000120	-0,017757	-0,023571	-0,021743	-0,009516	-0,007169	0,007196	0,013227	0,017364	0,019330	0,020627		
A <sub>7</sub>	-0,000003	-0,000021	-0,000167	0,000421	0,000403	-0,000923	-0,026533	-0,036734	-0,036878	-0,033754	-0,026964	-0,019019	-0,010905	0,020295	0,019322			
A <sub>8</sub>	0,000006	0,000097	0,000697	0,000524	0,0001029	-0,011303	-0,027976	-0,037814	-0,044188	-0,047769	-0,047223	-0,040721	-0,023228	-0,005557				
A <sub>9</sub>	0,000007	-0,000082	0,000044	0,000288	0,010920	0,006910	0,00076	-0,015429	-0,023607	-0,026739	-0,028217	-0,022623	-0,010657					
A <sub>10</sub>	0,000014	0,000292	0,000472	0,0007125	0,005361	-0,032711	-0,010007	-0,01441	-0,010802	-0,009516	-0,032386	-0,003775						
A <sub>11</sub>	-0,000001	-0,000036	0,000310	0,001500	0,003637	0,007253	0,012298	0,015445	-0,014654	0,011556	0,007050	0,012564						
A <sub>12</sub>	0,000190	0,001372	0,004197	0,008099	0,011741	0,012590	0,010390	0,005362	-0,010112	0,005370								
A <sub>13</sub>	0,000001	0,000115	0,000363	0,000696	0,001218	0,002094	0,003611	0,004280	0,005053	0,007759								
A <sub>14</sub>	0,000026	0,000147	0,000499	0,001690	0,003733	0,007036	0,010670	0,017451	0,016861									
A <sub>15</sub>	0,000004	0,000027	0,000117	0,000395	0,001075	0,002403	0,004096	0,002109	0,003026									
A <sub>16</sub>				0,000066	0,000206	0,000537	0,001045	0,003264	0,006008									
A <sub>17</sub>				0,000008	0,000039	0,000143	0,000379	0,002312	0,005649									
A <sub>18</sub>									0,000009	0,000032								
A <sub>19</sub>																		

Table 3.3

Coefficients of Legendre polynomial expansion of angular distributions of inelastically scattered neutrons at level 4<sup>+</sup>

Energy, MeV Coefficients	0.32	0.50	0.75	1.00	1.50	2.00	3.00	4.00	5.00	6.00	7.00	8.00	9.00	10.00	12.00	15.00	18.00			
A <sub>1</sub>	0.003715	0.022120	0.042085	0.065741	0.085602	0.107946	0.146634	0.145368	0.147553	0.152062	0.169152	0.200355	0.234935	0.264576	0.281319	0.311757	0.353454			
A <sub>2</sub>	-0.000157	-0.000992	-0.008932	-0.019332	-0.049344	-0.036835	-0.117627	-0.110578	-0.032653	-0.077369	-0.063707	-0.051527	-0.038678	-0.026365	-0.013604	0.019057	0.062036			
A <sub>3</sub>	-0.000757	-0.004210	-0.007745	-0.010440	-0.006280	-0.001532	-0.023580	-0.013674	-0.005592	-0.016492	-0.032783	-0.050365	-0.063212	-0.068504	-0.068544	-0.060555	-0.050357			
A <sub>4</sub>	-0.000168	-0.000833	0.000079	0.002046	0.007774	0.007996	-0.011322	-0.016566	-0.027037	-0.034717	-0.036839	-0.045602	-0.054746	-0.057449	-0.059146	-0.061211	-0.066671			
A <sub>5</sub>	0.000007	0.000114	0.000492	0.0000819	-0.000362	-0.005811	-0.005766	-0.006093	-0.009778	-0.003707	0.018049	0.019093	0.015053	0.012422	0.010052	-0.001701	-0.024635			
A <sub>6</sub>	-0.000003	-0.000076	-0.000239	-0.000312	0.000456	0.004552	0.000310	0.001081	0.007559	0.006689	0.002774	0.020396	0.004410	0.005576	0.003005	-0.002802				
A <sub>7</sub>		0.000007	0.000031	0.000287	0.000617	-0.000815	-0.004832	-0.002202	-0.000044	-0.002460	-0.002527	0.001850	0.005174	0.005557	0.009836	0.012659				
A <sub>8</sub>			-0.000002	-0.000039	-0.000367	-0.001020	0.004675	0.011022	0.010549	0.003771	0.003985	0.006171	0.003475	-0.000552	-0.000966	0.002351				
A <sub>9</sub>				0.000001	0.000039	0.000252	0.000236	0.000095	-0.001965	-0.000548	-0.000611	0.002234	0.001395	-0.000917	-0.002011	-0.002530				
A <sub>10</sub>					-0.000005	-0.000074	-0.001023	-0.001555	-0.000986	0.001933	0.004574	0.005389	0.009184	0.011181	0.014268	0.014234				
A <sub>11</sub>						0.000010	0.000050	0.000189	0.000639	0.001027	0.001105	0.001572	0.003475	0.005052	0.004253	0.004777				
A <sub>12</sub>							0.000007	-0.000095	-0.000204	-0.000522	-0.000363	-0.001235	-0.002007	-0.003445	-0.005201	0.001719				
A <sub>13</sub>								-0.000002	0.000018	0.000061	0.000136	0.000013	-0.000066	-0.001615	-0.002099	0.001572	0.007564			
A <sub>14</sub>									0.000002	0.000002	-0.000024	-0.0000101	-0.000034	0.000037	0.000418	0.002215	-0.001504			
A <sub>15</sub>										0.000001	0.000006	0.000027	0.000074	0.000175	0.000266	0.000155	-0.002374	-0.007014		
A <sub>16</sub>											0.000004	0.000002	-0.000024	-0.000132	-0.000531	-0.000060				
A <sub>17</sub>												0.000003	0.000014	0.000050	0.0000135	0.000004	0.001005			
A <sub>18</sub>															0.000007	0.003016				

Table 6.1

Group constants of  $^{242}\text{Pu}$  in the region of resolved resonances averaged over  
three standard spectra ( $f(E) = E^n$ ,  $n = -1, 0, 1$ )

No.	$E_1, E_{1+1},$ eV	$G_T$	$G_F$	$\lambda$	$G_d$	$\mu_c$	$\xi$	$G_T$	$G_F$	$\lambda$	$G_d$	$\mu_c$	$\xi$	$G_T$	$G_F$	$\lambda$	$G_d$	$\mu_c$	$\xi$
I5	465-1000	4,007	0,055	2,757	22,97I	0,003I	0,0082	3,824	0,058	2,757	22,174	0,003I	0,0082	3,64I	0,058	2,757	21,379	0,003I	0,0082
I6	215-465	6,144	0,018	2,757	25,II7	0,0029	0,0082	6,032	0,016	2,757	25,430	0,0029	0,0082	5,62I	0,014	2,757	25,I25	0,0029	0,0082
I7	100-215	10,30I	0,024	2,757	19,710	0,0028	0,0082	9,458	0,022	2,757	20,329	0,0028	0,0082	8,866	0,02I	2,757	21,304	0,0028	0,0082
I8	46,5-100	33,013	0,067	2,756	80,379	0,0028	0,0082	26,322	0,053	2,756	64,327	0,0028	0,0082	20,245	0,04I	2,756	50,048	0,0028	0,0082
I9	21,5-46,5	4,738		2,756	7,630	0,0028	0,0082	4,162		2,756	7,427	0,0028	0,0082	3,80I		2,756	7,225	0,0028	0,0082
20	10-21,5	1,617		2,756	8,893	0,0028	0,0082	1,57I		2,756	8,894	0,0028	0,0082	1,46I		2,756	8,777	0,0028	0,0082
21	4,65-10	0,70I		2,756	10,330	0,0028	0,0082	0,59I		2,756	10,177	0,0028	0,0082	0,495		2,756	10,040	0,0028	0,0082
22	2,15-4,65	I367,6I3		2,756	II6,880	0,0028	0,0082	1123,004		2,756	99,445	0,0028	0,0082	880,004		2,756	81,643	0,0028	0,0082
23	I,0-2,15	16,097		2,756	5,43I	0,0028	0,0082	18,142		2,756	5,13I	0,0028	0,0082	20,284		2,756	4,829	0,0028	0,0082
24	0,465-I,0	6,48I		2,756	7,509	0,0028	0,0082	6,556		2,756	7,460	0,0028	0,0082	6,628		2,756	7,4I3	0,0028	0,0082
25	0,215-0,465	6,7II		2,756	7,96P	0,0028	0,0082	6,636		2,756	7,952	0,0028	0,0082	6,568		2,756	7,936	0,0028	0,0082
T	0,0252	I8,636		2,756	8,245	0,0028	0,0082	18,636		2,756	8,245	0,0028	0,0082	I8,636	0,00I	2,756	8,245	0,0028	0,0082

Table 6.2

Group constants of  $^{242}\text{Pu}$  in the 1 keV-15 MeV region

No.	$E_i, E_{i+1}$	$G_t$	$\delta_f$	$\delta_d$	$\mu_e$	$\xi$	$G_{\alpha}$	$\delta_{\alpha,2n}$	$\delta_{\alpha,3n}$
HeB									
0	10.5-15	0.004	2.023	4.673	2.593	0.571	0.0017	0.307	0.659 0.037
I	6.5-10.5	0.005	1.984	4.043	3.199	0.867	0.0011	0.956	0.232
2	4.0-6.5	0.007	1.304	3.593	4.136	0.856	0.0012	1.950	
3	2.5-4.0	0.017	1.365	3.296	3.701	0.800	0.0017	2.762	
4	1.4-2.5	0.034	1.407	3.033	3.564	0.650	0.0029	2.044	
5	0.6-1.4	0.099	1.290	2.941	4.123	0.474	0.0049	1.431	
C	0.4-0.3	0.147	0.348	2.856	6.387	0.335	0.0055	1.293	
7	0.2-0.4	0.163	0.052	2.806	9.343	0.245	0.0062	1.093	
8	0.1-0.2	0.212	0.015	2.781	11.363	0.133	0.0072	0.301	
He3									
J	46.5-100	0.255	0.009	2.768	12.562	0.063	0.0077	0.323	
I0	21.5-46.5	0.616	0.007	2.762	13.243	0.021	0.0080	0.004	
II	10-21.5	0.965	0.008	2.759	13.755	0.015	0.0081		
I2	4.65-10	1.163	0.009	2.758	14.660	0.0090	0.0032		
I3	2.15-4.65	1.625	0.011	2.757	16.126	0.0043	0.0082		
I4	1.0-2.15	2.525	0.015	2.757	18.223	0.0036	0.0082		

Table 6.3

The matrix of inelastic transitions due to the  $(n,n')$ ,  $(n,2n)$  and  $(n,3n)$  reactions for  $^{242}\text{Pu}$

J	$\delta_{in} (\frac{1}{2}, \frac{1}{2} + K)$											
	K = 0	K = I	K = 2	K = 3	K = 4	K = 5	K = 6	K = 7	K = 8	K = 9	K = 10	K = II
0	0.259	0.030	0.017	0.070	0.317	0.481	0.416	0.155	0.050	0.016	0.004	0.001
I	0.319	0.042	0.034	0.115	0.179	0.277	0.270	0.126	0.039	0.010	0.002	
2	0.413	0.051	0.103	0.331	0.520	0.362	0.147	0.045	0.011	0.002		
3	0.488	0.124	0.220	0.524	0.455	0.240	0.035	0.021	0.004	0.001		
4	0.655	0.311	0.447	0.322	0.194	0.066	0.023	0.005	0.001			
5	0.811	0.292	0.193	0.113	0.040	0.009	0.003					
6	1.035	0.251	0.000	0.007	0.004	0.001						
7	0.764	0.331	0.004									
8	0.401	0.399	0.001									
9	0.050	0.187	0.059	0.075	0.003	0.001						
10	0.000	0.000	0.000	0.000	0.000	0.000	0.002	0.001	0.001			

Table 6.4

The matrix of inelastic transitions due to the  
(n,2n) reaction for  $^{242}\text{Pu}$

J	$G_{n,2n}(J, J+k)$										
	K = 0	K = I	K = 2	K = 3	K = 4	K = 5	K = 6	K = 7	K = 8	K = 9	K = 10
0	0,000	0,001	0,016	0,069	0,312	0,464	0,377	0,121	0,030	0,007	0,001
I	0,000	0,000	0,000	0,003	0,034	0,112	0,179	0,096	0,030	0,003	0,002

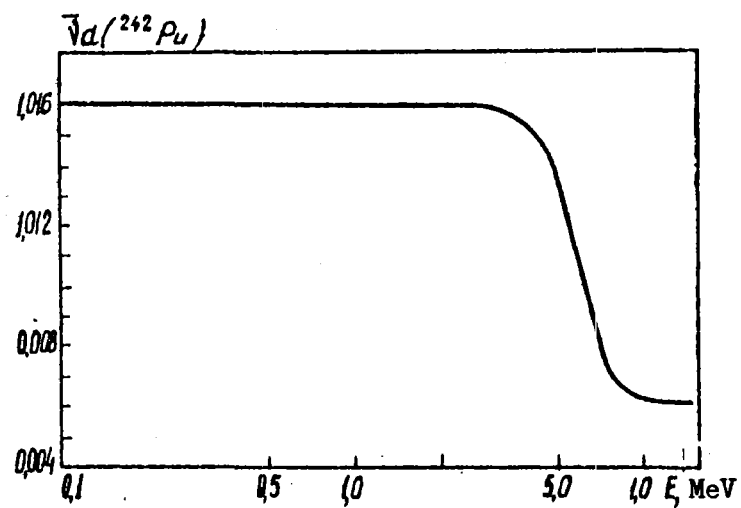
Table 6.5

The matrix of inelastic transitions due to the  
(n,3n) reaction for  $^{242}\text{Pu}$

J	$G_{n,3n}(J, J+k)$											
	K = I	K = I	K = 2	K = 3	K = 4	K = 5	K = 6	K = 7	K = 8	K = 9	K = 10	K = 11
0	0,000	0,000	0,000	0,000	0,001	0,012	0,034	0,032	0,019	0,009	0,003	0,001

Figure 1.1

The energy dependence of  $\bar{v}_d$  for  $^{242}\text{Pu}$



UDC 539.173.4

EVALUATION OF THE CHARACTERISTICS OF SECONDARY NEUTRONS AND  
GAMMA RAYS IN THE INTERACTION BETWEEN NEUTRONS AND THE  $^{242}\text{Pu}$   
NUCLEUS. V.A. Zenevich, A.B. Klepatskij, A.K. Krasin,  
V.M. Maslov and Yu.V. Porodzinskij in: Evaluation of  
 $^{242}\text{Pu}$  Nuclear Data in the  $10^{-5}$  eV-15 MeV Neutron Energy  
Region, A.V. Lykov Institute of Heat and Mass Exchange (ITMO),  
Byelorussian SSR Academy of Sciences, Minsk (1979) 112-183.

On the basis of calculations by various theoretical models the following characteristics of secondary neutrons and gamma rays for the  $^{242}\text{Pu}$  nucleus have been evaluated: fission neutron spectrum, value of  $\bar{v}$  for  $^{242}\text{Pu}$ , the angular and energy distributions of neutrons from the  $(n,n)$ ,  $(n,n')$ ,  $(n,2n)$ ,  $(n,3n)$ ,  $(n,n'f)$  and  $(n,2nf)$  reactions and the energy spectrum of the secondary gamma quanta. The group constants for  $^{242}\text{Pu}$  have been obtained. A print-out of the complete file of evaluated nuclear data for  $^{242}\text{Pu}$  in the ENDF/B format is reproduced.

Appendix

PRINT-OUT OF THE COMPLETE EVALUATED NUCLEAR DATA FILE FOR  $^{242}\text{Pu}$   
IN THE ENDF/B FORMAT [20]

The appendix reproduces a print-out from the magnetic tape containing evaluated data written in the form of 80-column punched cards, each of which is identified by three numbers: file number (columns 71, 72), section number (73-76) and card number (76-80).

File I comprises two sections: 451 (information) and 452 (neutron yield per fission). The data are written in the form of pairs of numbers ( $E, \bar{v}$ ) in the  $10^{-5}$  eV-15 MeV region.

File II (section 151) contains resonance parameters. The region of resolved resonances (punched cards 190-259) is represented by the Breit-Wigner parameters. The resonance energy and spin and the total, neutron, radiative and fission widths are given for each of the 69 resonances. In the region of unresolved resonances (punched cards 260-414), the energy dependence of the average resonance parameters is given. Entered here are the energy, average level spacing, average inelastic scattering width, average reduced neutron width, average radiation width and average fission width for all  $J$  at a given  $\ell$ ,  $\ell$  taking the values of 0, 1, 2.

File III contains cross-sections. It gives the total cross-section (section 1), elastic scattering cross-section (section 2), inelastic scattering cross-section (section 4), ( $n, 2n$ ) and ( $n, 3n$ ) cross-sections (sections 16, 17), fission cross-section (section 18), the ( $n, n'f$ ) and ( $n, 2n'f$ ) cross-sections (sections 20, 21), level excitation cross-sections (sections 51-63), cross-section of inelastic scattering to the continuous spectrum (section 91) and capture cross-section (section 102).

File IV is the file of angular distributions of secondary neutrons. The angular distributions for the cross-sections of sections 2, 51, 52 are presented as the coefficients of Legendre polynomials at different incident neutron energies. For example, punched card 1011 gives the incident neutron energy and the number of coefficients and punched card 1012 the Legendre coefficients, starting with the first. In the case of the other reactions, the angular distributions are assumed to be isotropic.

File V contains the energy distributions of secondary neutrons. For the  $(2,2n)$  and  $(n,3n)$  cross-sections the energy distributions are presented as arbitrary tabular functions for the first, second and third escaping neutrons. For example, punched cards 1272-1305 give the first neutron in the  $(n,2n)$  reaction, punched card 1272 gives the incident neutron energy and then pairs of numbers - the energy of the secondary neutron and the probability of its emission with this energy (punched cards 1274, 1275). The fission neutron spectrum is taken in the Maxwellian form. Pairs of numbers are entered: energy and effective nuclear temperature.

File XV contains the continuous photon spectrum, which is given for the inelastic interaction cross-section (section 3). The spectrum is given for five values of incident neutron energy (0.0253 eV; 3, 5, 10 and 15 MeV). For each energy pairs of numbers are given - energy and probability.

9.42420+04	2.39979+02	1	1	0	12025	1451	
0.00000+00	0.00000+00	0	0	0	02025	1451	1
0.00000+00	0.00000+00	0	0	97	502025	1451	2
94-FU-242 ITMO	EVAL-MAY79 KON'SHIN, SUKHOVITSKII, ANTSIPOV				2025	1451	3
	DIST-MAY79 REV1-MAY79				2025	1451	4
					2025	1451	5
					2025	1451	6
	EVALUATION PERFORMED IN THE FRAMEWORK				2025	1451	7
	OF THE IAEA-NDS COORDINATED RESEARCH				2025	1451	8
	PROGRAMME ON THE INTERCOMPARISON OF				2025	1451	9
	EVALUATION OF ACTINIDE NEUTRON NUCLEAR				2025	1451	10
	DATA (RESEARCH AGREEMENT N 2328/CF)				2025	1451	11
	BY				2025	1451	12
	G.V.ANTSIPOV, L.A.BAKHANOVICH, A.B.KLEPATSII,				2025	1451	13
	V.A.KON'SHIN, V.M.NASLOV, G.R.MOROGOVSKII,				2025	1451	14
	J.V.PORODZINSKII, E.SH.SUKHOVITSKII, V.A.ZENEVITCH				2025	1451	15
	*	*	*	*	2025	1451	16
	*	*	*	*	2025	1451	17
	THE EVALUATION OF NU-BAR IS BASED ON MUWERTON'S				2025	1451	18
	SYSTEMATICS (1) TAKING INTO ACCOUNT OUR EVALUATED				2025	1451	19
	SIGMA(N,N'F) AND SIGMA (N,2NF) AND AVERAGE ENERGIES OF				2025	1451	20
	NEUTRONS EMITTED BEFORE FISSION.				2025	1451	21
					2025	1451	22
					2025	1451	23
	MF = 2 RESONANCE PARAMETERS				2025	1451	24
					2025	1451	25
	RESONANCE PARAMETERS IN THE RESOLVED ENERGY RANGE FROM				2025	1451	26
	1.0E-5 EV TO 1 KEV ARE OBTAINED FROM THE DATA OF				2025	1451	27
	POORTMANS (2) ON RESONANCE ENERGIES, NEUTRON AND				2025	1451	28
	RADIATIVE CAPTURE WIDTHS. FISSION WIDTHS ARE EVALUATED				2025	1451	29
	FROM THE RESULTS OF AUCHAMPAUGH ET.AL.(3).				2025	1451	30
	IN THE ENERGY RANGE FROM 1.0E-5EV TO 2 EV A SPECIFIC				2025	1451	31

EVALUATION OF THE RESONANCE PARAMETERS FOR THE FIRST RESONANCE IS PERFORMED BY MAKING USE BOTH OF YOUNG ET.AL. DATA ON TOTAL CROSS SECTION (4,5) AND THE DATA AT 0,0253EV WITH TAKING INTO ACCOUNT ONE RESONANCE WITH NEGATIVE ENERGY. TO GENERATE NEUTRON CROSS SECTIONS IN THE RESOLVED RESONANCE ENERGY REGION FROM THE PARAMETERS GIVEN THE MULTILEVEL BREIT-WIGNER FORMALISM IS USED.	2025 1451	32
THE AVERAGE RESONANCE PARAMETERS IN THE UNRESOLVED RESONANCE ENERGY RANGE (FROM 1 KEV TO 200 KEV) ARE OBTAINED BY A SELF-CONSISTENT ANALYSIS BOTH OF THE RESOLVED RESONANCE PARAMETERS AND THE EXPERIMENTAL DATA ON RADIATIVE CAPTURE (6) AND FISSION CROSS SECTIONS (3).	2025 1451	33
THE SIGMA FISSION WAS CALCULATED TAKING INTO ACCOUNT A DOUBLE-HUMPED FISSION HARRIER CONCEPTION.	2025 1451	34
	2025 1451	35
	2025 1451	36
	2025 1451	37
	2025 1451	38
	2025 1451	39
	2025 1451	40
	2025 1451	41
	2025 1451	42
	2025 1451	43
	2025 1451	44
	2025 1451	45
	2025 1451	46
MF = 3 CROSS SECTIONS	2025 1451	47
	2025 1451	48
THE FISSION CROSS SECTION EVALUATION IN THE ENERGY RANGE FROM 200 KEV TO 15 MEV IS BASED ON EXPERIMENTAL DATA OF ALEKNAZOV, FURSOV, BEHRENS (7,8,9).	2025 1451	49
EVALUATED TOTAL, ELASTIC AND PARTIAL CROSS SECTIONS FOR DIRECT EXCITATION OF LOW-LYING LEVELS IN THE ENERGY REGION FROM 200KEV TO 15 MEV ARE OBTAINED BY COUPLED CHANNELS CALCULATIONS WITH A CAREFUL OPTIMIZATION OF POTENTIAL PARAMETERS FOR U-235.	2025 1451	50
THE RADIATIVE CAPTURE, INELASTIC SCATTERING, ( $n,2n$ ) AND ( $n,3n$ ) - CROSS SECTIONS ARE CALCULATED BY STATISTICAL MODEL TAKING INTO ACCOUNT THE COMPETITION PROCESSES ( $n,f$ ) ( $n,5n$ ), ( $n,6n$ ) AND NUCLEAR LEVEL COLLECTIVE MODES EFFECTS	2025 1451	51
	2025 1451	52
	2025 1451	53
	2025 1451	54
	2025 1451	55
	2025 1451	56
	2025 1451	57
	2025 1451	58
	2025 1451	59
	2025 1451	60
MF = 4 ANGULAR DISTRIBUTIONS	2025 1451	61
	2025 1451	62
THE ELASTIC AND INELASTIC NEUTRON SCATTERING ANGULAR DISTRIBUTIONS FROM 1 KEV TO 15 MEV ARE OBTAINED BY COUPLED CHANNELS CALCULATIONS WITH THE ISOTROPIC PART CALCULATED FROM THE COMPOUND PROCESS ADDED	2025 1451	63
	2025 1451	64
	2025 1451	65
	2025 1451	66
	2025 1451	67
	2025 1451	68
MF = 5 ENERGY DISTRIBUTION OF SECONDARY NEUTRONS	2025 1451	69
	2025 1451	70
	2025 1451	71
MT = 4 TO REPRODUCE THE ENERGY DISTRIBUTIONS IN THE REGION BELOW 5 MEV THE EVAPORATION MODEL SPECTRUM WAS USED. ABOVE 5 MEV THE CONTRIBUTION OF PREEQUILIBRIUM NEUTRONS WAS INCLUDED.	2025 1451	72
CALCULATIONS OF ( $n,2n$ ) AND ( $n,3n$ ) NEUTRON SPECTRA WERE MADE TAKING INTO ACCOUNT THE PREEQUILIBRIUM EMISSION OF THE FIRST NEUTRON.	2025 1451	73
	2025 1451	74
	2025 1451	75
	2025 1451	76
	2025 1451	77
	2025 1451	78
	2025 1451	79
MF = 15 CONTINUOUS PHOTON ENERGY SPECTRA	2025 1451	80
	2025 1451	81
GAMMA-RAY SPECTRA FROM THE INELASTIC NEUTRON PROCESSES WERE CALCULATED USING THE STATISTICAL MODEL, WHILE FISSION GAMMA-RAY SPECTRUM WAS TAKEN TO BE SIMILAR THAT OF FOR U-235 BASED ON THE EXPERIMENTAL DATA.	2025 1451	82
	2025 1451	83
	2025 1451	84
	2025 1451	85
	2025 1451	86
REFERENCES	2025 1451	87
	2025 1451	88
1. HOWERTON R.J., NUCL.SCI.ENG., 62, 1977, 438.	2025 1451	89
2. POORTMANS F., VANPHAEI G.J., NUCL.PHYS., A207, 1973, 342.	2025 1451	90
3. AUCHAMPAUGH G.F. ET.AL., NUCL.PHYS., A171, 1971, 31.	2025 1451	91
4. YOUNG T.E., REEDER S.D., NUCL.SCI.ENG., 40, 1970, 389.	2025 1451	92
5. YOUNG T.E., SIMPSON F.B., TATE R.E., NUCL.SCI.ENG., 43,	2025 1451	93

1971, 341.							
e. HOCKENBURY R.W. ET.AL., WASHINGTON CONF., 2, 1975, 584.						2025 1451	94.
7. ALCHAGOV I.D. ET.AL., KIEV CONF.V.6-V.9, 1975.						2025 1451	95
8. FURSOV B.I. ET.AL., ATOMNAYA ENERGIYA, 46, 1979, 35.						2025 1451	96
9. SFMRENS J.H. ET.AL., NUCL.SCI.ENG., 60, 1975, 433,						2025 1451	97
* * * * *						2025 1451	98
* * * * *						2025 1451	99.
0.00000+00 0.00000+00	1	451	150			12025 1451	100
0.00000+00 0.00000+00	1	452	31			12025 1451	101
0.00000+00 0.00000+00	2	151	230			12025 1451	102
0.00000+00 0.00000+00	3	1	94			12025 1451	103
0.00000+00 0.00000+00	3	2	94			12025 1451	104
0.00000+00 0.00000+00	3	4	27			12025 1451	105
0.00000+00 0.00000+00	3	16	9			12025 1451	107
0.00000+00 0.00000+00	3	17	5			12025 1451	108
0.00000+00 0.00000+00	3	18	44			12025 1451	109
0.00000+00 0.00000+00	3	20	9			12025 1451	110
0.00000+00 0.00000+00	3	21	5			12025 1451	111
0.00000+00 0.00000+00	3	51	27			12025 1451	112
0.00000+00 0.00000+00	3	52	24			12025 1451	113
0.00000+00 0.00000+00	3	53	43			12025 1451	114
0.00000+00 0.00000+00	3	54	6			12025 1451	115
0.00000+00 0.00000+00	3	55	11			12025 1451	116
0.00000+00 0.00000+00	3	56	11			12025 1451	117
0.00000+00 0.00000+00	3	57	10			12025 1451	118
0.00000+00 0.00000+00	3	58	10			12025 1451	119
0.00000+00 0.00000+00	3	59	9			12025 1451	120
0.00000+00 0.00000+00	3	60	10			12025 1451	121
0.00000+00 0.00000+00	3	61	9			12025 1451	122
0.00000+00 0.00000+00	3	62	9			12025 1451	123
0.00000+00 0.00000+00	3	63	9			12025 1451	124
0.00020+00 0.00000+00	3	91	15			12025 1451	125
0.00030+00 0.00000+00	3	102	94			12025 1451	126
0.00050+00 0.00000+00	6	2	79			12025 1451	127
0.00060+00 0.00000+00	6	16	2			12025 1451	128
0.00060+00 0.00000+00	6	17	2			12025 1451	129
0.00060+00 0.00000+00	6	18	2			12025 1451	130
0.00060+00 0.00000+00	6	20	2			12025 1451	131
0.00060+00 0.00000+00	6	51	71			12025 1451	132
0.00060+00 0.00000+00	6	52	69			12025 1451	133
0.00060+00 0.00000+00	6	53	2			12025 1451	134
0.00060+00 0.00000+00	6	54	2			12025 1451	135
0.00060+00 0.00000+00	6	55	2			12025 1451	136
0.00060+00 0.00000+00	6	56	2			12025 1451	137
0.00060+00 0.00000+00	6	57	2			12025 1451	138
0.00060+00 0.00000+00	6	58	2			12025 1451	139
0.00050+00 0.00000+00	6	59	2			12025 1451	140
0.00000+00 0.00000+00	6	60	2			12025 1451	141
0.00000+00 0.00000+00	6	61	2			12025 1451	142
0.00000+00 0.00000+00	6	62	2			12025 1451	143
0.00000+00 0.00000+00	6	63	2			12025 1451	144
0.00000+00 0.00000+00	6	91	2			12025 1451	145
0.00000+00 0.00000+00	5	15	153			12025 1451	146
0.00000+00 0.00000+00	5	17	83			12025 1451	147
0.00000+00 0.00000+00	5	18	17			12025 1451	148
0.00000+00 0.00000+00	5	91	117			12025 1451	149
0.00000+00 0.00000+00	15	3	45			12025 1451	150
0.00000+00 0.00000+00	0	0	0			02025 1 0	151
9.42420+04 2.39979+02	0	2	0			02025 1452	152
0.00000+00 0.00000+00	0	0	1			842025 1452	153
84         2						2025 1452	154
1.00000-05 2.75600+00	2.53000-02	2.75600+00	9.03000+02	2.75700+00	2025 1452	155	

1.00000+04	2.75800+00	1.00000+04	2.75920+00	2.20000+04	2.76000+002025	1452	156
2.70000+04	2.70100+00	3.30000+04	2.70200+00	3.00000+04	2.70300+002025	1452	157
4.50000+04	2.76400+00	5.10000+04	2.75500+00	5.00000+04	2.76600+002025	1452	158
7.20000+04	2.70700+00	6.80000+04	2.70800+00	7.40000+04	2.70900+002025	1452	159
8.00000+04	2.77400+00	8.50000+04	2.77100+00	9.10000+04	2.77200+002025	1452	160
1.00000+05	2.77400+00	1.20000+05	2.77700+00	1.40000+05	2.78000+002025	1452	161
1.60000+05	2.78400+00	1.40000+05	2.78700+00	2.00000+05	2.79100+002025	1452	162
2.20000+05	2.79400+00	2.40000+05	2.79800+00	2.60000+05	2.80100+002025	1452	163
2.30000+05	2.80500+00	3.00000+05	2.80800+00	3.20000+05	2.81100+002025	1452	164
3.40000+05	2.81500+00	3.50000+05	2.81400+00	3.60000+05	2.82200+002025	1452	165
4.00000+05	2.82500+00	4.20000+05	2.82900+00	4.40000+05	2.83200+002025	1452	166
6.80000+05	2.83500+00	4.90000+05	2.83900+00	5.00000+05	2.84200+002025	1452	167
5.50000+05	2.85100+00	6.00000+05	2.85600+00	6.50000+05	2.86800+002025	1452	168
7.00000+05	2.87700+00	7.50000+05	2.88500+00	8.00000+05	2.89400+002025	1452	169
8.50000+05	2.90300+00	9.00000+05	2.91100+00	9.50000+05	2.92000+002025	1452	170
1.00000+06	2.92200+00	1.10000+06	2.94600+00	1.20000+06	2.96300+002025	1452	171
1.40000+06	2.99700+00	1.60000+06	3.03200+00	1.80000+06	3.05600+002025	1452	172
2.00000+06	3.10000+00	2.20000+06	3.13500+00	2.40000+06	3.16900+002025	1452	173
2.50000+06	3.20400+00	2.37700+06	3.23800+00	3.00000+06	3.27200+002025	1452	174
3.20000+06	3.30700+00	3.45000+06	3.34100+00	3.60000+06	3.37600+002025	1452	175
7.26000+05	3.41000+00	4.00000+06	3.64300+00	4.50000+06	3.52900+002025	1452	176
5.00000+05	3.61400+00	5.50000+06	3.70200+00	6.00000+06	3.78900+002025	1452	177
7.50000+05	3.67200+00	7.00000+06	3.95300+00	7.50000+06	4.02300+002025	1452	178
8.00000+05	4.15700+00	8.50000+06	4.17700+00	9.00000+06	4.25600+002025	1452	179
9.50000+05	4.33600+00	1.00000+07	4.41900+00	1.05000+07	4.50500+002025	1452	180
1.10000+07	4.58470+00	1.15000+07	4.64700+00	1.20000+07	4.74500+002025	1452	181
1.40000+07	4.87070+00	1.40000+07	4.98400+00	1.50000+07	5.09800+002025	1451	182
1.00000+00	0.00000+00	0	0	0	02025 1 0	183	
6.00000+00	0.00000+00	0	0	0	02025 0 0	184	
9.42420+00	2.39970+02	0	0	1	02025 2151	185	
9.42420+00	1.00000+00	0	1	2	02025 2151	186	

.00000-15	1.00000+03	1	2	0	02025 2151	187	
.00000+00	9.14090-01	0	0	1	02025 2151	188	
.39999+02	0.00000+00	0	0	420	702025 2151	189	
1.00000+03	5.00000+01	1.00000+06-8.50000-08	1.08500+06	0.00000+002025	2151	190	
2.50000+03	5.00000+01	2.74200+02	1.97000+03	2.55000+02	0.00300+002025	2151	191
1.46000+01	5.00000+01	2.26700+02	3.10000+05	2.26900+02	0.00000+002025	2151	192
2.25600+01	5.00000+01	2.29190+02	3.10000+04	2.26090+02	0.00000+002025	2151	193
1.09300+01	5.00000+01	2.36790+02	4.70000+04	2.26090+02	0.00000+002025	2151	194
.346400+01	5.00000+01	7.32430+02	5.22000+02	2.12000+02	4.36000+052025	2151	195
.75700+01	5.00000+01	2.74470+02	4.40000+03	2.30000+02	4.70000+052025	2151	196
.84400+01	5.00000+01	2.31420+02	5.30000+04	2.26090+02	4.30000+052025	2151	197
.66000+02	5.00000+01	2.32070+02	6.02000+04	2.26090+02	0.00000+002025	2151	198
.07270+02	5.00000+01	3.40490+02	1.70000+02	2.12000+02	4.90000+052025	2151	199
1.31300+02	5.00000+01	3.26530+02	6.10000+03	2.45000+02	5.30000+052025	2151	200
1.41430+02	5.00000+01	2.27290+02	1.20000+04	2.26090+02	0.00000+002025	2151	201
1.49650+02	5.00000+01	3.55490+02	1.45000+02	2.10000+02	4.90000+052025	2151	202
1.63300+02	5.00000+01	2.30270+02	4.70000+04	2.26090+02	0.00000+002025	2151	203
2.04700+02	5.00000+01	7.20550+02	5.20000+02	2.00000+02	5.50000+052025	2151	204
2.09700+02	5.00000+01	2.30590+02	4.50000+04	2.26090+02	0.00000+002025	2151	205
2.15200+02	5.00000+01	2.79340+02	5.20000+03	2.26090+02	1.25000+042025	2151	206
2.19000+02	5.00000+01	2.28090+02	2.00000+04	2.26090+02	0.00000+002025	2151	207
2.32600+02	5.00000+01	2.77170+02	5.00000+03	2.26090+02	1.28000+042025	2151	208
2.64300+02	5.00000+01	2.29090+02	3.00000+04	2.26090+02	0.00000+002025	2151	209
2.71250+02	5.00000+01	2.27690+02	1.00000+04	2.26090+02	0.00000+002025	2151	210
2.73500+02	5.00000+01	3.36930+02	1.65000+02	2.20000+02	9.30000+052025	2151	211
2.74950+02	5.00000+01	2.27790+02	1.70000+04	2.26090+02	0.00000+002025	2151	212
2.81050+02	5.00000+01	2.27390+02	1.30000+04	2.26090+02	0.00000+002025	2151	213
2.98600+02	5.00000+01	3.47000+02	8.70000+03	2.60000+02	0.00000+002025	2151	214
3.03500+02	5.00000+01	4.03660+02	1.78000+02	2.25000+02	6.50000+052025	2151	215
3.19900+02	5.00000+01	2.202070+01	2.07000+01	2.20000+02	7.70000+052025	2151	216
3.27600+02	5.00000+01	2.31090+02	5.00000+04	2.26090+02	0.00000+002025	2151	217

3.32400+02	5.00000-01	9.51090+02	7.00000-02	2.50000-02	1.00000-042025	2151	218.
3.74240+02	5.00000-01	2.86400+02	6.00000-03	2.26090-02	3.10000-052025	2151	219
3.79630+02	5.00000-01	2.23790+02	2.70000-04	2.26090-02	0.00000+002025	2151	220
3.82300+02	5.00000-01	7.45210+02	5.40000-02	2.25000-02	2.10000-052025	2151	221
3.9e100+02	5.00000-01	2.51090+02	2.50000-03	2.26090-02	0.00000+002025	2151	222
3.209700+02	5.00000-01	2.48030+02	2.00000-03	2.26090-02	0.30000+002025	2151	223
4.10500+02	5.00000-01	3.06280+02	5.00000-03	2.26090-02	1.90000-052025	2151	224
4.26000+02	5.00000-01	2.76810+02	5.00000-03	2.26090-02	5.20000-052025	2151	225
4.25150+02	5.00000-01	2.23890+02	2.80000-04	2.26090-02	0.00000+002025	2151	226
4.74040+02	5.00000-01	2.39620+02	4.00000-04	2.26090-02	9.53000-042025	2151	227
4.23300+02	5.00000-01	4.74040+02	2.35000-02	2.35000-02	3.04000-042025	2151	228
4.24750+02	5.00000-01	2.28780+02	2.87000-04	2.26090-02	0.00000+002025	2151	229
5.03290+02	5.00000-01	1.72650+01	1.50000-01	2.26090-02	4.10000-052025	2151	230
5.36200+02	5.00000-01	1.21073+01	1.00000-01	2.10000-02	7.30000-052025	2151	231
5.48300+02	5.00000-01	9.30950+02	7.40000-02	2.50000-02	9.50000-052025	2151	232
5.76100+02	5.00000-01	5.26510+02	3.30000-02	2.26090-02	4.20000-052025	2151	233
5.94740+02	5.00000-01	5.90360+02	3.80000-02	2.10000-02	3.00000-052025	2151	234
5.99610+02	5.00000-01	3.17070+02	1.10000-02	2.26090-02	9.30000-052025	2151	235
6.11760+02	5.00000-01	3.46790+02	1.40000-02	2.26090-02	7.00000-052025	2151	236
6.36240+02	5.00000-01	2.76070+02	5.00000-03	2.26040-02	0.00000+002025	2151	237
6.85100+02	5.00000-01	2.53091+02	2.70000-03	2.26090-02	0.00000+002025	2151	238
7.69210+02	5.00000-01	3.57080+02	1.40000-02	2.26090-02	9.90000-052025	2151	239
8.92220+02	5.00000-01	6.72270+02	4.51000-02	2.20000-02	2.27000-042025	2151	240
9.11500+02	5.00000-01	1.42560+01	1.30000-01	1.95000-02	6.00000-052025	2151	241
2.27400+02	5.00000-01	2.56031+02	3.00000-03	2.26090-02	0.00000+002025	2151	242
7.36600+02	5.00010+01	1.21205+01	1.00000-01	2.26040-02	5.96000-042025	2151	243
2.54110+02	5.00010+01	1.51105+01	1.37000-01	2.26090-02	1.49000-032025	2151	244
2.61240+02	5.00000+01	5.94220+02	3.30000-03	2.26090-02	3.35200-022025	2151	245
2.228500+02	5.00000+01	7.586630+02	5.30000-02	2.26090-02	1.25000-032025	2151	246
7.03500+02	5.00000+01	1.07643+01	6.50000-02	2.26070-02	7.40000-052025	2151	247
8.23800+02	5.00000+01	2.50530+02	2.00000-03	2.26040-02	4.44000-042025	2151	248

8.37500+02	5.00000-01	5.80590+02	3.80000-02	2.00000+02	5.90000-052025	2151	249
8.56100+02	5.00000-01	5.91500+02	3.72000-02	2.20000+02	1.50000-042025	2151	250
8.55100+02	5.00000-01	3.25710+02	1.00000-02	2.26040+02	6.20000-052025	2151	251
8.72500+02	5.00000-01	8.30470+02	6.20000-02	2.60000+02	4.90000-052025	2151	252
8.86200+02	5.00000-01	5.10400+02	2.20000-02	2.90000+02	4.00000-052025	2151	253
9.22500+02	5.00000-01	8.20460+02	6.40000-02	1.80000+02	4.50000-052025	2151	254
9.35400+02	5.00000-01	3.36090+02	1.10000-02	2.26090+02	0.00000+002025	2151	255
9.39600+02	5.00000-01	3.26090+02	1.00000-02	2.26090+02	0.00000+002025	2151	256
9.49100+02	5.00000-01	4.60000+02	1.41000-02	2.60000+02	0.00000+002025	2151	257
9.77900+02	5.00000-01	3.71090+02	1.45000-02	2.26090+02	0.00000+002025	2151	258
1.00400+03	5.00000-01	6.56090+02	4.30000-02	2.26090+02	0.00000+002025	2151	259
1.00000+03	2.00000+05	- 2	2	0	02025	2151	260
5.00000+01	9.14070+01	0	0	3	02025	2151	261
2.39979+02	0.30000+00	0	0	1	02025	2151	262
5.00000+01	0.00000+00	- 3	0	174	282025	2151	263
0.00000+00	0.00000+00	2.00000+00	1.00000+00	0.00000+00	1.00000+002025	2151	264
1.00000+03	1.41980+01	0.00000+00	1.29202+03	2.26090+02	8.83000-012025	2151	265
1.50000+03	1.41820+01	0.00000+00	1.29056+03	2.26140+02	8.37000-012025	2151	266
2.00000+03	1.41600+01	0.00000+00	1.23911+03	2.26190+02	8.70000-012025	2151	267
2.50000+03	1.41500+01	0.00000+00	1.28765+03	2.26240+02	8.94000-012025	2151	268
3.00000+03	1.41350+01	0.00000+00	1.28628+03	2.26230+02	8.97000-012025	2151	269
4.00000+03	1.41030+01	0.00000+00	1.23337+03	2.26380+02	9.04000-012025	2151	270
5.00000+03	1.40720+01	0.00000+00	1.23055+03	2.26470+02	9.12000-012025	2151	271
6.00000+03	1.40400+01	0.00000+00	1.27754+03	2.26560+02	9.19000-012025	2151	272
7.00000+03	1.40090+01	0.00000+00	1.27482+03	2.26660+02	9.26000-012025	2151	273
2.00000+03	1.39780+01	0.00000+00	1.27200+03	2.26750+02	9.33000-012025	2151	274
9.00000+03	1.39470+01	0.00000+00	1.20918+03	2.26850+02	9.41000-012025	2151	275
1.00000+04	1.39150+01	0.00000+00	1.26536+03	2.26940+02	9.48000-012025	2151	276
1.50000+04	1.37420+01	0.00000+00	1.25234+03	2.27410+02	9.86000-012025	2151	277
2.00000+04	1.36090+01	0.00000+00	1.23842+03	2.27890+02	1.02600+002025	2151	278
2.50000+04	1.34590+01	0.00000+00	1.22477+03	2.28360+02	1.06700+002025	2151	279

3.00000+04	1.33100+01	0.00000+00	1.21121-03	2.28330-02	1.10900+002025	2151	280
4.00000+04	1.30170+01	0.00000+00	1.15455-03	2.29780-02	1.19900+002025	2151	281
5.00000+04	1.27320+01	8.00030-06	1.15851-03	2.30730-02	1.29500+002025	2151	282
6.00000+04	1.24520+01	9.40000-05	1.13313-03	2.31680-02	1.39900+002025	2151	283
7.00000+04	1.21790+01	3.06000-04	1.10829-03	2.32630-02	1.51000+002025	2151	284
8.00000+04	1.19120+01	6.63000-04	1.08399-03	2.33580-02	1.62900+002025	2151	285
9.00000+04	1.16520+01	1.19200-03	1.06033-03	2.34540-02	1.75700+002025	2151	286
1.00000+05	1.13970+01	1.38400-03	1.03713-03	2.35490-02	1.89400+002025	2151	287
1.20000+05	1.09050+01	3.77400-03	9.92355-04	2.37410-02	2.19900+002025	2151	288
1.40000+05	1.04340+01	9.31800-03	9.47496-04	2.39340-02	2.54800+002025	2151	289
1.60000+05	9.98500+00	9.46500-03	9.08635-04	2.41270-02	2.94700+002025	2151	290
1.80000+05	9.55600+00	1.31450-02	8.67590-04	2.43310-02	3.40300+002025	2151	291
2.00000+05	9.14600+00	1.72820-02	8.32280-04	2.45200-02	3.72300+002025	2151	292
2.39279+02	0.20000+00	1	0	2	02025	2151	293
-5.00000+01	0.00000+00	3	0	174	282025	2151	294
0.00000+00	0.00000+00	1.00000+00	1.00000+00	0.00000+00	2.00000+002025	2151	295
1.00000+03	1.41980+01	0.00000+00	3.54950-03	2.26090-02	8.83000-012025	2151	296
1.50000+03	1.41820+01	0.00000+00	3.54550-03	2.26140-02	8.37000-012025	2151	297
2.00000+03	1.41450+01	0.00000+00	3.54150-03	2.26190-02	8.30000-012025	2151	298
2.50000+03	1.41500+01	0.00000+00	3.53750-03	2.26240-02	8.94000-012025	2151	299
3.00000+03	1.41350+01	0.00000+00	3.53375-03	2.26280-02	8.97000-012025	2151	300
4.00000+03	1.41030+01	0.00000+00	3.52575-03	2.26380-02	9.04000-012025	2151	301
5.00000+03	1.40720+01	0.00000+00	3.51800-03	2.26470-02	9.12000-012025	2151	302
7.00000+03	1.40400+01	0.00000+00	3.51000-03	2.26560-02	9.19000-012025	2151	303
7.00000+03	1.40090+01	0.00000+00	3.50225-03	2.26660-02	9.26000-012025	2151	304
8.00000+03	1.39763+01	0.00000+00	3.49450-03	2.26750-02	9.33000-012025	2151	305
9.00000+03	1.39470+01	0.00000+00	3.43675-03	2.26850-02	9.41000-012025	2151	306
1.00000+04	1.39162+01	0.00000+00	3.47930-03	2.26940-02	9.48000-012025	2151	307
1.50000+04	1.37623+01	0.00000+00	3.44050-03	2.27410-02	9.36000-012025	2151	308
2.00000+04	1.3e993+01	0.00000+00	3.40225-03	2.27890-02	1.02600+002025	2151	309
2.50000+04	1.34590+01	0.00000+00	3.36475-03	2.28350-02	1.06700+002025	2151	310

3.00000+04	1.33100+01	0.00000+00	3.32750-03	2.28830-02	1.15900+002025	2151	311
4.00000+04	1.30170+01	0.00000+00	3.25425-03	2.29780-02	1.19900+002025	2151	312
5.00000+04	1.27320+01	4.97100-03	3.13300-03	2.30730-02	1.29500+002025	2151	313
6.00000+04	1.24520+01	2.04850-02	3.11300-03	2.31680-02	1.39900+002025	2151	314
7.00000+04	1.21790+01	4.01970-02	3.04475-03	2.32630-02	1.51000+002025	2151	315
8.00000+04	1.19120+01	6.21020-02	2.97800-03	2.33580-02	1.62900+002025	2151	316
9.00000+04	1.16520+01	8.51370-02	2.91300-03	2.34540-02	1.75700+002025	2151	317
1.00000+05	1.13970+01	1.09538-01	2.84925-03	2.35490-02	1.89400+002025	2151	318
1.20000+05	1.09050+01	1.55395-01	2.72025-03	2.37410-02	2.19900+002025	2151	319
1.40000+05	1.04340+01	2.00207-01	2.60950-03	2.39340-02	2.54800+002025	2151	320
1.40000+05	9.98500+00	2.41990-01	2.49625-03	2.41270-02	2.94730+002025	2151	321
1.30000+05	9.55600+00	2.80245-01	2.38970-03	2.43310-02	3.40300+002025	2151	322
2.00000+05	9.14600+00	3.14788-01	2.24650-03	2.45260-02	3.92300+002025	2151	323
-1.50000+00	0.00000+00	3	0	174	282025	2151	324
0.00000+00	0.00000+00	2.00000+00	1.00000+00	0.00000+00	4.00000+002025	2151	325
1.00000+03	7.25900+00	0.00000+00	1.81475-03	2.24950-02	4.52000-012025	2151	326
1.50000+03	7.25000+00	0.00000+00	1.81250-03	2.25000-02	4.53000-012025	2151	327
2.00000+03	7.24200+00	0.00000+00	1.81050-03	2.25050-02	4.55000-012025	2151	328
2.50000+03	7.23400+00	0.00000+00	1.80850-03	2.25090-02	4.57000-012025	2151	329
3.00000+03	7.22600+00	0.00000+00	1.80650-03	2.25140-02	4.59000-012025	2151	330
4.00000+03	7.21000+00	0.00000+00	1.80250-03	2.25240-02	4.62000-012025	2151	331
5.00000+03	7.19400+00	0.00000+00	1.70850-03	2.25330-02	4.66000-012025	2151	332
6.00000+03	7.17800+00	0.00000+00	1.77450-03	2.25420-02	4.70000-012025	2151	333
7.00000+03	7.16200+00	0.00000+00	1.77905-03	2.25520-02	4.73000-012025	2151	334
8.00000+03	7.14600+00	0.00000+00	1.78650-03	2.25610-02	4.77000-012025	2151	335
9.00000+03	7.13000+00	0.00000+00	1.78250-03	2.25710-02	4.81000-012025	2151	336
1.00000+04	7.11400+00	0.00000+00	1.77850-03	2.25800-02	4.85000-012025	2151	337
1.50000+04	7.03500+00	0.00000+00	1.75875-03	2.26270-02	5.04000-012025	2151	338
2.00000+04	6.95800+00	0.00000+00	1.73950-03	2.26740-02	5.24000-012025	2151	339
2.50000+04	6.88000+00	0.00000+00	1.72000-03	2.27210-02	5.45000-012025	2151	340
3.00000+04	6.80400+00	0.00000+00	1.70100-03	2.27680-02	5.67000-012025	2151	341

4.00000+04	6.65400+00	0.00000+00	1.67350-03	2.28630-02	6.13000-012025	2151	342
5.00000+04	6.50800+00	5.08300-03	1.62700-03	2.29580-02	6.02000-012025	2151	343
6.00000+04	6.36500+00	2.09430-02	1.59125-03	2.30520-02	7.15000-012025	2151	344
7.00000+04	6.22600+00	4.10940-02	1.55650-03	2.31470-02	7.72000-012025	2151	345
8.00000+04	6.03900+00	6.34860-02	1.52225-03	2.32430-02	8.33000-012025	2151	346
9.00000+04	5.95800+00	8.70330-02	1.48900-03	2.33380-02	8.98000-012025	2151	347
1.00000+05	5.82500+00	1.11055-01	1.45625-03	2.34330-02	9.68000-012025	2151	348
1.20000+05	5.57300+00	1.58848-01	1.34325-03	2.36250-02	1.12300+002025	2151	349
1.40000+05	5.33300+00	2.04541-01	1.43325-03	2.38170-02	1.30200+002025	2151	350
1.60000+05	5.10300+00	2.47338-01	1.27575-03	2.40100-02	1.50600+002025	2151	351
1.80000+05	4.33300+00	2.86424-01	1.22075-03	2.42140-02	1.73900+002025	2151	352
2.00000+05	4.67400+00	3.21714-01	1.15850-03	2.44080-02	2.00500+002025	2151	353
2.39970+02	0.00000+00	2	0	2	02025	2151	354
1.50000+04	0.00000+00	3	0	174	282025	2151	355
0.00000+00	0.00000+00	1.00000+00	1.00000+00	0.00000+00	4.00000+002025	2151	356
1.60000+03	7.25900+00	0.30000+00	6.62559-04	2.24950-02	4.52000-012025	2151	357
1.50000+03	7.25000+00	0.20000+00	6.59750-04	2.25000-02	4.53000-012025	2151	358
2.00000+03	7.24200+00	0.00000+00	6.59022-04	2.25050-02	4.55000-012025	2151	359
2.50000+03	7.23400+00	0.00000+00	6.55294-04	2.25090-02	4.57000-012025	2151	360
3.00000+03	7.22600+00	0.00000+00	6.57568-04	2.25140-02	4.59000-012025	2151	361
4.00000+03	7.21000+00	0.00000+00	6.55610-04	2.25240-02	4.62000-012025	2151	362
5.00000+03	7.19400+00	0.00000+00	6.54654-04	2.25330-02	4.66000-012025	2151	363
7.00000+03	7.17800+00	0.00000+00	6.53198-04	2.25420-02	4.70000-012025	2151	364
7.00000+03	7.16200+00	0.00000+00	6.51742-04	2.25520-02	4.73000-012025	2151	365
8.00000+03	7.14600+00	0.00000+00	6.50286-04	2.25610-02	4.77000-012025	2151	366
9.00000+03	7.13000+00	0.00000+00	6.45830-04	2.25710-02	4.81000-012025	2151	367
1.70000+04	7.11400+00	0.00000+00	6.47374-04	2.25800-02	4.35000-012025	2151	368
1.50000+04	7.03500+00	0.00000+00	6.43185-04	2.26270-02	5.04000-012025	2151	369
2.00000+04	6.95800+00	0.00000+00	6.33178-04	2.26740-02	5.24000-012025	2151	370
2.50000+04	6.38000+00	0.00000+00	6.24050-04	2.27210-02	5.45000-012025	2151	371
3.00000+04	6.80400+00	0.00000+00	6.19154-04	2.27680-02	5.67000-012025	2151	372

4.00000+04	6.65400+00	0.00000+00	6.05514-04	2.28630-02	6.13000-012025	2151	373
5.00000+04	6.50800+00	4.52790-02	5.92228-04	2.29580-02	6.52300-012025	2151	374
6.00000+04	6.36500+00	7.33130-02	5.79215-04	2.30520-02	7.15000-012025	2151	375
7.00000+04	6.22600+00	9.15060-02	5.65566-04	2.31470-02	7.72000-012025	2151	376
8.00000+04	6.08900+00	1.05475-01	5.54779-04	2.32430-02	8.33000-012025	2151	377
9.00000+04	5.95600+00	1.16547-01	5.41996-04	2.33330-02	8.95000-012025	2151	378
1.00000+05	5.82500+00	1.26407-01	5.30075-04	2.34330-02	9.56000-012025	2151	379
1.20000+05	5.57300+00	1.41748-01	5.07143-04	2.36250-02	1.12300+002025	2151	380
1.40000+05	5.33300+00	1.35829-01	4.85303-04	2.38170-02	1.30200+002025	2151	381
1.40000+05	5.10300+00	1.52996-01	4.64373-04	2.40100-02	1.50600+002025	2151	382
1.30000+05	4.88300+00	1.70602-01	4.44353-04	2.42140-02	1.73900+002025	2151	383
2.00000+05	4.07400+00	1.76815-01	4.25334-04	2.44080-02	2.00500+002025	2151	384
2.50000+04	0.00000+00	3	0	174	282025	2151	385
0.00000+00	0.00000+00	1.00000+00	1.00000+00	0.00000+00	6.00000+002025	2151	386
1.00000+03	5.02200+00	0.00000+00	4.57002-04	2.23070-02	3.12000-012025	2151	387
1.50000+03	5.01600+00	0.00000+00	4.55456-04	2.23120-02	3.14000-012025	2151	388
2.00000+03	5.01100+00	0.00000+00	4.55001-04	2.23160-02	3.15000-012025	2151	389
2.50000+03	5.00500+00	0.00000+00	4.55455-04	2.23210-02	3.16000-012025	2151	390
3.00000+03	4.99900+00	0.00000+00	4.54729-04	2.23260-02	3.17000-012025	2151	391
4.00000+03	4.98800+00	0.00000+00	4.53908-04	2.23350-02	3.20000-012025	2151	392
5.00000+03	4.97700+00	0.00000+00	4.52907-04	2.23450-02	3.22000-012025	2151	393
6.00000+03	4.96600+00	0.00000+00	4.51906-04	2.23540-02	3.25000-012025	2151	394
7.00000+03	4.95500+00	0.00000+00	4.50905-04	2.23630-02	3.28000-012025	2151	395
8.00000+03	4.94400+00	0.00000+00	4.49904-04	2.23730-02	3.30000-012025	2151	396
9.00000+03	4.93300+00	0.00000+00	4.48903-04	2.23820-02	3.33000-012025	2151	397
1.00000+04	4.92200+00	0.00000+00	4.47902-04	2.23910-02	3.35000-012025	2151	398
1.50000+04	4.86700+00	0.00000+00	4.42897-04	2.24380-02	3.49000-012025	2151	399
2.00000+04	4.81300+00	0.00000+00	4.37983-04	2.24850-02	3.63000-012025	2151	400
2.50000+04	4.76000+00	0.00000+00	4.33160-04	2.25320-02	3.77000-012025	2151	401
3.00000+04	4.70700+00	0.00000+00	4.28337-04	2.25790-02	3.92000-012025	2151	402
4.00000+04	4.60300+00	0.00000+00	4.12373-04	2.26730-02	4.24000-012025	2151	403

5.00000+04	6.50200+00	3.17350-02	4.09682-04	2.27680-02	4.58000-012025	2151	404	
6.00000+04	6.40300+00	5.07110-02	4.00673-04	2.28620-02	4.95000-012025	2151	405	
7.00000+04	4.30600+00	6.32900-02	3.91840-04	2.29570-02	5.34000-012025	2151	406	
5.00000+04	4.21100+00	7.29490-02	3.83201-04	2.30520-02	5.76000-012025	2151	407	
9.00000+04	4.11900+00	8.08110-02	3.74829-04	2.31470-02	6.21000-012025	2151	408	
1.00000+05	4.02900+00	8.74190-02	3.66639-04	2.32420-02	6.70000-012025	2151	409	
1.20000+05	3.85400+00	9.80200-02	3.53714-04	2.34320-02	7.77000-012025	2151	410	
1.40000+05	3.68700+00	1.06200-01	3.35517-04	2.36240-02	9.00000-012025	2151	411	
1.60000+05	3.52800+00	1.12715-01	3.21048-04	2.38170-02	1.04100-002025	2151	412	
1.80000+05	3.37600+00	1.18109-01	3.07216-04	2.40200-02	1.20200-002025	2151	413	
2.00000+05	3.23100+00	1.22719-01	2.94021-04	2.42140-02	1.38600-002025	2151	414	
0.00000+00	0.00000+00	0	0	0	02025	2	0	
0.00000+00	0.00000+00	0	0	0	02025	0	0	
9.42420+04	2.39979+02	0	99	0	02025	3	1	
0.00000+00	0.00000+00	0	0	2	2732025	3	1	
185	2	273	2	2025	3	1	419	
1.00000+05	3.40333+02	2.00000-05	2.52534+02	3.00000-05	2.14952+022025	3	1	420
4.00000+05	1.93237+02	5.00000-05	1.78836+02	6.00000-05	1.68479+022025	3	1	421
7.00000+05	1.65620+02	8.00000-05	1.54418+02	9.00000-05	1.49380+022025	3	1	422
1.00000+14	1.45189+02	2.00000-04	1.23437+02	3.00000-04	1.13820+022025	3	1	423
4.00000+04	1.07484+02	5.00000-04	1.02591+02	6.00000-04	9.85150+012025	3	1	424
7.00000+04	9.49800+01	8.00000-04	9.13460+01	9.00000-04	8.90250+012025	3	1	425
1.00000+03	8.64610+01	2.00000-03	6.92380+01	3.00000-03	5.96510+012025	3	1	426
4.00000+03	5.34130+01	5.00000-03	4.89700+01	5.00000-03	4.55080+012025	3	1	427
7.00000+03	4.29550+01	8.00000-03	4.07910+01	9.00000-03	3.39980+012025	3	1	428
1.00000+02	3.74690+01	1.50000-02	3.22470+01	2.00000-02	2.91230+012025	3	1	429
2.00000+02	2.69910+01	2.53000-02	2.68340+01	3.00000-02	2.54210+012025	3	1	430
3.00000+02	2.42040+01	4.00000-02	2.32260+01	4.50000-02	2.24160+012025	3	1	431
5.00000+02	2.17370+01	5.50000-02	2.11530+01	6.00000-02	2.06440+012025	3	1	432
6.00000+02	2.31980+01	7.00000-02	1.93200+01	7.50000-02	1.94470+012025	3	1	433
8.00000+02	1.71270+01	8.50000-02	1.88370+01	9.00000-02	1.85720+012025	3	1	434

9.50000+02	1.83330+01	1.00000-01	7.81060+01	1.10000-01	1.77100+012025	3	1	435
1.20000+01	1.73560+01	1.30000-01	1.70660+01	1.40000-01	1.68000+012025	3	1	436
1.50000+01	1.65630+01	1.60000-01	1.63510+01	1.70000-01	1.51600+012025	3	1	437
1.80000+01	1.59860+01	1.70000-01	1.58290+01	2.00000-01	1.56840+012025	3	1	438
2.10000+01	1.55521+01	2.20000-01	1.54310+01	2.30000-01	1.53170+012025	3	1	439
2.40000+01	1.52130+01	2.50000-01	1.51150+01	2.60000-01	1.50260+012025	3	1	440
2.70000+01	1.49430+01	2.80000-01	1.48650+01	2.90000-01	1.47920+012025	3	1	441
3.00000+01	1.47240+01	3.10000-01	1.46600+01	3.20000-01	1.46010+012025	3	1	442
3.30000+01	1.45450+01	3.40000-01	1.44930+01	3.50000-01	1.44460+012025	3	1	443
3.60000+01	1.43970+01	3.70000-01	1.43540+01	3.60000-01	1.43130+012025	3	1	444
3.90000+01	1.42740+01	4.00000-01	1.42410+01	4.10000-01	1.42060+012025	3	1	445
4.20000+01	1.41740+01	4.30000-01	1.41450+01	4.40000-01	1.41170+012025	3	1	446
4.50000+01	1.40920+01	4.60000-01	1.40670+01	4.70000-01	1.40460+012025	3	1	447
4.80000+01	1.40250+01	4.90000-01	1.40070+01	5.00000-01	1.39890+012025	3	1	448
5.20000+01	1.37570+01	5.40000-01	1.34310+01	5.60000-01	1.39100+012025	3	1	449
5.80000+01	1.38950+01	6.00000-01	1.38820+01	6.20000-01	1.38750+012025	3	1	450
6.40000+01	1.38710+01	6.50000-01	1.38720+01	6.80000-01	1.38770+012025	3	1	451
7.00000+01	1.38840+01	7.20000-01	1.38960+01	7.40000-01	1.39100+012025	3	1	452
7.60000+01	1.39300+01	7.80000-01	1.39520+01	8.00000-01	1.39770+012025	3	1	453
8.20000+01	1.40050+01	8.40000-01	1.40400+01	8.60000-01	1.40760+012025	3	1	454
8.80000+01	1.41150+01	9.00000-01	1.41610+01	9.20000-01	1.42070+012025	3	1	455
9.40000+01	1.42590+01	9.50000-01	1.43130+01	9.80000-01	1.43730+012025	3	1	456
1.00000+00	1.44350+01	1.05000+00	1.46120+01	1.10000+00	1.48200+012025	3	1	457
1.15000+00	1.50550+01	1.20000+00	1.53330+01	1.25000+00	1.56480+012025	3	1	458
1.30000+00	1.60100+01	1.35000+00	1.64250+01	1.40000+00	1.69020+012025	3	1	459
1.45000+00	1.74490+01	1.50000+00	1.80810+01	1.60000+00	1.96650+012025	3	1	460
1.70000+00	2.18310+01	1.80000+00	2.48710+01	1.90000+00	2.92870+012025	3	1	461
2.00000+00	3.59950+01	2.10000+00	4.68110+01	2.20000+00	6.57580+012025	3	1	462
2.30000+00	1.03218+02	2.40000+00	1.93197+02	2.50000+00	5.05059+022025	3	1	463
2.55000+00	1.06391+03	2.58000+00	1.99292+03	2.60000+00	3.47875+032025	3	1	464
2.61000+00	4.91240+03	2.62000+00	7.40109+03	2.63000+00	1.21898+042025	3	1	465

2.64000+00	2.26025+04	2.45000+00	4.62177+04	2.06000+00	8.09034+04	2025	3	1	466
2.67000+00	4.64778+04	2.68000+00	2.28658+04	2.69000+00	1.24060+04	2025	3	1	467
2.70000+00	7.57725+03	2.72000+00	3.60359+03	2.75000+00	1.65682+03	2025	3	1	468
2.80000+00	7.13744+02	2.90000+00	2.5774+02	3.00000+00	1.36612+02	2025	3	1	469
3.20000+00	6.25280+01	3.40000+00	3.00610+01	3.60000+00	2.85920+01	2025	3	1	470
3.80000+00	2.29710+01	4.00000+00	1.95770+01	4.20000+00	1.73550+01	2025	3	1	471
4.40000+00	1.58110+01	4.60000+00	1.46880+01	4.80000+00	1.38420+01	2025	3	1	472
5.00000+00	1.31540+01	5.20000+00	1.26620+01	5.40000+00	1.22380+01	2025	3	1	473
5.60000+00	1.18880+01	5.80000+00	1.15950+01	6.00000+00	1.13460+01	2025	3	1	474
6.20000+00	1.11320+01	6.40000+00	1.09470+01	6.60000+00	1.07840+01	2025	3	1	475
6.80000+00	1.06420+01	7.00000+00	1.05140+01	7.20000+00	1.04000+01	2025	3	1	476
7.40000+00	1.02970+01	7.60000+00	1.02040+01	7.80000+00	1.01200+01	2025	3	1	477
8.00000+00	1.00420+01	8.20000+00	9.97130+00	8.40000+00	9.90500+00	2025	3	1	478
8.60000+00	9.84500+00	8.50000+00	9.78900+00	9.00000+00	9.73600+00	2025	3	1	479
9.20000+00	9.68600+00	9.40000+00	9.64000+00	9.60000+00	9.59600+00	2025	3	1	480
9.80000+00	9.55500+00	1.00000+01	9.51500+00	1.00000+01	2.26890+01	2025	3	1	481
1.50000+03	2.05760+01	2.00000+03	1.93350+01	2.50000+03	1.84970+01	2025	3	1	482
3.00000+03	1.78840+01	4.00000+03	1.70380+01	5.00000+03	1.64730+01	2025	3	1	483
6.00000+03	1.60640+01	7.00000+03	1.57510+01	8.00000+03	1.55030+01	2025	3	1	484
9.00000+03	1.53020+01	1.00000+04	1.51330+01	1.50000+04	1.45820+01	2025	3	1	485
2.00000+04	1.42670+01	2.50000+04	1.40590+01	3.00000+04	1.39040+01	2025	3	1	486
4.00000+04	1.36790+01	5.00000+04	1.35090+01	6.00000+04	1.33670+01	2025	3	1	487
7.00000+04	1.32320+01	8.00000+04	1.31170+01	9.00000+04	1.30020+01	2025	3	1	488
1.00000+05	1.28880+01	1.20000+05	1.26610+01	1.40000+05	1.24420+01	2025	3	1	489
1.40000+05	1.22170+01	1.50000+05	1.19870+01	2.00000+05	1.17510+01	2025	3	1	490
2.20000+05	1.15080+01	2.40000+05	1.12710+01	2.60000+05	1.10190+01	2025	3	1	491
2.80000+05	1.07720+01	3.00000+05	1.05230+01	3.20000+05	1.02590+01	2025	3	1	492
3.40000+05	9.99200+00	3.60000+05	9.74700+00	3.80000+05	9.52000+00	2025	3	1	493
4.00000+05	9.28120+00	4.20000+05	9.07200+00	4.40000+05	8.92100+00	2025	3	1	494
4.60000+05	8.74500+00	4.80000+05	8.58700+00	5.00000+05	8.45300+00	2025	3	1	495
5.50000+05	8.19500+00	6.00000+05	7.95600+00	6.50000+05	7.77300+00	2025	3	1	496

7.19300+25	7.02100+00	7.50000+05	7.47500+00	8.00000+05	7.33900+00	2025	3	1	497
8.50000+25	7.22700+00	9.00000+05	7.14600+00	9.50000+05	7.06700+00	2025	3	1	498
1.00000+26	7.00200+00	1.10000+06	6.87400+00	1.20000+06	6.81300+00	2025	3	1	499
1.40000+26	6.78900+00	1.50000+06	6.83700+00	1.80000+06	6.96000+00	2025	3	1	500
2.00000+26	7.15200+00	2.20000+06	7.33100+00	2.46000+06	7.47500+00	2025	3	1	501
2.40000+26	7.58900+00	2.80000+06	7.66500+00	3.00000+06	7.71300+00	2025	3	1	502
3.20000+26	7.74000+00	3.40000+06	7.76400+00	3.60000+06	7.76800+00	2025	3	1	503
3.80000+26	7.75700+00	4.00000+06	7.74500+00	4.50000+06	7.64600+00	2025	3	1	504
5.00000+26	7.40000+00	5.00000+06	7.17900+00	6.00000+06	6.95200+00	2025	3	1	505
6.50000+26	6.74800+00	7.00000+06	6.55800+00	7.50000+06	6.39100+00	2025	3	1	506
9.00000+26	6.23200+00	8.50000+06	6.07800+00	9.00000+06	5.94700+00	2025	3	1	507
1.10000+27	5.65000+00	1.15000+07	5.64500+00	1.20000+07	5.54700+00	2025	3	1	508
1.30000+27	5.67700+00	1.40000+07	5.72500+00	1.50000+07	5.77500+00	2025	3	1	509
6.00000+26	0.50000+00	0	0	0	0	2025	3	1	510
2.42420+26	2.42970+02	0	0	0	0	2025	3	0	511
2.00000+26	3.00000+00	0	0	0	0	2025	3	2	512
1.155	2	273	2	2	273	2025	3	2	513
1.00000+05	1.29100+01	2.00000+05	1.28100+01	3.00000+05	1.27310+01	2025	3	2	514
4.00000+05	1.26450+01	5.00000+05	1.25620+01	6.00000+05	1.24810+01	2025	3	2	515
7.00000+05	1.24030+01	8.00000+05	1.23260+01	1.00000+05	1.22520+01	2025	3	2	516
1.05000+06	1.21800+01	2.00000+06	1.15540+01	3.00000+06	1.10670+01	2025	3	2	517
4.00000+06	1.00800+01	5.00000+06	1.03680+01	6.00000+06	1.01130+01	2025	3	2	518
7.00000+06	9.99100+00	8.00000+06	9.72400+00	9.00000+06	9.57400+00	2025	3	2	519
1.00000+06	9.44500+00	2.00000+06	8.78670+00	3.00000+06	8.55500+00	2025	3	2	520
4.00000+06	8.44700+00	5.00000+06	8.34900+00	6.00000+06	8.35300+00	2025	3	2	521
7.00000+06	8.32900+00	8.00000+06	8.31370+00	9.00000+06	8.30100+00	2025	3	2	522
1.30000+02	8.29200+00	1.50000+02	8.25700+00	2.00000+02	8.25600+00	2025	3	2	523
2.50000+02	8.24800+00	2.53000+02	8.24700+00	3.00000+02	8.24100+00	2025	3	2	524
3.50000+02	8.23600+00	4.00000+02	8.23100+00	4.50000+02	8.22700+00	2025	3	2	525
5.00000+02	8.22200+00	5.50000+02	8.21800+00	6.00000+02	8.21300+00	2025	3	2	526
5.50000+02	8.21300+00	6.00000+02	8.21000+00	6.50000+02	8.20700+00	2025	3	2	527

6.50000-02	8.20900+00	7.00000-02	8.20500+00	7.50000-02	8.20000+00	2025	3	2	528
6.00000-02	8.19600+00	8.50000-02	8.19200+00	9.00000-02	8.18700+00	2025	3	2	529
9.50000-02	8.18300+00	1.00000-01	8.17800+00	1.10000-01	8.17000+00	2025	3	2	530
1.20000-01	8.16100+00	1.30000-01	8.15300+00	1.40000-01	8.14400+00	2025	3	2	531
1.50000-01	8.13500+00	1.60000-01	8.12600+00	1.70000-01	8.11700+00	2025	3	2	532
1.80000-01	8.10800+00	1.90000-01	8.09900+00	2.00000-01	8.09000+00	2025	3	2	533
2.10000-01	8.08100+00	2.20000-01	8.07100+00	2.30000-01	8.06200+00	2025	3	2	534
2.40000-01	8.05200+00	2.50000-01	8.04300+00	2.60000-01	8.03300+00	2025	3	2	535
2.70000-01	8.02400+00	2.80000-01	8.01400+00	2.90000-01	8.00400+00	2025	3	2	536
3.00000-01	7.99400+00	3.10000-01	7.98400+00	3.20000-01	7.97400+00	2025	3	2	537
3.30000-01	7.96400+00	3.40000-01	7.95400+00	3.50000-01	7.94400+00	2025	3	2	538
3.60000-01	7.93300+00	3.70000-01	7.92300+00	3.80000-01	7.91200+00	2025	3	2	539
3.90000-01	7.90200+00	4.00000-01	7.89200+00	4.10000-01	7.88000+00	2025	3	2	540
4.20000-01	7.86900+00	4.30000-01	7.85800+00	4.40000-01	7.84600+00	2025	3	2	541
4.50000-01	7.83600+00	4.60000-01	7.82400+00	4.70000-01	7.81300+00	2025	3	2	542
4.80000-01	7.80200+00	4.90000-01	7.77100+00	5.00000-01	7.77900+00	2025	3	2	543
5.20000-01	7.75500+00	5.40000-01	7.73100+00	5.60000-01	7.70600+00	2025	3	2	544
5.80000-01	7.58200+00	6.00000-01	7.65600+00	6.20000-01	7.63100+00	2025	3	2	545
6.40000-01	7.50400+00	6.60000-01	7.57800+00	6.80000-01	7.55100+00	2025	3	2	546
7.00000-01	7.52300+00	7.20000-01	7.49500+00	7.40000-01	7.46500+00	2025	3	2	547
7.60000-01	7.43700+00	7.80000-01	7.40700+00	8.00000-01	7.37600+00	2025	3	2	548
8.20000-01	7.34600+00	8.40000-01	7.31400+00	8.60000-01	7.28100+00	2025	3	2	549
8.30000-01	7.24800+00	9.00000-01	7.21500+00	9.20000-01	7.18000+00	2025	3	2	550
9.40000-01	7.14600+00	9.60000-01	7.10900+00	9.80000-01	7.07300+00	2025	3	2	551
1.00000+00	7.03500+00	1.05000+00	6.83800+00	1.10000+00	6.83700+00	2025	3	2	552
1.15000+00	6.72800+00	1.20000+00	6.61500+00	1.25000+00	6.49200+00	2025	3	2	553
1.30000+00	6.36200+00	1.35000+00	6.22500+00	1.40000+00	6.07800+00	2025	3	2	554
1.45000+00	5.92000+00	1.50000+00	5.75200+00	1.60000+00	5.37700+00	2025	3	2	555
1.70000+00	4.94100+00	1.80000+00	4.42800+00	1.90000+00	3.82100+00	2025	3	2	556
2.00000+00	3.99800+00	2.10000+00	2.23900+00	2.20000+00	1.25400+00	2025	3	2	557
2.30000+00	2.77000-01	2.40000+00	3.24000-01	2.50000+00	8.36100+00	2025	3	2	558

2.55000+00	3.18450+01	2.53000+00	7.92240+01	2.60000+00	1.63545+022025	3	2	559
2.61000+00	2.49785+02	2.42000+00	4.05705+02	2.43000+00	7.18178+022025	3	2	560
2.64000+00	1.42720+03	2.55000+00	3.11944+03	2.56000+00	5.10099+032025	3	2	561
2.67000+00	3.55651+03	2.48000+00	1.85643+03	2.69000+00	1.06194+032025	3	2	562
2.70000+00	6.37857+02	2.72000+00	3.62851+02	2.75000+00	1.93557+022025	3	2	563
2.83000+00	1.02156+02	2.90000+00	5.16650+01	3.00000+00	3.56050+012025	3	2	564
3.20000+00	2.34990+01	3.40000+00	1.89310+01	3.50000+00	1.54850+012025	3	2	565
3.30000+00	1.49420+01	4.00000+00	1.39090+01	4.20000+00	1.31600+012025	3	2	566
4.40000+00	1.253940+01	4.00000+00	1.21510+01	4.80000+00	1.17960+012025	3	2	567
5.00000+00	1.15030+01	5.20000+00	1.12590+01	5.40000+00	1.10510+012025	3	2	568
5.60000+00	1.02710+01	5.80000+00	1.07160+01	6.00000+00	1.05790+012025	3	2	569
6.20000+00	1.04570+01	6.40000+00	1.03490+01	6.60000+00	1.02510+012025	3	2	570
6.80000+00	1.01630+01	7.00000+00	1.00820+01	7.20000+00	1.00020+012025	3	2	571
7.40000+00	9.94000+00	7.60000+00	9.87800+00	7.80000+00	9.32000+002025	3	2	572
8.00000+00	9.76600+00	8.20000+00	9.71500+00	8.40300+00	9.06800+002025	3	2	573
8.60000+00	9.52400+00	8.80000+00	9.53200+00	9.00000+00	9.54200+002025	3	2	574
9.20000+00	9.50400+00	9.40000+00	9.46800+00	9.50000+00	9.43400+002025	3	2	575
9.30000+00	9.40200+00	1.00000+01	9.37000+00	1.00000+03	1.94700+012025	3	2	576
1.55000+03	1.811e0+01	2.00000+03	1.72680+01	2.50000+03	1.66680+012025	3	2	577
3.00000+03	1.62230+01	4.00000+03	1.55830+01	5.00000+03	1.51550+012025	3	2	578
6.00000+03	1.48380+01	7.00000+03	1.45900+01	8.00000+03	1.44060+012025	3	2	579
9.00000+03	1.42520+01	1.00000+04	1.41250+01	1.50000+04	1.37170+012025	3	2	580
2.00000+04	1.35040+01	2.50000+04	1.33660+01	3.00000+04	1.32680+012025	3	2	581
4.00000+04	1.31230+01	5.00000+04	1.29570+01	6.00000+04	1.27420+012025	3	2	582
7.00000+04	1.25430+01	8.00000+04	1.23590+01	9.00000+04	1.21680+012025	3	2	583
1.00000+05	1.20250+01	1.20000+05	1.17130+01	1.40000+05	1.14130+012025	3	2	584
1.50000+05	1.11270+01	1.80000+05	1.08450+01	2.00000+05	1.05610+012025	3	2	585
2.20000+05	1.02860+01	2.40000+05	1.00140+01	2.50000+05	9.73600+002025	3	2	586
2.80000+05	9.46900+00	3.00000+05	9.17500+00	3.20000+05	2.90700+002025	3	2	587
3.40000+05	8.61200+00	3.60000+05	8.34300+00	3.60000+05	8.06500+002025	3	2	588
4.00000+05	7.81800+00	4.20000+05	7.59800+00	4.40000+05	7.39700+002025	3	2	589

4.60000+05	7.18600+00	4.80000+05	6.99400+00	5.00000+05	6.81900+002025	3	2	590
5.50000+05	6.46700+00	6.00000+05	6.13200+00	6.50000+05	5.35200+002025	3	2	591
7.00000+05	5.59800+00	7.50000+05	5.30400+00	8.00000+05	5.02900+002025	3	2	592
8.50000+05	4.76300+00	9.00000+05	4.54500+00	9.50000+05	4.35400+002025	3	2	593
1.00000+05	4.18700+00	1.10000+06	3.91000+00	1.20000+06	3.75800+002025	3	2	594
1.40000+05	3.61000+00	1.60000+06	3.47300+00	1.80000+06	3.43500+002025	3	2	595
2.00000+06	3.51200+00	2.20000+06	3.65400+00	2.40000+06	3.30200+002025	3	2	596
2.60000+06	3.793100+00	2.80000+06	4.04600+00	3.00000+06	4.14100+002025	3	2	597
3.20000+06	4.21400+00	3.40000+06	4.29300+00	3.60000+06	4.32400+002025	3	2	598
3.30000+06	4.33900+00	4.00000+06	4.35400+00	4.50000+06	4.31500+002025	3	2	599
3.00000+06	4.12900+00	5.50000+06	3.92900+00	6.00000+06	3.72400+002025	3	2	600
6.50300+06	3.53600+00	7.00000+06	3.35300+00	7.50000+06	3.21600+002025	3	2	601
8.00000+06	3.07100+00	8.50000+06	2.95200+00	9.00000+06	2.81300+002025	3	2	602
9.50000+06	2.71100+00	1.00000+07	2.67700+00	1.05000+07	2.56600+002025	3	2	603
1.10000+07	2.55300+00	1.15000+07	2.57200+00	1.20000+07	2.59200+002025	3	2	604
1.30000+07	2.67500+00	1.40000+07	2.76300+00	1.50000+07	2.82500+002025	3	2	605
0.00000+00	0.00000+00	0	0	0	02025	3	0	606
9.42420+04	2.39979+02	0	0	0	02025	3	4	607
0.00000+00-4.58100+04	0	0	1	722025	3	4	608	
10	2			2025	3	4	609	
4.60000+05	0.00000+00	5.00000+04	8.10000-02	6.00000+04	2.30000-012025	3	4	610
7.00000+05	3.51000-01	8.00000+04	4.49000-01	9.00000+04	5.30000-012025	3	4	611
1.00000+05	5.98000-01	1.20000+05	7.09000-01	1.40000+05	8.05000-012025	3	4	612
1.40000+05	8.73000-01	1.80000+05	9.32000-01	2.00000+05	9.81000-012025	3	4	613
2.20000+05	1.01600+00	2.40000+05	1.04800+00	2.60000+05	1.07900+002025	3	4	614
2.20000+05	1.09900+00	3.00000+05	1.11300+00	3.20000+05	1.13800+002025	3	4	615
3.40000+05	1.15700+00	3.60000+05	1.17400+00	3.80000+05	1.19200+002025	3	4	616
4.00000+05	1.21200+00	4.20000+05	1.22900+00	4.40000+05	1.24500+002025	3	4	617
4.70000+05	1.25700+00	4.80000+05	1.25700+00	5.00000+05	1.27900+002025	3	4	618
5.50000+05	1.30200+00	6.00000+05	1.31600+00	6.50000+05	1.32200+002025	3	4	619
7.00000+05	1.32100+00	7.50000+05	1.35400+00	8.00000+05	1.37600+002025	3	4	620
10	2			2025	3	4	621	
8.00000+05	1.36900+00	9.00000+05	1.36700+00	9.50000+05	1.36900+002025	3	4	622
1.00000+05	1.32000+00	1.10000+06	1.44000+00	1.20000+06	1.52200+002025	3	4	623
1.40000+05	1.71500+00	1.50000+06	1.90000+00	1.80000+06	2.03100+002025	3	4	624
2.00000+05	2.13100+00	2.20000+06	2.20100+00	2.40000+06	2.25200+002025	3	4	625
2.20000+05	2.24800+00	2.60000+06	2.21700+00	3.00000+06	2.17800+002025	3	4	626
3.20000+05	2.14500+00	3.40000+06	2.10400+00	3.60000+06	2.09200+002025	3	4	627
3.80000+05	2.08100+00	4.00000+06	2.07000+00	4.50000+06	2.04900+002025	3	4	628
5.00000+05	2.02800+00	5.50000+06	1.99400+00	6.00000+06	1.77700+002025	3	4	629
6.50000+05	1.45500+00	7.00000+06	1.22600+00	7.50000+06	9.82000-012025	3	4	630
7.00000+05	6.63000-01	8.50000+06	4.43000-01	9.00000+06	3.08000-012025	3	4	631
7.50000+05	3.48000-01	1.00000+07	3.23000-01	1.05000+07	3.17000-012025	3	4	632
1.10000+07	3.13000-01	1.15000+07	3.09000-01	1.20000+07	3.02000-012025	3	4	633
1.30000+07	2.89000-01	1.40000+07	2.83000-01	1.50000+07	2.82000-012025	3	4	634
0.00000+00	0.00000+00	0	0	0	02025	3	0	634
9.42420+04	2.39977+02	0	99	0	02025	3	16	635
0.00000+00-6.30400+06	0	0	1	1e2025	3	16	636	
10	2			2025	3	16	637	
6.33000+06	0.00000+00	6.50000+06	2.00000+03	7.00000+06	3.50000-022025	3	16	638
7.50000+06	1.45000+01	8.00000+06	3.95000+01	8.50000+06	5.87000-012025	3	16	639
9.00000+06	5.56000+01	9.50000+06	6.85000+01	1.00000+07	7.20000-012025	3	16	640
1.05000+07	7.43000+01	1.10000+07	7.58000+01	1.15000+07	7.05000-012025	3	16	641
1.20000+07	7.55000+01	1.30000+07	5.14000+01	1.40000+07	2.56000-012025	3	16	642
1.50000+07	1.72000+01				2025	3	16	643
0.00000+00	0.00000+00	0	0	0	02025	3	0	644
9.42420+04	2.39979+02	0	99	0	02025	3	17	645
0.00000+00-1.15420+07	0	0	1	52025	3	17	646	
5	2			2025	3	17	647	
1.15900+07	0.00000+00	1.20000+07	1.00000+03	1.30000+07	1.70000-012025	3	17	648
1.40000+07	2.80000+01	1.50000+07	3.23000+01		2025	3	17	649
0.00000+00	0.00000+00	0	0	0	02025	3	0	650
9.42420+04	2.39979+02	0	99	0	02025	3	18	651

0.00000+00	0.00000+00	0	0	2	1212025	3 18	652
33	2	121	2		2025	3 18	653
1.00000-05	3.80000-02	2.00000-05	2.70000-02	3.00000-05	2.20000-022025	3 18	654
4.00000-05	1.90000-02	5.00000-05	1.70000-02	6.00000-05	1.50000-022025	3 18	655
7.00000-05	1.40000-02	8.00000-05	1.30000-02	9.00000-05	1.30000-022025	3 18	656
1.00000-04	1.20000-02	2.00000-04	8.00000-03	3.00000-04	7.00000-032025	3 18	657
4.00000-04	6.00000-03	5.00000-04	5.00000-03	6.00000-04	5.00000-032025	3 18	658
7.00000-04	4.00000-03	8.00000-04	4.00000-03	9.00000-04	4.00000-032025	3 18	659
1.00000-03	4.00000-03	2.00000-03	3.00000-03	3.00000-03	2.00000-032025	3 18	660
4.00000-03	2.00000-03	5.00000-03	2.00000-03	6.00000-03	2.00000-032025	3 18	661
7.00000-03	1.00000-03	8.00000-03	1.00000-03	1.00000-02	1.00000-032025	3 18	662
2.53000-02	1.00000-03	4.00000-02	1.00000-03	5.50000-02	1.00000-032025	3 18	663
6.00000-02	0.00000+00	1.00000+00	0.00000+00	1.00000+01	0.00000+002025	3 18	664
1.00000+03	1.80000-02	1.50000+03	1.50000-02	2.00000+03	1.30000-022025	3 18	665
2.50000+03	1.20000-02	3.00000+03	1.10000-02	4.00000+03	1.00000-022025	3 18	666
5.00000+03	9.00000-03	6.00000+03	9.00000-03	7.00000+03	9.00000-032025	3 18	667
8.00000+03	8.00000-03	9.00000+03	8.00000-03	1.00000+04	8.00000-032025	3 18	668
1.50000+04	6.00000-03	2.00000+04	7.00000-03	2.50000+04	7.00000-032025	3 18	669
3.00000+04	7.00000-03	4.00000+04	7.00000-03	5.00000+04	8.00000-032025	3 18	670
6.00000+04	8.00000-03	7.00000+04	9.00000-03	8.00000+04	9.00000-032025	3 18	671
9.00000+04	1.00000-02	1.00000+05	1.00000-02	1.20000+05	1.20000-022025	3 18	672
1.40000+05	1.40000-02	1.50000+05	1.70000-02	1.80000+05	2.00000-022025	3 18	673
2.00000+05	2.30000-02	2.20000+05	2.70000-02	2.40000+05	3.30000-022025	3 18	674
2.50000+05	3.30000-02	2.30000+05	4.40000-02	3.00000+05	5.30000-022025	3 18	675
3.20000+05	6.10000-02	3.40000+05	7.20000-02	3.60000+05	8.00000-022025	3 18	676
3.80000+05	9.10000-02	4.00000+05	1.02000-01	4.20000+05	1.16000-012025	3 18	677
4.40000+05	1.30000-01	4.60000+05	1.53000-01	4.80000+05	1.79000-012025	3 18	678
5.00000+05	2.06000-01	5.50000+05	2.77000-01	6.00000+05	3.59000-012025	3 18	679
6.50000+05	4.51000-01	7.00000+05	5.55000-01	7.50000+05	6.07000-012025	3 18	680
8.00000+05	8.00000-01	8.50000+05	9.72000-01	9.00000+05	1.12000+002025	3 18	681
9.50000+05	1.23900+00	1.00000+06	1.33500+00	1.10000+06	1.45200+002025	3 18	682

1.20000+00	1.44700+00	1.40000+06	1.38300+00	1.60000+06	1.36300+002025	3 18	683
1.20000+05	1.42400+00	2.00000+06	1.44400+00	2.20000+06	1.41500+002025	3 18	684
2.40000+05	1.33100+00	2.50000+06	1.33000+00	2.80000+06	1.38500+002025	3 18	685
3.30000+05	1.37800+00	3.20000+06	1.36300+00	3.40000+06	1.35600+002025	3 18	686
3.50000+05	1.36300+00	3.30000+06	1.32700+00	4.00000+06	1.31400+002025	3 18	687
4.50000+05	1.27500+00	5.00000+06	1.23800+00	5.50000+06	1.25100+002025	3 18	688
7.50000+05	1.44600+00	6.50000+06	1.75000+00	7.00000+06	1.93400+002025	3 18	689
7.50000+05	2.03700+00	3.00000+06	2.09400+00	8.50000+06	2.11200+002025	3 18	690
9.00000+05	2.10600+00	9.20000+06	2.08700+00	1.00000+07	2.06400+002025	3 18	691
1.05000+05	2.04400+00	1.10000+07	2.02200+00	1.15000+07	2.00200+002025	3 18	692
1.20000+05	1.24500+00	1.30000+07	2.02500+00	1.40000+07	2.13400+002025	3 18	693
1.50000+05	2.16300+00				2025	3 18	694
0.00000+00	0.00000+00	0	0	0	02025	3 0	695
0.42420+04	2.32979+02	0	98	0	02025	3 20	696
6.00000+03	-5.37800+06	0	20	1	182025	3 20	697
13	2				2025	3 20	698
5.40000+06	6.00000+00	5.50000+06	5.10400-02	6.00000+06	2.55900-012025	3 20	699
6.30000+06	5.05100-01	7.00000+06	7.49000-01	7.50000+06	6.57000-012025	3 20	700
8.00000+06	9.24000-01	8.50000+06	9.47000-01	9.00000+06	9.55900-012025	3 20	701
9.50000+06	9.51300-01	1.00000+07	9.44100-01	1.05000+07	9.36900-012025	3 20	702
1.10000+07	2.22000-01	1.15000+07	9.09700-01	1.20000+07	8.95200-012025	3 20	703
1.30000+07	8.89000-01	1.40000+07	8.91900-01	1.50000+07	8.71900-012025	3 20	704
0.00000+00	0.00000+00	0	0	0	02025	3 0	705
9.42420+04	2.39979+02	0	98	0	02025	3 21	706
6.00000+00	-1.13500+07	0	21	1	52025	3 21	707
5	2				2025	3 21	708
1.19000+07	0.00000+00	1.20000+07	1.93500-02	1.30000+07	8.00600-022025	3 21	709
1.40000+00	2.13000-01	1.50000+07	2.81200-01		2025	3 21	710
6.00000+00	0.00000+00	0	0	0	02025	3 0	711
9.42420+04	2.32979+02	0	1	0	02025	3 51	712
0.00000+00	-4.58100+04	0	0	1	722025	3 51	713

72	2						2025	3	51	714
4.60000+04	0.00000+00	5.00000+04	8.10000-02	6.00000+04	2.30000-012025	3 51	715			
7.00000+04	3.51000-01	8.00000+04	4.49000-01	9.00000+04	5.30000-012025	3 51	716			
1.00000+05	5.98000-01	1.20000+05	7.09000-01	1.40000+05	8.05000-012025	3 51	717			
1.50000+05	8.73000-01	1.50000+05	9.29000-01	2.00000+05	9.73000-012025	3 51	718			
2.20000+05	1.00300+00	2.40000+05	1.03000+00	2.60000+05	1.05500+002025	3 51	719			
2.80000+05	1.06800+00	3.00000+05	1.07900+00	3.20000+05	1.09000+002025	3 51	720			
3.40000+05	1.09900+00	3.60000+05	1.10700+00	3.80000+05	1.11500+002025	3 51	721			
4.00000+05	1.12300+00	4.20000+05	1.13000+00	4.40000+05	1.13500+002025	3 51	722			
4.60000+05	1.13600+00	4.80000+05	1.13500+00	5.00000+05	1.13400+002025	3 51	723			
5.50000+05	1.12900+00	6.00000+05	1.11500+00	6.50000+05	1.09600+002025	3 51	724			
7.00000+05	1.07100+00	7.50000+05	1.02100+00	8.00000+05	9.04000-012025	3 51	725			
8.50000+05	9.10000-01	9.00000+05	8.31000-01	9.50000+05	7.83000-012025	3 51	726			
1.00000+06	7.48000-01	1.10000+06	6.82000-01	1.20000+06	6.42000-012025	3 51	727			
1.40000+06	5.85000-01	1.50000+06	5.41000-01	1.80000+06	5.04000-012025	3 51	728			
2.00000+06	4.72000-01	2.20000+06	4.47000-01	2.40000+06	4.27000-012025	3 51	729			
2.60000+06	4.14000-01	2.80000+06	4.00000-01	3.00000+06	3.90000-012025	3 51	730			
3.20000+06	3.83000-01	3.40000+06	3.75000-01	3.60000+06	3.68000-012025	3 51	731			
3.80000+06	3.61000-01	4.00000+06	3.54000-01	4.50000+06	3.38000-012025	3 51	732			
5.00000+06	3.25000-01	5.50000+06	3.12000-01	6.00000+06	3.00000-012025	3 51	733			
6.50000+06	2.39000-01	7.00000+06	2.82000-01	7.50000+06	2.67000-012025	3 51	734			
8.00000+06	2.58000-01	8.50000+06	2.50000-01	9.00000+06	2.43000-012025	3 51	735			
9.50000+06	2.37000-01	1.00000+07	2.31000-01	1.05000+07	2.30000-012025	3 51	736			
1.10000+07	2.28000-01	1.15000+07	2.26000-01	1.20000+07	2.25000-012025	3 51	737			
1.30000+07	2.27000-01	1.40000+07	2.32000-01	1.50000+07	2.37000-012025	3 51	738			
0.00000+00	0.00000+00	0	0	0	02025	3 0	39			
9.42420+04	2.39979+02	0	2	0	02025	3 52	740			
0.00000+00-1	4.7386+05	0	0	1	632025	3 52	741			
63	2				2025	3 52	742			
1.48000+05	0.00000+00	1.30000+05	3.00000-03	2.00000+05	8.00000-032025	3 52	743			
2.20000+05	1.30000-02	2.40000+05	1.83000-02	2.60000+05	2.40000-022025	3 52	744			

2.80000+05	3.10000-02	3.00000+05	3.90000-02	3.20000+05	4.80000-022025	3 52	745
3.40000+05	5.80000-02	3.50000+05	6.70000-02	3.80000+05	7.70000-022025	3 52	746
4.00000+05	8.90000-02	4.20000+05	9.90000-02	4.40000+05	1.10000-012025	3 52	747
4.50000+05	1.21000-01	4.80000+05	1.32000-01	5.00000+05	1.44000-012025	3 52	748
5.50000+05	1.72000-01	6.00000+05	1.99000-01	6.50000+05	2.23000-012025	3 52	749
7.00000+05	2.46000-01	7.50000+05	2.57000-01	8.00000+05	2.67000-012025	3 52	750
8.50000+05	2.69000-01	9.00000+05	2.65000-01	9.50000+05	2.54000-012025	3 52	751
1.00000+06	2.65000-01	1.10000+06	2.63000-01	1.20000+06	2.61000-012025	3 52	752
1.40000+06	2.51000-01	1.50000+06	2.42000-01	1.80000+06	2.27000-012025	3 52	753
2.00000+06	2.08000-01	2.20000+06	1.91000-01	2.40000+06	1.77000-012025	3 52	754
2.60000+06	1.67000-01	2.30000+06	1.59000-01	3.00000+06	1.53000-012025	3 52	755
3.20000+06	1.49000-01	3.40000+06	1.44000-01	3.60000+06	1.41000-012025	3 52	756
3.80000+06	1.38000-01	4.00000+06	1.35000-01	4.50000+06	1.28000-012025	3 52	757
5.00000+06	1.23000-01	5.50000+06	1.15000-01	6.00000+06	1.05000-012025	3 52	758
6.50000+06	1.00000-01	7.00000+06	9.50000-02	7.50000+06	8.50000-022025	3 52	759
8.00000+06	8.00000-02	8.50000+06	7.30000-02	9.00000+06	6.80000-022025	3 52	760
9.50000+06	6.40000-02	1.00000+07	6.20000-02	1.05000+07	5.00000-022025	3 52	761
1.10000+07	5.90000-02	1.15000+07	5.80000-02	1.20000+07	5.70000-022025	3 52	762
1.30000+07	5.50000-02	1.40000+07	5.30000-02	1.50000+07	5.10000-022025	3 52	763
0.00000+00	0.00000+00	0	0	0	02025	3 0	764
9.42420+04	2.39979+02	0	3	0	07025	3 53	765
0.00000+00-3	0.6722+05	0	0	1	282025	3 53	766
28	2				2025	3 53	767
3.08000+05	0.50000+00	5.00000+05	1.00000-03	5.50000+05	1.00000-032025	3 53	768
6.00000+05	2.00000-03	6.50000+05	3.00000-03	7.00000+05	4.00000-032025	3 53	769
7.50000+05	6.00000-03	8.00000+05	7.00000-03	8.50000+05	9.00000-032025	3 53	770
9.00000+05	1.00000-02	9.50000+05	1.10000-02	1.00000+06	1.20000-022025	3 53	771
1.10000+06	1.50000-02	1.20000+06	1.70000-02	1.40000+06	2.30000-022025	3 53	772
1.60000+06	2.60000-02	1.80000+06	2.40000-02	2.00000+06	1.70000-022025	3 53	773
2.20000+06	1.30000-02	2.40000+06	9.00000-03	2.60000+06	6.00000-032025	3 53	774
2.80000+06	4.00000-03	3.00000+06	2.00000-03	3.20000+06	1.00000-032025	3 53	775

3.40000+05	1.00000+03	3.00000+06	1.00000+03	3.60000+06	0.00000+00	2025	3 53	776
1.50000+07	0.00000+00					2025	3 53	777
0.00000+00	0.00000+00	0	0	0	0	02025	3 0	778
9.42420+04	2.39979+02	0	4	0	0	02025	3 54	779
0.00000+00-5.16340+03		0	0	1	02025	3 54	780	
2					2025	3 54	781	
5.10000+05	0.00000+00	1.50000+06	1.00000+03	1.80000+06	1.00000+00	2025	3 54	782
2.00000+05	1.00000+03	2.20000+06	1.00000+03	2.40000+06	1.00000+00	2025	3 54	783
2.00000+05	1.00000+03	2.60000+06	0.00000+00	1.50000+07	0.00000+00	2025	3 54	784
0.00000+00	0.00000+00	0	0	0	0	02025	3 0	785
9.42420+04	2.39979+02	0	5	0	0	02025	3 55	786
0.00000+00-7.15023+05		0	0	1	242025	3 55	787	
24	2				2025	3 55	788	
2.16200+05	0.00000+00	7.50000+05	7.80000+02	8.00000+05	1.40000+01	2025	3 55	789
5.50000+05	1.50000+01	9.00000+05	1.77000+01	9.50000+05	1.77000+01	2025	3 55	790
1.00000+06	1.72000+01	1.10000+06	1.54000+01	1.20000+06	1.46000+01	2025	3 55	791
1.40000+06	1.20000+01	1.50000+06	9.40000+02	1.50000+06	6.70000+02	2025	3 55	792
2.00000+05	4.50000+02	2.20000+06	3.00000+02	2.40000+06	1.90000+02	2025	3 55	793
2.40000+05	1.10000+02	2.60000+06	7.00000+03	3.00000+06	4.00000+03	2025	3 55	794
3.20000+05	2.00000+03	3.40000+06	1.03000+03	3.60000+06	1.00000+03	2025	3 55	795
3.40000+05	1.00000+03	3.30000+06	0.00000+00	1.50000+07	0.00000+00	2025	3 55	796
0.00000+00	0.00000+00	0	0	0	0	02025	3 0	797
9.42420+04	2.39979+02	0	6	0	0	02025	3 56	798
0.00000+00-8.22543+05		0	0	1	232025	3 56	799	
23	2				2025	3 56	800	
3.53000+05	0.00000+00	8.50000+05	1.20000+02	9.00000+05	3.70000+02	2025	3 56	801
5.50000+05	5.00000+02	1.00000+06	6.50000+02	1.10000+06	7.00000+02	2025	3 56	802
1.20000+05	3.10000+02	1.40000+06	8.80000+02	1.60000+06	8.30000+02	2025	3 56	803
1.30000+05	5.40000+02	2.10000+06	4.50000+02	2.20000+06	3.20000+02	2025	3 56	804
2.40000+06	2.10000+02	2.50000+06	1.30000+02	2.80000+06	8.00000+02	2025	3 56	805
3.50000+05	5.00000+03	3.20000+06	3.00000+03	3.40000+06	2.00000+03	2025	3 56	806

3.00000+05	1.00000+03	3.80000+06	1.00000+03	4.00000+06	1.00000+03	2025	3 56	807
4.00000+06	0.00000+00	1.50000+07	0.00000+00			2025	3 56	808
0.00000+00	0.00000+00	0	0	0	0	02025	3 0	809
9.42420+04	2.39979+02	0	7	0	0	02025	3 57	810
0.00000+00-3.61410+05		0	0	1	212025	3 57	811	
21	2				2025	3 57	812	
8.65000+05	0.00000+00	9.00000+05	4.70000+02	9.50000+05	8.00000+02	2025	3 57	813
1.00000+06	9.50000+02	1.10000+06	1.11000+01	1.20000+06	1.12000+01	2025	3 57	814
1.40000+06	1.05000+01	1.60000+06	8.90000+02	1.80000+06	6.70000+02	2025	3 57	815
2.00000+06	4.20000+02	2.20000+06	2.80000+02	2.40000+06	1.30000+02	2025	3 57	816
2.50000+05	1.10000+02	2.80000+06	6.00000+03	3.00000+06	4.00000+03	2025	3 57	817
3.20000+05	2.00000+03	3.40000+06	1.00000+03	3.60000+06	1.00000+03	2025	3 57	818
3.80000+05	1.00000+03	3.30000+06	0.00000+00	1.50000+07	0.00000+00	2025	3 57	819
0.00000+00	0.00000+00	0	0	0	0	02025	3 0	820
9.42420+04	2.39979+02	0	8	0	0	02025	3 58	821
0.00000+00-9.23153+05		0	0	1	192025	3 58	822	
19	2				2025	3 58	823	
9.27000+05	0.00000+00	1.00000+06	1.00000+03	1.10000+04	4.00000+03	2025	3 58	824
1.20000+06	7.00000+03	1.40000+06	1.30000+02	1.60000+06	1.80000+02	2025	3 58	825
1.50000+05	1.80000+02	2.00000+06	1.50000+02	2.20000+06	1.20000+02	2025	3 58	826
2.40000+05	9.00000+03	2.50000+06	6.00000+03	2.80000+06	4.00000+03	2025	3 58	827
3.00000+05	3.00000+03	3.20000+06	2.00000+03	3.40000+06	1.00000+03	2025	3 58	828
3.50000+05	1.00000+03	3.50000+06	1.00000+03	3.80000+06	0.00000+00	2025	3 58	829
1.50000+07	0.00000+00				2025	3 58	830	
0.00000+00	0.00000+00	0	0	0	0	02025	3 0	831
9.42420+04	2.39979+02	0	9	0	0	02025	3 59	832
0.00000+00-9.52033+05		0	0	1	182025	3 59	833	
18	2				2025	3 59	834	
9.50000+05	0.00000+00	1.00000+06	1.70000+02	1.10000+06	4.10000+02	2025	3 59	835
1.20000+06	4.90000+02	1.40000+06	5.00000+02	1.60000+06	4.30000+02	2025	3 59	836
1.80000+06	3.20000+02	2.00000+06	2.00000+02	2.20000+06	1.40000+02	2025	3 59	837

2.40000+00	9.00000-03	2.00000+06	5.00000-03	2.00000+06	3.00000-032025	3 59	838.
3.00000+00	2.00000-03	3.20000+06	1.00000-03	3.40000+06	1.00000-032025	3 59	839
3.60000+00	0.00000+00	3.60000+06	0.00000+00	1.50000+07	0.00000+002025	3 59	840
0.00000+00	0.00000+00	0	0	0	02025	3 0	841
9.42420+04	2.39979+02	0	10	0	02025	3 0	842
0.00000+00	1.00000-03	0	0	1	182025	3 60	843
1.00000+00	1.00000+00	2			2025	3 60	844
0.00000+00	0.00000+00	1.00000+06	2.00000-03	1.10000+06	6.40000-022025	3 60	845
0.00000+00	0.00000+00	1.40000+06	1.17000-01	1.60000+06	1.09000-012025	3 60	846
1.30000+00	2.20000-02	2.00000+06	5.70000-02	2.20000+06	4.00000-022025	3 60	847
2.40000+00	2.60000-02	2.40000+06	1.50000-02	2.80000+06	1.00000-022025	3 60	848
3.00000+00	6.00000-03	3.20000+06	3.00000-03	3.40000+06	2.00000-032025	3 60	849
3.60000+00	1.00000-03	3.30000+06	1.00000-03	3.80000+06	0.00000+002025	3 60	850
1.50000+07	0.00000+00				2025	3 60	851
0.00000+00	0.00000+00	0	0	0	02025	3 0	852
0.42420+04	2.39979+02	0	11	0	02025	3 61	853
0.00000+00	1.01577+06	0	0	1	182025	3 61	854
13	2				2025	3 61	855
1.02000+00	0.00000+00	1.10000+06	2.50000-02	1.20000+06	4.20000-022025	3 61	856
1.40000+00	6.10000-02	1.30000+06	2.40000-02	1.80000+06	5.50000-022025	3 61	857
2.00000+00	3.30000-02	2.20000+06	2.70000-02	2.40000+06	1.90000-022025	3 61	858
2.40000+00	1.20000-02	2.50000+06	7.00000-03	3.00000+06	5.30000-032025	3 61	859
3.20000+00	3.00000-03	3.40000+06	2.00000-03	3.60000+06	1.00000-032025	3 61	860
3.50000+00	1.10000-03	3.30000+06	0.00000+00	1.50000+07	0.00000+002025	3 61	861
0.00000+00	0.00000+00	0	0	0	02025	3 0	862
0.42420+04	2.39979+02	0	12	0	02025	3 62	863
0.00000+00	1.01577+06	0	0	1	182025	3 62	864
19	2				2025	3 62	865
1.10200+06	0.00000+00	1.20000+06	4.40000-02	1.40000+06	9.00000-022025	3 62	866
1.70000+06	9.40000-02	1.20000+06	7.90000-02	2.00000+06	5.30000-022025	3 62	867
2.20000+06	3.80000-02	2.40000+06	2.60000-02	2.40000+06	1.50000-022025	3 62	868

2.80000+00	9.00000-03	3.00000+06	5.00000-03	3.20000+06	3.00000-032025	3 02	869
3.40000+00	2.00000-03	3.60000+06	1.00000-03	3.80000+06	1.00000-032025	3 62	870
4.20000+00	0.30000+00	4.00000+06	0.00000+00	1.50000+07	0.00000+002025	3 62	871
0.00000+00	0.00000+00	0	0	0	02025	3 0	872
0.42420+04	2.39979+02	0	13	0	02025	3 63	873
0.00000+00	1.11734+06	0	0	1	182025	3 63	874
16	2				2025	3 03	875
1.12200+00	0.00000+00	1.20000+06	1.00000-03	1.40000+06	6.00000-032025	3 03	876
1.50000+00	1.10000-02	1.30000+06	1.30000-02	2.00000+06	1.10000-022025	3 63	877
2.20000+00	9.00000-03	2.40000+06	7.00000-03	2.60000+06	5.00000-032025	3 63	878
2.80000+00	3.00000-03	3.00000+06	2.00000-03	3.20000+06	2.00000-032025	3 63	879
3.40000+00	1.30000-03	3.60000+06	1.00000-03	3.60000+06	0.00000+002025	3 63	880
1.50000+07	0.00000+00				2025	3 63	881
0.00000+00	0.00000+00	0	0	0	02025	3 0	882
0.42420+04	2.39979+02	0	98	0	02025	3 91	883
0.00000+00	1.12700+06	0	0	1	352025	3 91	884
35	2				2025	3 91	885
1.13200+06	0.00000+00	1.20000+06	2.60000-02	1.40000+06	2.09000-012025	3 91	886
1.60000+00	4.85000-01	1.90000+06	7.94000-01	2.00000+06	1.10600+002025	3 91	887
2.20000+00	1.31900+00	2.40000+06	1.43600+00	2.10000+06	1.56600+002025	3 91	888
2.80000+00	1.59300+00	3.00000+06	1.59700+00	3.20000+06	1.59100+002025	3 91	889
3.40000+00	1.57100+00	3.60000+06	1.57400+00	3.80000+06	1.57500+002025	3 91	890
4.00000+00	1.57900+00	4.50000+06	1.56300+00	5.00000+06	1.58000+002025	3 91	891
5.50000+00	1.56700+00	6.00000+06	1.37200+00	6.50000+06	1.06600+002025	3 91	892
7.00000+00	8.49000-01	7.50000+06	6.30000-01	8.00000+06	3.30000-012025	3 91	893
8.50000+00	1.20000-01	9.00000+06	5.70000-02	7.50000+06	4.70000-022025	3 91	894
1.00000+07	3.50000-02	1.05000+07	2.70000-02	1.10000+07	2.60000-022025	3 91	895
1.15000+07	2.50000-02	1.20000+07	2.00000-02	1.30000+07	7.00000-032025	3 91	896
1.40000+07	3.00000-03	1.50000+07	0.00000+00		2025	3 91	897
0.00000+00	0.00000+00	0	0	0	02025	3 0	898
0.42420+04	2.39979+02	0	0	0	02025	3 162	899

0.00000+00	3.02000+00	0	0	2	2732025	3102	900.
1.00000-15	3.27355+00	2.00000-05	2.32658+02	3.00000-05	2.02100+022025	3102	901
4.00000-05	1.50573+02	5.00000-05	1.64257+02	6.00000-05	1.55953+022025	3102	902
7.00000-15	1.48265+02	5.00000-05	1.42075+02	5.00000-05	1.37115+022025	3102	903
1.00000-04	1.32997+02	2.00000-04	1.11925+02	3.00000-04	1.92752+022025	3102	904
4.00000-04	9.67980+01	5.00000-04	9.22180+01	5.00000-04	8.83970+012025	3102	905
7.00000-14	8.56750+01	8.00000-04	8.21190+01	9.00000-04	7.94475+012025	3102	907
1.00000-03	7.70120+01	2.00000-03	8.04490+01	3.00000-03	5.10490+012025	3102	908
4.00000-03	4.49640+01	5.00000-03	4.05720+01	6.00000-03	3.12530+012025	3102	909
7.00000-13	3.44250+01	8.00000-03	3.24830+01	9.00000-03	3.06960+012025	3102	910
1.00000-02	2.91760+01	1.50000-02	2.37720+01	2.00000-02	2.02550+012025	3102	911
2.50000-02	1.87420+01	2.53000-02	1.66380+01	3.00000-02	1.71790+012025	3102	912
3.50000-02	1.55670+01	4.00000-02	1.469940+01	4.50000-02	1.41900+012025	3102	913
1.00000-02	1.35140+01	5.50000-02	1.29340+01	6.00000-02	1.24310+012025	3102	914
4.50000-12	1.14640+01	7.00000-02	1.15970+01	7.50000-02	1.12470+012025	3102	915
7.00000-12	1.09310+01	8.50000-02	1.04450+01	9.00000-02	1.03850+012025	3102	916
9.50000-12	1.01470+01	1.00000-01	9.92300+00	1.10000-01	9.54000+002025	3102	917
1.20000-11	9.28560+00	1.30000-01	8.91300+00	1.40000-01	8.95600+002025	3102	918
1.50000-11	8.42840+00	1.70000-01	8.22500+00	1.70000-01	8.04300+002025	3102	919
1.80000-11	7.87240+00	1.70000-01	7.73000+00	2.00000-01	7.50400+002025	3102	920
2.10000-11	7.47160+00	2.20000-01	7.35900+00	2.30000-01	7.25500+002025	3102	921
2.40000-11	7.16100+00	2.50000-01	7.07300+00	2.60000-01	6.99300+002025	3102	922
2.70000-11	6.91200+00	2.50000-01	6.85100+00	2.50000-01	6.78500+002025	3102	923
3.00000-11	6.73060+00	3.10000-01	6.67000+00	3.20000-01	6.62700+002025	3102	924
3.30000-11	6.58100+00	3.40000-01	6.53900+00	3.50000-01	6.50000+002025	3102	925
3.60000-11	6.46400+00	3.70000-01	6.43100+00	3.80000-01	6.40100+002025	3102	926
3.90000-11	6.37440+00	4.00000-01	6.34900+10	4.10000-01	6.32400+002025	3102	927
4.20000-11	6.30500+00	4.30000-01	6.28700+00	4.40000-01	6.27100+002025	3102	928
4.50000-11	6.25600+00	4.60000-01	6.24300+00	4.70000-01	6.23300+002025	3102	929
4.80000-11	6.22300+00	4.90000-01	6.21600+00	5.00000-01	6.21000+002025	3102	930

5.20000-01	6.20200+00	5.40000-01	6.20000+00	5.60000-01	6.28400+002025	3102	931
5.80000-01	6.21300+00	6.00000-01	6.22600+00	6.20000-01	6.24400+002025	3102	932
7.40000-01	6.26700+00	7.00000-01	6.29400+00	6.80000-01	6.32600+002025	3102	933
7.00000-11	6.36100+00	7.20000-01	6.40100+00	7.40000-01	6.44500+002025	3102	934
7.60000-01	6.49300+00	7.80000-01	6.54500+00	8.00000-01	6.00100+002025	3102	935
9.20000-01	6.66200+00	6.40000-01	6.72600+00	8.60000-01	6.79500+002025	3102	936
8.80000-01	6.88800+00	9.00000-01	6.94500+00	9.20000-01	7.02700+002025	3102	937
9.40000-01	7.11300+00	9.50000-01	7.20400+00	9.80000-01	7.30000+002025	3102	938
1.00000+00	7.40000+00	1.05000+00	7.67400+00	1.10000+00	7.96300+002025	3102	939
1.15000+00	8.33000+00	1.20000+00	8.71900+00	1.25000+00	9.15600+002025	3102	940
1.30000+00	9.64800+00	1.35000+00	1.02000+01	1.40000+00	1.02240+012025	3102	941
1.45000+00	1.15290+01	1.50000+00	1.23290+01	1.60000+00	1.42880+012025	3102	942
1.70000+00	1.08700+01	1.50000+00	2.04430+01	1.90000+00	2.54660+012025	3102	943
2.00000+00	3.28970+01	2.10000+00	4.45720+01	2.20000+00	6.45040+012025	3102	944
2.30000+00	1.02021+02	2.40000+00	1.92873+02	2.50000+00	4.96598+022025	3102	945
2.55000+00	1.03200+03	2.58000+00	1.91370+03	2.60000+00	3.31520+032025	3102	946
2.80000+00	4.86262+03	2.62000+03	6.99539+03	2.63000+00	1.14716+042025	3102	947
2.84000+00	2.11753+04	2.65000+00	4.3u982+04	2.66000+00	6.58024+042025	3102	948
2.87000+00	4.29213+04	2.68000+00	2.10094+04	2.69000+00	1.13398+042025	3102	949
2.70000+00	6.88940+03	2.72006+00	3.24073+03	2.75000+00	1.47326+032025	3102	950
2.80000+00	6.11584+02	2.90000+00	2.05809+02	3.00000+00	1.01007+022025	3102	951
3.20000+00	3.88290+01	3.40000+00	2.00800+01	3.60000+00	1.21070+012025	3102	952
3.80000+00	8.02200+00	4.00000+00	5.00800+00	4.20000+00	4.19500+002025	3102	953
4.40000+00	3.21700+00	4.60000+00	2.53700+00	4.80000+00	2.04600+002025	3102	954
5.00000+00	1.68100+00	5.20000+00	1.40300+00	5.40000+00	1.18700+002025	3102	955
5.60000+00	1.01700+00	5.80000+00	8.79000+01	6.00000+00	7.07000+012025	3102	956
6.20000+00	6.75000+01	6.40000+00	5.98000+01	6.00000+00	5.33000+012025	3102	957
6.80000+00	4.79000+01	7.00000+00	4.32000+01	7.20000+00	3.92000+012025	3102	958
7.40000+00	3.57000+01	7.60000+00	3.26000+01	7.80000+00	3.00000+012025	3102	959
8.00000+00	2.76000+01	8.20000+00	2.56000+01	8.40000+00	2.37000+012025	3102	960
8.60000+00	2.21000+01	8.60000+00	2.07000+01	9.00000+00	1.94000+012025	3102	961

9.28661+00	1.42000+01	2.40000+00	1.72000+01	2.00000+00	1.02000-01	2025	3102	962.
9.80000+00	1.53000+01	1.00000+01	1.45000+01	1.00000+03	3.20100+00	2025	3102	963
1.50000+03	2.44700+00	2.00000+03	2.05600+00	2.50000+03	1.51700+00	2025	3102	964
3.00000+03	1.65000+00	4.00000+03	1.44000+00	5.00000+03	1.30400+00	2025	3102	965
6.00000+03	1.21700+00	7.00000+03	1.12600+03	8.00000+03	1.08900+00	2025	3102	966
9.00000+03	1.04200+03	1.00000+04	1.00000+00	1.50000+04	8.57000-01	2025	3102	967
2.00000+04	7.58000+01	2.50000+04	6.85000+01	3.00000+04	6.29000-01	2025	3102	968
6.00000+04	5.40000+01	5.00000+04	4.63000+01	5.00000+04	3.87000-01	2025	3102	969
7.00000+04	3.35000+01	8.00000+04	3.00000+01	9.00000+04	2.74000-01	2025	3102	970
1.00000+05	2.55000+01	1.20000+05	2.20000+01	1.40000+05	2.10000-01	2025	3102	971
1.50000+05	1.92000+01	1.00000+05	1.93000+01	2.00000+05	1.36000-01	2025	3102	972
2.00000+05	1.72000+01	2.40000+05	1.72000+01	2.00000+05	1.06000-01	2025	3102	973
2.50000+05	1.60000+01	3.00000+05	1.54000+01	3.20000+05	1.53000-01	2025	3102	974
3.00000+05	1.51000+01	3.50000+05	1.50000+01	3.60000+05	1.49000-01	2025	3102	975
4.00000+05	1.49000+01	4.20000+05	1.49000+01	4.40000+05	1.49000-01	2025	3102	976
4.50000+05	1.49000+01	4.50000+05	1.49000+01	5.00000+05	1.49000-01	2025	3102	977
5.50000+05	1.49000+01	6.00000+05	1.47000+01	5.50000+05	1.48000-01	2025	3102	978
7.00000+05	1.47000+01	7.50000+05	1.46000+01	8.00000+05	1.32000-01	2025	3102	979
8.50000+05	1.42300+01	9.00000+05	1.42000+01	9.50000+05	1.05000-01	2025	3102	980
1.00000+06	1.00000+01	1.10000+06	9.20000+02	1.20000+06	8.60000-022025	3102	981	
1.40000+06	8.00000+02	1.00000+06	7.60000+02	1.80000+06	7.00000-022025	3102	982	
2.00000+06	6.10000+02	2.20000+06	5.10000+02	2.40000+06	4.10000-022025	3102	983	
2.50000+06	3.00000+02	2.80000+06	2.10000+02	3.00000+06	1.20000-022025	3102	984	
3.20000+06	1.70000+02	3.40000+06	1.10000+02	3.60000+06	9.00000-032025	3102	985	
3.80000+06	8.00000+02	4.00000+06	7.01000+03	4.50000+06	6.00000-032025	3102	986	
5.00000+06	5.00000+03	5.50000+06	5.00000+03	6.00000+06	5.00000-032025	3102	987	
5.50000+06	5.00000+03	7.00000+06	5.00000+03	7.50000+06	5.00000-032025	3102	988	
7.00000+06	4.00000+03	8.50000+06	4.00000+03	9.00000+06	4.30000-032025	3102	989	
9.50000+06	4.00000+03	1.00000+07	4.00000+03	1.05000+07	4.00000-032025	3102	990	
1.10000+07	4.00000+03	1.15000+07	4.00000+03	1.20000+07	4.00000-032025	3102	991	
1.30000+07	4.00000+03	1.40000+07	4.00000+03	1.50000+07	4.00000-032025	3102	992	

5.00000+00	0.00000+00	0	0	0	02025	3	0	993
0.00000+00	0.00000+00	0	0	0	02025	0	0	994
9.42420+04	2.39972+02	0	1	0	02025	4	2	995
0.00000+00	2.39970+02	0	2	0	02025	4	2	996
0.00000+00	0.00000+00	0	0	1	242025	4	2	997
24	2				2025	4	2	998
2.93400+02	1.00000+05	0	0	1	02025	4	2	999
0.00000+00					2025	4	2	1000
2.93400+02	9.00000+02	0	0	1	02025	4	2	1001
0.00000+00					2025	4	2	1002
2.93400+02	1.00000+03	0	0	1	02025	4	2	1003
5.23+00+04					2025	4	2	1004
2.93400+02	3.00000+03	0	0	2	02025	4	2	1005
1.94800+03	4.49534+06				2025	4	2	1006
2.93400+02	1.10000+04	-	0	0	02025	4	2	1007
7.82069+03	5.68387+05				2025	4	2	1008
2.93400+02	3.00000+04	0	0	3	02025	4	2	1009
2.58286+02	5.20937+04	4.91904+06			2025	4	2	1010
2.93400+02	1.00000+05	0	0	4	02025	4	2	1011
8.53562+02	7.34571+03	3.26433+04	1.01012+05		2025	4	2	1012
2.93400+02	2.50000+05	0	0	5	02025	4	2	1013
2.28932+01	4.59893+02	5.49577+03	3.05419+04	1.42776+06	2025	4	2	1014
2.93400+02	5.00000+05	0	0	6	02025	4	2	1015
3.06736+01	1.03945+01	3.09543+02	5.27952+03	1.05952+04	1.63677+052025	4	2	1016
2.93400+02	7.50000+05	0	0	7	02025	4	2	1017
3.81542+01	1.68594+01	8.45960+02	2.23510+02	1.02795+03	2.50161+042025	4	2	1018
1.57826+05					2025	4	2	1019
2.93400+02	1.00000+06	0	0	8	02025	4	2	1020
4.60293+01	2.43685+01	1.55476+01	6.05871+02	6.13177+03	1.52649+032025	4	2	1021
1.15104+04	4.11480+06				2025	4	2	1022
2.93400+02	1.50000+06	0	0	9	02025	4	2	1023

5.40701-01	3.72347-01	5.30261-01	1.73156-01	4.59607-02	1.2e972-022025	4	2	1024.
1.53277-03	1.27255-04	5.65523-05			2025	4	2	1025
2.930-0+02	2.00007+06	0	0	10	02025	4	2	1026
0.80722-03	5.19121-01	4.71420-01	2.92846-01	1.23181-01	4.16910-022025	4	2	1027
2.00354-03	1.60573-03	1.72121-04	1.39172-05		2025	4	2	1028
2.03500+02	3.00000+06	0	0	11	02025	4	2	1029
7.93210-01	0.25002-01	4.32803-01	3.30398-01	2.34374-01	1.08420-012025	4	2	1030
3.70522-02	1.03352-02	2.04059-03	2.67511-04	1.52721-05	2025	4	2	1031
2.03000+02	6.00007+06	0	0	13	02025	4	2	1032
3.393-0-11	6.33423-01	5.50202-01	4.29578-01	2.96041-01	1.03560-012025	4	2	1033
7.40227-02	3.21032-02	1.01279-02	2.12672-03	4.42708-04	5.50235-052025	4	2	1034
2.38526-00						4	2	1035
2.030-0+02	5.00000+06	0	0	14	02025	4	2	1036
3.59453-01	7.27245-01	0.01985-01	4.74607-01	3.45295-01	2.12371-012025	4	2	1037
1.10100-01	0.43433-02	2.75200-02	8.37475-03	2.27404-03	4.45221-042025	4	2	1038
5.342-0-05	7.46223-00				2025	4	2	1039
2.03100+02	0.00000+06	0	0	15	02025	4	2	1040
1.00759-01	7.47315-01	0.35092-01	5.13967-01	3.89011-01	2.01025-012025	4	2	1041
1.00653-01	1.02235-01	5.59903-02	2.25979-02	7.77053-03	1.36298-032025	4	2	1042
3.21076-14	5.31052-05	3.54445-06			2025	4	2	1043
2.03100+02	7.00000+06	0	0	15	02025	4	2	1044
3.07300-01	7.32054-01	6.52306-01	5.42115-01	4.25171-01	3.06674-012025	4	2	1045
2.031-0-01	1.04167-01	2.29314-02	4.73229-02	1.03931-02	5.71796-032025	4	2	1046
1.22265-03	2.42354-04	2.16604-05			2025	4	2	1047
2.030-0+02	8.00000+06	0	0	17	02025	4	2	1048
3.55020-01	7.0-3677-01	4.52644-01	5.50097-01	4.51877-01	3.45884-012025	4	2	1049
2.47761-01	1.02057-01	1.34953-01	8.39172-02	4.13781-02	1.43293-022025	4	2	1050
4.033-0-03	1.05922-03	1.24245-04	2.83798-05	2.00760-06	2025	4	2	1051
2.03270+02	9.00000+06	0	0	17	02025	4	2	1052
0.62910-01	7.35583-01	0.42333-01	5.58190-01	4.07302-01	3.75099-012025	4	2	1053
2.87466-01	2.21307-01	1.75992-01	1.24629-01	7.02087-02	2.37237-022025	4	2	1054

9.59040-03	2.39413-03	6.27923-04	1.07442-04	9.44088-06		2025	4	2	1055
2.03000+02	1.00000+07	0	0	17	02025	4	2	1056	
8.04170-01	7.33003-01	0.34052-01	5.54227-01	4.70403-01	3.97995-012025	4	2	1057	
3.22001-01	2.59302-01	2.14248-01	1.65016-01	1.04008-01	4.25829-022025	4	2	1058	
1.05600-02	6.55610-03	1.04447-03	3.23929-04	3.35314-05	2025	4	2	1059	
2.73000+02	1.10000+07	0	0	17	02025	4	2	1060	
8.44793-01	7.27604-01	6.24304-01	5.45451-01	4.77184-01	4.11092-012025	4	2	1061	
2.40400-01	2.90297-01	2.46279-01	2.00031-01	1.37285-01	7.44344-022025	4	2	1062	
3.33197-02	1.24002-02	3.50771-04	7.84266-04	0.40020-05	2025	4	2	1063	
2.03000+02	1.30000+07	0	0	19	02025	4	2	1064	
8.81090-01	7.48190-01	6.33250-01	5.55865-01	4.5957(-01	4.35175-012025	4	2	1065	
3.34015-01	3.39102-01	2.95771-01	2.51622-01	1.95521-01	1.29035-012025	4	2	1066	
7.21238-02	3.44717-02	1.34931-02	4.53604-03	1.25253-03	2.58920-042025	4	2	1067	
2.72539-05					2025	4	2	1058	
2.93000+02	1.30000+07	0	0	19	02025	4	2	1059	
9.03077-01	7.34872-01	6.75758-01	5.82347-01	5.16538-01	4.50637-012025	4	2	1070	
4.10737-01	3.66634-01	3.24170-01	2.89526-01	2.23412-01	1.05043-012025	4	2	1071	
1.04526-01	5.72435-02	2.52013-02	1.03552-02	3.43450-03	8.07458-042025	4	2	1072	
1.02331-04					2025	4	2	1073	
0.00000+00	0.00000+00	0	0	0	02025	4	0	1074	
9.42420+04	2.39979+02	0	0	0	02025	4	16	1075	
0.00000+00	2.39979+02	1	2	0	02025	4	16	1076	
0.00000+00	0.00000+00	0	0	0	02025	4	0	1077	
9.42420+04	2.39979+02	0	0	0	02025	4	17	1078	
0.00000+00	2.39979+02	1	2	0	02025	4	17	1079	
0.00000+00	0.00000+00	0	0	0	02025	4	0	1080	
9.42420+04	2.39979+02	0	0	0	02025	4	18	1081	
0.00000+00	2.39979+02	1	2	0	02025	4	18	1082	
0.00000+00	0.00000+00	0	0	0	02025	4	0	1083	
9.42420+04	2.39979+02	0	0	0	02025	4	20	1084	
0.00000+00	2.39979+02	1	2	0	02025	4	20	1085	

0.30340+00	0.31863+00	0	0	0	02025	4	0	1086	
5.42420+04	2.39979+02	0	1	0	02025	4	51	1087	
0.00000+00	2.99979+02	0	2	0	02025	4	51	1088	
0.00000+00	0.00000+00	0	0	1	02025	4	51	1089	
20	2				2025	4	51	1090	
2.93060+02	1.00000+05	0	0	1	02025	4	51	1091	
0.00000+00					2025	4	51	1092	
2.93060+02	1.00000+05	0	0	1	02025	4	51	1093	
0.00000+00					2025	4	51	1094	
2.93060+02	1.20000+05	0	0	3	02025	4	51	1095	
-6.76176+04	-7.71562+04	5.05513+05			2025	4	51	1096	
2.93000+02	2.50000+05	0	0	5	02025	4	51	1097	
-5.56954+03	-3.34513+03	1.39582+03	2.37076+05	5.12647+00	2025	4	51	1098	
2.93000+02	5.00000+05	0	0	0	02025	4	51	1099	
-1.43546+02	-1.14472+02	4.21461+03	-0.18936+04	-7.28556+05	1.00199+05	02025	4	51	1100
2.93000+02	7.50000+05	0	0	7	02025	4	51	1101	
-7.22333+02	-1.35232+02	4.10950+03	-1.52106+03	-5.82867+05	1.05398+04	02025	4	51	1102
-7.74726+00					2025	4	51	1103	
2.93000+02	-1.10000+05	0	0	8	02025	4	51	1104	
-3.55124+02	-2.13726+02	5.50522+03	-4.05779+03	-1.76505+04	4.92171+04	02025	4	51	1105
-2.93024+02	0.20379+00				2025	4	51	1106	
2.93000+02	1.50000+05	0	0	9	02025	4	51	1107	
-4.32551+02	-3.70803+02	1.52051+02	-0.12755+03	2.15113+03	1.99349+03	02025	4	51	1108
-1.47440+04	-2.71553+05	7.44515+06			2025	4	51	1109	
2.93000+02	2.10000+05	0	0	11	02025	4	51	1110	
-3.13156+02	-6.47249+02	2.93431+02	5.01544+03	1.27917+02	2.27410+03	02025	4	51	1111
4.21274+04	4.27329+04	5.16193+05	1.39294+05	-1.08849+06		2025	4	51	1112
2.93000+02	3.00000+05	0	0	11	02025	4	51	1113	
7.66372+02	-7.23840+02	1.51707+02	2.14152+02	3.81446+02	1.19572+04	02025	4	51	1114
4.63265+03	3.52422+03	4.44692+05	2.91952+04	-3.55881+05		2025	4	51	1115
2.93000+02	4.00000+06	0	0	13	02025	4	51	1116	

1.37327+01	-4.32745+02	-6.36877+03	2.64877+02	3.44693+02	-1.71369+02	02025	4	51	1117
-9.02272+13	1.02430+03	6.26802+03	3.47226+03	3.09757+04	1.99253+04	02025	4	51	1118
0.29590+12						2025	4	51	1119
2.93000+02	5.00000+06	0	0	15		02025	4	51	1120
1.58620+01	-5.30837+02	-3.04705+02	2.99515+02	2.20557+02	-2.83705+02	02025	4	51	1121
-2.95333+02	-1.13029+02	1.09198+02	7.12482+03	1.49952+03	1.37204+03	02025	4	51	1122
1.14715+04	2.64741+05	3.76380+06				2025	4	51	1123
2.93000+02	6.00000+06	0	0	15		02025	4	51	1124
1.770+05	-5.77731+02	-5.38700+02	1.69672+02	2.31555+02	-2.17433+02	02025	4	51	1125
-3.67345+02	-2.79753+02	6.90981+03	5.36057+03	3.63068+03	4.19685+03	02025	4	51	1126
3.62574+04	1.46673+04	2.56889+05				2025	4	51	1127
2.93040+02	7.00000+06	0	0	15		02025	4	51	1128
2.07359+01	-5.58323+02	-6.90505+02	1.77340+03	3.17401+02	-9.51557+03	02025	4	51	1129
-3.68777+02	-3.78144+02	-4.07573+03	-2.81101+03	7.28277+03	8.09940+03	02025	4	51	1130
6.95334+04	4.39557+04	1.17316+04				2025	4	51	1131
2.93000+02	8.00000+06	0	0	17		02025	4	51	1132
2.41317+01	-4.10751+02	-7.42593+02	-1.33057+02	2.83451+02	-1.38783+04	02025	4	51	1133
-3.37537+02	-4.41882+02	-1.54288+02	-1.00068+02	1.22976+02	1.17411+02	02025	4	51	1134
1.21833+03	1.69003+03	3.95263+04	6.58231+05	8.30952+06		2025	4	51	1135
2.93000+02	9.00000+06	0	0	17		02025	4	51	1136
2.61165+01	-1.78895+02	-7.72429+02	-2.59701+02	1.75269+02	7.19559+03	02025	4	51	1137
-2.68644+02	-4.77604+02	-2.26067+02	-1.14406+02	1.54450+02	1.25905+02	02025	4	51	1138
2.09416+03	3.73317+03	1.07470+03	2.05669+04	3.94219+05		2025	4	51	1139
2.93000+02	1.00000+07	0	0	17		02025	4	51	1140
3.25499+01	1.23371+02	-7.10292+02	-3.12318+02	8.76883+03	1.32267+02	02025	4	51	1141
-1.20191+02	-4.72233+02	-2.57395+02	-1.04345+02	1.46944+02	1.03896+02	02025	4	51	1142
3.11074+03	7.03520+03	2.40294+03	5.35974+04	1.42555+04		2025	4	51	1143
2.93000+02	1.10000+07	0	0	17		02025	4	51	1144
3.59611+01	3.98228+02	-6.12737+02	-2.87455+02	5.08628+03	1.73638+02	02025	4	51	1145
-1.09448+02	-4.07209+02	-2.56168+02	-9.31615+03	1.15561+02	5.36179+03	02025	4	51	1146
4.07973+03	1.06701+02	4.09596+03	1.04492+03	3.83850+04		2025	4	51	1147

2.93000+02	1.30000+07	0	0	10	02025	4	51	1148
6.14722+01	9.55242+02+2.27235+02-1.04633+02	0	1.17243+03	1.39293+022025	4	51	1149	
2.09515+03+2.32376+02+2.20231+02+4.36530+03	7.05042+03-1.01242+032025	4	51	1150				
5.03337+03	1.74511+02	9.14385+03	3.2+3+0+03	2.31228+03	4.31982+042025	4	51	1151
8.75751+06					2025	4	51	1152
2.93030+02	1.50000+07	0	0	10	02025	4	51	1153
4.56218+01	1.41261+01	9.99278+03	3.09702+03	2.27037+02	2.90270+022025	4	51	1154
1.83225+02+5.55674+03+1.06969+02+3.79468+03	1.29637+02	5.37993+032025	4	51	1155			
7.79404+03	1.62611+02	3.02606+03	0.05833+03	5.64934+03	1.23314+032025	4	51	1156
3.22705+05					2025	4	51	1157
0.00000+00	0.00000+00	0	0	0	02025	4	0	1158
0.42420+04	2.19973+02	0	1	0	02025	4	52	1159
0.00000+00	2.39979+02	0	2	0	02025	4	52	1160
0.000010+00	0.00000+00	0	0	1	192025	4	52	1161
					2025	4	52	1162
2.93000+02	1.00000+05	0	0	1	02025	4	52	1163
0.00000+00					2025	4	52	1164
2.93000+02	3.10000+05	0	0	1	02025	4	52	1165
0.00000+00					2025	4	52	1166
2.93000+02	3.20000+05	0	0	5	02025	4	52	1167
3.71451+03+1.57303+04+2.57147+04-1.65258+04	7.44238+08				2025	4	52	1168
2.93000+02	5.00000+05	0	0	0	02025	4	52	1169
2.21197+02+2.21096+04+4.20945+03+5.33144+04	1.13910+04-2.71957+062025	4	52	1170				
2.93000+02	7.50000+05	0	0	7	02025	4	52	1171
4.20950+02+4.43223+03+7.74525+03	7.95935+05	4.92045+04-7.58758+052025	4	52	1172			
0.56312+00					2025	4	52	1173
2.93000+02	1.00000+04	0	0	8	02025	4	52	1174
4.57478+02+1.93317+02+1.04339+02	2.0+566+03	8.19206+04-2.39011+042025	4	52	1175			
3.08132+05+1.99202+05					2025	4	52	1176
2.93000+02	1.50000+06	0	0	8	02025	4	52	1177
5.56221+02+4.93443+02+0.28016+03	7.97391+03+5.62280+04+8.11760+042025	4	52	1178				

2.36908+04-3.39734+05					2025	4	52	1179
2.03000+02	2.00000+05	0	0	10	02025	4	52	1180
1.07948+11+8.02353+02-1.53191+03	7.99574+03+5.84122+03	4.56415+042025	4	52	1181			
6.17152+04-3.67049+04	3.48315+05+5.13320+06				2025	4	52	1182
2.93000+02	3.00000+06	0	0	11	02025	4	52	1183
1.46695+01+1.17623+01+2.35796+02-1.13818+02+5.76850+03	4.55184+032025	4	52	1184				
+0.14599+04+1.01997+03	2.52307+04-7.42532+05	9.63523+06			2025	4	52	1185
2.93000+02	4.00000+06	0	0	13	02025	4	52	1186
1.45369+01+1.10579+01+1.36746+02+1.66658+02+6.09347+03	3.09944+042025	4	52	1187				
+4.89159+03	4.67529+03	8.36057+04-1.02293+03	4.96198+05	6.98427+062025	4	52	1188	
+1.93942+00					2025	4	52	1189
2.93000+02	5.00000+06	0	0	14	02025	4	52	1190
1.47453+01+4.26522+02+5.59159+03+2.72371+02+9.77837+03	1.08448+032025	4	52	1191				
+2.20132+03	1.10219+02	3.94582+04-1.55518+03	1.88645+04-3.49781+052025	4	52	1192		
1.78103+05	1.53903+06				2025	4	52	1193
2.93000+02	6.00000+06	0	0	15	02025	4	52	1194
1.52057+01+7.73684+03+1.74025+02+3.47168+02	3.70462+03	7.55899+032025	4	52	1195			
+4.36688+05	1.05495+02+1.96506+03+9.85615+04	0.38508+04-2.04457+042025	4	52	1196			
6.11075+05	1.65066+06	4.12441+06			2025	4	52	1197
2.93000+02	7.00000+06	0	0	13	02025	4	52	1198
1.69152+01+6.37049+02+3.27831+02+3.68386+02	1.80489+02	6.06856+032025	4	52	1199			
+2.46046+03	3.77022+03+3.54772+03	1.93811+03	1.02695+03+5.32015+042025	4	52	1200		
1.35613+04+2.40749+05	2.09720+05				2025	4	52	1201
2.93000+02	8.00000+06	0	0	17	02025	4	52	1202
2.00345+01+5.19271+02+5.03648+02+4.56017+02	1.90933+02	2.77425+032025	4	52	1203			
+2.52683+03	3.93465+03+3.01047+04	4.57411+03	1.10498+03+6.03353+042025	4	52	1204		
1.77425+05+1.29902+06	7.44541+05	4.10658+06	2.99762+06		2025	4	52	1205
2.93000+02	9.00000+06	0	0	17	02025	4	52	1206
2.34935+01+3.28781+02+6.32110+02+5.47463+02	1.50535+02	2.08640+032025	4	52	1207			
1.25008+03	6.17099+03	2.23415+03	0.38949+03	1.57195+03+1.23520+032025	4	52	1208	
+6.05700+04+3.36718+05	1.74969+04	2.10433+06	1.35789+05		2025	4	52	1209

2.93000+02	1.00000+07	0	0	17	02025	4	52	1210.	
2.64570+01	-2.63651+02	-6.35039+02	-5.74491+02	1.24214+02	4.40996+03	2025	4	52	1211
5.17357+03	3.47533+03	1.39514+03	9.18430+03	3.48568+03	-2.09654+03	2025	4	52	1212
-1.41510+03	3.66546+05	2.66087+06	-2.35409+05	4.96264+05		2025	4	52	1213
2.93000+02	1.10007+07	0	0	17	02025	4	52	1214	
2.81819+01	-1.36042+02	-6.35636+02	-5.81459+02	1.00518+02	5.37629+03	2025	4	52	1215
6.65661+03	-5.52393+04	-6.47334+04	1.18150+02	5.05221+03	-3.44508+03	2025	4	52	1216
-2.68872+03	4.18280+04	1.55325+04	-1.32698+04	1.35067+04		2025	4	52	1217
2.93000+02	1.30000+07	0	0	19	02025	4	52	1218	
3.11756+01	1.90575+02	-9.36648+02	-8.1c111+02	-1.70407+03	3.00540+03	2025	4	52	1219
6.53752+03	-9.66245+04	-2.01147+03	1.42678+02	4.28315+03	-5.20074+03	2025	4	52	1220
1.57069+03	2.21461+03	-2.37436+03	-6.30930+04	8.03674+04	1.98768+05	2025	4	52	1221
-6.54158+06						2025	4	52	1222
2.93000+02	1.50000+07	0	0	19	02025	4	52	1223	
3.53486+01	4.29257+02	-5.33565+02	-6.66713+02	-1.46392+02	-2.80039+03	2025	4	52	1224
1.26794+02	2.35046+03	-2.53790+03	1.42338+02	4.57764+03	1.71896+03	2025	4	52	1225
7.64336+03	-1.50442+03	-7.01358+03	-4.60414+04	1.60527+03	9.83664+05	2025	4	52	1226
4.90465+05						2025	4	52	1227
0.00000+00	0.00000+00	0	0	0	02025	4	0	1228	
9.42420+04	2.39979+02	0	0	0	02025	4	53	1229	
0.00000+00	2.39979+02	1	2	0	02025	4	53	1230	
0.00000+00	0.00000+00	0	0	0	02025	4	0	1231	
0.42420+04	2.39979+02	0	0	0	02025	4	54	1232	
0.00000+00	2.39979+02	1	2	0	02025	4	54	1233	
0.00000+00	0.00000+00	0	0	0	02025	4	0	1234	
0.42420+04	2.39979+02	0	0	0	02025	4	55	1235	
0.00000+00	2.39979+02	1	2	0	02025	4	55	1236	
0.00000+00	0.00000+00	0	0	0	02025	4	0	1237	
0.42420+04	2.39979+02	0	0	0	02025	4	56	1238	
0.00000+00	2.39979+02	1	2	0	02025	4	56	1239	
0.00000+00	0.00000+00	0	0	0	02025	4	0	1240	

0.42420+04	2.39979+02	0	0	0	02025	4	57	1241
0.00000+00	2.39979+02	1	2	0	02025	4	57	1242
0.00000+00	0.00000+00	0	0	0	02025	4	0	1243
0.42420+04	2.39979+02	0	0	0	02025	4	58	1244
0.00000+00	2.39979+02	1	2	0	02025	4	58	1245
0.00000+00	0.00000+00	0	0	0	02025	4	0	1246
0.42420+04	2.39979+02	0	0	0	02025	4	59	1247
0.00000+00	2.39979+02	1	2	0	02025	4	59	1248
0.00000+00	0.00000+00	0	0	0	02025	4	0	1249
0.42420+04	2.39979+02	0	0	0	02025	4	60	1250
0.00000+00	2.39979+02	1	2	0	02025	4	60	1251
0.00000+00	0.00000+00	0	0	0	02025	4	0	1252
0.42420+04	2.39979+02	0	0	0	02025	4	61	1253
0.00000+00	2.39979+02	1	2	0	02025	4	61	1254
0.00000+00	0.00000+00	0	0	0	02025	4	0	1255
0.42420+04	2.39979+02	0	0	0	02025	4	62	1256
0.00000+00	2.39979+02	1	2	0	02025	4	62	1257
0.00000+00	0.00000+00	0	0	0	02025	4	0	1258
0.42420+04	2.39979+02	0	0	0	02025	4	63	1259
0.00000+00	2.39979+02	0	0	0	02025	4	63	1260
0.00000+00	0.00000+00	1	2	0	02025	4	0	1261
0.42420+04	2.39979+02	0	0	0	02025	4	91	1262
0.00000+00	2.39979+02	1	2	0	02025	4	91	1263
0.00000+00	0.00000+00	0	0	0	02025	4	0	1264
0.00000+00	0.00000+00	0	0	0	02025	0	0	1265
0.42420+04	2.39979+02	0	0	2	02025	3	16	1266
0.00000+00	0.00000+00	0	1	1	02025	5	16	1267
2	2				2025	5	16	1268
0.33000+06	5.00000+01	1.50000+07	3.00000+01		2025	5	16	1269
0.00000+00	0.00000+00	0	0	1	02025	5	16	1270
9	2				2025	5	16	1271

0.00000+00	7.00000+00	0	0	1	52025	5	16	1272
5	2				2025	5	16	1273
0.00000+00	0.00000+00	1.16667+05	7.11963-01	3.50000+05	7.87238-012025	5	16	1274
5.33333+05	6.43657-01	6.70000+05	0.00000+00		2025	5	16	1275
0.00000+00	0.00000+06	0	0	1	112025	5	16	1276
11	2				2025	5	16	1277
0.00000+00	0.00000+00	1.50000+05	3.87735-01	4.50000+05	4.03762-012025	5	16	1278
7.50000+03	3.10574-01	1.05000+05	2.10877-01	1.35000+06	1.43682-012025	5	16	1279
1.65000+05	9.18263-02	1.95000+06	5.70574-02	2.25000+07	3.46113-022025	5	16	1280
2.55000+06	2.05415-02	2.67000+06	0.00000+00		2025	5	16	1281
0.00000+00	1.10000+07	0	0	1	152025	5	16	1282
15	2				2025	5	16	1283
0.00000+00	0.00000+00	1.83333+05	3.50445-01	2.50000+05	3.45854-012025	5	16	1284
9.16667+05	2.51893-01	1.28333+06	1.66383-01	1.65000+06	1.04152-012025	5	16	1285
2.01667+05	6.28274-02	2.38333+06	3.68031-02	2.75000+06	2.10203-022025	5	16	1286
3.11667+05	1.17307-02	3.48333+06	5.40289-03	3.85000+06	3.41904-032025	5	16	1287
4.21667+05	1.78553-03	4.58333+06	9.11458-04	4.67000+06	0.00000+002025	5	16	1288
0.00000+00	1.30000+07	0	0	1	172025	5	16	1289
17	2				2025	5	16	1290
0.00000+00	0.00000+00	2.16667+05	9.15987-02	6.50000+05	1.84931-012025	5	16	1291
1.08333+06	2.34327-01	1.51667+06	2.52699-01	1.95000+06	1.56159-012025	5	16	1292
2.58333+05	3.93552-02	2.81667+06	4.95990-02	3.25000+06	2.68128-022025	5	16	1293
3.48333+06	1.41452-02	4.11557+06	7.28903-03	4.55000+06	3.66941-032025	5	16	1294
4.96433+05	1.80397-03	5.41667+06	8.75383-04	5.85000+06	4.04578-042025	5	16	1295
6.28333+05	1.84034-04	6.67000+06	0.00000+00		2025	5	16	1296
0.00000+00	1.50000+07	0	0	1	192025	5	16	1297
19	2				2025	5	16	1298
0.00000+00	0.00000+00	2.50000+05	2.04570-02	7.50000+05	4.28480-022025	5	16	1299
1.25000+06	6.73139-02	1.75000+06	9.72290-02	2.25000+06	1.34008-012025	5	16	1300
2.75000+00	1.75781-01	3.25000+06	2.05743-01	3.75000+06	1.30996-012025	5	16	1301
4.25000+06	6.56018-02	6.75000+06	3.20507-02	5.25000+06	1.52776-022025	5	16	1302

5.75000+00	7.10172-03	6.25000+06	3.21531-03	6.75000+06	1.41726-032025	5	16	1303
7.25000+00	8.05545-04	7.75000+06	2.51549-04	8.25000+06	1.00613-042025	5	16	1304
3.47000+00	3.00000+00				2025	5	16	1305
0.00000+00	0.00000+00	0	1	1	22025	5	16	1306
1	2				2025	5	16	1307
2.33000+10	5.00000+01	1.50000+07	5.00000+01		2025	5	16	1308
0.00000+00	0.00000+00	0	0	1	52025	5	16	1309
5	2				2025	5	16	1310
0.00000+00	7.30000+05	0	0	1	162025	5	16	1311
15	2				2025	5	16	1312
2.00000+00	0.100000+00	4.00000+04	2.29597-01	3.00000+04	6.77991-012025	5	16	1313
1.26000+05	1.10995+00	1.50000+05	1.42581+00	2.00000+05	1.52358+002025	5	16	1314
2.40000+05	1.58933+00	2.30000+05	1.47275+00	3.20000+05	1.27212+002025	5	16	1315
3.60000+05	1.01713+00	4.00000+05	8.04554-01	4.40000+05	5.92036-012025	5	16	1316
4.90000+05	3.94951-01	5.20000+05	2.30818-01	5.60000+05	4.52554-022025	5	16	1317
5.00000+05	0.00000+00				2025	5	16	1318
0.00000+00	9.00000+05	0	0	1	522025	5	16	1319
52	2				2025	5	16	1320
0.00000+00	0.00000+00	4.00000+04	1.85858-02	8.00000+04	6.53238-022025	5	16	1321
1.20000+05	1.29311-01	1.60000+05	1.98905-01	2.00000+05	2.70679-012025	5	16	1322
2.40000+05	3.39200-01	2.30000+05	4.02946-01	3.20000+05	4.54390-012025	5	16	1323
3.50000+05	4.98333-01	4.00000+05	5.32331-01	4.40000+05	5.56684-012025	5	16	1324
4.50000+05	5.71663-01	5.20000+05	5.78109-01	5.60000+05	5.76831-012025	5	16	1325
5.00000+05	5.56881-01	6.40000+05	5.55026-01	5.80000+05	5.36462-012025	5	16	1326
7.20000+05	5.14054-01	7.60000+05	4.83677-01	8.00000+05	4.01141-012025	5	16	1327
8.40000+05	4.32163-01	8.30000+05	4.02330-01	9.20000+05	3.72345-012025	5	16	1328
9.60000+05	3.42523-01	1.20000+06	3.13319-01	1.04000+06	2.85037-012025	5	16	1329
1.08000+06	2.57934-01	1.12000+06	2.32200-01	1.16000+06	2.07966-012025	5	16	1330
1.20000+06	1.35322-01	1.24000+06	1.64318-01	1.28000+06	1.44966-012025	5	16	1331
1.32000+06	1.27253-01	1.40000+06	9.65951-02	1.44000+06	8.35146-022025	5	16	1332
1.52000+06	5.14365-02	1.20000+06	4.42011-02	1.04000+06	3.71623-022025	5	16	1333

1.72000+05	2.57957-02	1.30000+06	1.74242-02	1.38000+06	1.14128-022025	5	16	1334	
1.26000+05	7.21340-03	2.04000+06	4.39907-03	2.12000+06	2.54775-032025	5	16	1335	
2.20000+05	1.38253-03	2.28000+06	6.92831-04	2.36000+06	3.20746-042025	5	16	1336	
2.44000+05	1.20473-04	2.48000+06	6.33934-05	2.52000+06	2.59811-052025	5	16	1337	
2.56000+05	0.20000+07					2025	5	16	1338
0.00000+00	1.10000+07					602025	5	16	1339
80	2					2025	5	16	1340
0.00000+00	0.00000+00	4.00000+04	7.23048-03	5.00000+04	2.51838-022025	5	16	1341	
1.20000+05	5.33092-02	1.60000+05	8.57180-02	2.00000+05	1.21081-012025	5	16	1342	
2.40000+05	1.57549-01	3.20000+05	2.23354-01	4.00000+05	2.90314-012025	5	16	1343	
6.5.20000+05	3.55601-01	6.00000+05	3.66508-01	6.80300+05	4.00909-012025	5	16	1344	
7.20000+05	4.03555-01	7.00000+05	4.03495-01	8.00000+05	4.00942-012025	5	16	1345	
8.40000+05	3.26180-01	9.20000+05	3.31059-01	1.00000+06	3.50072-012025	5	16	1346	
1.08000+05	3.35020-01	1.20000+06	2.93150-01	1.28000+06	2.64223-012025	5	16	1347	
1.40000+05	2.21605-01	1.48000+06	1.94636-01	1.60000+06	1.57615-012025	5	16	1348	
1.68000+05	1.35472-01	1.30000+06	1.06292-01	1.88000+06	8.95426-022025	5	16	1349	
2.00000+05	6.32505-02	2.30000+06	5.66151-02	2.20000+06	4.18035-022025	5	16	1350	
2.23000+05	3.39111-02	2.40000+06	2.44233-02	2.48000+05	1.94333-022025	5	16	1351	
2.60000+05	1.35864-02	2.70000+06	1.05913-02	2.80000+06	7.17116-032025	5	16	1352	
2.80010+05	5.66534-03	3.00000+06	3.57147-03	3.08000+06	2.65417-032025	5	16	1353	
3.15000+05	1.95044-03	3.20000+06	1.56452-03	3.28000+06	1.20076-032025	5	16	1354	
3.40000+05	7.17006-04	3.48000+06	4.93951-04	3.56000+06	3.1346-042025	5	16	1355	
3.70000+05	2.80355-04	3.72000+06	1.50515-04	3.80000+05	9.65029-052025	5	16	1356	
3.95010+05	5.02849-05	3.90000+06	3.63912-05	4.00000+06	2.78563-052025	5	16	1357	
4.04000+05	2.10535-05	4.12000+06	1.16079-05	4.20000+06	6.05527-062025	5	16	1358	
4.28000+05	2.22939-05	4.32000+06	1.93919-06	4.40000+06	7.23631-072025	5	16	1359	
4.44000+05	3.34582-07	4.48000+06	1.65322-07	4.52000+06	0.00000+002025	5	16	1360	
0.00000+00	1.30000+07					812025	5	16	1361
81	2					2025	5	16	1362
0.00000+00	0.00000+00	4.00000+04	3.31254-03	3.00000+04	1.22180-022025	5	16	1363	
1.20000+05	2.52814-02	1.60000+05	4.13272-02	2.00000+05	5.93580-022025	5	15	1364	

3.41000+05	9.53132-02	2.30000+05	1.21552-01	3.20000+05	2.44752-012025	5	16	1365	
4.10000+15	1.93976-01	4.40000+05	2.12243-01	5.20000+05	2.49848-012025	5	16	1366	
6.30000+05	2.30012-01	4.30000+05	3.02322-01	3.00000+05	3.21397-012025	5	16	1367	
2.40000+05	3.24434-01	9.20000+05	3.27468-01	9.00000+05	3.25161-012025	5	16	1368	
1.04000+05	3.14934-01	1.12000+06	3.03511-01	1.20000+06	2.45508-012025	5	16	1369	
1.25000+05	2.772873-01	1.40000+06	2.53578-01	1.48000+06	2.35018-012025	5	16	1370	
1.70000+05	2.14944-01	1.48000+06	1.83345-01	1.80000+06	1.51866-012025	5	16	1371	
1.85000+05	1.45257-01	2.00000+06	1.22253-01	2.03000+06	1.08292-012025	5	16	1372	
2.20000+05	3.27227-02	2.21000+06	7.83271-02	2.40000+06	5.36242-022025	5	16	1373	
2.48010-00	5.55005-02	2.50000+06	4.41309-02	2.68000+06	3.77328-022025	5	16	1374	
2.40010-00	2.17927-02	2.33000+06	2.51878-02	3.00000+06	1.75239-022025	5	16	1375	
3.10000+05	1.164910-02	3.20000+06	1.25140-02	3.24000+06	1.03966-022025	5	16	1376	
3.45000+05	7.51234-03	3.48000+06	6.42341-03	3.61000+06	6.74934-032025	5	16	1377	
3.56000+05	3.441107-03	3.30000+06	2.81632-03	3.83000+06	2.25553-032025	5	16	1378	
4.08000+05	1.00923-03	4.03030+06	1.13545-03	4.20000+06	5.33692-042025	5	16	1379	
4.28000+05	6.99387-04	4.40000+06	4.71771-04	4.48000+06	3.58989-042025	5	16	1380	
4.50000+05	2.445515-04	4.53000+06	1.35715-04	4.80000+06	1.21313-042025	5	16	1381	
4.36000+05	9.00894-05	5.00000+06	5.55789-05	5.08000+06	4.11119-052025	5	16	1382	
5.20000+05	2.33904-05	5.28000+06	1.75546-05	5.40000+06	1.01395-052025	5	16	1383	
5.46000+05	6.70228-06	5.56000+06	4.52323-06	5.64000+06	3.03522-062025	5	16	1384	
5.72000+05	1.95375-06	5.30000+06	1.22312-06	5.88000+06	7.47258-072025	5	16	1385	
5.95000+05	4.39065-07	5.04000+06	2.43240-07	5.12000+06	1.34616-072025	5	16	1386	
6.20000+05	6.82032-08	5.24000+06	4.67393-08	6.28000+06	3.39625-082025	5	16	1387	
6.32000+05	1.32162-08	6.36000+06	1.10763-08	6.40000+06	6.30330-092025	5	16	1388	
6.44000+05	2.83518-09	6.48000+06	5.94750-10	6.52000+06	0.00000+002025	5	16	1389	
0.00000+00	1.50000+07					802025	5	16	1390
80	2					2025	5	16	1391
0.00000+00	0.26000+00	4.00000+04	1.92985-03	3.00000+04	7.18494-032025	5	16	1392	
1.20000+05	1.50638-02	1.70000+05	2.47502-02	2.00000+05	3.63287-022025	5	16	1393	
2.40000+05	5.13334-02	2.30000+05	6.47671-02	3.60000+05	9.27770-022025	5	16	1394	
4.00000+05	1.00433-01	4.30000+05	1.32176-01	5.00000+05	1.55129-012025	5	16	1395	

6.80000+05	1.52480-01	8.00000+05	2.20175-01	8.50000+05	2.28475-012025	5	16	1396
1.00000-06	2.33871-01	1.04000-06	2.33946-01	1.08000-06	2.53350-012025	5	16	1397
1.16000+06	2.30043-01	1.28000+06	2.54659-01	1.40000+06	2.39614-012025	5	16	1398
1.46000+06	2.27867-01	1.50000+06	2.08636-01	1.68000+06	1.75217-012025	5	16	1399
1.30000+06	2.14255-01	1.92000+06	1.910-2-01	2.08000+06	1.59419-012025	5	16	1400
2.16000+06	1.45089-01	2.30000+06	1.71243-01	2.24000+06	1.53168-012025	5	16	1401
2.32000+06	1.47721-01	2.40000+06	1.33257-01	2.55000+06	1.07342-012025	5	16	1402
2.72000+06	8.53711-02	3.00000+06	5.55736-02	3.12000+06	4.57495-022025	5	16	1403
3.28000+06	3.49642-02	3.40000+06	2.83821-02	3.60000+06	1.97275-022025	5	16	1404
3.30000+06	1.35738-02	4.00000+06	9.1-153-03	4.20000+06	6.08314-032025	5	16	1405
0.40000+06	3.97210-03	4.60000+06	2.51936-03	4.80000+06	1.50724-032025	5	16	1406
5.00000+05	9.94466-04	5.20000+06	6.03252-04	5.40000+06	3.58319-042025	5	16	1407
5.60000+06	2.08067-04	5.30000+06	1.17951-04	5.00000+06	6.50285-052025	5	16	1408
8.08000+06	5.08420-05	6.20000+06	3.48206-05	6.28000+06	2.06775-052025	5	16	1409
6.40000+06	1.80356-05	6.58000+06	1.37226-05	6.60000+06	8.99625-062025	5	16	1410
6.66000+06	6.73372-05	6.80000+06	4.29398-06	6.85000+06	3.15575-062025	5	16	1411
7.00000+06	1.85255-05	7.12000+06	1.14213-05	7.20000+06	8.34054-072025	5	16	1412
7.32000+06	4.86084-07	7.60000+06	3.31042-07	7.52000+06	1.81971-072025	5	16	1413
7.60000+06	1.19446-07	7.72000+06	6.10252-08	7.80000+06	3.77997-082025	5	16	1414
7.88000+06	2.27246-08	6.00000+06	9.92861-09	8.08000+06	5.47467-092025	5	16	1415
8.16000+06	2.74028-09	8.24000+06	1.25288-09	8.26000+06	7.980-8-102025	5	16	1416
8.32000+06	4.79307-10	8.35000+06	2.03421-10	8.40000+06	1.23160-102025	5	16	1417
8.44000+06	3.51062-11	5.48000+06	0.00000+00		2025	5	16	1418
0.00000+00	0.00000+00	0	0	0	02025	5	0	1419
4.42420+04	2.39979+02	0	0	3	02025	5	17	1420
0.00000+00	0.00000+00	0	1	1	22025	5	17	1421
2	2				2025	5	17	1422
1.15900+07	3.33333-01	1.50000+07	3.33333-01		2025	5	17	1423
0.00000+00	0.00000+00	0	0	1	22025	5	17	1424
2	2				2025	5	17	1425
0.00000+00	1.30000+07	0	0	1	52025	5	17	1426

5	2				2025	5	17	1427
0.00000+00	0.00000+00	2.16667+05	6.57552-01	6.50000+05	1.06299-012025	5	17	1428
1.06333+06	2.36857-03	1.41000+06	0.00000+00		2025	5	17	1429
0.70000+00	1.50000+07	-	0	0	02025	5	17	1430
0	2				2025	5	17	1431
0.30000+00	0.00000+00	1.75000+06	7.23910-03	2.25000+06	1.07502-032025	5	17	1432
2.75000+06	5.84387-05	3.25000+06	1.61198-07	3.41000+06	0.00000+002025	5	17	1433
0.00000+00	0.00000+00	0	1	1	22025	5	17	1434
0	2				2025	5	17	1435
1.15940+07	3.33333-01	1.50000+07	3.33333-01		2025	5	17	1436
0.00000+00	0.00000+00	0	0	1	22025	5	17	1437
2	2				2025	5	17	1438
0.00000+00	1.30000+07	0	0	1	272025	5	17	1439
27	2				2025	5	17	1440
0.00000+00	0.00000+00	4.00000+04	3.63464-02	8.00000+04	1.15046-012025	5	17	1441
1.20000+05	2.03914-01	1.60000+05	2.64224-01	2.00000+05	3.46457-012025	5	17	1442
2.40000+05	7.04626-01	2.80000+05	8.03642-01	3.20000+05	7.57611-012025	5	17	1443
4.00000+05	6.26167-01	4.40000+05	6.30270-01	5.20000+05	4.97785-012025	5	17	1444
8.00000+05	3.57721-01	6.80000+05	2.37250-01	7.60000+05	1.44883-012025	5	17	1445
8.00000+05	1.09463-01	6.60000+05	5.76245-02	7.20000+05	3.97683-022025	5	17	1446
9.40000+05	2.63303-02	1.00000+06	1.65643-02	1.04000+06	9.76860-032025	5	17	1447
1.08000+06	5.27346-03	1.12000+06	2.50240-03	1.16000+06	9.57007-042025	5	17	1448
1.20000+06	2.29407-04	1.24000+06	1.49125-06	1.28000+06	0.00000+002025	5	17	1449
0.00000+00	1.50000+07	0	0	1	512025	5	17	1450
51	2				2025	5	17	1451
0.00000+00	0.00000+00	4.60000+04	1.0e313-02	8.00000+04	3.73966-022025	5	17	1452
1.20000+05	7.39170-02	1.60000+05	1.15316-01	2.00000+05	1.58134-012025	5	17	1453
2.40000+05	1.99370-01	2.80000+05	2.37327-01	3.60000+05	2.99052-012025	5	17	1454
4.40000+05	3.35951-01	5.20000+05	3.57462-01	5.60000+05	3.59570-012025	5	17	1455
6.00000+05	3.57551-01	5.80000+05	3.43240-01	7.60000+05	3.20015-012025	5	17	1456
2.40000+05	2.88723-01	9.20000+05	2.54289-01	1.00000+00	2.19230-012025	5	17	1457

1.08000+06	5.85387-01	1.20000+06	1.42603-01	1.28000+06	1.15195-012025	5	17	1458
1.40000+06	8.12312-02	1.48000+06	6.31480-02	1.60000+06	4.20813-022025	5	17	1459
1.68000+06	3.15020-02	1.80000+06	2.21586-02	1.88000+06	1.57701-022025	5	17	1460
2.00000+06	9.15334-03	2.08000+06	6.21703-03	2.12000+06	5.08410-032025	5	17	1461
2.20000+06	6.32055-03	2.26000+06	4.19970-03	2.32000+06	3.28680-032025	5	17	1462
2.40000+06	2.04512-03	2.48000+06	1.23375-03	2.56000+06	7.16450-042025	5	17	1463
2.60000+06	5.37061-04	2.68000+06	2.90293-04	2.76000+06	1.47226-042025	5	17	1464
2.80000+06	1.01643-04	2.84000+06	6.84080-05	2.86000+06	4.46671-052025	5	17	1465
2.92000+06	2.51126-05	2.96000+06	1.68998-05	3.00000+06	9.57354-062025	5	17	1466
3.04000+06	5.00282-06	3.08000+06	2.32366-06	3.12000+06	8.89608-072025	5	17	1467
3.16000+06	2.29180-07	3.20000+06	1.07129-08	3.24000+06	0.00000+002025	5	17	1468
0.00000+00	0.00000+00	0	1	1	22025	5	17	1469
2	2				2025	5	17	1470
1.15900+07	3.33333-01	1.50000+07	3.33333-01		2025	5	17	1471
0.00000+00	0.00000+00	0	0	1	22025	5	17	1472
2	2				2025	5	17	1473
0.00000+00	1.30000+07	0	0	1	272025	5	17	1474
27	2				2025	5	17	1475
0.00000+00	0.00000+00	4.00000+04	9.37009-01	8.00000+04	1.05726+002025	5	17	1476
1.20000+05	1.02784+00	1.50000+05	9.38817-01	2.00000+05	8.25764-012025	5	17	1477
2.20000+05	5.94151-01	3.60000+05	3.94088-01	4.00000+05	3.21071-012025	5	17	1478
4.80000+05	1.29550-01	5.60000+05	1.17365-01	6.00000+05	8.34846-022025	5	17	1479
6.30000+05	4.82970-02	7.20000+05	3.46596-02	7.60000+05	2.43052-022025	5	17	1480
8.00000+05	1.44819-02	8.40000+05	1.13491-02	8.80000+05	7.55440-032025	5	17	1481
9.20000+05	4.81600-03	9.50000+05	2.89826-03	1.00000+06	1.58511-032025	5	17	1482
1.04000+06	8.31986-04	1.08000+06	5.24999-04	1.12000+06	3.09552-042025	5	17	1483
1.16000+06	1.63868-04	1.20000+06	6.98330-05	1.24000+06	0.00000+002025	5	17	1484
3.00000+00	1.50000+07	0	0	?	462025	5	17	1485
46	2				2025	5	17	1486
0.00000+00	0.00000+00	4.00000+04	4.19201-01	8.00000+04	5.21345-012025	5	17	1487
1.20000+05	5.01031-01	1.40000+05	5.63711-01	2.00000+05	5.57692-012025	5	17	1488

2.10000+05	5.06241-01	4.00000+05	4.03582-01	4.80000+05	3.35936-012025	5	17	1489
5.30000+05	2.45695-01	6.80000+05	1.97324-01	8.00000+05	1.38127-012025	5	17	1490
3.40000+05	1.37496-01	1.00000+06	7.24927-02	1.08000+06	5.51099-022025	5	17	1491
1.20000+05	3.59154-02	1.28000+06	2.65930-02	1.40000+06	1.56066-022025	5	17	1492
1.42000+05	1.21994-02	1.50000+06	7.40242-03	1.68000+06	5.23447-032025	5	17	1493
1.80000+05	3.04647-03	1.88000+06	2.09047-03	2.00000+06	1.15793-032025	5	17	1494
2.00000+05	7.05902-04	2.16000+06	4.99313-04	2.20000+06	4.00042-042025	5	17	1495
2.20000+05	2.52301-04	2.35000+06	1.55619-04	2.40000+06	1.22178-042025	5	17	1496
2.48000+05	7.27393-05	2.50000+06	4.19142-05	2.60000+06	3.13216-052025	5	17	1497
2.58000+05	1.32385-05	2.75000+06	9.04881-06	2.80000+06	6.37162-062025	5	17	1498
2.24000+05	4.33920-06	2.88000+06	2.84185-07	2.92000+06	1.97825-062025	5	17	1499
2.26000+05	1.30957-06	3.00000+06	8.30787-07	3.04000+06	4.96699-072025	5	17	1500
3.05000+05	2.71344-07	3.12000+06	1.25769-07	3.16000+06	3.46553-082025	5	17	1501
5.20000+00	0.00000+00				2025	5	17	1502
0.00000+00	0.00000+00	0	0	0	02025	5	0	1503
0.42420+04	2.39979+02	0	0	1	02025	5	18	1504
-2.00000+07	0.00000+00	0	7	1	22025	5	18	1505
2	2				2025	5	18	1506
1.60000+05	1.00000+00	1.50000+07	1.00000+00		2025	5	18	1507
0.00000+00	0.00000+00	0	0	1	332025	5	18	1508
33	2				2025	5	18	1509
1.00000+05	1.34100+05	2.53000+02	1.34100+06	1.00000+04	1.34200+062025	5	18	1510
4.50000+04	1.34200+06	6.00000+04	1.34300+06	1.00000+05	1.34400+062025	5	18	1511
2.00000+05	1.34600+06	2.40000+05	1.34700+06	3.00000+05	1.34800+062025	5	18	1512
4.00000+05	1.35000+06	5.00000+05	1.35300+06	6.00000+05	1.35500+062025	5	18	1513
7.00000+05	1.35700+06	8.00000+05	1.35900+06	9.00000+05	1.36200+062025	5	18	1514
1.00000+06	1.36400+06	1.50000+06	1.37700+06	2.00000+06	1.38600+062025	5	18	1515
2.40000+06	1.37400+06	3.00000+06	1.40700+06	3.40000+06	1.41000+062025	5	18	1516
4.00000+06	1.42800+06	5.00000+06	1.44800+06	6.00000+05	1.44800+062025	5	18	1517
7.00000+06	1.44300+06	8.00000+06	1.45400+06	9.00000+06	1.47100+062025	5	18	1518
1.00000+07	1.45800+06	1.10000+07	1.50800+06	1.20000+07	1.52400+062025	5	18	1519

1.30000+07	1.53300+06	1.40000+07	1.53400+06	1.50000+07	1.54200+06	2025	5	18	1520
0.00000+00	0.00000+00	0	0	0	0	02025	5	0	1521
9.42420+04	2.39979+02	0	0	1	1	02025	5	91	1522
0.00000+00	0.00000+00	0	1	1	1	22025	5	91	1523
2	2					2025	5	91	1524
1.13200+06	1.00000+00	1.50000+07	1.00000+00			2025	5	91	1525
0.00000+00	0.00000+00	0	0	1	1	112025	5	91	1526
11	2					2025	5	91	1527
0.00000+00	1.50000+06	0	0	1	1	92025	5	91	1528
9	2					2025	5	91	1529
0.00000+00	0.00000+00	2.50000+04	2.30771+00	7.50000+04	3.24767+00	2025	5	91	1530
1.25000+05	3.38415+00	1.75000+05	3.23852+00	2.25000+05	2.94909+00	2025	5	91	1531
2.75000+05	2.60704+00	3.25000+05	2.25582+00	3.68000+05	0.00000+00	2025	5	91	1532
0.00000+00	2.00000+05	0	0	1	1	122025	5	91	1533
12	2					2025	5	91	1534
0.00000+00	0.00000+00	2.33333+05	2.91497+00	3.00000+05	2.56593+00	2025	5	91	1535
3.66667+05	2.19168+00	4.33333+05	1.83022+00	5.00000+05	1.50197+00	2025	5	91	1536
5.66667+05	1.21429+00	6.33333+05	9.68486-01	7.00000+05	7.62861-01	2025	5	91	1537
7.66667+05	5.93692-01	3.33333+05	4.56566-01	8.68000+05	0.00000+00	2025	5	91	1538
0.00000+00	3.00000+06	0	0	1	1	212025	5	91	1539
21	2					2025	5	91	1540
0.00000+00	0.00000+00	5.00000+04	1.18593+00	1.50000+05	1.53145+00	2025	5	91	1541
2.50000+05	1.46639+00	3.50000+05	1.27952+00	4.50000+05	1.06428+00	2025	5	91	1542
5.50000+05	8.57604+01	6.50000+05	6.75129-01	7.50000+05	5.21518-01	2025	5	91	1543
8.50000+05	3.96313-01	9.50000+05	2.96711-01	1.05000+06	2.19325-01	2025	5	91	1544
1.15000+06	1.59483-01	1.25000+06	1.14539-01	1.35000+06	9.27423-02	2025	5	91	1545
1.45000+06	6.47293-02	1.55000+06	4.44899-02	1.65000+06	3.00805-02	2025	5	91	1546
1.75000+06	1.99731-02	1.35000+06	1.30128-02	1.86500+06	0.00000+00	2025	5	91	1547
0.00000+00	4.00000+06	0	0	1	1	242025	5	91	1548
24	2					2025	5	91	1549
0.00000+00	0.00000+00	6.66667+04	1.05364+00	2.00000+05	1.30636+00	2025	5	91	1550

3.33333+02	1.19430+00	4.70000+05	9.94435-01	6.00000+05	7.38245-01	2025	5	91	1551
7.33333+02	0.04344+01	2.00000+05	4.52931-01	1.00000+05	3.32500-01	2025	5	71	1552
1.13333+02	2.30334+01	1.20000+06	1.71225+01	1.40000+05	1.12772-01	2025	5	91	1553
1.53333+02	0.18244+02	1.05452+06	5.55230+02	1.80000+06	3.70557-02	2025	5	91	1554
1.93333+02	2.43285+02	2.00000+06	1.55671+02	2.20000+06	9.94201-03	2025	5	91	1555
2.33333+02	6.17017+03	2.46667+06	3.74420+03	2.00000+06	2.21575-03	2025	5	91	1556
2.73333+02	1.27575+03	2.84667+06	7.10718+04	2.86300+06	0.00000+00	2025	5	91	1557
0.00000+10	9.00000+06	0	0	1	1	252025	5	91	1558
25	2					2025	5	91	1559
0.00000+05	0.00000+00	8.33333+04	9.70212+01	2.50000+05	1.15111+00	2025	5	91	1560
4.16667+03	1.01042+00	5.33333+05	8.07142+01	7.50000+05	6.13273-01	2025	5	91	1561
9.16667+03	4.50237+01	1.08333+06	3.21023+01	1.25000+05	2.26593-01	2025	5	91	1562
1.41667+03	1.55175+01	1.53333+06	1.05755+01	1.75000+05	7.04354-02	2025	5	91	1563
1.91667+03	4.61477+02	2.08333+06	2.07226+02	2.25000+06	1.38351-02	2025	5	91	1564
2.41667+03	1.71742+02	2.53333+06	7.15130+03	2.75000+06	4.27563-03	2025	5	91	1565
2.91667+03	2.49454+03	3.08313+06	1.42548+03	3.25000+06	7.20741-04	2025	5	91	1566
3.41667+03	4.25030+04	3.53333+06	2.21373+04	3.75000+06	1.09520-04	2025	5	91	1567
0.00000+00	1.00000+00					2025	5	91	1568
26	2					2025	5	91	1569
0.00000+00	0.00000+00	1.00000+05	5.53535+01	3.00000+05	6.38666-01	2025	5	91	1570
5.00000+05	1.08000+00	7.00000+05	8.31502+01	9.00000+05	6.08101-01	2025	5	91	1571
1.10000+05	4.27852+01	1.30000+06	2.90044+01	1.50000+06	1.39493-01	2025	5	91	1572
1.70000+05	1.31841+01	1.92000+06	8.55000+02	2.10000+06	5.45560-02	2025	5	91	1573
2.30000+05	3.41813+02	2.50000+06	2.10358+02	2.70000+06	1.27098-02	2025	5	91	1574
2.90000+05	7.53040+03	3.10000+06	4.3073+03	3.30000+06	1.27098-02	2025	5	91	1575
3.50000+06	1.37384+03	3.70000+06	7.40640+04	3.20000+06	2.43055-03	2025	5	91	1576
4.10000+06	1.95809+04	4.30000+06	9.51362+05	4.50000+06	4.41270+05	2025	5	91	1577
4.70000+06	1.93585+05	4.48400+06	0.00000+00			2025	5	91	1578
0.00000+00	7.00000+06	0	0	1	1	272025	5	91	1579
27	2					2025	5	91	1580
						2025	5	91	1581

0.00000+00	0.00000+00	1.16607+05	7.59464-01	3.50000+05	5.40010-012025	5	91	1562	
5.33333+05	6.87025-01	8.10667+05	5.10699-01	1.05000+06	3.00593-012025	5	91	1583	
1.28333+00	2.45922-01	1.51607+06	3.26574-01	1.75000+05	2.11996-012025	5	91	1584	
1.98333+00	1.34853-01	2.21667+06	8.41596-02	2.45000+06	5.15552-022025	5	91	1585	
2.68333+00	3.10004-02	2.91667+06	1.82991-02	3.15000+06	1.05803-022025	5	91	1586	
3.38333+06	5.39452-03	3.61667+06	3.32176-03	3.85000+05	1.79707-032025	5	91	1587	
4.08333+00	9.47042-04	4.31667+06	4.84812-04	4.55000+05	2.40249-042025	5	91	1588	
4.78333+00	1.14741-04	5.01667+06	5.25153-05	5.25000+05	2.28627-052025	5	91	1589	
5.48333+00	9.37263-06	5.71667+06	3.54712-06	5.86800+06	0.00000+002025	5	91	1590	
0.00000+00	9.00000+06		0	0	1	282025	5	91	1591
28	2					2025	5	91	1592
0.00000+00	0.00000+00	1.50000+05	7.58525-01	4.50000+05	7.91903-012025	5	91	1593	
7.50000+05	6.10145-01	1.05000+06	4.24524-01	1.35000+05	2.82770-012025	5	91	1594	
1.65000+06	1.80803-01	1.95000+06	1.12389-01	2.25000+05	6.82011-022025	5	91	1595	
2.55000+06	4.64932-02	2.85000+06	2.35492-02	3.15000+06	1.34195-022025	5	91	1596	
3.45000+06	7.42220-03	3.75000+06	8.19186-03	4.05000+06	4.38127-032025	5	91	1597	
4.35000+06	2.289+9-03	4.05000+06	1.10704-03	4.95000+06	5.79083-042025	5	91	1598	
5.25000+06	2.78922-04	5.45000+06	1.30088-04	5.85000+06	5.34750-052025	5	91	1599	
6.15000+06	2.52117-05	6.45000+06	1.03594-05	6.75000+06	4.02253-062025	5	91	1600	
7.05000+06	1.45921-06	7.35000+06	4.86617-07	7.65000+06	1.45649-072025	5	91	1601	
7.84800+06	7.00000+06					2025	5	91	1602
0.00000+00	1.10000+07		0	0	1	292025	5	91	1603
29	2					2025	5	91	1604
0.00000+00	0.00000+00	1.33333+05	6.70544-01	5.50000+05	6.84657-012025	5	91	1605	
9.16007+05	5.07915-01	1.23333+06	3.39910-01	1.65000+06	2.14080-012025	5	91	1606	
2.01007+06	1.30253-01	2.36333+06	7.65750-02	2.75000+05	4.38299-022025	5	91	1607	
3.11607+06	2.44904-02	3.48333+06	1.33774-02	3.85000+06	7.16700-032025	5	91	1608	
4.21607+06	3.73432-03	4.58333+06	1.90707-03	4.95000+06	9.50902-042025	5	91	1609	
5.31607+06	4.62224-04	5.68333+06	4.37372-04	6.05000+06	2.00387-042025	5	91	1610	
6.41607+06	5.93255-05	6.78333+06	3.83153-05	7.15000+06	1.57855-052025	5	91	1611	
7.51607+06	6.21129-06	7.28333+06	2.31770-06	8.25000+06	8.12489-072025	5	91	1612	

5.11467+06	2.64217-07	9.06333+06	7.82940-08	9.35000+06	2.05897-082025	5	91	1613	
9.71667+06	4.60537-09	9.36800+06	9.00000+30			2025	5	91	1614
0.00000+00	1.30000+07		0	0	1	292025	5	91	1615
29	2					2025	5	91	1616
0.00000+00	0.00000+00	2.10607+05	5.276+6-01	5.50000+05	6.01342-012025	5	91	1617	
1.08333+06	4.48611-01	1.51607+06	2.90045-01	1.95000+05	1.36201-012025	5	91	1618	
2.38333+06	1.10263-01	2.91607+06	6.27320-02	3.25000+06	3.44771-022025	5	91	1619	
3.68333+06	1.03615-02	4.11607+06	9.53196-03	4.55000+06	4.31562-032025	5	91	1620	
4.98333+06	2.37194-03	5.41607+06	1.13920-03	5.85000+06	5.32632-042025	5	91	1621	
6.28333+06	2.42505-04	6.71607+06	1.07170-04	7.15000+06	4.58728-052025	5	91	1622	
7.58333+06	3.79170-05	8.01667+06	1.50719-05	7.45000+06	5.73451-062025	5	91	1623	
7.88333+06	2.07540-06	9.31667+06	7.09358-07	9.75000+06	2.26520-062025	5	91	1624	
1.01937+07	6.66698-08	1.16167+07	1.77379-08	1.10500+07	4.14499-092025	5	91	1625	
1.14033+07	8.12360-10	1.18680+07	0.00000+00			2025	5	91	1626
0.00000+00	1.50000+07		0	0	1	302025	5	91	1627
30	2					2025	5	91	1628
0.00000+00	0.00000+00	2.50000+05	3.85517-01	7.50000+05	4.40419-012025	5	91	1629	
1.25000+06	3.73029-01	1.75000+06	2.87158-01	2.25000+06	2.08853-012025	5	91	1630	
2.75000+06	1.38274-01	3.25000+06	7.91256-02	3.75000+06	4.32372-022025	5	91	1631	
4.25000+06	2.26462-02	4.75000+06	1.14093-02	5.25000+06	5.34675-032025	5	91	1632	
5.75000+06	2.60855-02	6.25000+06	1.18917-03	6.75000+06	5.25707-042025	5	91	1633	
7.25000+06	2.25337-04	7.75000+06	9.35295-05	8.25000+06	3.75073-052025	5	91	1634	
8.75000+06	1.44862-04	9.25000+06	5.30631-06	9.75000+06	3.79366-062025	5	91	1635	
1.02500+07	1.27114-06	1.07500+07	4.00436-07	1.12500+06	1.17293-072025	5	91	1636	
1.17500+07	3.14770-08	1.22500+07	7.57960-09	1.27500+07	1.58778-092025	5	91	1637	
1.32500+07	2.75302-10	1.37500+07	3.61045-11	1.38760+07	0.10000+002025	5	91	1638	
0.00000+00	0.00000+00		0	0	0	02025	5	0	1639
0.00000+00	0.00000+00		0	0	0	02025	0	0	1640
9.42420+04	2.30974+02		0	0	1	0202515	3	1641	
0.00000+00	0.00000+00		0	1	1	2202515	3	1642	
2	2					202515	3	1642	

1.00000-05	1,00000+00	1.50000+07	1,00000+00		202515	3 1646
0 00000+00	0,00000+00	0	0	1	5202515	3 1645
5	2				202515	3 1646
0.00000+00	2,53000-02	0	0	1	13202515	3 1647
13	2				202515	3 1648
0.00000+00	0,00000+00	5,00000+04	2,09080-04	1,00000+05	1,10813-02202515	3 1649
2.00000+05	6,33517-02	4,00000+05	3,74047-01	6,00000+05	5,71210-01202515	3 1650
8.00000+05	6,24526-01	1,00000+06	6,14699-01	1,50000+06	4,32589-01202515	3 1651
2.00000+06	2,49015-01	3,00000+06	5,66611-02	4,00000+06	8,36326-04202515	3 1652
5.00000+06	0,00000+00				202515	3 1653
0.00000+00	3,00000+06	0	0	1	16202515	3 1654
16	2				202515	3 1655
0.00000+00	0,00000+00	5,00000+04	1,86455-03	1,00000+05	1,05422-01202515	3 1656
2.00000+05	5,50439-01	4,00000+05	7,30671-01	6,00000+05	7,14002-01202515	3 1657
6.00000+05	6,75665-01	1,00000+06	5,83313-01	1,50000+06	2,86725-01202515	3 1658
2.00000+06	1,33742-01	3,00000+06	2,31490-02	4,00000+06	9,26855-03202515	3 1659
5.00000+06	2,79526-03	^,00000+06	1,44000-03	8,00000+06	1,02602-04202515	3 1660
1.00000+07	0,00000+00				202515	3 1661
0.00000+00	5,00000+06	0	0	1	16202515	3 1662
1e	2				202515	3 1663
0.00000+00	0,00000+00	5,00000+04	2,31242-03	1,00000+05	1,58864-01202515	3 1664
2.00000+05	3,00113-01	4,00000+05	9,85671-01	6,00000+05	8,63261-01202515	3 1665
8.00000+05	6,32769-01	1,00000+06	4,94372-01	1,50000+06	1,86336-01202515	3 1666
2.00000+06	1,01223-01	3,00000+06	1,82658-02	4,00000+06	7,35974-03202515	3 1667
5.00000+06	2,22669-03	6,00000+06	1,14130-03	8,00000+06	1,53830-04202515	3 1668
1.00000+07	0,00000+00				202515	3 1669
0.00000+00	1,00000+07	0	0	1	16202515	3 1670
16	2				202515	3 1671
6.00000+00	0,00000+00	5,00000+04	2,17495-03	1,00000+05	1,39106-01202515	3 1672
2.00000+05	7,23948-01	4,00000+05	9,08095-01	6,00000+05	8,14602-01202515	3 1673
8.00000+05	6,14821-01	1,00000+06	4,90720-01	1,50000+06	2,03713-01202515	3 1674

2.00000+00	1,13717-01	3,00000+06	3,47997-02	4,00000+05	1,26784-02202515	3 1675
5.00000+00	5,77907-03	6,00000+06	1,94426-03	8,00000+06	1,46463-04202515	3 1676
1.00000+07	0,00000+00				202515	3 1677
0.00000+00	1,50000+07	0	0	1	17202515	3 1678
17	2				202515	3 1679
0.00000+00	0,00000+00	5,00000+04	2,19906-03	1,00000+05	1,42526-01202515	3 1680
2.00000+05	7,14505-01	4,00000+05	9,23167-01	5,00000+05	8,20989-01202515	3 1681
8.00000+05	8,04199-01	1,00000+06	4,85815-01	1,50000+06	1,90151-01202515	3 1682
2.00000+06	1,08035-01	3,00000+06	3,02901-02	4,00000+06	1,40691-02202515	3 1683
5.00000+06	4,16717-03	6,00000+06	2,05228-03	8,00000+06	1,47549-04202515	3 1684
1.00000+07	5,25321-07	1,20000+07	0,00000+00		202515	3 1685
0.00000+00	0,00000+00	0	0	0	0202515	0 1686
0.00000+00	0,00000+00	0	0	0	02025 0	0 1687
0.00000+00	0,00000+00	0	0	0	0 0 0	0 1688